
IMPACTS OF CLIMATE CHANGE ON REGIONAL PRIMARY AND FISHERIES PRODUCTIVITY IN AN AUSTRALIAN UPWELLING SYSTEM

Anne-Elise Nieblas

BSc (Honours), University of Tasmania
BSc & BA, University of California, Los Angeles

Submitted in fulfilment of the requirements for the degree of

Doctor of Philosophy in Quantitative Marine Science
(A joint CSIRO and UTAS PhD program in Quantitative Marine Science)

University of Tasmania
June 2010

Supervisors
Dr Bernadette M. Sloyan
Prof. Richard Coleman
Dr Anthony J. Richardson
Dr Alan J. Butler



For my parents with love

STATEMENT OF ORIGINALITY

To the best of my knowledge, this thesis contains no material that has been accepted for a degree or a diploma by the University of Tasmania or other institutions, or has been previously published or written by another person except by way of background information that has been duly acknowledged in the text of this thesis, nor does this thesis contain any material that infringes copyright.



Anne Elise Nieblas

28/6/10

Date

STATEMENT OF AUTHORITY OF ACCESS

I, the undersigned, the author of this thesis, understand that the University of Tasmania will make it available for use within the university library and, by microfilm or other photographic means, allow access to users in other approved libraries. All users consulting this thesis will have to sign the following statement:

'In consulting this thesis I agree not to copy or closely paraphrase it in whole or in part, or use the results in any other work (written or otherwise) without the signed consent of the author; and to make proper written acknowledgement for any other assistance which I have obtained from it.'

This thesis may be made available for loan and limited copying in accordance with the Copyright Act 1968.

Beyond this, I do not wish to place any restrictions on access to this thesis.



Anne Elise Nieblas

28/6/10

Date

STATEMENT OF PUBLICATION AND CO-AUTHORSHIP

Publications produced as part of this thesis include:

Chapter 3

Nieblas A-E, BM Sloyan, AJ Hobday, R Coleman, and AJ Richardson (2009) Variability of biological production in low wind-forced regional upwelling systems: a case study off southeastern Australia. *Limnology and Oceanography*, 54(5): 1548–1558.

To be submitted:

Chapter 2.1

Nieblas A-E, M Haddon, BM Sloyan, AJ Butler, and AJ Richardson (*in prep*) Ecosystem trophic control assessed across a suite of Australian marine habitats.

Chapter 2.2

Nieblas A-E, M Haddon, BM Sloyan, AJ Butler, and AJ Richardson (*in prep*) 'Ocean triad' features in tropical and temperate Australian marine ecosystems: an investigation of physical mechanisms affecting fish and invertebrate spawning habitats.

Chapter 4

Nieblas A-E, M Haddon, BM Sloyan, AJ Butler, and AJ Richardson (*in prep*) Environmental mechanisms driving variability in catch rates of two contrasting marine species: arrow squid (*Nototodarus gouldi*) and gummy shark (*Mustelus antarcticus*) in an Australian upwelling region.

Chapter 5

Nieblas A-E, M Haddon, BM Sloyan, AJ Butler, and AJ Richardson (*in prep*) Impacts of climate on environment, primary productivity, and tertiary productivity of arrow squid (*Nototodarus gouldi*) in an Australian upwelling region.

The following people and institutions contributed to the publication of the work undertaken as part of this thesis:

Bernadette M. Sloyan (CSIRO Marine and Atmospheric Research), Richard Coleman (University of Tasmania & CSIRO Marine and Atmospheric Research), Anthony J. Richardson (University of Queensland & CSIRO Marine and Atmospheric Research), and Alan J. Butler (CSIRO Marine and Atmospheric Research) have provided guidance and supervision in all aspects of my PhD.

Alistair J. Hobday (CSIRO Marine and Atmospheric Research) provided assistance in the development of methods and contributed to Nieblas et al. (2009). Malcolm Haddon (CSIRO Marine and Atmospheric Research) provided assistance in the development of methods and contributed to Chapters 4 and 5.

I the undersigned agree with the above stated "proportion of work undertaken" for each of the above published (or submitted) peer-reviewed manuscripts contributing to this thesis:



Bernadette Sloyan
Candidate Supervisor

 29.6.10

Craig Johnson
Divisional Director
Institute for Marine and Antarctic Science

ABSTRACT

Coastal upwelling regions account for 20% of global ocean productivity. These extremely productive wind-driven ecosystems are vulnerable to climate change. Here, I investigate relationships between the physical environment, primary productivity, and fisheries productivity in an Australian upwelling ecosystem. This study examines the likely impacts of climate change on the ecosystem productivity of a historically low-wind upwelling system. These results provide insight into the vulnerability of the ecosystem to climate change to help inform an ecosystem approach to marine management.

The large-scale investigation in Chapter 2.1 reveals bottom-up trophic control across a diverse suite of Australian marine bioregions, indicating that changes in primary productivity will cascade throughout foodwebs. Though primary productivity is clearly important, other oceanographic conditions are necessary for the viability of fisheries. Chapter 2.2 presents a comparative analysis of key oceanographic characteristics of several productive Australian ecosystems to assess how enrichment, concentration, and retention mechanisms regulate fisheries recruitment.

These large-scale physics-to-biology relationships are then assessed at the regional scale for the most productive upwelling system in Australia: the Bonney Upwelling. The Bonney Upwelling in south eastern Australia has classic enrichment, concentration, and retention features. This wind-driven system is vulnerable to climate change because of potential future changes in large-scale wind forcing. The productivity of wind-driven upwelling systems depends on an “optimal environmental window” in which wind speed is strong enough to promote vertical mixing of nutrients that enhance productivity, but is not so strong as to lead to deleterious turbulent mixing or pronounced advection that may

reduce productivity or lose spawning products to oligotrophic offshore waters. In Chapter 3, I show that the Bonney Upwelling region currently operates at low wind velocities ($\sim 4 \text{ m s}^{-1}$), and hence suboptimal productivity as wind velocities are less than the optimal environmental window ($5\text{--}6 \text{ m s}^{-1}$). Statistical models are developed that describe between 40%–50% of the variation in phytoplankton biomass, using alongshore wind stress and the size of the upwelling plume as predictors.

In Chapter 4, I develop biophysical statistical models that describe relationships between regional and large-scale environmental drivers, primary productivity and catches of two commercial marine species. These species have contrasting r - (arrow squid, *Nototodarus gouldi*) and K -selected (gummy shark, *Mustelus antarcticus*) life history traits. I develop significant physics to biology relationships that describe $\sim 77\%$ of variance for arrow squid catch rates and $\sim 50\%$ of variance for gummy shark catch rates. Arrow squid are closely related to upwelling forcing and the regional environment on a seasonal time scale, and gummy shark have closer links to large-scale climate drivers (El Niño–Southern Oscillation) at periods of up to 3 years. The arrow squid biophysical model is useful for present-day and future predictions; however, due to complicated (non-linear) interactions in the gummy shark biophysical model, predictions for gummy shark populations are not useful.

In Chapter 5, climate models are used to make projections of potential impacts of climate change on ecosystem productivity for two likely CO_2 emission scenarios (Special Report on Emissions Scenarios A1B, and A2). I find that the Bonney Upwelling is projected to remain a low-wind system as the magnitude of the wind is not predicted to substantially increase. However, alongshore wind stress events are predicted to intensify and become more prevalent, especially in the upwelling season. This is due to the southward migration of the subtropical ridge. The “business-as-usual” emissions scenario (A2) predicts an extension of the upwelling season by one month that affects intra-annual upwelling phases by shortening the onset of upwelling, extending the sustained phase of upwelling, and shortening or delaying the quiescent phase of upwelling. Primary productivity is expected to increase linearly with wind stress, with potential shifts in seasonal peaks. Arrow squid catch rates are predicted to increase due to stronger upwelling and warmer ocean temperature.

In this thesis, I apply ecological theory at both large and regional scales to Australian marine ecosystems. I develop robust, relatively simple methods to describe complex environment-biology interactions. This thesis demonstrates the value of simple statistical models to investigate complex ecosystem response to future climate change.

ACKNOWLEDGMENTS

Firstly, I would like to acknowledge my primary supervisor Dr Bernadette Sloyan whose dedicated efforts and unwavering support have enabled me to finish this thesis. Bernadette is a superior scientist with clear priorities between family and work that make her an inspiring role model for women in science. Bernadette has helped me through the most difficult aspects of my PhD and has always kept my best interests at heart.

I would like to thank Prof. Richard Coleman, Dr Anthony Richardson, and Dr Alan Butler for accepting me as a student mid-way through my candidature. The myriad of opinions I've received over the last couple years has been both a challenge and a blessing! My manuscripts are top-quality due to the abundance of critical thought and rigorous review. Special thanks also go to Prof. Malcolm Haddon for his statistical and methodological help, critical comments to my fourth and fifth chapters, and his constructive comments on the final version of this thesis. Thanks as well to Nicole Hill for her constructive comments on the final draft of this thesis.

I would like to thank the Quantitative Marine Science program, the CSIRO Climate Adaptations National Research Flagship, and the International Postgraduate Research Scholarship for the generous funding provided throughout this PhD. I'd also like to thank the Australian Research Council Network for Earth System Sciences for assistance with international travel funding.

There have been many people that have helped me along the way by taking the time to chat with me about my ideas, help me with data handling, and assist me with programming. Thanks go to Mike Fuller for his help and patience assisting me with the

Australian Fisheries Management Authority logbook dataset. Thank you to Dr Peter Rothlisberg, Dr Michele Burford, and Dr Scott Condie for their expert advice on the Gulf of Carpentaria.

As this thesis was a wholly computer-based endeavour, I'd like to thank the people that let me tag along on their field projects so that I could continue to maintain my diving and field skills, especially Mark Green for diving fun with endangered spotted handfish, Tim Alexander for Maria Island adventures, and Adam Barnett for a great day dancing with sharks.

Thanks to my fellow PhD students both at CSIRO and TAFI – the after work beers, weekend barbeques, camping trips and fancy dress parties have made this PhD fly by. Special thanks to the CSIRO cubicle crew. Thanks Laura for the running and tea breaks – they helped keep me fit and gave me much-needed breathers. An acknowledgements page would not be complete if I didn't specially thank Paul Durack for answering (?) the multitude of mini-questions I've thrown over the top of the cubicle. Whilst I'm not listing you as first author as per your request, you get a special mention.

To my family: Jo Ann, Peter, Marie, Kari, Joey, Jonas, Donna, and Dan – thank you for the constant encouragement. I have been unusually lucky to end up with a family as loving, tolerant, and supportive as you. I've discovered that homesickness is never cured. Thank you for phone calls, emails, and plane tickets home for Christmas. I have missed you all so much, and I can't wait to spend more time with you.

There are few people that make a place like a home, and I've had the good luck to know three during my time in Tassie. Thanks to Sarah Metcalf who was my faithful early-to-the-pub-on-Friday-afternoon buddy for the first 2 years, and my almost-hourly-sarcastic-humour-provider every Monday through Friday for the subsequent two years. Big thanks to Jane Alpine, who has set the standard for best friends since 2004. This PhD would have been a far more quiet, sober, perhaps quicker, hugely less eventful and definitely, extraordinarily, more boring undertaking without you. What can I say – you're the best.

And finally, my biggest thanks go to Ben Smethurst. You have given me invaluable friendship, love and support. You have had the thankless job of being a Domestic God for a distracted and unappreciative partner. Without you, the bills wouldn't be paid, the dishes would never be done, I would be eating refried beans from a can, and the stress would have killed me months ago. Thank you for always being there to pick up the pieces, make me laugh, and put me back together again. I couldn't have done it without you.

CONTENTS

STATEMENT OF ORIGINALITY	ii
STATEMENT OF AUTHORITY OF ACCESS	ii
STATEMENT OF PUBLICATION AND CO-AUTHORSHIP	iii
ABSTRACT	v
ACKNOWLEDGMENTS	vii
CONTENTS	ix
LIST OF TABLES	xi
LIST OF FIGURES	xiii
INTRODUCTION 1	1
1.1 IMPACTS OF CLIMATE CHANGE ON MARINE SYSTEMS	2
1.2 COASTAL UPWELLING ECOSYSTEMS	6
LARGE-SCALE RELATIONSHIPS 2	11
2.1 LARGE-SCALE RELATIONSHIPS BETWEEN PRIMARY AND FISHERIES PRODUCTIVITY	12
Ecosystem Trophic Control Assessed across a Suite of Australian Marine Habitats	12
2.2 LARGE-SCALE RELATIONSHIPS BETWEEN OCEAN PHYSICS AND FISHERIES PRODUCTIVITY	27
‘Ocean Triad’ Features in Tropical and Temperate Australian Marine Ecosystems: an Investigation of Physical Mechanisms Affecting Fish and Invertebrate Spawning Habitats	27
REGIONAL-SCALE RELATIONSHIPS: PHYSICS TO PRIMARY PRODUCTIVITY 3	53
3 REGIONAL-SCALE RELATIONSHIPS BETWEEN OCEAN PHYSICS AND PRIMARY PRODUCTIVITY	54
Variability of Biological Production in Low Wind-Forced Regional Upwelling Systems: a Case Study off Southeastern Australia	54
REGIONAL-SCALE RELATIONSHIPS: PHYSICS TO FISHERIES PRODUCTIVITY 4	75

4 REGIONAL-SCALE RELATIONSHIPS BETWEEN OCEAN PHYSICS AND FISHERIES PRODUCTIVITY	76
Environmental Mechanisms Driving Variability in Catch Rates of Two Contrasting Marine Species: Arrow Squid (<i>Nototodarus gouldi</i>) and Gummy Shark (<i>Mustelus antarcticus</i>) in an Australian Upwelling Region	76
CLIMATE CHANGE IMPACTS 5	101
5 PROJECTIONS OF THE IMPACTS OF CLIMATE CHANGE ON REGIONAL-SCALE UPWELLING PHYSICS, PRIMARY PRODUCTIVITY, AND FISHERIES PRODUCTIVITY	102
Impacts of Climate Change on Environment, Primary Productivity, and Tertiary Productivity of Arrow Squid (<i>Nototodarus gouldi</i>) in an Australian Upwelling Region	102
DISCUSSION 6	127
6 GENERAL DISCUSSION	128
REFERENCES	a

LIST OF TABLES

Table 2.1.1: Correlation coefficients (r) for the linear regression between Chl and CPUE for each functional group based on trophic level with 3.75 as a threshold, and habitat preference, indicating the strength and direction of the relationship. Significant r values are in bold with significance levels indicated as $p<0.1^*$, $p<0.05^{**}$, $p<0.001^{***}$, $p<0.0001^{****}$. _____ 16

Table 2.1.2: Trophic level and percent biomass of the 20 most abundant fish and invertebrate species based on catch (t). Percent biomass is calculated as the catch (t) of the specific species divided by the total catch (t) from all Australian Commonwealth fisheries. _____ 18

Table 2.2.1: A list of common marine organism spawning patterns and behaviour in the regions examined in this study. Bolded species are investigated in this paper. Location codes: North (N), South (S), East (E), West (W); Australia (Aus), Tasmania (Tas), Flinders Current System (FCS), New South Wales (NSW). Footnotes are provided for species that are not referenced in the text. ____ 34

Table 2.2.2: Mechanisms for ocean triad features for each region examined in this study. Abbreviations as: North (N), South (S), East (E), West (W), Tasmania (Tas), Subtropical Front (STF), and East Australia Current (EAC). _____ 41

Table 3.1: Interannual variability of the mean number of days of upwelling-favourable wind stress per year, the mean number of upwelling events per year, annual mean duration of upwelling events (d), wind stress ($N\ m^{-2}$), length of periods of quiescence between upwelling events (d), $ASST_a$ (km^2), and $[Chl\ a]$ ($mg\ m^{-3}\ km^{-2}$). *, **, *** Indicate significant interannual REGWQ groupings between years in ascending value order (e.g., * lowest grouping, *** highest grouping). _____ 65

Table 3.2: REGWQ multiple range test groupings and orders for frequency of upwelling days per month, wind stress intensity ($N\ m^{-2}$), and duration of upwelling events (d). Separate groupings delineated by commas, and are listed in descending order. _____ 67

Table 4.1: Optimal lag periods of environmental indices for arrow squid and gummy shark catch rates. Lag periods expressed in months. Only significant ($\alpha = 0.05$) correlation coefficients, r , listed. Ln represents a natural logarithmic transformation. _____ 86

Table 4.2: Best fit step-wise linear modelling of environmental predictors against arrow squid CPUE (2003–2007) and gummy shark catch (1998–2007) with adjusted coefficients of determination (adj r ²) and the Akaike Information Criterion (AIC) indicating goodness-of-fit. Significance codes for each predictor variable in the ANOVA are represented as ***' <0.001, '**' <0.01, '*'<0.05, '~'<0.1. ____	88
Table 4.3: Models for arrow squid and gummy shark with optimal predictive performance (M1). Mn refers to the mean year parameter. _____	90
Table 4.4: Best models parameter estimates and retrospective analysis of environmental predictors against arrow squid CPUE and gummy shark catch. Mean of all year factor estimates listed. Adjusted coefficients of determination (adj r ²) show goodness-of-fit. Significance codes of each predictor in the ANOVA are represented as '***' <0.001, '**' <0.01, '*'<0.05, '~'<0.1. 2008 column represents adj r ² of each model's 2008 predictions against 2008 arrow squid CPUE or gummy shark catch data. ____	90
Table 5.1: Details of climate models used in this study. Geophysical Fluid Dynamics Laboratory (GFDL); the National Oceanic and Atmospheric Administration (NOAA); Model for Interdisciplinary Research on Climate 3.2 medium-resolution (MIROC3.2 (medres)); the Center for Climate System Research (CCSR); the National Institute for Environmental Studies (NIES); the Frontier Research Center for Global Change (FRCGC); the Japan Agency for Marine-Earth Science and Technology (JAMSTEC); the U.K. Met Office Hadley Centre Coupled Model, version 3 (UKMO-HadCM3); Parallel Climate Model, version 1.1 (PCM 1); the National Center for Atmospheric Research; the Goddard Institute of Space Studies Model E/Russel (GISSer); the National Aeronautics and Space Administration (NASA); the Centre National de Recherches Meteorologiques (CNRM); and the Commonwealth Scientific and Industrial Research Organisation (CSIRO)._____	109
Table 5.2: Best fit step-wise linear modelling of observed environmental predictors against arrow squid CPUE (2003–2007) with adjusted coefficients of determination (Adj r ²) and the Akaike Information Criterion (AIC) indicating goodness-of-fit. 'ln' represents the natural log. Significance codes for each predictor variable in the ANOVA are represented as ***' <0.001, '**' <0.01, '*'<0.05. _____	112
Table 5.3: Model parameter estimates and retrospective analysis of observed environmental predictors against arrow squid CPUE. Mean of all year factor estimates listed. Adjusted coefficients of determination (adj r ²) show goodness-of-fit. Significance codes of each predictor in the ANOVA are represented as '***' <0.001, '**' <0.01, '*'<0.05. 2008 column represents adjusted r ² of each model's 2008 predictions against 2008 arrow squid CPUE._____	113

LIST OF FIGURES

Fig. 1.1.1: Important physical and chemical changes in atmospheric, terrestrial, and oceanographic features due to climate change (from Poloczanska et al. 2007). _____ 3

Fig. 1.2.1: Ekman transport and coastal upwelling in the southern hemisphere. Equatorward, alongshore winds drive surface waters to the left due to the Coriolis force. Water from depth is then vertically upwelled to replace surface waters. _____ 7

Fig. 1.2.2: The optimal environmental window (adapted from Cury & Roy 1989). _____ 8

Fig. 2.1.1: Combined inshore and offshore bioregions used in this study (bold black lines) derived from bioregions defined in the Integrated Marine and Coastal Regionalisation of Australia Version 4.0. Also shown are divisions between inshore and offshore (light black lines) of the original 41 bioregions. _____ 15

Fig. 2.1.2: Spatial distribution for Australian bioregions of (a) Chl (mg m^{-3}), and CPUE (t shot^{-1}) for (b) total fish species, (c) pelagic fish, (d) benthic fish, (e) lower trophic level fish (f) lower trophic level pelagic fish, (g) lower trophic level benthic fish, (h) higher trophic level fish, (i) higher trophic level pelagic fish, and (j) higher trophic level benthic fish. See bioregion labels in Fig. 2.1.1. _____ 19

Fig. 2.1.3: Correlations of overall mean log Chl versus overall mean log CPUE (t shot^{-1}) for (a) Total species combined, (b) lower trophic level species (LT), (c) higher trophic level species (GT), (d) pelagic and benthopelagic species (P), (e) lower trophic level pelagic and benthopelagic species (LTP), (f) higher trophic level pelagic and benthopelagic species (GTP), (g) benthic species (B), (h) lower trophic level benthic species (LTB), and (i) higher trophic level benthic species (GTB). Dashed lines represent ± 1 standard error; “ns” represents “not significant”. Data labels represent bioregions as in Fig. 2.1.1. _____ 21

Fig. 2.1.4: Interannual variability of (a) the Chl (mg m^{-3}) for bioregions A–S (see Fig. 2.1.1) with >50 shots per year and (b) all fish species CPUE with a split panel for enhanced readability. _____ 22

Fig. 2.1.5: The log of CPUE for all species as a function of the log of Chl for the Tasmanian bioregion (I) with no time lag; “ns” represents “not significant”. _____ 23

Fig. 2.2.1: Coastline of (a) the Gulf of Carpentaria with regions of seagrass bed (black) (widths not to scale), which is suitable spawning and nursery habitat for this region, adapted from Poiner et al. 1987, and (b) south eastern Australia with spawning habitat of blue grenadier (*Macruronus novaezelandiae*; blue) taken from Thresher et al. 1988; egg and larval distributions of sardine (*Sardinops sagax*; dark gray) and Australian anchovy (*Engraulis australis*; dark gray) taken from Dimmlich et al. 2004 and Ward et al. 2008, and the Larval Fish Database compiled by Bruce et al. 2001a; spawning area of King George whiting (*Sillaginodes punctata*; light blue) from Jenkins et al. 2000; egg and larval distributions of redbait (*Emmelichthys nitidus*; light gray) from Neira et al. 2009; larval distributions of (*Nemadactylus macropterus*; red) and redfish (*Centroberyx affinis*; white) and beaked salmon (*Gonorhynchus greyi*; white) from the Larval Fish Database compiled by Bruce et al. 2001a, with boxes indicating regions where mean annual chlorophyll *a* concentration was calculated. Also shown are regions discussed in text: Bonney Coast, Bass Strait, western Tasmania (W.Tas), eastern Tasmania (E. Tas), Kangaroo Island (KI), and Eyre Peninsula (EP). (c) Satellite ocean colour image from 5 January 1998 showing productivity around the south east of Australia. Note the high chlorophyll *a* concentration due to eddies off the east coast, an upwelling plume off Bonney Coast and Eyre Peninsula, and the Subtropical Front apparent in the latitudinal band approximately between 42°S–45°S. The tall black box on the coast represents the region where eddy productivity was calculated and smaller black box offshore represents the region where background chlorophyll *a* concentrations were taken in the Tasman Sea, (d) Australian altimetry image from 7 January 1998 showing eddies off the east coast due to EAC extension, also note the low SSH in the Flinders Current system, indicating coastal upwelling. The black box represents same as in (c), and black line follows the 200m isobath (continental shelf) in both (c) and (d).

31
Fig. 2.2.2: Mean annual (a) satellite Chl (mg m^{-3}) (b) BRAN surface salinity and (c) 10 m CARS nitrate (black), silicate (red), and phosphate (green) (μM) for nearshore zone, and (d) wind turbulence index, w^3 ($\text{m}^3 \text{s}^{-3}$). Potential density (kg m^{-3}) distribution along 139.5°E latitude for the (e) wet and (f) dry seasons based on BRAN salinity and temperature, black lines at -16.67°S indicate the location of the 20 m contour, and BRAN mean surface currents for the (g) wet and (h) dry seasons for the Gulf of Carpentaria, with a solid black line indicating the line of longitude of the density distribution (e,f). Dots represent points where mean current is near zero (in central Gulf), and where BRAN does not resolve the nearshore region.

38
Fig. 2.2.3: Seasonal distribution of wind speed cubed (W^3 ; units: $\text{m}^3 \text{s}^{-3}$) in Australian waters for (a) summer, (b) autumn, (c) winter, and (d) spring.

42
Fig. 2.2.4: Oceanographic variables from south eastern Australia including (a) mean annual Chl for the fisheries hotspots in south eastern Australia calculated from boxes in Fig. 2.2.1b, and (b) productivity related to cold- (blue line) and warm-core (red line) eddies relative to background Chl from the Tasman Sea (black line).

42
Fig. 2.2.5: Bonney Coast (a) mean summer Ekman transport per unit width (January–February), (b) mean summer satellite Chl (December–February), (c) characteristic summer BRAN surface currents (February 2006), note currents are plotted every third grid point for clarity; and (d) mean summer/autumn frontal activity (December–April) (red indicates high activity, blue indicates low

activity) with locations mentioned in the text. White or black lines indicate 200 m isobath (continental shelf). _____ 43

Fig. 2.2.6: Western Tasmania mean austral winter (June–August) ocean dynamics including (a) BRAN surface currents, note currents were plotted every third grid point for clarity; (b) sea surface temperature, and (c) frontal activity (red indicates high activity, blue indicates low activity). Black or white lines indicate the 200 m isobath (continental shelf). _____ 46

Fig. 2.2.7: Ocean dynamics of south eastern Australia, including (a) mean summer and (b) mean winter frontal activity (red indicates high activity, blue indicates low activity); and characteristic surface currents for (c) austral summer (February 2006), and (d) austral winter (June 2005), note currents were plotted every second grid point for clarity. White or black lines indicate the 200 m isobath (continental shelf). _____ 49

Fig. 3.1: (a) The Bonney Coast is encompassed by Cape Jaffa and Portland. NCEP-NCAR gridded wind locations (blue arrows) over the south eastern Australian ocean region. Numbered grid locations (1 to 4) identify wind values adjacent to the Bonney Coast. The boxed grid point (3) was used to represent wind values along the Bonney Coast, and developed into the upwelling wind index. The dashed black arrow along the coast indicates the dominant angle of the Bonney Coast near grid point 3 ($\beta \approx 314^\circ$). The 200 m contour represents the continental shelf (solid (a) black and (b) white lines). A polygon is defined by the northern and southern limits (red lines) and the 1000 m bathymetric contour defines the seaward edge of the upwelling region (dashed (a) black and (b) white lines) of the Bonney Coast upwelling region. The pink lines show the area of (a) anomalously low SST and (b) anomalously high SSC that represent the upwelling plume for each variable. _____ 57

Fig. 3.2: Wavelet transform (colour bar indicates power, black contours = 5% significance) and time series of (a) daily alongshore wind stress (1994–2006) (positive wind stress is easterly and upwelling-favourable), (b) daily ASST_a (1994–2006), and (c) 8-day [Chl *a*] (1998–2006) for the Bonney Coast. 61

Fig. 3.3: Seasonal variability between the non-upwelling season (May–October) and the upwelling season (November–April) for (a) the mean frequency of upwelling events per season, duration of events (days), length of periods of quiescence between events (days), (b) the mean overall wind stress (N m^{-2}) (positive wind stress is easterly and upwelling-favourable), (c) ASST_a (km^2), and (d) [Chl *a*] ($\text{mg m}^{-3} \text{ km}^{-2}$). Error bars represent standard error around the mean. _____ 63

Fig. 3.4: Interannual variation of (a) number of upwelling days and frequency of upwelling events per year (b) mean annual duration of upwelling events and quiescent periods, and mean annual wind stress intensity (N m^{-2}), and (c) mean annual [Chl *a*] ($\text{mg m}^{-3} \text{ km}^{-2}$) and ASST_a (km^2) of the upwelling season (November to April). _____ 64

Fig. 3.5: Seasonal variation of (a) number of upwelling days per month, duration of upwelling events (d), and wind stress intensity (N m^{-2}), and (b) ASST_a (km^2) over 1994–2006, and (c) [Chl *a*] ($\text{mg m}^{-3} \text{ km}^{-2}$) over 1998–2006 for the months within the upwelling season (November–April). Error bars represent standard errors of means. _____ 66

Fig. 3.6: A comparison of the observed [Chl *a*] as derived from the SeaWiFS satellite (solid line) against the modelled [Chl *a*] from wind + ASST_a (dashed line), and wind (dotted line). _____ 68

Fig. 3.7: CSIRO Atlas of Regional Seas (CARS; Dunn & Ridgway 2002, Ridgway et al. 2002) (a) mixed layer depth, and (b) phosphate and (c) nitrate concentration ($\mu\text{mol L}^{-1}$) at the surface (0 m), base of the summer mixed layer (20 m), and base of the winter mixed layer (80 m) on the continental shelf at a point off the Bonney Coast (-38.5° latitude, 141° longitude) and (d) mean SST climatology (heavy line) ± 1 standard deviation (light lines) within the upwelling plume. _____ 70

Fig. 4.1: The Bonney Coast with the $\sim 15^\circ\text{C}$ upwelling plume. The South East Scalefish and Shark Fishery zone 50 is shown by the black box. Red arrows indicate reanalysed wind positions and the yellow-circled vector 3 value at 39°S , 140.5°E is used to represent wind stress that directly influences the Bonney Coast. Black full and dashed lines represent the 200- and 1000-m contours, respectively, and the colour bar represents sea surface temperature ($^\circ\text{C}$). _____ 80

Fig. 4.2: Histogram of the natural log of (a) arrow squid CPUE and (b) gummy shark catch. Red lines indicate a normal distribution curve. _____ 82

Fig. 4.3: Interannual and seasonal variability of (a,c) arrow squid and (b,d) gummy shark catch (t) in South East Scalefish and Shark Fishery zone 50. Error bars represent standard errors of means. _ 86

Fig. 4.4: (a) 2003–2008 arrow squid $\ln(\text{CPUE})$ time series (black) with full MI_{squid} linear model with each year parameter value (grey, dashed), full MI_{squid} with mean year parameter value (red), predicted until 2008. (b) 1998–2008 gummy shark $\ln(\text{catch})$ time series (black) with the optimal linear model using the Year factor ($\text{Year} + \text{SST}_{\text{R-9}}$; red), and mean Year fact ($\text{mnYear} + \text{SST}_{\text{R-9}}$; blue), predicted until 2008. (c) 1998–2008 full MI_{shark} linear model (red), predicted until 2008. _____ 89

Fig. 4.5: Time series of (a) arrow squid $\ln(\text{CPUE})$ and environmental variables with incorporated optimal lag periods, including (b) negatively-related $\text{SSH}_{\text{R-5}}$, (c) positively-related $\text{Area}_{\text{UI-2}}$, and (d) negatively-related Nino_{-13} . _____ 93

Fig. 4.6: Time series of (a) gummy shark $\ln(\text{catch})$ and environmental variables with incorporated optimal lag periods, including (b) positively-related Nino_{-31} , (c) negatively-related FRE_{-24} , (d) positively-related DMI_{-1} , and (e) positively-related UI_{-10} . _____ 97

Fig. 5.1: The Bonney Coast off south eastern Australia with schematic coastline. The colour bar represents sea surface temperature ($^\circ\text{C}$), and the upwelling plume is signified by cool ($\sim 15^\circ\text{C}$) water off the coast. Red arrows represent observed wind stress, the continental shelf is represented by the 200 m (black line) and 1000 m (dashed black line) contours. The black box represents the South East Scalefish and Shark Fishery zone 50. _____ 104

Fig. 5.2: Schematic diagram of the data sources and methods used in this study. _____ 106

Fig. 5.3: (a) Chl of the Bonney Upwelling plume ($\text{mg m}^{-3} \text{ km}^{-2}$) as measured from SeaWiFS satellite data (black) and predicted by Eq. 5.1 (blue). (b) Squid catch rate (t hr^{-1}) for the South East Scalefish and Shark Fishery zone 50 as reported by AFMA logbook data (black) and predicted by M5_{squid} (red). _____ 111

Fig. 5.4: Climate model 20th century runs of (a) SST ($^\circ\text{C}$), (b) u -component of wind speed (m s^{-1}), (c) v -component of wind speed (m s^{-1}), and (d) UI (N m^{-2}) plotted against present day observations. Cyan lines represent the ensemble means of the seven different climate models. Model name abbreviations as listed in Table 5.1. _____ 114

Fig. 5.5: Validation of biophysical models forced by 20th century climate models and present-day environmental indices against (a) observed Chl, and (b) observed squid catch rate. Black dots represent individual climate model predictions for the 20th century. _____ 115

Fig. 5.6: Climate model ensemble means for the 20th century (1990–1999; white bar), and 21st century A1B (2090–2099; blue bar), and A2 (2090–2099; red bar) scenarios for (a) SST (°C), and (b) the wind stress-based upwelling index (N m^{-2}). Individual model and scenario predictions for the 20th century (black dot) and projections of the 21st century A1B (blue dot) and A2 (red dot) scenarios are given to show the full range of model predictions. _____ 117

Fig. 5.7: As for Fig. 5.6, but for (a) Chl of the upwelling plume ($\text{mg m}^{-3} \text{ km}^{-2}$) and (b) squid catch rate (t hr^{-1}). _____ 120

INTRODUCTION **I**

1.1 IMPACTS OF CLIMATE CHANGE ON MARINE SYSTEMS

Climate change is having significant and rapid impacts on the physical environment and will likely have unprecedented effects on organisms and ecosystems (Walther et al. 2002). The majority of studies on the impacts of climate change have to date focused on terrestrial systems, with a much smaller number investigating marine systems (Richardson & Poloczanska 2008). However, the majority of the heat energy due to enhanced greenhouse gas emissions is stored in the oceans, especially in the upper 700 m (Murphy et al. 2009). Most marine organisms inhabit this upper layer, suggesting that marine ecosystems could be significantly affected by climate change. As marine fisheries provide up to 16% of global animal protein (FAO 2007) and oceans account for ~63% of global ecosystem services (Costanza et al. 1997), it is imperative to understand the effects that climate change will have on the marine environment.

Increasing atmospheric CO₂ concentration have resulted in changes to atmospheric and oceanic temperature, which will alter atmospheric and ocean interactions and circulation, ocean stratification, storm frequency and intensity, sea level, and ocean chemistry (Harley et al. 2006, IPCC 2007a, Poloczanska et al. 2007) (Fig. 1.1.1). Ecological impacts of climate change have been documented for most taxa, on each continent, and in every ocean (Hoegh-Guldberg 1999, Hughes 2000, Peñuelas & Filella 2001, Walther et al. 2002, Parmesan & Yohe 2003, Badeck et al. 2004, Hoegh-Guldberg 2005, Walther et al. 2005, Parmesan 2006, IPCC 2007b). These include direct and indirect influences on the physiology, abundance, distribution and phenology of species, and impacts on the composition, interaction, structure and dynamics of communities (Walther et al. 2002, Harley et al. 2006, Poloczanska et al. 2007).

In this thesis, I focus on the potential effect of climate change on Australian marine ecosystems. I initially take a large-scale perspective of marine ecosystems to describe the key relationships between physical drivers, primary productivity and fisheries productivity. I then refine the examination by focussing on the most productive upwelling habitat in Australia, the Bonney Upwelling system. I describe present-day characteristics and create quantitative relationships that can be used to predict specific changes to the ecosystem. Finally, I discuss the implications of the potential climate change in relation to adaptive management.

IMPACTS OF CLIMATE CHANGE ON AUSTRALIAN SYSTEMS

Marine fisheries and aquaculture account for ~AUD\$2.2 billion in gross value (ABARE 2008), and are important components of Australian socio-economic wellbeing. Fishing pressure is high, and several commercially-important fish stocks are classified as overfished

or uncertain (Larcombe et al. 2007). Climate change contributes an additional pressure on marine fisheries that may have positive or negative effects.

Australia's marine systems are distinctive due to the poleward-flowing currents that border both the east (the East Australia Current, EAC) and west coasts (the Leeuwin Current) that originate from oligotrophic tropical and subtropical waters. The Leeuwin Current suppresses the large-scale, eastern boundary upwelling that would otherwise occur off the west coast (Hanson et al. 2005a). As a consequence, and because of the aridity of the continent, Australian waters are generally nutrient-poor. These two major poleward ocean currents can advect tropical species into higher latitudes compared to other continents (Maxwell & Cresswell 1981), however the zonal orientation of the southern coastline limits poleward migration for temperate species that are already at their upper thermal limits (Poloczanska et al. 2007). Australian marine flora and fauna have a high degree of endemism (O'Hara & Poore 2000, Phillips 2001) and many species face serious risk to their populations if they cannot find appropriate habitats in the future.

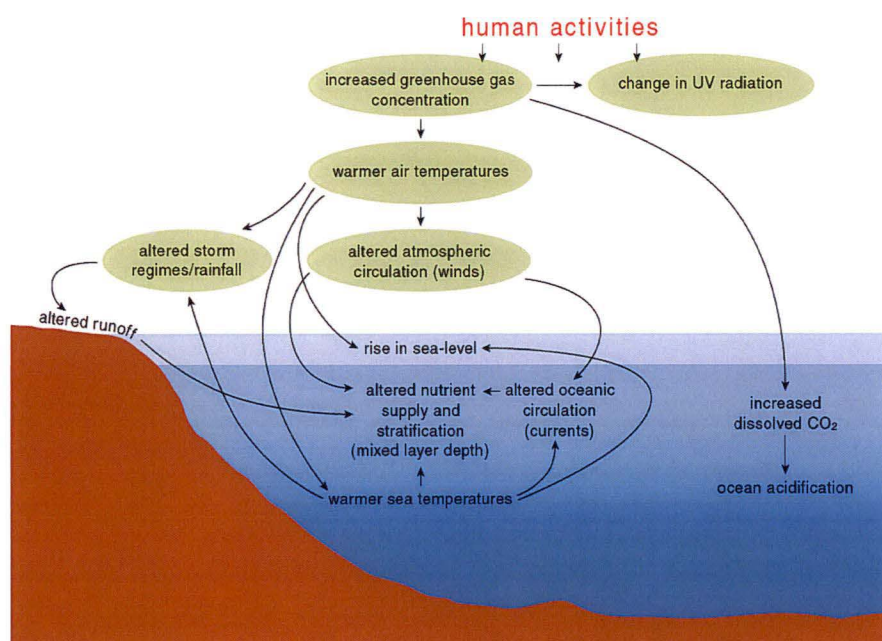


Fig. 1.1.1: Important physical and chemical changes in atmospheric, terrestrial, and oceanographic features due to climate change (from Poloczanska et al. 2007).

Physical changes

Waters around Australia are projected to warm by 0.12°C per decade due to increased solar radiation and changes in circulation (Lough 2008). The greatest warming will be in the south east, resulting from the southward extension of the EAC. This is due to the spin up of the subtropical gyre driven by the southward trend in the subpolar westerly winds (Oke

& England 2004, Cai 2006, Roemmich et al. 2007). On the west coast, the Leeuwin Current is projected to weaken slightly (Feng et al. 2009); however, westward transport along the south coast of the Great Australian Bight is expected to increase (Poloczanska et al. 2007).

Most nutrients around the Australian coastline are brought to the surface by seasonal convective mixing. Annual mean mixed layer depths are expected to decline (Poloczanska et al. 2007); however ocean stratification is projected to increase as the ocean warms (Bopp et al. 2001). Therefore, more mixing energy may be required to replenish nutrients at the surface and productivity is likely to decrease in these regions in the future, possibly having severe effects throughout the food web. Although substantial large-scale, wind-driven upwelling is absent from Australian coastlines, regional upwelling is often associated with seasonal counter-currents (e.g. Flinders Current off South Australia, Ningaloo Current off north west Australia, and the Capes and Cresswell Currents off south west Australia) (Suthers & Waite 2007) that can either enhance or suppress wind-forced upwelling. These upwelling systems are important to regional productivity, but have not yet been closely studied for the effects of climate change.

Ecological changes

Biological responses to these physical changes are far less clear, but may be profound. Predictions of alterations to distribution and abundance of marine species can be made with greater confidence than potential changes in community structure (Hobday et al. 2008). Warming may impose direct physiological stress on plants and animals (Shaw et al. 2002, Pandolfi et al. 2003, Philippart et al. 2003). It may enhance or slow growth rates, depending on the food supply and how close populations are to their thermal optimum and maximum (Munday et al. 2008). Changes in warming, wind forcing and ocean circulation will impact on larval transport and primary and secondary productivity. Increased ultraviolet radiation is projected to have deleterious effects on fish larvae (Häder et al. 2003), affecting the recruitment of key species. Phytoplankton, zooplankton, and fish are expected to shift their distributions southward due to rising ocean temperatures and the southward extension of the EAC (Hobday & Matear 2005, Hallegraeff et al. 2009, Richardson et al. 2009a, Richardson et al. 2009b). Changes in phytoplankton abundance are anticipated due to reduced nutrients with warming and increased ocean stratification (Boyd & Doney 2002), though a recent study using nutrient-phytoplankton-zooplankton (NPZ) models predict an increase in nutrients in Australian waters leading to enhanced productivity (Brown et al. 2009). On the other hand, ocean acidification may cause declines in health and abundance of phyto- and zooplankton species with calcareous shells (Hays et al. 2005). Warming may also lead to an earlier appearance of reproductive or recruitment behaviours of phyto- and zooplankton species. This may decouple temporal coincidence of zooplankton from

phytoplankton, having potentially dramatic impacts for the higher trophic levels such as fish (Edwards & Richardson 2004), and affecting community composition.

Regional vulnerability

Most regions around Australia are thought to have medium to high vulnerability to climate change, with the eastern central and south eastern Australian marine regions indicated as the most vulnerable (Hobday et al. 2006). Both regions are host to ecologically and socio-economically important marine fisheries. The eastern central region has many endemic threatened, endangered, and protected species, and a high chance of change in physical features (e.g. sea surface temperature, sub-surface temperature, and surface winds) (Hughes 2003). The south eastern region, as well as having high likelihood of changes in physical ocean features (e.g. warming due to the extension of the EAC, changes in surface winds), is also subject to heavy commercial fishing, and a variety of other anthropogenic factors (e.g. heavy metals and chemical dumps) that already stress the ecosystem. The south eastern region is an important area as it includes the largest regional and productive upwelling system in Australia, the Bonney Upwelling off South Australia (Butler et al. 2002).

The projected ecological responses to changes in the physical environment are many and complex. Additionally, there is uncertainty surrounding ecological projections due to the seemingly large range of climate and oceanographic predictions and the non-linear or threshold response of ecological systems (e.g. Hughes et al. 1999, Worm et al. 2005). Changes in physical and ecological systems with climate change have the potential to cause catastrophic collapses in communities or shifts to alternate stable states, whereby ecosystem recovery becomes difficult and protracted (Scheffer & Carpenter 2003, Collie et al. 2004). Changes in fish distributions, abundances, and community composition will undoubtedly affect the humans that rely on these resources (Roessig et al. 2004). Therefore there is a great need to investigate the implications of climate change for marine fisheries and ecosystems.

1.2 COASTAL UPWELLING ECOSYSTEMS

Upwelling systems are often characterised by high primary and fish productivity. Coastal upwelling regions are <1% of the global ocean by area but account for >20% of global ocean productivity (Pauly & Christensen 1995). Coastal upwelling is mainly driven by wind forcing, and is thus extremely sensitive to climate change (Bakun 1990, Peterson et al. 1995, Summerhayes et al. 1995). It is believed that alterations in upwelling can have significant effects on ecosystem functions, and profound changes in productivity levels (Snyder et al. 2003). Therefore, it is important to have a good understanding of these systems, the processes that drive them, and how they may change temporally and spatially.

Upwelling occurs everywhere there is surface divergence of water, which must be replaced by subsurface water (Smith 1968, Summerhayes et al. 1995). There are many mechanisms that drive upwelling at a variety of different space and time scales defined by the geographic location and the type of physical forcing (Summerhayes et al. 1995, Roughan & Middleton 2002, Rykaczewski & Checkley 2008). These mechanisms are closely related and often interact to induce coastal upwelling. However, coastal upwelling is generally a wind-driven phenomenon. The classic type of upwelling is forced by alongshore winds that flow parallel to shore and deflect water to the left (right) in the Southern (Northern) Hemisphere due to the Coriolis force. Depending on the orientation of the coastline, surface water can be deflected offshore creating an Ekman divergence of surface waters. This surface water is replaced by water from depth that is often colder and nutrient-rich. As the water is upwelled, nutrients are brought into the euphotic zone where they can be taken up by primary producers such as phytoplankton (Fig. 1.2.1). Alternatively, if surface water is deflected onshore a surface Ekman convergence results in downwelling of surface waters.

Most major upwelling systems are located on the eastern boundary of ocean basins (Pond & Pickard 1983, Mann & Lazier 1996), such as off the west coast of the USA, Peru, and South Africa. This type of upwelling is absent off the west coast of Australia due to the unique poleward-flowing Leeuwin Current, which suppresses otherwise upwelling-favourable conditions (Hanson et al. 2005a). Therefore, wind-driven upwelling in Australia is relegated to smaller, regional systems such as off the Gascoyne region of Western Australia (Hanson et al. 2005a), off south western Western Australian (Suthers & Waite 2007) and off the Bonney Coast of South Australia (Rochford 1977, Lewis 1981).

BIOLOGICAL IMPACTS OF UPWELLING

Coastal upwelling systems are associated with the most productive regions and the largest fish populations in the world (Ryther 1969, Cushing 1971, Bakun 1996). Upwelling systems

generally have high productivity and high biomass, low biodiversity and short trophic links between primary productivity and fish productivity (Ryther 1969, Sommer et al. 2002). Therefore, variability in the abundance of higher trophic levels can be closely related to environmental fluctuations (Cole & McGlade 1998).

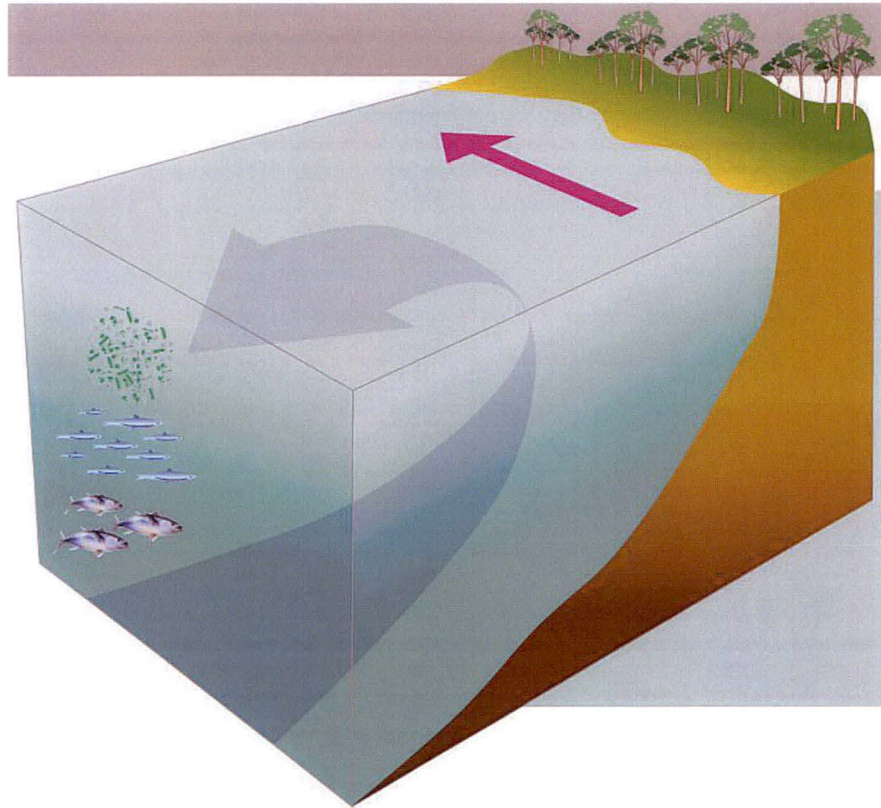


Fig. 1.2.1: Ekman transport and coastal upwelling in the southern hemisphere. Equatorward, alongshore winds drive surface waters to the left due to the Coriolis force. Water from depth is then vertically upwelled to replace surface waters.

Whether an upwelling wind event leads to enhanced productivity depends on the timing, persistence, direction, strength and quiescence of the wind. For significant biological activity, the timing of winds needs to correspond to a shallow mixed layer to introduce new nutrients (Rutllant & Montecino 2002), high light levels (Kudela & Dugdale 2000, Pennington et al. 2006), and relatively warm water temperature (Pierce 2004). Each of these environmental factors increases phytoplankton growth (Brown & Field 1986, Brink et al. 1995) and varies seasonally (Mann 2000). Upwelling-favourable winds should be persistent to penetrate the mixed layer (Pickett & Schwing 2006), but periods of quiescence are also necessary for phytoplankton to take up new nutrients in calm, stable conditions (Lasker 1975, 1978).

Upwelling regions can be challenging habitats for fish reproduction. Previous studies of numerous upwelling systems have described a parabolic relationship between wind and productivity in wind-driven upwelling ecosystems (Cury & Roy 1989, Botsford et al. 2003, 2006). An “optimal environmental window” of wind speeds has been defined, where winds are strong enough to promote vertical mixing, but not so strong as to cause vigorous turbulent mixing or advection from the system (Fig. 1.2.2; Cury & Roy 1989). Low upwelling winds do not enhance productivity. Low turbulence does not encourage encounter rates between larvae and prey for successful larval feeding. In contrast, excessively high levels of upwelling lead to offshore advection of eggs and larvae. In addition, high levels of turbulent mixing suppress productivity, which needs periods of calm to develop blooms (Lasker 1975, 1978). Therefore, an intermediate level of upwelling activity encourages an optimal trade-off between physical forcing and productivity (Fig. 1.2.2, Cole & McGlade 1998). This theory was successfully investigated for small pelagic fish populations in California, Peru, Chile, the Iberian Peninsula, and north west Africa where it was found that population productivity was maximised at moderate levels of turbulence and Ekman transport (Cury & Roy 1989, Roy et al. 1995, Serra et al. 1998). These studies suggest that the general wind speed for fish recruitment is $\sim 5\text{--}6\text{ m s}^{-1}$; however a recent study indicates that the optimal wind speed varies depending on shelf width and latitude (Botsford et al. 2006).

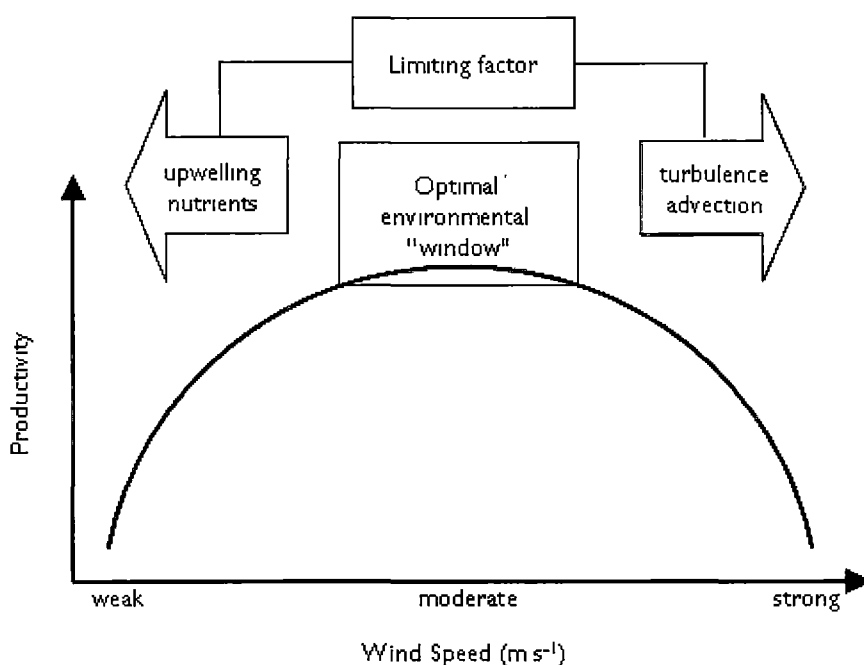


Fig. 1.2.2: The optimal environmental window (adapted from Cury & Roy 1989).

Fish tend to have distinct spawning, transport, and nursery habitats that select for key oceanographic characteristics beneficial for recruitment success. Through a series of comparative oceanographic studies of fish spawning habitat (Parrish et al. 1983, Bakun & Parrish 1990, 1991, Bakun 1996, 1998, Durand et al. 1998), an integrated conceptual framework emerged of how the environment can impact fish recruitment success. This “ocean triad” concept described fundamental oceanographic mechanisms that influence recruitment: enrichment, which supplies nutrients and thus enhances primary production; concentration, which aggregates primary producers and larvae; and retention, which retains or transports fish eggs and larvae within or towards suitable nursery habitat (Bakun 1996). In a coastal upwelling habitat, enrichment is via upwelling of nutrient-rich water from below the pycnocline; concentration is via a stable water column or formation of convergence zones that concentrate food particles; and retention is via reduced offshore transport or advection of other waters into the system (Cole & McGlade 1998). This theory is most commonly applied to small pelagic fish in coastal habitats; however it is equally applicable to other types of fish and invertebrates, the majority of which have pelagic larval stages (Bakun 1996, Agostini & Bakun 2002).

POTENTIAL CLIMATE CHANGE IMPACTS ON UPWELLING ECOSYSTEMS

As most types of upwelling are forced by wind-driven processes, upwelling systems are sensitive to climatic change (Peterson et al. 1995) and through feedbacks in biogeochemical cycles, upwelling systems may also influence climate (Peterson et al. 1995, Bakun & Weeks 2004). One can infer the sensitivity of wind-driven upwelling by analysing differences in wind stress in different climate regimes (or differing levels of CO₂) (Snyder et al. 2003). However, one should note that analysing upwelling only via atmospheric factors (i.e. wind), provides an incomplete picture of actual oceanographic responses to changing climate patterns. For example, although upwelling-favourable winds or currents may intensify due to climate change, stronger thermal stratification and a deeper thermocline may inhibit the upwelling of cool, nutrient-rich water to the surface (Roemmich & McGowan 1995). Therefore, predictions of ecosystem response to climate change may improve if oceanic and atmospheric responses are coupled and regional bathymetry is included (Snyder et al. 2003).

With climate change, upwelling intensity is predicted to increase (Bakun 1990, Bakun et al. 2009), with changes already observed over the last 30 years in some regions (Snyder et al. 2003). Upwelling off the coast of Namibia has intensified to the point where the resultant productivity appears to be unused, and is rapidly transported offshore where it sinks, builds up on the ocean floor and eventually results in massive eruptions of noxious gas (Bakun & Weeks 2004). In California, delays in peak upwelling events have led to

unprecedented low recruitment of marine species (Barth et al. 2007) as species are reliant on seasonal temperature cues and ocean productivity for their reproductive cycle.

Coastal wind-driven upwelling around Australia coincides with regions that are ranked as highly vulnerable under climate change due to rapid warming and changing circulation patterns (Hobday et al. 2006). These regions are already heavily exploited through fishing. Further effects of climate change may push these critical upwelling ecosystems into alternate and degraded states from which recovery may be difficult. A closer inspection of the potential impacts of climate change on upwelling systems may help inform how best to manage these ecosystems.

This thesis assesses climate change impacts on a regional upwelling ecosystem off south eastern Australia: the Bonney Upwelling. The remainder of this thesis is divided into 5 chapters. Chapter 2 is a large-scale approach that investigates the drivers of fisheries productivity, and is comprised of two independent subchapters. Chapter 2.1 examines the linkages between primary productivity and fisheries productivity to assess the type of trophic control that dominates Australian marine bioregions over long temporal and large spatial scales. Chapter 2.2 examines broad-scale physical forcing in regions of high primary productivity and qualitatively relates these physical characteristics to previous accounts of fish spawning and recruitment behaviour. The remaining chapters concentrate on a region of high primary productivity, the Bonney Upwelling. In Chapter 3, I describe the seasonal, interannual, and intra-annual variability of the upwelling and assess how it affects phytoplankton biomass in the region. I develop statistical models of upwelling drivers to predict phytoplankton biomass at annual to decadal scales. In Chapter 4, I examine the relationships between physical features within the Bonney Upwelling region and two contrasting, commercially-important marine animal species – arrow squid (*Nototodarus gouldi*) and gummy shark (*Mustelus antarcticus*). I develop statistical models that describe physics-to-biology relationships and can be used for prediction. In Chapter 5, I use the statistical models developed in the previous two chapters and force them with climate models to generate projections of how the upwelling ecosystem might change in response to climate change. I examine changes in physical drivers of the upwelling and investigate how this may affect both primary and fisheries productivity of the Bonney Upwelling. Large portions of this thesis have been prepared for publication as papers in journals, and are presented here in that format. Therefore, repetition in the Introduction and Methods sections of each chapter is unavoidable. In Chapter 6, I discuss the links between the chapters and provide continuity for the thesis, as well as present the general findings.

LARGE-SCALE RELATIONSHIPS

2

2.1 LARGE-SCALE RELATIONSHIPS BETWEEN PRIMARY AND FISHERIES PRODUCTIVITY

Ecosystem Trophic Control Assessed across a Suite of Australian Marine Habitats

Anne-Elise Nieblas^{a,b,*}, Bernadette M. Sloyan^{c,d}, Alan J. Butler^c and Anthony J. Richardson^{e,f}

^a University of Tasmania, School of Zoology, Sandy Bay, Tasmania, Australia.

^b Commonwealth Scientific and Industrial Research Organisation (CSIRO) Climate Adaptation Flagship National Research Flagship, CSIRO Marine and Atmospheric Research, Hobart, Tasmania, Australia.

^c CSIRO Wealth from Oceans National Research Flagship, CSIRO Marine and Atmospheric Research, Hobart, Tasmania, Australia.

^d Centre for Australian Weather and Climate Research, CSIRO Marine and Atmospheric Research, Hobart, Tasmania, Australia

^e CSIRO Climate Adaptation National Research Flagship, CSIRO Marine and Atmospheric Research, Cleveland, Queensland, Australia.

^f School of Mathematics and Physics, University of Queensland, St Lucia, Queensland, Australia.

*Corresponding author: Anne.Nieblas@csiro.au

ACKNOWLEDGEMENTS

A.E.N. is supported by a joint Commonwealth Scientific and Industrial Research Organisation (CSIRO)–University of Tasmania Ph.D. scholarship in Quantitative Marine Science (QMS) and a CSIRO Climate Adaptations National Research Flagship Ph.D. stipend. B.M.S. was funded by CSIRO Wealth from Oceans Flagship and the Australian Climate Change Science Program. I thank the National Aeronautics and Space Administration for Sea-viewing Wide Field-of-view Sensor ocean colour data. Satellite data were accessed using the Spatial Dynamics Ocean Data Explorer – customised software provided by Alistair Hobday, Klaas Hartmann, Jason Hartog, and Sophie Bestley. I thank the Australian Fisheries Management Authority (AFMA) for fish catch data and Mike Fuller for his help with AFMA data manipulation.

INTRODUCTION

Ecologists frequently seek to investigate the primary control of marine biomass production: bottom up (resource-driven) or top-down (predator-driven) dynamics. Previous studies have shown that top-down control is important for many lakes and a few marine systems, where top predators can cause trophic cascades throughout the ecosystem (Pace et al. 1999, Frank et al. 2005, Daskalov et al. 2007). Trophic cascades arise from predator-prey interactions that modify the abundance, biomass or productivity across more than one trophic level in a food web (Pace et al. 1999). However, other studies argue that resource levels at the base of the food web (e.g. primary productivity) act as the 'carrying-capacity' for the ecosystem (Richardson & Schoeman 2004, Ware & Thomson 2005, Chassot et al. 2007), with effects that propagate through the food web to impact all trophic levels (Hunter & Price 1992, Frederiksen et al. 2006). Additionally, 'wasp-waist' dynamics, which are often found in upwelling ecosystems, may control systems with one or a few abundant mid-trophic level species that influence the food web both upwards to higher trophic levels and downwards on lower levels (Bakun 1996, Cury et al. 2000, Bakun 2006).

The strength of the bottom-up relationships between primary and fish productivity may vary in space and time (Hunter & Price 1992, Frank et al. 2006, Chassot et al. 2007). The relative strength of trophic controls can alter in different habitats or across trophic levels, and can be influenced by biotic (e.g. competition) and abiotic (e.g. climate, nutrients) factors that impact consumer efficiency (Hunter & Price 1992, Cury et al. 2003, Dyer & Letourneau 2003, Chassot et al. 2007). An understanding of trophic control is important when considering potential impacts of natural variability or anthropogenic change on marine ecosystems. For example, depending on whether a system has top-down or bottom-up control, different perturbations such as overfishing (e.g. Frank et al. 2005) or climate change (e.g. Brown et al. 2009), can have significant effects on fish productivity and the structure and function of marine ecosystems.

Trophic control can be assessed by examining the relationship between primary productivity and fish productivity. If the relationship is positive or weak, bottom-up control is suspected, and if it is negative, top-down control is deduced (Frank et al. 2006). The ability to assess trophic control over large spatial scales in marine systems has improved with the advent of satellite-based observations. Several studies have correlated satellite-based estimates of chlorophyll *a* concentration to fish productivity in northern hemisphere temperate marine ecosystems (Ware & Thomson 2005, Frank et al. 2006, Chassot et al. 2007). They used a variety of methods that found bottom-up trophic linkages between chlorophyll *a* concentrations and fish catch. Chassot et al. (2007) found this relationship to be consistent through time in European seas, but Frank et al. (2006) highlight temporal and

spatial variability in the balance between top-down and bottom-up control in the western North Atlantic.

Here, I investigate large-scale relationships between primary productivity and fish to develop an understanding of the type of trophic control regulating Australian fisheries over a suite of marine food webs. Australia's marine system is distinctive due to oligotrophic poleward currents that border both the east and west coasts (the East Australia Current (EAC) and the Leeuwin Current, respectively). The Leeuwin Current suppresses large-scale, eastern boundary upwelling that would otherwise occur off the west coast (Hanson et al. 2005a). As a consequence of this and the aridity of the land-mass, Australian waters are generally oligotrophic. Australian marine ecosystems range from tropical to polar food webs, and the relationship between primary productivity and fish catch is generally asserted rather than demonstrated (e.g. Harris et al. 1992, Ward et al. 2001). I characterise Australian bioregions based on their resource carrying-capacity (satellite-derived estimates of chlorophyll *a* concentration (Chl) as a proxy for phytoplankton biomass) and an index of fish biomass (catch per unit effort (CPUE)). I use spatial comparisons of Chl and CPUE to investigate the dominant trophic control. To better resolve the association between Chl and CPUE, I have considered different habitat types, trophic levels of fish, and whether the relationship between Chl and CPUE is persistent in space and time. This study is designed to provide valuable insight into how fisheries may change under different productivity scenarios as climate changes.

DATA

Australian bioregions

The geographical scope of this study includes the Exclusive Economic Zone of the Australian continent, excluding the distant offshore fishing zones of Christmas/Cocos (Keeling) Island, Macquarie Island, Heard and MacDonald Islands, the Australian Antarctic Territory, and Norfolk Island. Australian marine bioregions based on oceanography and biogeography have been defined by the Integrated Marine and Coastal Regionalisation of Australia Version 4.0 (Commonwealth of Australia 2006) (Fig. 2.1.1). Bioregions on the shelf are distinct from those on the slope and beyond. However, the shelf bioregions as defined were too fine for the spatial scale of fish data available for this study. Therefore, I modified the 41 provincial bioregions by combining on-shelf and offshelf bioregions based on similar surface water types as defined by the Integrated Marine and Coastal Regionalisation of Australia Version 4.0, giving 19 bioregions (Fig. 2.1.1).

Chlorophyll data

Chl from Sea-viewing Wide Field-of-view Sensor ocean colour images were used as an estimate of primary productivity. Chl data were 8-day composites with a spatial resolution

of 0.0833° latitude by 0.0833° longitude. These data were mapped onto the 0.25° Australian Fisheries Management Authority grid. Interannual and overall mean chlorophyll *a* concentrations were calculated for each bioregion from January 1998 to December 2007 (units: mg m^{-3}).

Satellite colour data are used extensively as a proxy for phytoplankton biomass, though it has limitations (Sathyendranath et al. 1991, Alvain et al. 2008). Chl estimates around Australia and New Zealand have known calibration errors (Clementson et al. 2001, Hendiarti et al. 2004, Richardson et al. 2004). The largest errors are in shallow, turbid, coastal (Case 2) waters where suspended particles or dissolved organic matter introduce a significant, but unquantified contribution to the ocean colour signal (Condie & Dunn 2006). Therefore, absolute Chl values may be unreliable and overestimated in some bioregions. However, Chl patterns are likely to be indicative of surface concentrations at the large temporal and spatial scale of this analysis (Fig. 2.1.1; McClain et al. 2004; Condie and Dunn 2006).

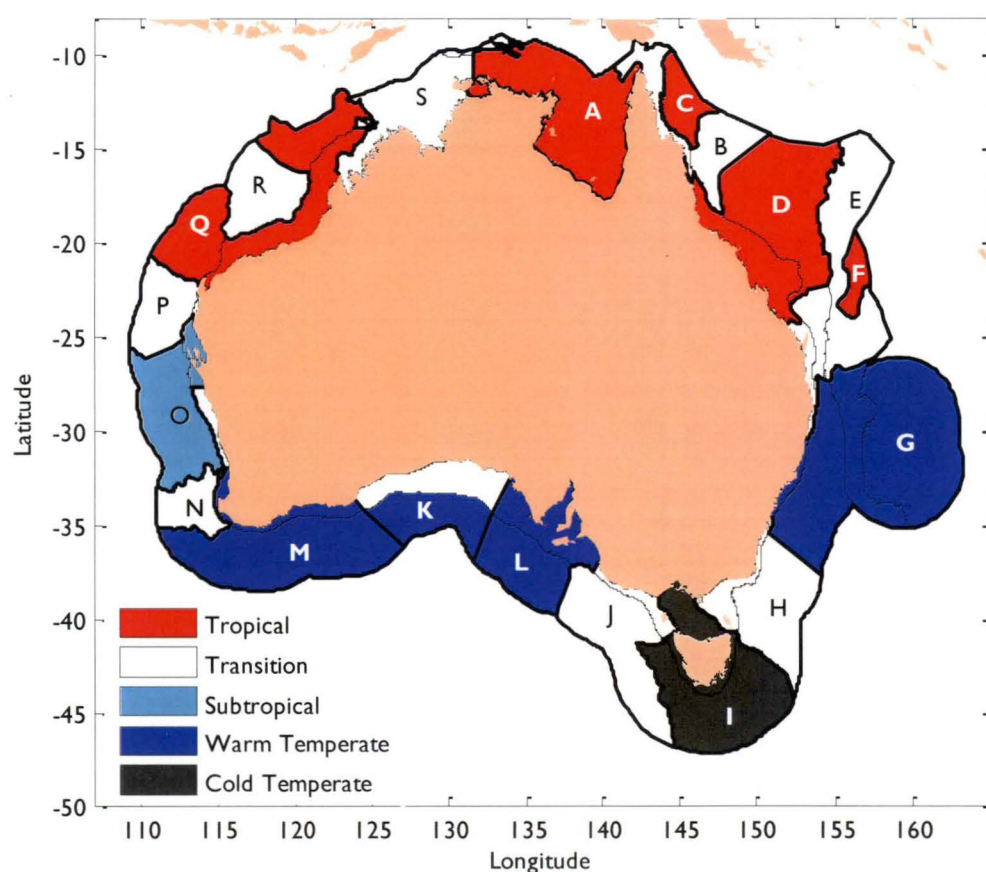


Fig. 2.1.1: Combined inshore and offshore bioregions used in this study (bold black lines) derived from bioregions defined in the Integrated Marine and Coastal Regionalisation of Australia Version 4.0. Also shown are divisions between inshore and offshore (light black lines) of the original 41 bioregions.

Fisheries data

Fisheries data were obtained from the Australian Fisheries Management Authority logbook data, and were binned into 0.25° latitude by 0.25° longitude grid. Catch records were examined from January 1998 to December 2007 to match the time span of Chl data. The Australian Fisheries Management Authority dataset contains 7.5 million catch records for 610 species. Catch values were reported in tonnes (t) of total fish caught, excluding discards. Zero values were ignored as they are not accurate assessments of zero catch in this dataset, due to variable reporting methods across different fisheries (e.g. Salthaug and Godø 2000). The number of shots was the only consistent measure of effort across the dataset. “Shot” here is defined as the number of logbook entries per day for all fisheries and included multiple gear types (e.g. purse seine, trawl, long-line; Table 2.1.2). A nominal catch per unit effort (CPUE) was calculated as monthly catch divided by the number of shots for that month (units: t shot⁻¹) (e.g. Cushing 1992, Tuck 2006).

Table 2.1.1: Correlation coefficients (r) for the linear regression between Chl and CPUE for each functional group based on trophic level with 3.75 as a threshold, and habitat preference, indicating the strength and direction of the relationship. Significant r values are in bold with significance levels indicated as *p*<0.1*, *p*<0.05**, *p*<0.001***, *p*<0.0001****.

Functional Group	No. of Species	r
Total Fish	610	0.43 *
< 3.75	292	0.58**
≥ 3.75	310	0.07
Benthic	437	0.77****
Pelagic & Benthopelagic	154	0.12
< 3.75xBenthic	245	0.75****
< 3.75xPelagic & Benthopelagic	43	-0.02
≥ 3.75xBenthic	190	0.61**
≥ 3.75xPelagic & Benthopelagic	111	0.08

To identify biological processes that might drive trophic interactions, functional groups based on trophic level and habitat preference from FishBase (www.fishbase.org) for fish species and CephBase (www.cephbase.org) for cephalopods were assigned to CPUE data where possible (Table 2.1.1). Trophic level information for the remaining invertebrates was taken from an Australian marine ecosystem model (Metcalf 2009). Following Christensen et al. (2003), a trophic level <3.75 separated planktivorous fish species from higher order predators. Habitats were defined as benthic (demersal, reef, bathydemersal), or pelagic (pelagic, bathypelagic, benthopelagic). Interannual and overall mean CPUE were calculated for each region with >50 total logbook observations. To account for changes in fish catchability through time, linear trends were removed from annual means of CPUE by

taking residuals, although this could potentially also remove some interannual variation in fish abundance.

There are several caveats associated with the use of fish catch data as an index of abundance. First, fish catch is generally standardised by effort using sophisticated statistical techniques to create an unbiased relative abundance index that accounts for biases such as effort creep and variations in catchability. However, these techniques are challenging, as many factors affect catch rate that cannot be fully taken into account using methods of standardisation (Maunder & Punt 2004, Bishop et al. 2008). The large scale of this study, inclusive of 610 diverse species over most Australian Commonwealth fisheries (e.g. Table 2.1.2), prevents a fishery-specific calculation of effort. In this study, I characterise catch rates by dividing fish catch by number of shots. A shot as defined here does not delineate between different gear types. Gear types represent different units of effort, and may influence the spatial distribution of catch rates. However, this simple index of catch rate and the removal of trends substantially reduces the biases in the dataset and is suitable for the large-scale analysis presented here. Second, logbook data have their own weaknesses in terms of the handling of discards, and the general difficulty of data collection and data quality control (Chassot et al. 2007). The Australian Fisheries Management Authority logbook program has been in existence for >40 years, with high coverage and sufficient consistency in the reporting by Commonwealth fisheries operating in Australian waters in the recent period (Rohan 1999). Finally, the findings in this study are only applicable to the region beyond the coastal zone. There are two reasons for this: the satellite imagery used in this study is not accurate in very nearshore zones; and Australian state fisheries observations (mostly <3 nautical miles from the coast) are not included in the Australian Fisheries Management Authority database.

Analysis

I first characterised the productivity and fisheries yield of Australian marine bioregions using overall mean values of Chl and CPUE for the period 1998–2007. I then investigated spatial trophic linkages in Australian marine ecosystems by relating the overall mean of Chl and CPUE using linear regression as an indicator of the strength of the association. Strong and weak positive associations indicated bottom-up dynamics, and strong negative associations indicated top-down dynamics (Worm & Myers 2003, Frank et al. 2006). A visual inspection of residuals indicated that a log-log transform was appropriate for these regressions. Finally, linear trends were removed from annual means of CPUE and residuals were correlated with Chl to investigate whether trophic linkages were variable in space and time. Chl was lagged behind CPUE by 0 to 2 years to account for the influence of primary productivity on spawning or larval success and subsequent recruitment to fisheries. Though many of the

LARGE SCALE RELATIONSHIPS

species included in this study recruit to the fishery at 4-8 years, longer lag periods were not possible due to the relatively short temporal period of the Chl dataset.

Table 2.1.2: The habitat, dominant gear type, trophic level and percent biomass of the 20 most abundant fish and invertebrate species based on catch (t). Percent biomass is calculated as the catch (t) of the specific species divided by the total catch (t) from all Australian Commonwealth fisheries.

Common name	Species name	Habitat	Gear type	Trophic level	Percent biomass
Blue grenadier	<i>Macrurus novaezelandiae</i>	B	drop line	4.47	10.20%
Southern bluefin tuna	<i>Thunnus maccoyii</i>	P	purse seine	3.93	8.60%
Orange roughy	<i>Hoplostethus atlanticus</i>	P	trawl	4.3	7.00%
Redbait	<i>Emmelichthys spp</i>	P	trawl	3.62	6.40%
Flathead	<i>Neoplatycephalus richardsoni</i>	B	trawl	3.87	4.70%
Spotted warehou	<i>Seriola punctata</i>	P	trawl	3.4	4.70%
Broad billed swordfish	<i>Xiphias gladius</i>	P	trawl	4.49	4.40%
Jack mackerel	<i>Trachurus declivis</i>	P	trawl	3.93	3.80%
Yellowfin tuna	<i>Thunnus albacares</i>	P	rod and reel	4.34	3.70%
Skipjack tuna	<i>Katsuwonus pelamis</i>	P	purse seine	4.35	2.90%
Gummy shark	<i>Mustelus antarcticus</i>	B	gillnet	4.31	2.80%
Arrow squid	<i>Nototodarus gouldi</i>	P	trawl, jig	3.76	2.50%
Ling	<i>Genypterus blacodes</i>	B	trawl	4.34	2.30%
Deepwater flathead	<i>Neoplatycephalus conatus</i>	B	trawl	4.2	2.10%
Penaeid prawns	<i>Fenneropenaeus indicus</i> & <i>Fenneropenaeus merguensis</i>	B	trawl	2.35	2.00%
Bigeye tuna	<i>Thunnus obesus</i>	P	longline	4.49	1.70%
Albacore	<i>Thunnus alalunga</i>	P	longline	4.31	1.50%
Jackass morwong	<i>Nemadactylus macropterus</i>	B	trawl	3.41	1.40%
Alfonsino	<i>Beryx splendens</i>	P	trawl	4.38	1.40%
Tiger prawns	<i>Penaeus esculentus</i> , <i>Penaeus semisulcatus</i> & <i>Penaeus monodon</i>	B	trawl	2.35	1.30%

RESULTS

Characterisation of Australian marine bioregions

There was high spatial variability of phytoplankton biomass in Australian waters (Fig. 2.1.2a). There appears to be a consistent overall pattern of high overall mean Chl in the north (Bioregions A, S) of up to 1.15 mg m⁻³ (Fig. 2.1.2a), and another peak in primary productivity in the south east (0.4–0.6 mg m⁻³) (Bioregions H–K; Fig. 2.1.2a). Bioregions

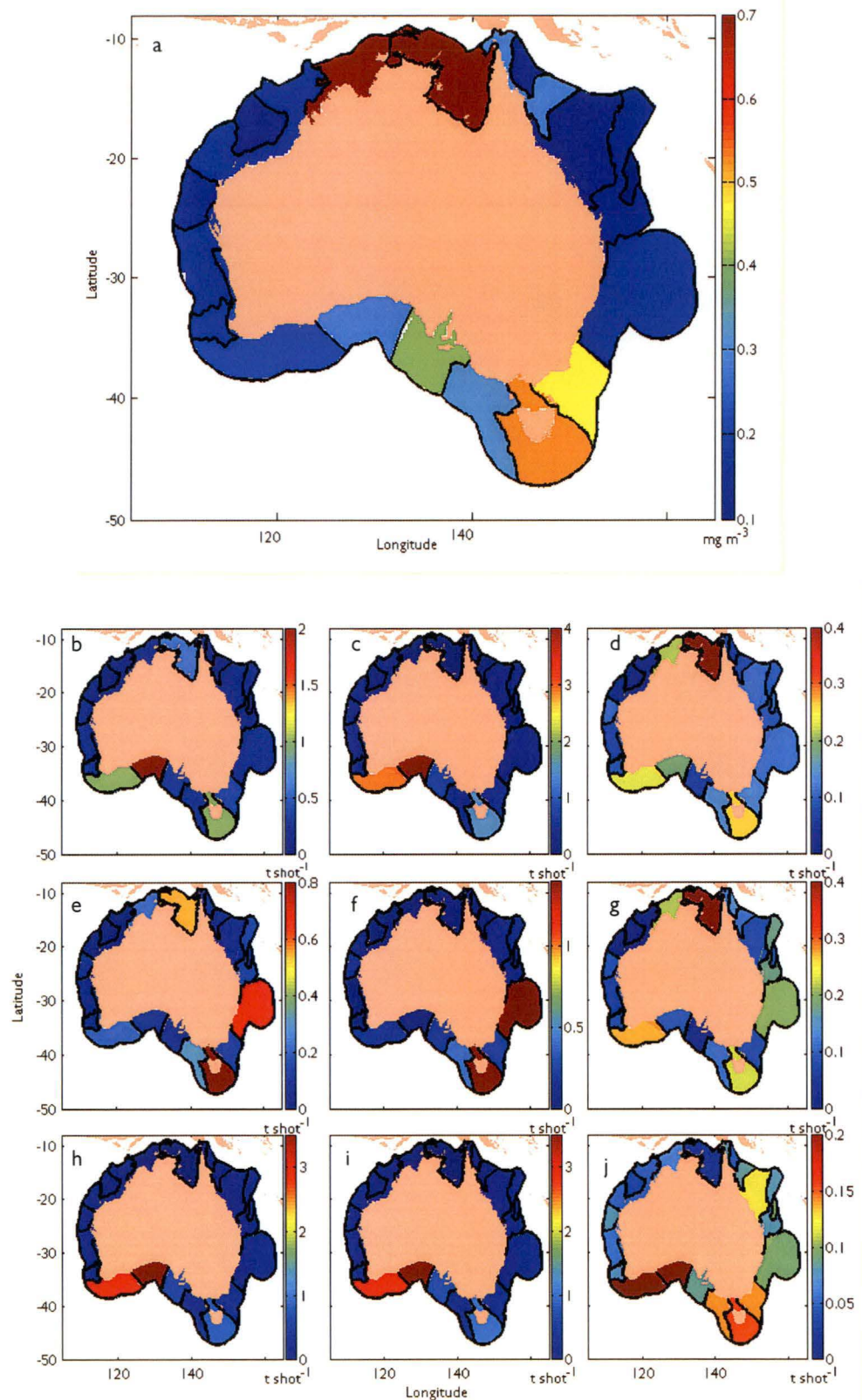


Fig. 2.1.2: Spatial distribution for Australian bioregions of (a) Chl (mg m^{-3}), and CPUE (t shot^{-1}) for (b) total fish species, (c) pelagic fish, (d) benthic fish, (e) lower trophic level fish (f) lower trophic level pelagic fish, (g) lower trophic level benthic fish, (h) higher trophic level fish, (i) higher trophic level pelagic fish, and (j) higher trophic level benthic fish. See bioregion labels in Fig. 2.1.1 and definition of each functional group in Table 2.1.1.

with lowest levels of Chl were the east and west tropical bioregions, especially in the Coral Sea and the Great Barrier Reef (Bioregions D–F, Fig. 2.1.2a).

Total CPUE indicates that most fish are caught in the north and south of Australia (Fig. 2.1.2), broadly consistent with bioregions of high primary productivity in the north and south east. Bioregions of lowest CPUE are in the Coral Sea and waters of the Great Barrier Reef (Bioregions B–F, Fig. 2.1.2), and tropical and subtropical waters off the west coast of Australia (Bioregions N–R, Fig. 2.1.2). CPUE for Australian marine fisheries is dominated by pelagic fisheries CPUE (Fig. 2.1.2c), which are up to an order of magnitude more than benthic CPUE (Fig. 2.1.2d). Pelagic fisheries have their highest CPUE in southern Western Australia and the Great Australian Bight (Bioregions M and L, Fig. 2.1.2c, i) where southern bluefin tuna are caught. Lower trophic level pelagic CPUE dominates the Lord Hol Rise (Bioregion G) and south eastern Tasmania (Bioregion I; Fig. 2.1.2f), where the small pelagic fishery operates. Benthic CPUE is more evenly distributed around the Australian bioregions (Fig. 2.1.2d). However, benthic fish yield is highest in the Gulf of Carpentaria (Bioregion A; Fig. 2.1.2d, g), with catch being dominated by penaeid prawns. Bioregions of low productivity in the north east (Bioregions D–F) and north west to south west (Bioregions N–R) have correspondingly low catch rates (Fig. 2.1.2). Chl and CPUE have generally consistent spatial patterns with high primary and fish productivity in the north and south east, except for Bioregions M and L where CPUE is high and Chl is relatively low. However, although northern bioregions have the most primary productivity, highest overall fisheries yields are more generally derived from south and south eastern waters.

Trophic linkages

Spatial variability of Chl and CPUE

Strong positive relationships were found between overall mean Chl and CPUE (Fig. 2.1.3), suggesting a bottom-up trophic link exists between Chl and CPUE in the Australian marine environment. However, this relationship is not consistent across functional groups with regards to trophic level or habitat usage of species caught (Fig. 2.1.3, Table 2.1.1). While a marginally non-significant association between Chl and CPUE was found for total species ($r=0.43$, $p=0.06$, $n=19$; Fig. 2.1.3a), a marginally significant positive relationship was found for all lower trophic level species ($r=0.58$, $p=0.04$, $n=13$; Fig. 2.1.3b). Benthic species had a significant, strong positive relationship to Chl ($r=0.77$, $p<0.001$, $n=15$; Fig. 2.1.3c). This strong association was consistent for both the lower and higher trophic levels of benthic species ($r=0.75$, $p=0.005$, $n=12$, and $r=0.61$, $p=0.03$, $n=12$, respectively; Fig. 2.1.3d, e), though slightly less strong for the higher trophic level benthic species. No significant relationships were found between Chl and pelagic CPUE of either lower or higher trophic levels (Fig. 2.1.3d–f). Leverage effects were marginal for relationships between Chl and CPUE with significant correlations. Overall, these results suggest that in the Australian

LARGE SCALE RELATIONSHIPS

marine environment bottom-up control operates between regional productivity and the CPUE of particularly benthic fish for which Chl explains over 60% of the variability as measured by the coefficient of determination.

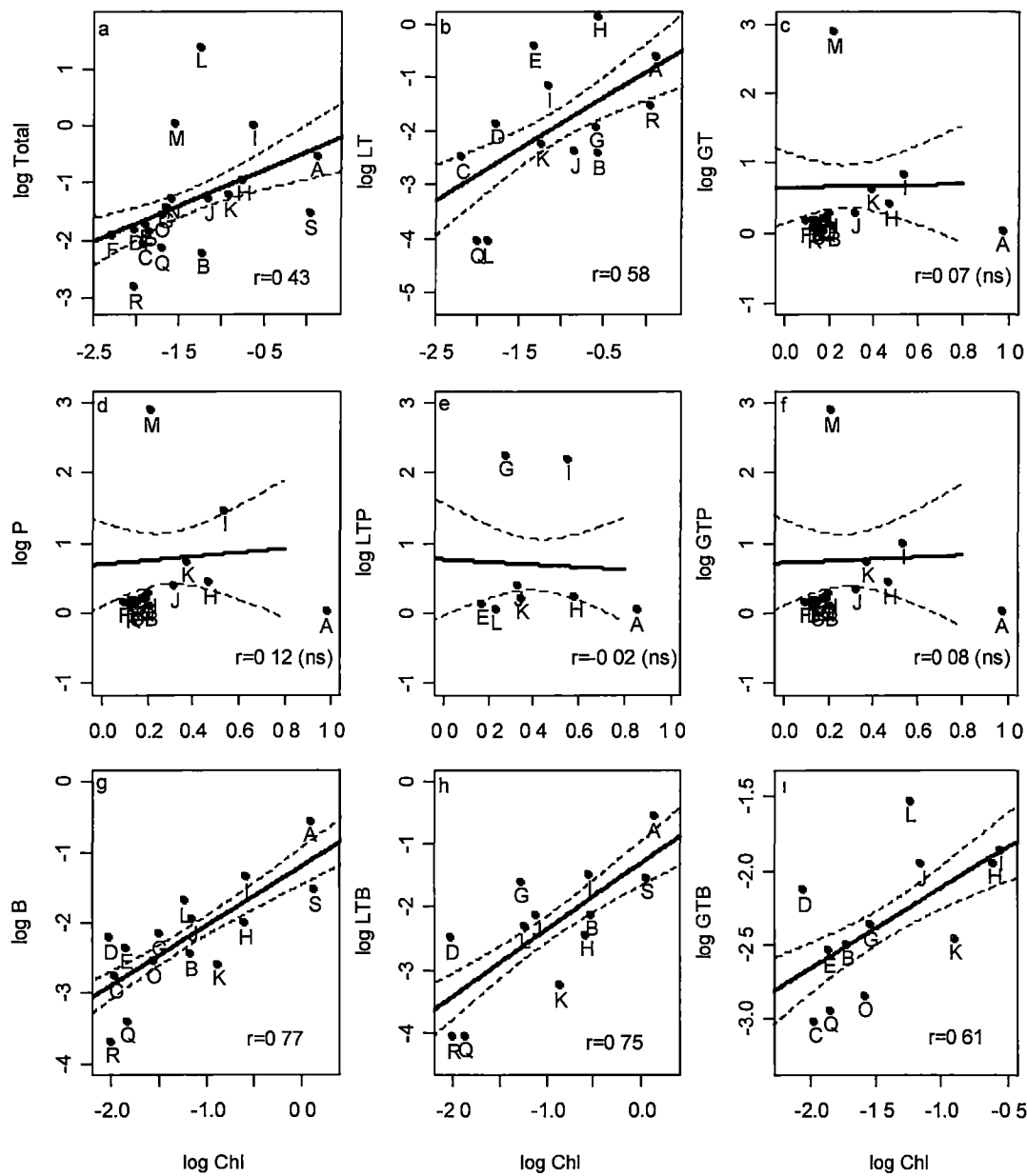


Fig. 2.1.3: Correlations of overall mean log Chl versus overall mean log CPUE ($t \text{ shot}^{-1}$) for (a) Total species combined, (b) lower trophic level species (LT), (c) higher trophic level species (GT), (d) pelagic and benthopelagic species (P), (e) lower trophic level pelagic and benthopelagic species (LTP), (f) higher trophic level pelagic and benthopelagic species (GTP), (g) benthic species (B), (h) lower trophic level benthic species (LTB), and (i) higher trophic level benthic species (GTB). Dashed lines represent ± 1 standard error; "ns" represents "not significant". Data labels represent bioregions as in Fig. 2.1.1.

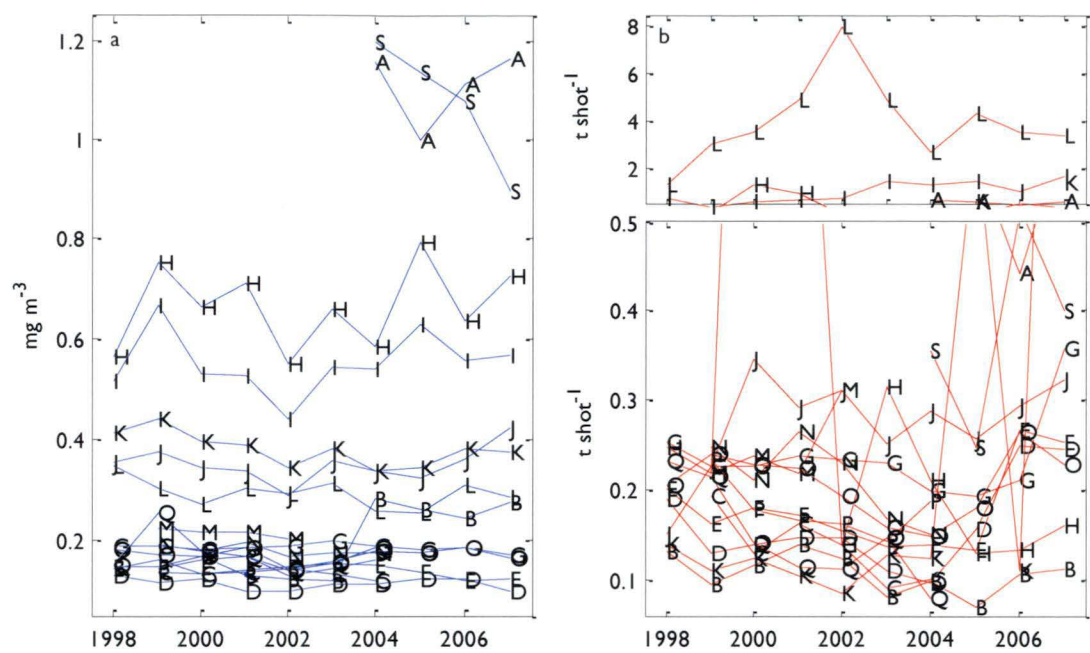


Fig. 2.1.4: Interannual variability of (a) the Chl (mg m^{-3}) for bioregions A–S (see Fig. 2.1.1) with >50 shots per year and (b) all fish species CPUE with a split panel for enhanced readability.

Temporal and Regional Variability

Chl interannual variability is greatest for Tasmania, the EAC extension, the Gulf of Carpentaria, and the Northwest Shelf (Bioregions I, H, A, and S, respectively) (Fig. 2.1.4a). The highest interannual variability of CPUE is found in the Great Australian Bight, Tasmania, the EAC extension, the Northwest Shelf, and the Gulf of Carpentaria (Bioregions L, I, H, S, A, respectively) (Fig. 2.1.4b). The majority of bioregions with the highest Chl variability also have high variability in CPUE. The Great Australian Bight (Bioregion L) is an exception as it has high CPUE variability due to the southern bluefin tuna fishery (Fig. 2.1.4b), but it does not have high Chl variability. Benthic fish species show smaller interannual variability for all bioregions (not shown). Although there is some interannual variability for Chl (Fig. 2.1.4a), it is apparent that the spatial variability among bioregions is greater than the interannual variability within each bioregion (Fig. 2.1.2, 2.1.4a). In contrast, CPUE shows high variability spatially, temporally (Fig. 2.1.2, 2.1.4b) and amongst functional groups (not shown).

There were no consistent relationships for the interannual correlations within each bioregion between spatially matched annual Chl and CPUE residuals for any functional group for 0, 1, and 2 year time lags (e.g. Fig. 2.1.5). These results indicate that the interannual variability of Chl does not account for the interannual variability of CPUE for any of the functional groups at the spatial scales examined here.

DISCUSSION

This study is the first large-scale analysis of phytoplankton biomass and fish productivity for the Australian marine ecosystem. I find several significant associations of estimated phytoplankton biomass and fish productivity amongst different functional groups in the diverse bioregions of the Australian Exclusive Economic Zone. This indicates that many Australian marine fisheries

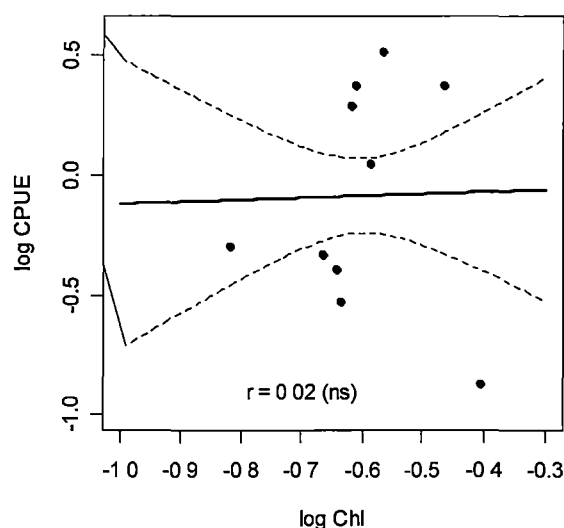


Fig. 2.1.5: The log of CPUE for all species as a function of the log of Chl for the Tasmanian bioregion (I) with no time lag; “ns” represents “not significant”.

are regulated by bottom-up control at large spatial scales (6.1×10^4 – 9.3×10^5 km²). There was no evidence for top-down control of phytoplankton productivity at the spatial or temporal scale of this study. Fisheries production in Australian seas thus appears to be controlled by resource levels or primary productivity of the underlying marine ecosystem, similar to northern hemisphere oceans (Harley et al. 2001, Maunder et al. 2006, Bishop et al. 2008). In addition, our study indicates that similar trophic mechanisms control ecosystem functions across a large suite of diverse food webs ranging from tropical to cold temperate latitudes, and inclusive of a wide range of species including invertebrates.

Bioregions shown to have the highest phytoplankton biomass are in the north and south east and the lowest phytoplankton biomass is along the western and eastern coasts. Northern bioregions (A and S), are Case 2 waters (Condie & Dunn 2006) and phytoplankton biomass estimates are likely overestimated. However, as these regions only had marginal leverage on correlations between CPUE and Chl (benthic and lower trophic level benthic species), the overestimation of the chlorophyll concentration in these waters

does not detract from the relationships found here. Areas of lowest phytoplankton biomass are where oligotrophic conditions prevail; suggesting nutrients limit productivity in many areas (Condie and Dunn 2006). I note that satellite chlorophyll data have limitations, as subsurface productivity is not detected and the absolute magnitude of chlorophyll *a* concentration may not be reliable. Nevertheless, it is reasonable to assume that satellite data are indicative of surface chlorophyll *a* concentrations at large temporal and spatial scales, as in this study (Menge et al. 1997, Chassot et al. 2007). In addition, several studies have shown that satellite ocean colour data correspond reasonably well to *in situ* data in tropical to subpolar regions (e.g. the Gulf of Carpentaria, Burford and Rothlisberg 1999; the Banda Sea, Moore et al. 2003; the Southern Ocean, Clementson et al. 2001).

In general, bioregions of high primary productivity also have high fish productivity, and vice versa, conforming to the general pattern of resource-limited production (e.g. Ware & Thomson 2005, Richardson & Schoeman 2004). Interesting exceptions of this pattern are the bioregions with the highest CPUE and relatively low surface Chl: southern Western Australia and the Great Australian Bight (Bioregions M, L; Fig. 2.2). These bioregions are dominated by the southern bluefin tuna fishery. Southern bluefin tuna migrate to the Great Australian Bight from their spawning ground in the Indonesian-Australian Bight (off Bioregions Q, R). They aggregate in the Great Australian Bight as juveniles during the summer and autumn and achieve >80% of their annual growth during this period (Gunn & Young 1996, Young et al. 1996, Young et al. 1997). Though surface Chl is not high, subsurface productivity is derived from upwelling on the eastern side of the Great Australian Bight that spreads along the thermocline of the continental shelf (Hearn 1986, Young et al. 1999). This subsurface productivity is not detectable from near-surface Chl observations, and may support prey for juvenile southern bluefin tuna. It is also thought that these tuna use the relatively warm waters of the central Great Australian Bight as a thermal respite (Kloser et al. 1998) from which to forage outside of the region of highest catch (Ward et al. 2006).

Benthic fish appear to have the closest relationship to Chl of all functional groups. This may be due to the high residence time of benthic fish species in a bioregion (Ward et al. 2006), which suggests that these fish are more influenced by regional productivity than species that are migratory or transient and often move between boundaries of the defined bioregions. Pelagic fish are more mobile than benthic species and other life history characteristics and behaviours (e.g. spawning or feeding aggregations) may govern their CPUE more strongly than primary productivity. Therefore, migratory fish recruitment would not necessarily be linked to phytoplankton biomass in bioregions where they are caught as their early life stages are more influenced by remote oceanographic and productivity conditions.

Lower trophic level fish are more directly related to phytoplankton biomass because many of them feed directly on either phytoplankton or zooplankton. Therefore, it is not surprising that lower trophic level fish have a significant association to phytoplankton biomass. Lower trophic level benthic species have strong bottom-up linkages, likely due to a close trophic link to Chl and high residence time. Higher trophic level benthic fish have a significant, though weaker link to Chl than lower trophic level benthic fish, indicating that resource limitations ‘cascade up’ (Menge et al. 1997, Ware & Thomson 2005) the benthic food web. Our results concur with previous studies (e.g. Ware & Thomson, Chassot et al. 2007) that indicate that bottom-up effects “cascade up” the food web (Hunter & Price 1992) to affect higher trophic levels. Therefore, benthic fish of a higher trophic level are farther removed from Chl; however, as their planktivorous prey is tightly linked to Chl they are also reliant on regional productivity. This propagation is likely due to energy transfers between trophic levels, but may also be due to interactions between species (Hunter & Price 1992). This may include direct impacts of prey availability on predator growth, reproduction and recruitment, and indirect effects of competition between predators for prey (Hunter & Price 1992).

The temporal variability of Chl did not relate to CPUE variability at the large scale of this study. In contrast to Frank et al. (2006) I did not find any consistent latitudinal pattern for trophic control varying from top-down in higher latitudes and bottom-up in lower latitudes. Factors other than Chl contribute to the interannual variability of CPUE. These may include a variety of biotic and abiotic processes that influence fish catch variability, for example, inter-specific competition for prey, reproductive success, temperature, ocean circulation variability, and time lags between environmental drivers and recruitment (Chassot et al. 2007). The 0–2 year time lag I analysed did not elucidate any significant relationships, but it is appropriate only for short-lived species (e.g. prawns, jack mackerel, redbait). The short Chl time series (1998–2007) does not allow for appropriate time lags to account for the influence of primary productivity on larval success and recruitment to the fishery for most species. Variability related to primary productivity may also have been masked by species interactions (Micheli 1999, Frank et al. 2005, Chassot et al. 2007). Further, both bottom-up and top-down dynamics can control ecosystems simultaneously, impacting on the strength of the association between Chl and CPUE at a regional scale over short time scales (Micheli 1999). Finally, the aggregation of many different species over large spatial scales results in highly smoothed data, removing short timescale variability. Species-specific behaviours vary at multiple temporal and spatial scales (Pinaud & Weimerskirch 2007), and it may be more appropriate in some cases to examine species individually.

Previous large scale studies have examined the trophic dynamics in marine systems over limited latitudinal range; generally temperate to warm temperate waters, e.g. north

LARGE SCALE RELATIONSHIPS

east Atlantic (Cury et al. 2003, Frank et al. 2006), north east Pacific (Frank et al. 2005) and European seas (Ware & Thomson 2005). Here, I find regional productivity is the dominant limiting factor of fisheries productivity in benthic and reef ecosystems at large temporal and spatial scales. This relationship applies throughout the diverse tropical, subtropical, and warm and cold temperate marine ecosystems of Australia. In this study, Chl explains 60% of overall mean variability of the fish catch. However, I note that quantitative studies at small spatial and short temporal scales would need to consider other biological interactions and physical parameters in addition to chlorophyll *a* concentration.

2.2 LARGE-SCALE RELATIONSHIPS BETWEEN OCEAN PHYSICS AND FISHERIES PRODUCTIVITY

‘Ocean Triad’ Features in Tropical and Temperate Australian Marine Ecosystems: an Investigation of Physical Mechanisms Affecting Fish and Invertebrate Spawning Habitats

Anne-Elise Nieblas^{a,b,*}, Bernadette M. Sloyan^{c,d}, Alan J. Butler^c and Anthony J. Richardson^{e,f}

^a University of Tasmania, School of Zoology, Sandy Bay, Tasmania, Australia.

^b Commonwealth Scientific and Industrial Research Organisation (CSIRO) Climate Adaptation Flagship National Research Flagship, CSIRO Marine and Atmospheric Research, Hobart, Tasmania, Australia.

^c CSIRO Wealth from Oceans National Research Flagship, CSIRO Marine and Atmospheric Research, Hobart, Tasmania, Australia.

^d Centre for Australian Weather and Climate Research, CSIRO Marine and Atmospheric Research, Hobart, Tasmania, Australia

^e CSIRO Climate Adaptation National Research Flagship, CSIRO Marine and Atmospheric Research, Cleveland, Queensland, Australia.

^f School of Mathematics and Physics, University of Queensland, St Lucia, Queensland, Australia.

*Corresponding author: Anne.Nieblas@csiro.au

ACKNOWLEDGEMENTS

A.E.N. is supported by a joint Commonwealth Scientific and Industrial Research Organisation (CSIRO)–University of Tasmania Ph.D. scholarship in Quantitative Marine Science (QMS) and a CSIRO Climate Adaptations National Research Flagship Ph.D. stipend. B.M.S. was funded by CSIRO Wealth from Oceans Flagship and the Australian Climate Change Science Program. I thank the following agencies for environmental data: 1) sea surface temperature – National Oceanic and Atmospheric Administration (NOAA) and National Aeronautics and Space Administration (NASA), 2) Sea-viewing Wide Field-of-view Sensor ocean colour – NASA, and 3) wind – National Centre for Environmental Prediction–National Centre for Atmospheric Research. Satellite data were accessed using the Spatial Dynamics Ocean Data Explorer (SDODE) – customised software provided by Alistair Hobday, Klaas Hartmann, Jason Hartog, and Sophie Bestley. I thank Scott Condie, Peter Rothlisberg, and Michele Burford for their expert advice in the Gulf of Carpentaria.

INTRODUCTION

Fish abundance and population dynamics are related to recruitment success (Myers et al. 1995), although ecological drivers that cause recruitment variability remain obscure. Resource limitation, or bottom-up control (where primary productivity drives ecosystem functions), is assumed to have a major influence on fish population dynamics (Ware & Thomson 2005, Chassot et al. 2007, Chapter 2.1). In addition, other oceanographic conditions (e.g. retentive circulation, concentration of food sources) are necessary for suitable reproductive habitat and successful recruitment and ultimately, high fisheries yield (Agostini & Bakun 2002). Perturbations to the dominant physical mechanisms in spawning habitats can influence reproductive success, and will thus potentially have large effects on the structure and function of fish productivity. Therefore, an improved knowledge of the underlying ocean dynamics that influence fish spawning and recruitment is needed to understand potential drivers of ecosystem variability.

Fish tend to have distinct spawning, transport, and nursery habitats that self-select key characteristics beneficial for recruitment success. Through a series of comparative oceanographic studies of fish spawning habitat (Parrish et al. 1983, Bakun & Parrish 1990, 1991, Bakun 1996, 1998, Durand et al. 1998) an integrated conceptual framework identified key ocean features that regulate successful fisheries recruitment. The 'ocean triad' hypothesis describes these key features: enrichment, which supplies nutrients and thus enhances primary production; concentration, which aggregates primary producers and larvae through convergence zones or water column stability; and retention, which retains or transports fish eggs and larvae within or towards suitable nursery habitat (Bakun 1996). This ecological concept has most often been applied in eastern boundary upwelling habitats to small pelagic fish, although the concept arose from observations of a wide range of fisheries and habitats (Cole & McGlade 1998). It is therefore equally applicable in other coastal habitats and to other fish and invertebrates, the majority of which have pelagic larval stages (Bakun 1996, Agostini & Bakun 2002). This theory is difficult to test empirically as two of the three processes (concentration and retention) are difficult to quantify in a consistent manner (Cole & McGlade 1998, Hardman-Mountford et al. 2003). However, the ocean triad does provide a clear conceptual framework of the underlying mechanisms that influence fish recruitment and can be useful when examining environmental dynamics in particular ecosystems (Cole & McGlade 1998).

The Australian marine environment exists under generally oligotrophic conditions; however there are several regions of relatively high productivity that support valuable fisheries. Australia's marine system is distinctive due to the warm, nutrient-poor poleward-flowing currents that border both the east and west coast (the East Australia Current (EAC) and the Leeuwin Current, respectively) that originate from oligotrophic tropical and

subtropical waters. The Leeuwin Current suppresses the large-scale, eastern boundary upwelling that would otherwise occur off the west coast (Hanson et al. 2005a). In contrast to the general pattern, the tropical north (Gulf of Carpentaria (GoC)) and temperate south east of Australia both have high levels of primary productivity (Condie & Dunn 2006) and high fish catch (Chapter 2.1). They are also known spawning sites for a variety of residential and migratory species (Rothlisberg et al. 1985, Prince 2001). The northern, tropical region is dominated by a strong annual cycle driven by an Asian-Australian monsoon. In contrast, the south east region is one of the most oceanographically complex and dynamic Australian marine ecosystems due to the high variability of the eastern boundary current (EAC), seasonally reversing boundary currents, and the latitudinal movement of major ocean boundaries (the Subtropical Front).

Catch for the entire GoC bioregion (Fig. 2.2.1a) is dominated by penaeid prawns taken by the Northern Prawn Fishery (Condie et al. 1999), which was valued at AU\$72 million in 2007–08 (Australian Fisheries Management Authority 2009a). The several species of penaeid prawn that are caught by this fishery both spawn and recruit in the GoC. Similarly, the south east hosts one of the oldest and most valuable Australian fisheries (Tilzey 1994), valued at over AU\$95 million in 2006–08 (Commonwealth South East Scalefish and Shark Fishery; Australian Fisheries Management Authority 2009b), in addition to several significant state fisheries. In the south east, there are several productive regions driven by different physical forcing mechanisms that are also key fishing and spawning grounds and hotspots of biodiversity (Prince 2001). These include the Bonney Coast, the west coast of Tasmania, and the east coast of Australia (Fig 2.2.1b, c).

Here I contrast spawning habitats in Australian tropical and temperate waters within the context of the ocean triad. I relate broad-scale ocean dynamics to primary productivity, spawning behaviour, and recruitment of commercially-important species from significant and contrasting fisheries in the GoC and south eastern Australia. I use ocean colour, wind, ocean surface currents, temperature, salinity, and nutrient data to develop several different oceanographic indices to discuss spawning characteristics and habitat usage of commercially-important marine species. I underline how ocean triad features are used by species with diverse life history characteristics. This study enhances our understanding of how fisheries productivity is influenced by oceanographic and climatological features, characteristics that are likely to change in coming decades.

REGIONAL OCEAN DESCRIPTIONS

Gulf of Carpentaria

The GoC is a shallow (<70 m) semi-enclosed sea on the continental shelf of tropical Australia (Fig. 2.2.1a) that is dominated by tidal and wind mixing (Forbes 1984, Wolanski & Ridd 1990, Burford et al. 2009). The GoC is nitrogen-limited, with low, suboptimal nitrate

(N): phosphate (P) ratios (Rothlisberg et al. 1989, Rothlisberg et al. 1994, Burford & Rothlisberg 1999) in relation to the Redfield ratio of 16N:1P (Redfield 1958). The GoC is subject to high turbidity, especially in the nearshore zone, causing light-limiting conditions for primary productivity (Rothlisberg et al. 1994, Burford & Rothlisberg 1999). The GoC is forced by a seasonal monsoon, with weak, moist north westerly winds that dominate the wet season (December–March), and stronger, more arid south easterly winds that dominate the dry season (April–November) (Burford et al. 1995). The GoC is classified into two zones: the shallow, nearshore coastal zone (<20 m) and the deeper, offshore central gulf zone (>20 m), which are separated by a coastal boundary current (Wolanski & Ridd 1990, Burford et al. 1995).

Bonney Coast

A complex ocean current system exists along the Bonney Coast in south eastern Australia (Fig. 2.2.1b) that includes seasonally reversing coastal boundary currents (Nieblas et al. 2009) and wind-driven upwelling (Flinders Current System; Ward et al. 2006). South easterly winds drive offshore Ekman transport along the Bonney Coast (Lewis 1981, Schahinger 1987, Griffin et al. 1997). These upwelling winds are due to the seasonal migration of the subtropical high pressure system that forces south easterly winds during the late spring and summer period and westerly winds for the remainder of the year. Offshore water transport is replaced by subsurface, nutrient-rich water drawn from beneath the nutricline into the euphotic zone, driving primary productivity. The Bonney Upwelling is the largest and most predictable upwelling around Australia (Butler et al. 2002). Seasonal winds drive upwelling at Kangaroo Island as well (Fig. 2.2.1b), and upwelled water off the Eyre Peninsula is supplied by the Kangaroo Island upwelling pool (McClatchie et al. 2006).

Western Tasmania

The west coast of Tasmania (Fig. 2.2.1b) is dominated by the poleward-flowing, relatively narrow (~40 km wide) Zeehan Current, the seasonal cycle of which is influenced by the Leeuwin Current (Baines et al. 1983). The Zeehan Current is restricted largely to the continental shelf, with maximum speeds of about $\sim 0.5 \text{ m s}^{-1}$ (Baines et al. 1983). It is weakest in summer and strongest in winter when it transports relatively warm ($1\text{--}2^\circ\text{C}$ higher than surrounding waters) and saline waters (Thresher et al. 1988) poleward along the west coast and around the southern tip of Tasmania. These waters are then entrained by remnants of the EAC extension (Ridgway 2007).

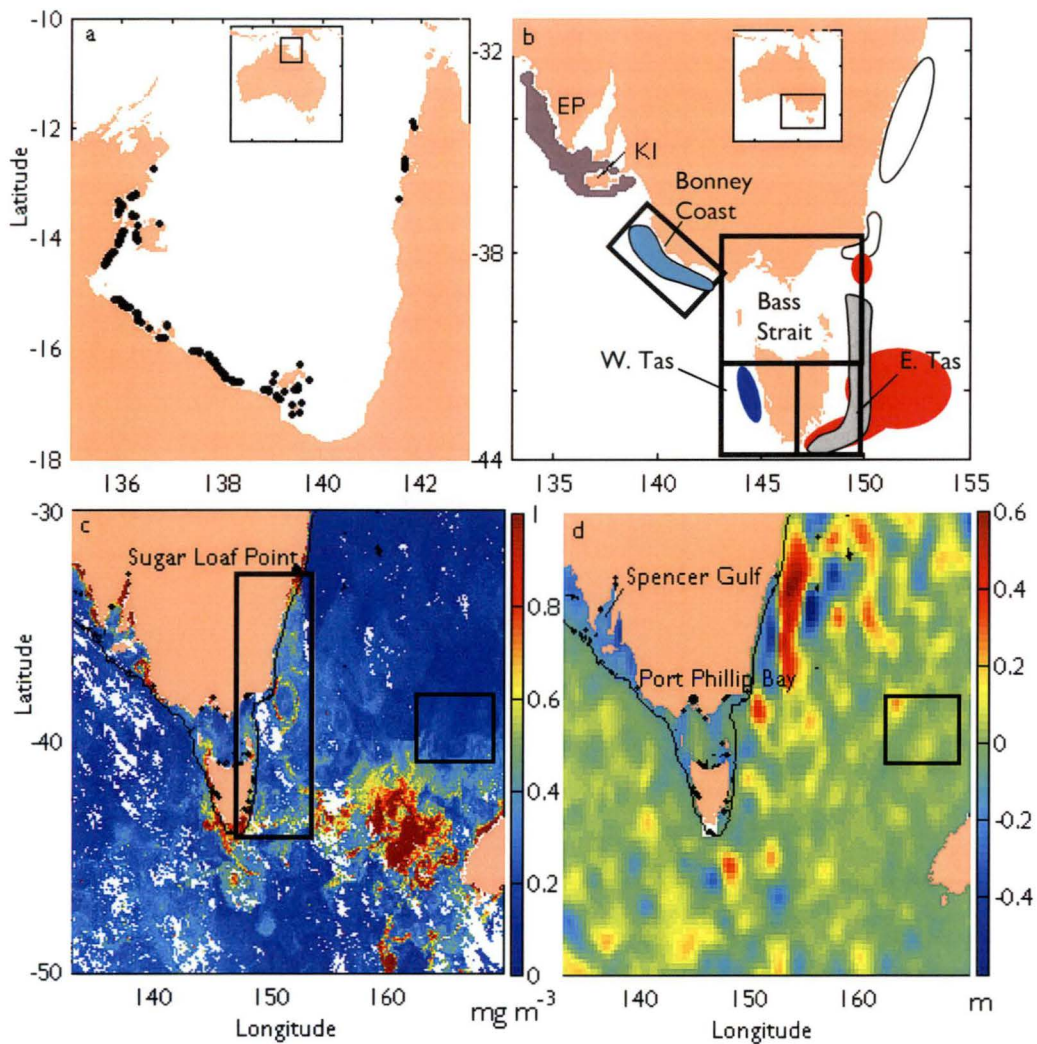


Fig. 2.2.1: Coastline of (a) the Gulf of Carpentaria with regions of seagrass bed (black) (widths not to scale), which is suitable spawning and nursery habitat for this region, adapted from Poiner et al. 1987, and (b) south eastern Australia with spawning habitat of blue grenadier (*Macruronus novaezelandiae*; blue) taken from Thresher et al. 1988; egg and larval distributions of sardine (*Sardinops sagax*; dark gray) and Australian anchovy (*Engraulis australis*; dark gray) taken from Dimmlich et al. 2004 and Ward et al. 2008, and the Larval Fish Database compiled by Bruce et al. 2001a; spawning area of King George whiting (*Sillaginodes punctata*; light blue) from Jenkins et al. 2000; egg and larval distributions of redbait (*Emmelichthys nitidus*; light gray) from Neira et al. 2009; larval distributions of (*Nemadactylus macropterus*; red) and redfish (*Centroberyx affinis*; white) and beaked salmon (*Gonorhynchus greyi*; white) from the Larval Fish Database compiled by Bruce et al. 2001a, with boxes indicating regions where mean annual chlorophyll *a* concentration was calculated. Also shown are regions discussed in text: Bonney Coast, Bass Strait, western Tasmania (W.Tas), eastern Tasmania (E. Tas), Kangaroo Island (KI), and Eyre Peninsula (EP). (c) Satellite ocean colour image from 5 January 1998 showing productivity around the south east of Australia. Note the high chlorophyll *a* concentration due to eddies off the east coast, an upwelling plume off Bonney Coast and Eyre Peninsula, and the Subtropical Front apparent in the latitudinal band approximately between 42°S–45°S. The tall black box on the coast represents the region where eddy productivity was calculated and smaller black box offshore represents the region where background chlorophyll *a* concentrations were taken in the Tasman Sea, (d) altimetry image from 7 January 1998 showing eddies off the east coast due to EAC extension, also note the low SSH in the Flinders Current system, indicating coastal upwelling. The black box represents same as in (c), and black line follows the 200m isobath (continental shelf) in both (c) and (d).

Eastern Australia

Off the east coast of Australia (Fig. 2.2.1c), western boundary and large-scale gyre dynamics influence the strength of the poleward-flowing, warm, nutrient-poor EAC. The EAC has a strong seasonal flow from 25°S to 40°S, with its maximum strength and southern extent in the austral summer (Ridgway & Godfrey 1997). The EAC separates from the coast at 31°S–34°S (Nilsson & Cresswell 1981, Roughan & Middleton 2002) and forms the Tasman Front, which extends across the Tasman Sea. The remainder of the EAC, named the EAC extension continues southward to the east coast of Tasmania. The EAC extension is dominated by eddies that frequently encroach over the continental shelf and slope (Smith & Suthers 1999). The EAC extension meets with cooler, nutrient-rich subantarctic water, and forms the Subtropical Front (Wyrtki 1960), which varies in latitude seasonally and interannually (Harris et al. 1987). Productivity patterns off eastern Australia are influenced by the position of the Subtropical Front and eddy dynamics in the EAC system.

DATA & ANALYSIS

Our focus was to assess seasonal distributions of key oceanographic variables for major productive bioregions in Australia and determine whether these conform to the triad features of enrichment, concentration, and retention. These variables included chlorophyll *a* concentration (Chl), surface currents, water property distribution (temperature, salinity, density and nutrient concentration), turbulent mixing, Ekman transport, and eddy and frontal activity. The period considered was from January 1998 to December 2007, coincident with the period of satellite-derived Chl from Sea-viewing Wide Field-of-view Sensor. Ocean colour images were 8-day composites with 0.0833° latitude by 0.0833° longitude spatial resolution. In this study I consider the GoC and south east Australian fisheries bioregions (Fig 1a, b, c) as they have high primary productivity (Chapter 2.1) and fisheries productivity (Chapter 2.1, Prince 2001).

Satellite colour data are used extensively as a proxy for phytoplankton biomass (e.g. Sathyendranath et al. 1991, Alvain et al. 2008), despite limitations. Chl estimates have the largest calibration errors in shallow, turbid, coastal (Case 2) waters (e.g. GoC) where suspended particles or dissolved organic matter introduce a significant, but unquantified contribution to the ocean colour signal (Condie & Dunn 2006). Though absolute values may be unreliable in these regions, the spatial pattern of ocean colour is likely to be indicative of surface concentrations (McClain et al. 2004, Condie & Dunn 2006).

Three-dimensional ocean currents, temperature and salinity variables were taken from the Commonwealth Scientific and Industrial Research Organisation BLUElink Reanalysis 2.1 (BRAN) ocean general circulation model (Oke et al. 2005). BRAN output has a spatial resolution of 0.1° latitude by 0.1° longitude in Australian waters, with vertical

resolution of 10 m in the upper 200 m and > 10 m otherwise (in total 47 levels). Six-hourly 10 m wind data were taken from National Center for Environmental Prediction–National Center for Atmospheric Research Reanalysis Project (Kalnay et al. 1996) and have a spatial resolution of 1.9° latitude by 1.88° longitude. I use local area coverage sea surface temperature (SST) data from the National Oceanic and Atmospheric Administration's Advanced Very High Resolution Radiometer, which was processed into 6-day composites (Griffin et al. 2004) with spatial resolution of 0.036° latitude by 0.042° longitude. Climatological nutrient data were taken from the Commonwealth Scientific and Industrial Research Organisation Atlas of Regional Seas (CARS2006) (see <http://www.marine.csiro.au/~dunn/cars2006/>; Dunn & Ridgway 2002). Nutrient data have a spatial resolution of 0.5° latitude by 0.5° longitude and 79 standard depths. I also used weekly TOPEX/POSEIDON, Jason-1, Jason-2, ERS-1, ERS-2, GFO, and Envisat composite satellite altimetry anomaly data for the Australian region with 0.193° latitude by 0.333° longitude spatial resolution. Altimeter products were produced by Ssalto/Duacs and distributed by AVISO, with support from CNES (<http://www.aviso.oceanobs.com/duacs/>).

Oceanographic indices

I develop several oceanographic indices that represent the ocean triad of enrichment, concentration, and retention (Bakun 1996). To investigate the physical drivers of productive Australian marine bioregions and their influence on fisheries recruitment, I examined the seasonal distributions of these oceanographic indices, and qualitatively related them to the descriptions of spawning for species investigated in previous studies (Table 2.2.1). The species I examine here were selected based on the relatively high level of information regarding their spawning and recruitment patterns.

Ocean surface (10 m) circulation was examined using eastward and northward velocity (U, V, respectively) from BRAN. The circulation provides an indication of physical dynamics that may act as concentration, retention, or transport mechanisms of planktonic particles in surface waters. Potential density at each model depth was calculated from temperature and salinity profiles (Gill 1982) to give an indication of stratification throughout the water column.

Wind data were used to calculate a proxy for wind-driven turbulent mixing: viz. wind speed cubed (W^3) (Elsberry & Garwood 1978). This index has been used in numerous comparative studies of continental shelf habitats to identify the wind-driven turbulence threshold for small pelagic fish spawning habitats around the world (Husby & Nelson 1982, Parrish et al. 1983, Bakun & Parrish 1990, 1991). From these studies, a consistent pattern emerged that fish generally spawn in regions where the seasonal average of wind mixing does not exceed $250 \text{ m}^3 \text{ s}^{-3}$ (Bakun 1993, Agostini & Bakun 2002). Exceptions occur in

LARGE SCALE RELATIONSHIPS

Table 2.2.1: A list of common marine organism spawning patterns and behaviour in the regions examined in this study. Bolded species are investigated in this paper. Location codes: North (N), South (S), East (E), West (W); Australia (Aus), Tasmania (Tas), Flinders Current System (FCS), New South Wales (NSW). Footnotes are provided for species that are not referenced in the text.

Region	Species	Spawning season	Spawning location	Nursery location	Larval transport	Adult movement
GoC	Penaeid prawns	Sep–Oct, Jan–Mar	Nearshore seagrass beds, offshore central Gulf	Nearshore seagrass beds	Selective tidal stream transport	
FCS	Australian anchovy, <i>Engraulis australis</i>	Spring–summer	Shelves, gulfs	Shelves, mouths of gulfs	NW coastal current, dispersed over shelf, concentrated in bays, straits, and northern gulfs	
FCS	Australian sardine or pilchard, <i>Sardinops sagax</i>	All year, but peak in Jan–Apr	Shelves, gulfs	Shelves, mouths of gulfs	NW coastal current, dispersed over shelf, concentrated in bays, and straits	
FCS	<i>Spratelloides robustus</i> ¹	Multiple batches of demersal eggs, Oct–Feb			Low densities in gulfs and straits, nearshore	
FCS	<i>Hyperlophus vittatus</i> ¹	Batch spawning Oct–Feb, peaks in Nov	Gulf waters, nearshore			
FCS	<i>Etrumeus teres</i> ¹	All year, but peak in Jan–Apr	Shelves, gulfs			
FCS	<i>Scomber australasicus</i> ¹		Mid-shelf S Aus, location highly variable			
FCS, E Aus	<i>Trachurus declivis</i> ^{1,2}	Summer, Dec–Feb	Shelf FCS, S NSW			
FCS	King George whiting, <i>Sillaginoides punctata</i>	Winter	Bonney Coast shelf	Pt. Phillip Bay	E coastal current	Adults return to Bonney Coast to spawn

LARGE SCALE RELATIONSHIPS

W Tas	Blue grenadier, <i>Macruronus novaezelandiae</i>	Winter	Mid-W coast Tas, some evidence for second spawning area off SE mainland ³	SE Tas, estuaries and nearshore, some retained on west coast	Advection by Zeehan Current	Adults return to W Tas to spawn
E Aus	Redbait, <i>Emmelichthys nitidus</i>	Distinct peak, Oct	Shelf edge		Widely dispersed nearshore, shelf, offshore	
E Aus	Jackass morwong, <i>Nemadactylus macropterus</i>	Multiple batches, Feb–Jun	Nearshore, E Tas, SE mainland	Bays and estuaries S Tas and Bass Strait	Variable but with some return to native location	
E Aus	<i>Maurolicus muelleri</i> ⁴	Late winter, spring (Jul–Oct)				
E Aus	Redfish, <i>Centroberyx affinis</i>	Summer	Nearshore, SE mainland		Passively dispersed onshore	
E Aus	Beaked salmon or sand eel, <i>Gonorynchus greyi</i>	Protracted, multiple-batch spawning, summer–autumn	Outer shelf		Shelf break, mostly passive dispersal in early stages, then actively swim to maintain outer shelf location	
SE Aus	<i>Seriola brama</i> ^{5,6}	Winter–spring, Jun–Oct off Bonney Coast, May–Aug off E Aus			Widely distributed on shelf and slope, Kangaroo Island–southern NSW	
SE Aus	<i>S. punctata</i> ⁵	Winter–spring (Jul–Aug), spawning one month earlier E of Bass Strait than W			High concentrations off W Tas and S NSW, low distributions between S Tas and S NSW	

¹Ward et al. 2008, ²Jordan et al. 1995, ³Bruce et al. 2001b, ⁴Clarke 1982, ⁵Bruce et al. 2001c,

⁶Knuckey & Sivakumaran 2001

regions where mixing is inhibited due to large freshwater surface inputs, or large overflows of less dense water masses (Bakun 1996). This threshold should be valid for species with pelagic larvae whose survival depends on first feeding success requiring concentrated patches of phytoplankton (Bakun 1996, Agostini & Bakun 2002). This index has often been applied to continental shelf upwelling regions (e.g. Parrish et al. 1983, Payá & Ehrhardt 2005); I note that this threshold level may not be appropriate for shallow, stable regions, and consider this further with regard to the GoC.

Wind data were also used to indicate potential upwelling activity by calculations of Ekman transport per unit width ($\text{m}^2 \text{s}^{-1}$):

$$Q_y = -\frac{\tau_x}{\rho f}; \quad Q_x = \frac{\tau_y}{\rho f} \quad (2.2.1)$$

where τ_x and τ_y are the eastward and northward component of the wind stress (N m^{-2}) respectively, ρ is the density of water (kg m^{-3}), and f is the Coriolis parameter ($f = 2\Omega \sin\phi$), where Ω represents the angular velocity of the earth ($7.242 \times 10^{-5} \text{ radians s}^{-1}$) and ϕ denotes latitude (Pond & Pickard 1983).

To estimate eddy activity due to variability in the strength of the EAC, I found continuous areas of sea surface height (SSH) anomaly fields off the continental shelf ($>200 \text{ m}$) of south eastern Australia (44.5°S – 32°S , 147°E – 154°E) (Fig. 2.2.1c), based on ± 1 standard deviation from the mean ($0.05 \text{ m} \pm 0.18 \text{ m}$). These regions were classified as eddies if they were less than twice as long as they were wide, giving them a roughly elliptical shape, with anomalously high (low) SSH representing warm (cold) core eddies (Alpine & Hobday 2007). Phytoplankton biomass associated with eddies was assessed by finding the nearly-coincident mean Chl from satellite colour images to SSH images with an additional 0.25° radial increase to account for eddy edge phytoplankton biomass. To assess whether eddy fields enhance regional phytoplankton biomass, eddy Chl was compared to background Chl computed for a box in the Tasman Sea (41°S – 37°S , 162.5°E – 169.2°E ; Fig. 2.2.1c, d) outside the region of eddy influence.

Position and persistence of ocean fronts were estimated using SST gradients. These were derived using the single-image SST edge detection algorithm developed by Cayula and Cornillon (1992) as implemented by Alpine and Hobday (2007). This is a multi-level (picture, window, local) approach that uses bimodality of the histogram in a window as the basic edge detector to clearly identify two spatially-compact temperature populations (Ullman & Cornillon 2000). This method is not based on the absolute strength of the frontal gradient, rather how well pixels separate into bimodal peaks (Kahru et al. 1995).

The frontal index has no units, but higher values indicate longer persistence or higher detection frequency of a front in the region.

RESULTS & DISCUSSION

Tropical marine ecosystem

Gulf of Carpentaria

Ocean dynamics

Penaeid prawn spawning occurs nearshore and offshore, although spawning is most effective nearshore (Catchpole & Auliciems 1999) where seagrass beds are used as spawning and nursery habitat. I therefore examine the mean seasonal distribution of the oceanographic variables for the wet and dry season for the nearshore zone. Also, due to high turbidity and light-limited conditions in the GoC, I only examine surface layer (0–10 m) nutrient concentrations. I find high Chl in the coastal zone of the GoC (Fig. 2.2.2a) relative to other Australian waters (e.g. see Fig. 2.2.4). Though the Case 2 waters of the GoC are due to turbidity of sediments, the high Chl found here may be indicative of surface concentrations of Chl. This is supported by *in situ* measurements of Burford & Rothlisberg (1999) who found high primary productivity in the surface waters that depleted rapidly in the turbid, light-limited water column. The nearshore peak in Chl is in the summer wet season (January–March) (Fig. 2.2.2a), coinciding with low salinities (Fig. 2.2.2b). BRAN model data indicate that surface salinities peak towards the end of the dry season (October–November, 35.1), and begin to decline from November to reach the lowest point in April (33.4) (Fig. 2.2.2b). This shows the influence of riverine inputs during the wet season. The GoC is surrounded by large rivers that input up to 92,000 GL of freshwater that is trapped nearshore by the coastal boundary current (Burford et al. 2009), thus lowering salinities nearshore during periods of high riverine input. CARS2006 shows relatively low concentrations of N (0.47–1.14 μM) and P (0.21–0.26 μM) in the surface layer for the nearshore region of the Gulf and relatively high concentrations of silicate (Si, 3.05–4.94 μM) (Fig. 2.2.2c) throughout the year. Seasonal peaks in nutrient concentration (Fig. 2.2.2c) are due to terrestrial runoff that enriches the nutrient concentrations in the coastal zone during the wet season. The nearshore zone is dominated by seagrass beds in the north east, south west, and west (Poiner et al. 1987, Condie et al. 1999) (Fig. 2.2.1a) that contribute to the nitrogen budget by nitrogen-fixation from epiphytic and bacterial activity (Moriarty & O'Donohue 1993, Burford et al. 2009). However, the ratio of nitrate to phosphate ($\sim 4\text{N:1P}$) indicates a nitrogen-limited system. BRAN density profiles show the nearshore zone is well-mixed throughout the year, though less dense during the wet season (Fig 2.2.2e, f), indicating nutrients may be continuously resuspended from the sediment in the coastal zone. This is contrary to the offshore GoC, where stratification increases during the wet season (Fig. 2.2.2e).

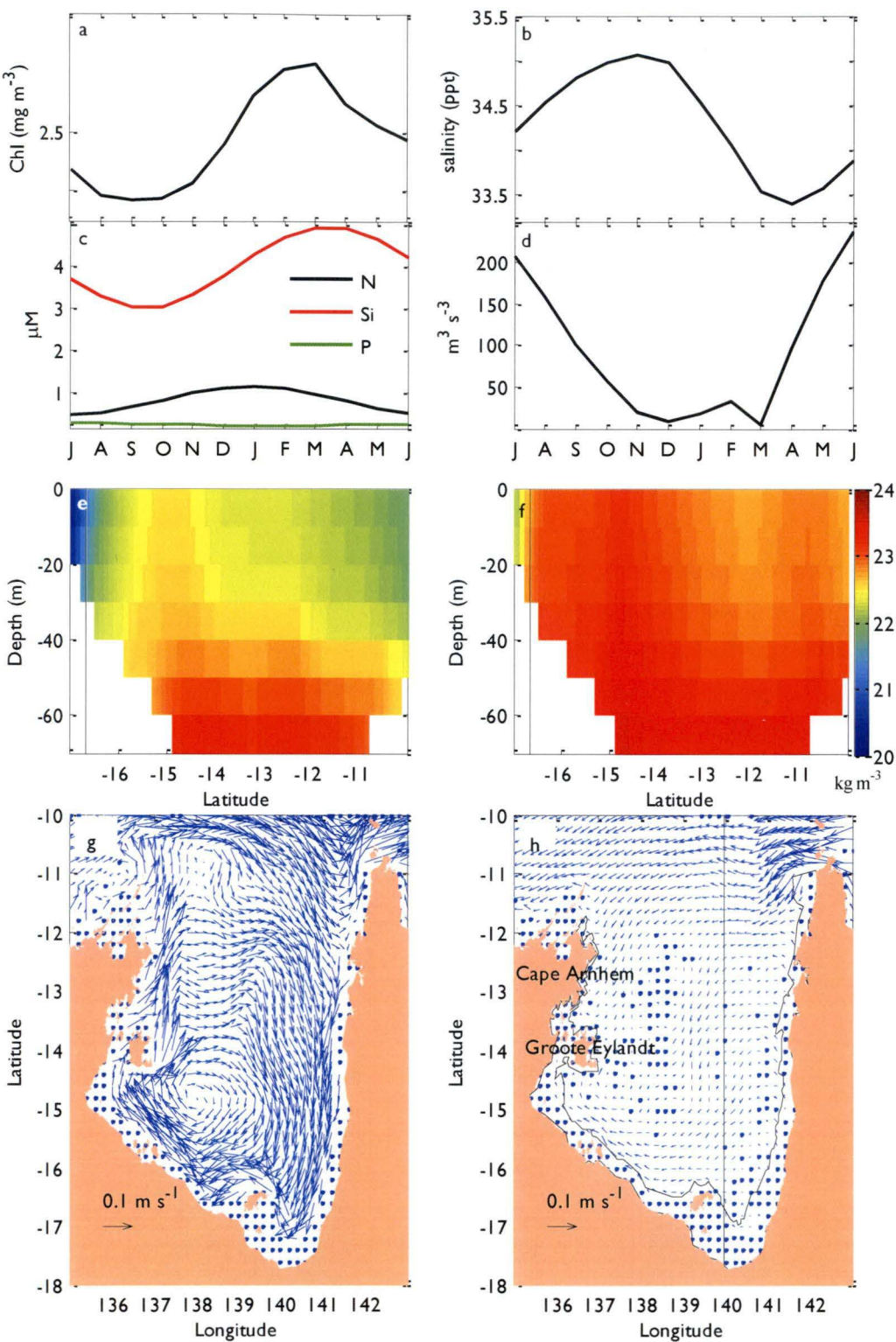


Fig. 2.2.2: Mean annual (a) satellite Chl (mg m^{-3}) (b) BRAN surface salinity and (c) 10 m CARS nitrate (black), silicate (red), and phosphate (green) (μM) for nearshore zone, and (d) wind turbulence index, w^3 ($\text{m}^3 \text{s}^{-3}$). Potential density (kg m^{-3}) distribution along 139.5°E Longitude for the (e) wet and (f) dry seasons based on BRAN salinity and temperature, black lines at -16.67°S Latitude indicate the location of the 20 m contour, and BRAN mean surface currents for the (g) wet and (h) dry seasons for the Gulf of Carpentaria, with a solid black line indicating the line of longitude of the density distribution (e,f). Dots represent points where mean current is near zero (in central Gulf), and where BRAN does not resolve the nearshore region.

I find that regional mean W^3 in the GoC never exceeds the $250 \text{ m}^3 \text{ s}^{-3}$ threshold (maximum $237.1 \text{ m}^3 \text{ s}^{-3}$; Fig. 2.2.2d, 2.2.3) for deleterious wind mixing that contributes to dispersion of larvae and food patches (Bakun 1996) and has extremely low wind mixing from November to March ($8\text{--}32 \text{ m}^3 \text{ s}^{-3}$; Fig. 2.2.2d, 2.2.3a, d). However, I note that though the $250 \text{ m}^3 \text{ s}^{-3}$ threshold is not reached, some wind mixing may have deleterious effects on some algal species, for example the nitrogen-fixing raft-forming cyanobacterium, *Trichodesmium*. This species occurs in higher concentrations in the calm periods of the wet season when W^3 values are minimum, and the biggest blooms occur in years of little wind (Burford et al. 1995). As the GoC has high freshwater inputs and acts more like a shallow lake than an open-ocean influenced continental shelf, apart from the tidal forcing, the $250 \text{ m}^3 \text{ s}^{-3}$ threshold is not suitable. Notwithstanding, there is little phytoplankton species succession and low seasonal variability of phytoplankton in this region, indicating water column stability (Burford et al. 1995).

The broad-scale circulation of the GoC from BRAN shows a slow, permanent clockwise circulation for most of the year, which is stronger in the wet season than in the dry season (Fig. 2.2.2g, h). Forbes and Church (1983), using satellite-tracked drogued buoys indicate that this east to west flow occurs within the coastal boundary as well. During the wet season, north westerly winds enhance the clockwise circulation, and during the dry season, the strong south easterly winds weaken the flow (Fig. 2.2.2i, j) (Forbes & Church 1983). BRAN data does not resolve the nearshore circulation of the GoC. However, due to the seasonal progression of the diurnal tide relative to day-night cycles, particle advection is oriented away from the coast in the wet season (March) and towards the coast in the dry season (October) (Rothlisberg & Church 1994). There is little exchange between waters in the northern Gulf and the Arafura or Coral Seas, with water residence times of up to 3 years (Forbes & Church 1983), indicating a retentive system.

Spawning patterns

The Northern Prawn Fishery is seasonally closed (June–July) to protect pre-spawning penaeid prawn adults (Condie et al. 1999) from overfishing. Typically, tropical prawn species (e.g. grooved tiger prawn, *P. semisulcatus* and banana prawn, *Penaeus merguensis*), spawn in two distinct peaks in austral spring (August–October) and autumn (January–March) (Rothlisberg et al. 1985, Rothlisberg et al. 1987, Crocos & van der Velde 1995) (Table 2.2.1). The initial spawning period (August–October) coincides with the end of the dry season when Chl is low, but nearshore nutrient enrichment is increasing and wind-driven turbulence is decreasing, and the second spawning period (January–March) coincides with the latter half of the wet season when Chl is high and the W^3 is minimum (Fig. 2.2.2a,d). The reproductive output of the August–October spawning period is generally weaker than the January–March spawning period (Staples & Vance 1985). Penaeids have a

brief period (12–25 days) during their early life stages where they are entirely dependent on phytoplankton for food (Dall et al. 1990). The spawning periods appear to coincide with periods of increasing or high nutrient enrichment. Turbulent mixing is low throughout the year, likely leading to concentrated patches of phytoplankton during critical life stages.

Horizontal dispersal of marine larvae is largely determined by interactions of larval behaviour, environmental stimuli, and local currents (see McEdward 1995 for review). These prawn species have a larval period where they have no horizontal swimming ability (Rothlisberg et al. 1996), but penaeids migrate vertically as postlarvae and use selective tidal stream transport to gain access to their estuarine or seagrass nursery grounds (Dall et al. 1990). The Gulf's clockwise circulation may broaden their 'advective envelope' (Rothlisberg et al. 1996, Condie et al. 1999) along nearshore seagrass beds (Fig. 2.2.1a), increasing the likelihood of successful establishment in suitable nursery habitat. In contrast, offshore spawning is not effective (Condie et al. 1999), possibly because larvae cannot transport to suitable nursery grounds due to the coastal boundary current, which acts as a barrier to the nearshore seagrass. Conditions are favourable for inshore advection during the August–October spawning period. Therefore, though the peak reproductive output is in the January–March spawning period, the small peak in August–October may supply most of the postlarvae that recruit to the fishery 6–7 months later (Rothlisberg & Church 1994).

Triad features

Although the relevant parameter values are different from those on open continental shelves (e.g. W^3), the GoC has regional-scale ocean dynamics that produce key ocean triad features for the Northern Prawn Fishery (Table 2.2.2). Enrichment occurs throughout the water column in the nearshore zone due to terrestrial runoff and consistent tidal-driven mixing, and epiphytic activity, though light-limited due to turbidity (Rothlisberg et al. 1994, Burford & Rothlisberg 1999). Concentration transpires through water column stability with minimal turbulent mixing during the November to March wet season. Advective conditions during the August–October spawning season appear to act as “retention” features that deliver eggs and larvae into appropriate spawning habitat. The coastal boundary current is a retentive feature as it is an effective barrier that separates nearshore and offshore waters. In addition, the large-scale, slow, clockwise GoC circulation is a concentrating and retention feature for GoC phytoplankton biomass. The timings of these key triad features coincide with periods of peak spawning and recruitment, and probably contribute to the success of penaeid prawn populations in this coastal region.

LARGE SCALE RELATIONSHIPS

Table 2.2.2: Mechanisms for ocean triad features for each region examined in this study. Abbreviations as: North (N), South (S), East (E), West (W), Tasmania (Tas), Subtropical Front (STF), and East Australia Current (EAC).

Region	Enrichment	Concentration		Retention
			W^3	
Gulf of Carpentaria	Terrestrial runoff, epiphytic/bacterial activity, resuspension due to tidal mixing, peak in Jan–Mar	Coastal boundary current	Max 237.1 $m^3 s^{-3}$, min Nov–Mar	Permanent clockwise circulation, coastal boundary current
Bonney Coast	Summer upwelling	High frontal activity in straits and along upwelling plume	$< 250 m^3 s^{-3}$ all season	NW or SE flow towards different nursery habitats
W Tas	STF-driven large spring, minor autumn blooms	Persistent front at S-SE Tas coast	$< 250 m^3 s^{-3}$ summer, autumn, $> 250 m^3 s^{-3}$ winter	Nearshore "pockets", S-SE advection E Tas nursery via Zeehan Current
E Australia	STF-driven large spring, minor autumn blooms; eddy enrichment, sporadic summer upwelling	High frontal activity due to mesoscale features	$> 250 m^3 s^{-3}$ winter and spring in S Tas, $< 250 m^3 s^{-3}$ all year N of Tas	EAC onshore transport, some eddies may be pelagic retention cells

Temperate marine ecosystems

Bonney Coast

Ocean dynamics

Ekman transport vectors show mean summer offshore Ekman transport for most of the Flinders Current System (Fig. 2.2.5a). I find phytoplankton biomass peaks in the late austral summer (Fig. 2.2.4a), due to enrichment by upwelling (Nieblas et al. 2009). Chl declines in autumn (Fig. 2.2.4a) due to the return of downwelling-favourable winds (Nieblas et al. 2009). Upwelling plumes are apparent from seasonally-averaged satellite imagery (Fig. 2.2.5b), indicating a large seasonal effect on regional productivity. The turbulent wind index does not reach the $250 m^3 s^{-3}$ threshold where deleterious mixing hinders recruitment processes in any season in this region, even during summer upwelling (Fig. 2.2.3). Although upwelling is a dispersive process, Australian upwelling systems are relatively low-wind systems compared with eastern boundary upwelling systems (Nieblas et al. 2009). Further, Spencer Gulf and Gulf St. Vincent (Fig. 2.2.5d) are known to be shallow "inverse estuaries", that are especially stable in their northern reaches (Dimmlich et al. 2004, Shepherd et al. 2008). BRAN surface currents show that during the upwelling season, there is a weak north westward flow that carries surface water from off the Bonney Coast to semi-enclosed bays further west (e.g. Encounter Bay, and the continental shelf region of the eastern Great

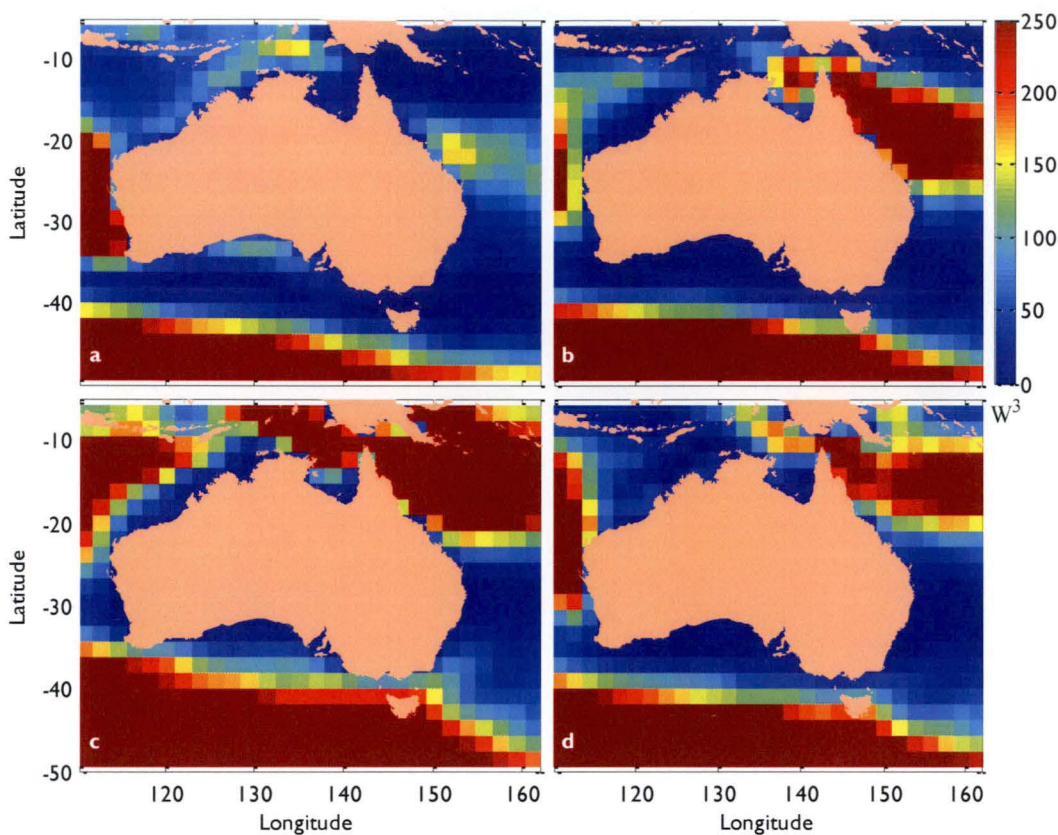


Fig. 2.2.3: Seasonal distribution of wind speed cubed (W^3 ; units: $m^3 s^{-3}$) in Australian waters for (a) summer, (b) autumn, (c) winter, and (d) spring.

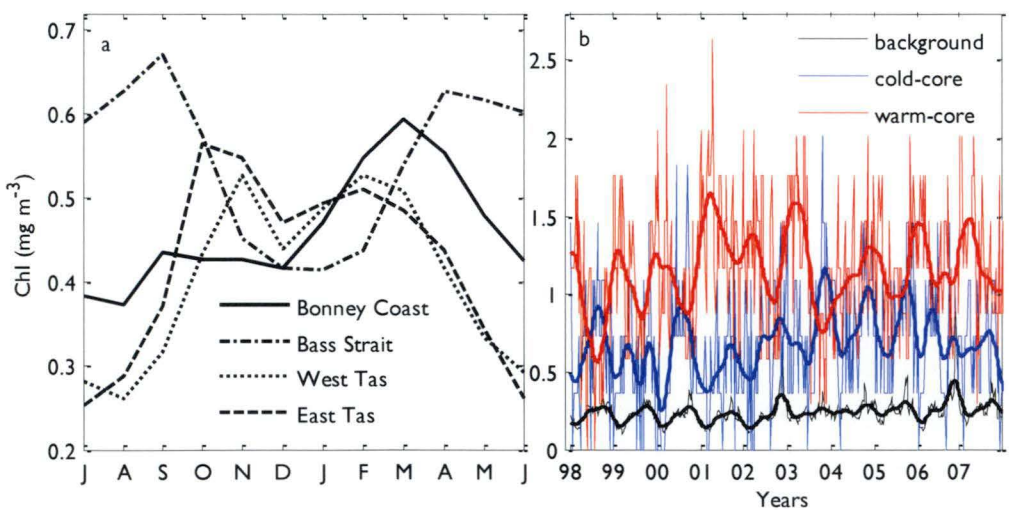


Fig. 2.2.4: Oceanographic variables from south eastern Australia including (a) mean annual Chl for the fisheries hotspots in south eastern Australia calculated from boxes in Fig. 2.2.1b, and (b) Chl related to cold- (blue line) and warm-core (red line) eddies relative to background Chl from the Tasman Sea (black line).

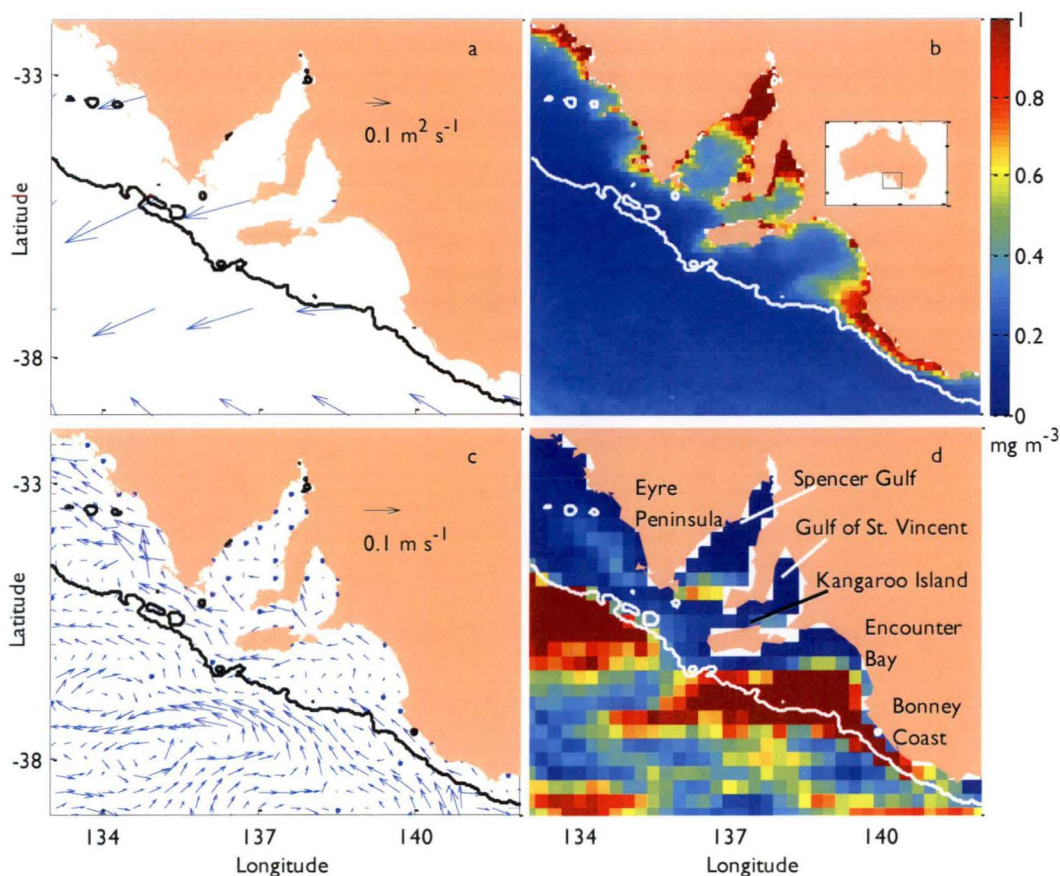


Fig. 2.2.5: Bonney Coast (a) mean summer Ekman transport per unit width (January–February), (b) mean summer satellite Chl (December–February), (c) characteristic summer BRAN surface currents (February 2006), note currents are plotted every third grid point for clarity; and (d) mean summer/autumn frontal activity (December–April) (red indicates high activity, blue indicates low activity) with locations mentioned in the text. White or black lines indicate 200 m isobath (continental shelf).

Australian Bight), and to Spencer Gulf and Gulf St. Vincent (Fig. 2.2.5c). This is the coastal current that flows north westward during summer and reverses to a strong, south eastward flow in the winter (Middleton & Platov 2003). I find high SST gradient activity in the Investigator Strait north of Kangaroo Island, at the mouths of the two gulfs, and along the continental shelf of the eastern Great Australian Bight (Fig. 2.2.5d). Intense SST gradients are also found at the edge of the upwelling plumes, with the strongest and most frequent SST gradient activity off the Bonney Coast (Fig. 2.2.5d). SST gradient activity is highest in summer and autumn, during and after the upwelling period.

Spawning patterns

Small pelagic fish are distributed throughout southern Australia, but the centre of their distribution is in the Flinders Current System where they spawn and are abundant (Ward et al. 2008). There are 11 main species within the state-managed small pelagic fishery (Table

2.2.1), but Australian anchovy (*Engraulis australis*) and sardine (*Sardinops sagax*) dominate the catch (Ward et al. 2008). Similar to other small pelagic fish worldwide, these species spawn in the gulfs, lagoons, and along the continental shelf of the region in the spring and summer, during peak upwelling productivity (Dimmlich et al. 2004). Eggs of these two species are abundant in the frontal regions at the mouths of the gulfs and Investigator Strait, and on the continental shelf of the eastern Great Australian Bight (Dimmlich et al. 2004, Ward et al. 2006), downstream from upwelling plumes (Fig. 2.2.1b). Larvae found on the shelf and at the mouths of gulfs are dominated by sardine, and only anchovy eggs and larvae are found in the far north of the gulfs. The northern regions of the gulfs have high salinity and warm temperatures, which are tolerated by anchovy but not by sardine, therefore acting as a 'refuge' for anchovy (Dimmlich et al. 2004).

King George whiting (*Sillaginodes punctata*) spawn off the Bonney Coast; however, this species spawns in the winter months (Jenkins et al. 2000) (Fig. 2.2.1b, Table 2.2.1) when downwelling conditions are prominent (Nieblas et al. 2009) and Chl is low (Fig. 2.2.4a). During this period, eggs and larvae of these fish are advected eastwards to Bass Strait in the strong south eastward-flowing coastal current (not shown) thereby reaching their nursery ground in Port Phillip Bay, Victoria (Jenkins et al. 2000) at the time of peak Chl (Fig. 2.2.4a).

Triad features

The Flinders Current System appears to have appropriate triad features coincident in time with small pelagic species that dominate fisheries in the region (Table 2.2.2). Sardines and anchovy are known to have faster growth and more fatty reserves in the Flinders Current System than in the rest of their southern Australian range (Ward et al. 2006), probably due to the higher and more predictable primary productivity inputs from seasonal upwelling enrichment. The Flinders Current System is analogous to larger eastern boundary upwelling systems world-wide (Nieblas et al. 2009) that also support small pelagic fish spawning. One example is the California Current System where anchovies and sardines have similar life history characteristics (Bakun 1996). "Retention" in the system is achieved by summer north westward coastal currents that transport eggs and larvae to frontal regions and stable nursery habitats. Frontal features of the Flinders Current System likely act to spatially concentrate prey and larvae, increasing food availability for larval feeding. Additionally, the Flinders Current System also appears to function as an appropriate spawning region during its period of lowest phytoplankton biomass for fish with life histories different from anchovy and sardine (e.g. King George whiting). For these species spawning is coincident with coastal current features that enhance advection of their eggs and larvae to preferred nursery habitat.

Western Tasmania*Ocean dynamics*

The BRAN model data clearly show the Zeehan Current flowing poleward along the west coast of Tasmania (Fig. 2.2.6a). Satellite data show relatively warm water advected poleward by the Zeehan Current off the west coast of Tasmania in winter (Fig. 2.2.6b). I find a clear spring bloom (September–November), which declines moderately in mid-summer, and ramps up again to form a summer to early autumn bloom (January–March, Fig. 2.2.4a). This pattern is characteristic of phytoplankton biomass driven by Subtropical Front dynamics (Harris et al. 1987) that influence the southern and temperate regions of Australia. I find western Tasmania has strong westerly winds (autumn–spring), leading to the highest levels of W^3 in south eastern Australia (Fig. 2.2.3). However, W^3 only becomes $> 250 \text{ m}^3 \text{ s}^{-3}$ in the winter, and is lower than this threshold in all other seasons (Fig. 2.2.3), indicating that deleterious mixing is absent during spring through autumn. I find temperature gradients on the west coast are relatively weak, but a persistent, well-defined SST gradient frontal feature is found off the south-south eastern Tasmanian shelf in the winter (Fig 2.2.6c). This SST gradient is likely due to the convergence of the Zeehan Current with the EAC eddies (Ridgway 2007) that concentrate food and larval particles. Retention mechanisms may occur on the west coast of Tasmania as “pockets” of relatively static nearshore water that are not entrained in the general southward flow (Thresher et al. 1988). These static waters have been hypothesized to occur, but have not been observed, nor do I observe them in this study (Fig. 2.2.6a), because the spatial resolution of BRAN model is too large to resolve such features.

Spawning patterns

Though few fisheries studies have been undertaken on the west coast of Tasmania, it is known to be the main spawning site of blue grenadier, *Macrurus novaezelandiae* (Table 2.2.1), an important commercial fish in the South East Scalefish and Shark Fishery, valued at ~AU\$31 million for 2006–07 (Vieira et al. 2008). Spawning occurs during winter on the mid-west coast of Tasmania (Fig. 2.2.1b) (Thresher et al. 1988, Gunn et al. 1989). The majority of eggs and larvae are advected by the Zeehan Current towards nursery grounds in the estuaries and coastal regions of the south east coast of Tasmania though some are retained on the west coast (Thresher et al. 1988). Retained young larvae (<15–20d) on the west coast grow faster in comparison to young larvae that have been advected south and south eastward, indicating that for this age and time of year, the mid-west coast is most beneficial for growth (Thresher et al. 1988). This could be due to higher phytoplankton biomass of the Tasmanian west coast compared to the Tasmanian east coast during this period (May–July) (Fig. 2.2.4). Also the relative warmth of the Zeehan Current (Fig. 2.2.6b)

may affect growth rates as gadoid growth is positively related to water temperature (Lawrence 1978). However, older larvae (>25d) grow faster off the south east than west coast of Tasmania (Thresher et al. 1988) when Chl is higher than the west coast towards the end of winter (Fig. 2.2.4a), indicating that food availability contributes to the regional differences in larval growth rates.

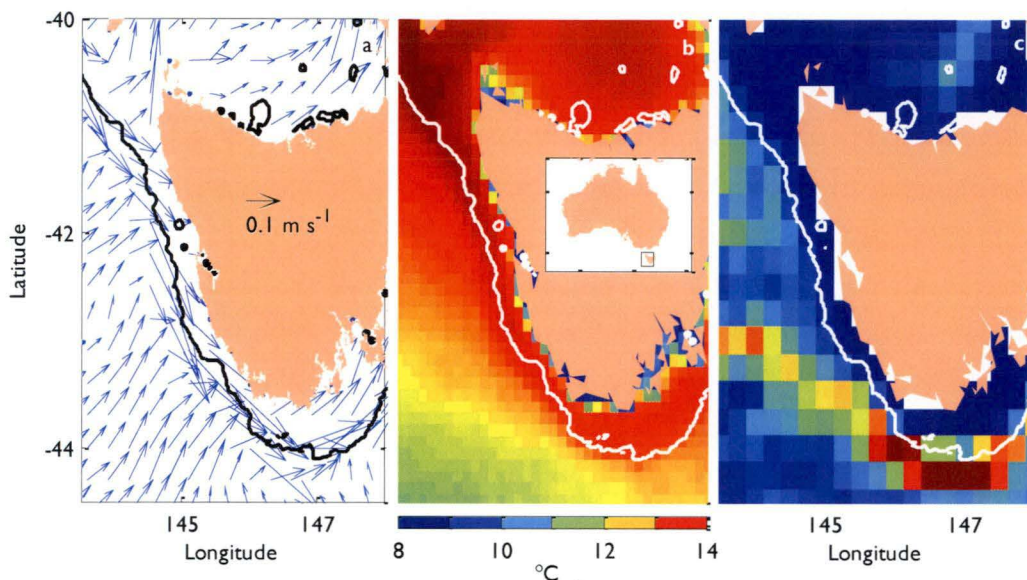


Fig. 2.2.6: Western Tasmania mean austral winter (June–August) ocean dynamics including (a) BRAN surface currents, note currents were plotted every third grid point for clarity; (b) sea surface temperature, and (c) frontal activity (red indicates high activity, blue indicates low activity). Black or white lines indicate the 200 m isobath (continental shelf).

Triad features

Overall it appears that there are features of the ocean triad off the west coast of Tasmania: enhanced phytoplankton biomass at different points in the year; there are periods when the wind fields are below the $250 \text{ m}^3 \text{ s}^{-3}$ turbulence threshold; and a good “retention” mechanism that advects larvae to the appropriate nursery grounds on the south east coast; and concentration mechanisms at the end of the advection pathway (Table 2.2.2). However, the seasonal distributions of these features do not coincide with the spawning season of *M. novaezelandiae*. In fact, the main spawning season (winter) coincides with the lowest phytoplankton biomass and highest turbulence for the west coast. It is apparent that conditions are beneficial for larval growth for the early larval stages that are retained off the Tasmanian west coast. Nevertheless, blue grenadier appear to have life histories similar to King George whiting, in that the majority of larvae are delivered by current advection to the preferred nursery habitat for later larval stages.

Eastern Australia*Ocean dynamics*

Off eastern Tasmania, I show a large spring bloom (September–November) and a minor autumn bloom (February) (Fig. 2.2.4a), due to the variability of the Subtropical Front. During the winter, the oligotrophic EAC extension retreats along the east coast and nutrient-rich subantarctic water migrates northwards with the Subtropical Front. When days lengthen in the spring, high nutrient levels in the water column lead to phytoplankton blooms (September–November). In summer, the EAC extension progresses further south, extending warm, oligotrophic water southward along the east coast, and suppressing phytoplankton biomass (December–January). In the autumn, the EAC extension again retreats northward, and there is a secondary peak in Chl (February) as nutrient-rich subantarctic waters again move northward (Condie & Dunn 2006).

Chl levels are also enhanced above background levels due to eddies in the EAC extension and the Subtropical Front (Fig. 2.2.4b). Mesoscale features (warm- and cold-core eddies) within the current drive regional Chl that is up to 3–5 times higher than similar waters not influenced by eddy activity (e.g. the Tasman Sea) (Fig. 2.2.4b). This is due to upwelling of nutrient-rich water from depth either in the eddy interior or at the eddy edges. Further, primary productivity is also enhanced in this region due to sporadic upwelling nearshore and south of the separation zone of the EAC (Griffin & Middleton 1992). Here, regional bathymetry combines with local upwelling-favourable (north westerly) winds to induce episodic upwelling during the summertime (Smith et al. 1999) and enhance productivity. Productivity is high in general during the summer period off the south east coast (Smith et al. 1999), however seasonal means show little phytoplankton biomass (Condie & Dunn 2006). This is likely due to the episodic and dynamic nature of the productivity drivers in this region whose signals are diminished by large-scale means.

In the south east of eastern Tasmania, the turbulent wind index exceeds the $250 \text{ m}^3 \text{ s}^{-3}$ threshold during winter, with relatively high wind turbulence in spring as well that reduces to low levels by summer (Fig. 2.2.3). However, north of this the W^3 index remains substantially lower than $250 \text{ m}^3 \text{ s}^{-3}$ for all seasons. During the summer, dynamic SST gradient activity extends along the eastern Australian coastline to Tasmania and retreats equatorward in the winter (Fig. 2.2.7a, b) due to the interaction of the Subtropical Front and the EAC, the EAC extension, and episodic upwelling fronts. BRAN surface current fields show strong eddy activity extending to southern Tasmania in the summer, and weaker activity in the winter (Fig. 2.2.7c, d). Eddies can concentrate particles along the eddy-edge, as well as entrain surrounding water. Eddies can act as either dispersive or retentive features, depending on their persistence and movement. Some eddies in the region entrain highly productive surrounding water, as well as enhance productivity through

their own dynamic properties, and persist up to 18 months along the coast (Nilsson & Cresswell 1981). The overall southward flow of the EAC extension eddy field can carry particles as far south as the south eastern tip of Tasmania (Fig. 2.2.7c, d). Nearshore transport over the shelf is typically shoreward in response to EAC forcing, driving cross-shelf flows, recirculation cells and incursions of the EAC water onto the shelf (Smith 2003). Here, I examine fish species that firstly, spawn off the east coast of Tasmania, and secondly, spawn off the east coast of Australia.

Spawning patterns

Tasmanian east coast – Numerous and diverse fish species spawn nearshore off the east coast of Tasmania (Table 2.2.1). Some have a distinct spawning peak (e.g. redbait, *Emmelichthys nitidus*; Neira et al. 2009), and some have an extended spawning period with multiple batches (e.g. jackass morwong, *Nemadactylus macropterus*; Bruce et al. 2001d). Globally, most species spawn and are retained nearshore and those species that spawn offshore are associated with particular retentive oceanographic features (Hare & Cowan 1993). If not, they are considered a loss or emigration of larvae (Nelson et al. 1977). Similarly, most eggs and larvae are retained nearshore off eastern Tasmania (e.g. redbait; Neira et al. 2009), but there are interesting exceptions of species transported offshore (e.g. jackass morwong; Bruce et al. 2001d).

Redbait has a distinct peak spawning period in October off the east coast of Tasmania (Fig. 2.2.1b) (Neira et al. 2009), when Chl levels are at their highest (Fig. 2.2.4a). The southernmost extent of spawning is 43.5°S, at the frontal zone where the Zeehan Current meets the EAC; south of this, the cold water is suboptimal for egg and larval health. Redbait appears to prefer the shelf edge to spawn, but surface currents disperse its larvae evenly across nearshore, shelf, and offshore regions (Neira et al. 2009); indicating that nearshore retention is not high in this region.

In contrast to the redbait, jackass morwong spawn over an extended period from February to June (Lyle & Ford 1993), with nursery areas in bays and estuaries of southern Tasmania and Bass Strait (Tilzey et al. 1990). Larvae are spawned nearshore off eastern Tasmania, and south eastern Australia, but are quickly transported offshore by the EAC and Subtropical Front where they are retained during their long pelagic larval phase (Vooren 1972). However, both populations are also known to be self-sustaining, with their advection pathways occasionally returning them within a few kilometres of their nursery grounds. In addition, directed swimming towards the end of their extended larval period likely returns them to nearshore nursery grounds (Bruce et al. 2001d).

Both species have spawning and life history characteristics that take advantage of the variability of the region's features. Redbait spawns in a distinct period when phytoplankton biomass is highest, though retention does not appear to be optimal for the

majority of the eggs and larvae. The reproductive strategy of this species may be to spawn during a period when the majority of eggs and larvae may be lost or expatriated due to advection from appropriate nursery habitat, but the minority that are retained succeed due to optimal food availability. In contrast, jackass morwong spawns over a protracted period that does not always have high Chl. Their eggs and larvae are then entrained in circulation features (fronts and eddies) that advect them offshore, where the conditions appear suitable for their long pelagic larval phase. By the end of this phase, they are either transported nearshore or swim toward preferred nearshore nursery habitats. Due to high oceanographic variability in this region, protracted spawning increases the likelihood of coincidence with oceanographic and productivity features favourable for recruitment success and decreases the impact of environmental variation (Bobko & Berkeley 2004).

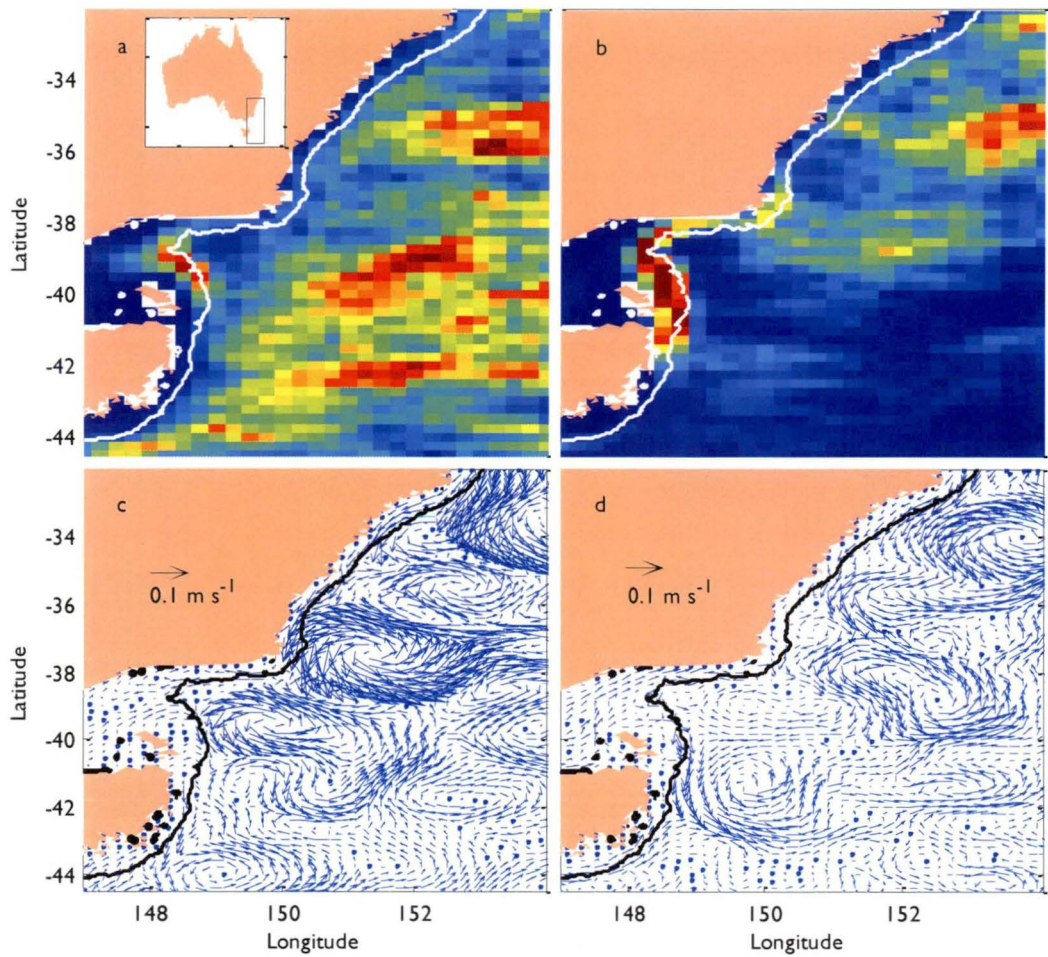


Fig. 2.2.7: Ocean dynamics of south eastern Australia, including (a) mean summer and (b) mean winter frontal activity (red indicates high activity, blue indicates low activity); and characteristic surface currents for (c) austral summer (February 2006), and (d) austral winter (June 2005), note currents were plotted every second grid point for clarity. White or black lines indicate the 200 m isobath (continental shelf).

Continental Australian east coast – The south east coast of Australia is a biologically diverse region reflecting the mixing of tropical and temperate species (111 ichthyoplankton families; Smith & Suthers 1999) caused by the interaction of the EAC and subantarctic waters. Similar to the east coast of Tasmania, most species spawn and are mostly retained nearshore due to retentive onshore transport (Table 2.2.1). However, for some species, an offshore larval phase is necessary, thus the highly variable, short-term offshore advection events are important for successful recruitment (Smith et al. 1999). Examples of the diversity of life histories in this region are given by redfish (*Centroberyx affinis*) and beaked salmon (*Gonorynchus greyi*).

Redfish spawn nearshore in summer and their larvae are retained at the Sydney shelf (Smith & Suthers 1999). This species is passively dispersed throughout their larval stage and seems to reflect the onshore or nearshore oceanographic variability (Smith et al. 1999). In contrast, beaked salmon have protracted spawning in the austral summer to autumn with multiple batch spawning on the outer shelf, with their larvae found at the shelf break (Smith 2000). In their early larval stages, beaked salmon have mostly passive dispersal and occur near the surface, making them particularly susceptible to wind and surface currents. They are often found in high densities in frontal regions (Kingsford & Suthers 1994, Gray 1996). As they age, their swimming abilities improve, and they can swim against the cross-shelf flows to maintain their near-surface distribution over the outer shelf-slope. Phytoplankton biomass is higher here due to the southward flow of the EAC along the shelf edge that uplifts nutrient-rich slope water through bottom-boundary layer transport (Tranter et al. 1986). Additionally, eddies at the shelf edge enhance regional Chl (Fig. 2.2.4d), and form SST gradients (Fig. 2.2.7a) that are beneficial for the growth of these larvae.

Triad features

Triad features are apparent off eastern Australia (Table 2.2.2), with high Chl enhancement due to upwelling, eddies, and interacting water masses. Concentration features are seen with frontal activity of these mesoscale features, the spatially-variable Subtropical Front, and turbulent wind mixing below the $250 \text{ m}^3 \text{ s}^{-3}$ threshold for much of the year. Depending on fish life history, “retention” features exist such that EAC forcing creates onshore transport in nearshore waters and eddies can act as dynamic pelagic retention cells depending on their persistence and movement. Additionally, it appears southward advection is contained in suitably warm waters for larval survival north of 43.5°S . The east coast of Australia has extremely variable oceanographic conditions. Species in this region have life histories adapted to deal with variable conditions, having protracted spawning periods or multiple

batch spawning, increasing the likelihood of their eggs and larvae coinciding with favourable oceanographic conditions, which may be localised in space as well as time.

CONCLUSIONS

Ocean triads in diverse habitats

This study has shown that the Australian marine ecosystems examined are driven by diverse oceanographic and atmospheric forcing, and elements of the ocean triad (enrichment, concentration, retention) occur across all these systems. However, the influence of the ocean triad and the specific mechanisms that produce its key features are variable in each region. Additionally, the relative importance of the different triad features is dependent on individual life histories of the reproductively active fish population. Tradeoffs between triad mechanisms are frequent for many species and different features become important at different larval stages. Some species take advantage of one aspect of the triad (i.e. transport) at the cost of another (i.e. spawning during peak productivity). For some species, these tradeoffs function well. However, many species only succeed due to high spawning output that enables sufficient larvae to survive and close the lifecycle, despite large and variable losses.

Our investigation into the physical drivers of Australian bioregions with high phytoplankton biomass is complementary to previous remote and *in situ* studies; however our interdisciplinary study makes links between distinct ocean features and their relevance to spawning and recruitment success for a variety of different regions and a suite of marine species. I believe that a firm understanding of the underlying regional oceanographic and atmospheric conditions driving recruitment to different fisheries is imperative to comprehending the likely impacts of perturbations to marine ecosystems. I find that while general principles are useful guides in marine ecosystem function, regional ecosystems and species are highly variable and should be examined individually.

**REGIONAL-SCALE RELATIONSHIPS:
PHYSICS TO PRIMARY PRODUCTIVITY**

3

3 REGIONAL-SCALE RELATIONSHIPS BETWEEN OCEAN PHYSICS AND PRIMARY PRODUCTIVITY

Variability of Biological Production in Low Wind-Forced Regional Upwelling Systems: a Case Study off Southeastern Australia

Anne-Elise Nieblas,^{a,b,*} Bernadette M. Sloyan,^c Alistair J. Hobday,^b Richard Coleman,^{c,d} and
Anthony J. Richardson^{e,f}

^a University of Tasmania, School of Zoology, Sandy Bay, Tasmania, Australia.

^b Climate Adaptation Flagship, Commonwealth Scientific and Industrial Research Organisation (CSIRO) Marine and Atmospheric Research, Hobart, Tasmania, Australia.

^c Centre for Australian Weather and Climate Research, CSIRO Marine and Atmospheric Research, Hobart, Tasmania, Australia.

^d University of Tasmania, Centre for Marine Science, Sandy Bay, Tasmania, Australia.

^e Climate Adaptation Flagship, CSIRO Marine and Atmospheric Research, Cleveland, Queensland, Australia.

^f University of Queensland, School of Physical Sciences, St Lucia, Queensland, Australia.

*Corresponding author: Anne.Nieblas@csiro.au

ACKNOWLEDGEMENTS

A. E. N. is supported by a joint Commonwealth Scientific and Industrial Research Organisation (CSIRO)–University of Tasmania Ph.D. scholarship in Quantitative Marine Science and a CSIRO Climate Adaptations National Research Flagship Ph.D. stipend. B. M. S. was funded by CSIRO Wealth from Oceans Flagship and the Australian Climate Change Science Program. I thank the following agencies for environmental data: 1) sea surface temperature – National Oceanic and Atmospheric Administration and National Aeronautics and Space Administration (NASA), 2) Sea-viewing Wide Field-of-view Sensor ocean colour – NASA, and 3) wind – National Centre for Environmental Prediction–National Centre for Atmospheric Research. Satellite data were accessed using the Spatial Dynamics Ocean Data Explorer– customised software provided by Alistair Hobday, Klaas Hartmann, Jason Hartog and Sophie Bestley. The manuscript was improved by constructive comments of two anonymous reviewers.

INTRODUCTION

Major coastal upwelling systems are driven primarily by winds that make this process highly sensitive to climate change (Bakun 1990, Snyder et al. 2003). Coastal upwelling systems account for up to 20 percent of global fish production (Mann 2000) and support major fisheries worldwide (Ryther 1969, Cushing 1971, Mann 2000). Climate change and variability, in addition to overexploitation, may severely affect fisheries production or disrupt functioning systems. A careful understanding of the present variability of these wind-driven upwelling systems is the first step before making predictions of future production and the response of fisheries to changes in the physical environment.

Coastal wind-driven upwelling is the process by which water is forced offshore by Ekman transport and is largely compensated by subsurface onshore flow from below the Ekman layer. This typically results in the upwelling of cold, nutrient-rich water into the euphotic zone. Upwelling systems are generally characterised as having high productivity, high biomass, low biodiversity, and low numbers of trophic linkages from primary to fish productivity (Ryther 1969, Sommer et al. 2002). Environmental and primary productivity fluctuations are tightly linked, and can be related closely to higher trophic level variability (Cole and McGlade 1998). Dynamic upwelling systems are mostly seasonal in their wind forcing (Mann 2000, Snyder et al. 2003), and the biological response to upwelling-favourable wind events depends on the timing, persistence, direction, and strength of the wind and the background environmental conditions (e.g., shallow mixed layer, high light levels, and warm surface water temperature).

Most major upwelling systems are located along eastern boundaries of ocean basins (Pond and Pickard 1983, Mann & Lazier 1996), such as off the coasts of California, Peru, Namibia and South Africa. The west coast of Australia does not conform to the classic eastern boundary system, as large-scale upwelling is absent. This is due to the Leeuwin Current (a unique, poleward flowing, eastern boundary current (Cresswell & Golding 1980)) that suppresses otherwise favourable upwelling conditions (Hanson et al. 2005a). Therefore, upwelling in Australia is relegated to smaller, regional systems such as those in the Gascoyne region of Western Australia (Hanson et al. 2007), the separation point of the East Australian Current from the east coast of Australia at Sugar Loaf Point (32°30'S) (Roughan & Middleton 2002), and off the Bonney Coast in south eastern Australia between Cape Jaffa and Portland (Rochford 1977, Lewis 1981, Schahinger 1987).

The Bonney Coast has the largest and most predictable upwelling in the south eastern Australian region (Butler et al. 2002) (Fig. 3.1). It supports a productive fishing ground, seabird and seal colonies, and is one of the few known feeding grounds for the endangered blue whale, *Balaenoptera musculus* (Butler et al. 2002, Gill 2002). Hynd and Robins (1967) and Rochford (1977) were among the first to suggest an upwelling off the Bonney Coast during the austral summer months. The upwelling is driven by the seasonal

migration of the subtropical ridge: a zone of high atmospheric pressure. In the austral winter, the ridge lies over the Australian continent, driving westerly, downwelling-favourable winds along south eastern Australia (Rochford 1975). During the austral summer (November to April) the ridge moves southward to lie over the Great Australian Bight (Linacre & Hobbs 1977, Sturman & Tapper 1996) and drives south easterly, upwelling-favourable winds along the Bonney Coast (Lewis 1981, Schahinger 1987, Griffin et al. 1997). Lewis (1981) noted three upwelling centres along the Bonney Coast's narrow shelf (~20–50 km wide) (Fig. 3.1b), while Gill (2004) showed that additional subsurface upwelling occurs to the east of the surface plumes.

Wind forcing is the primary driver of the Bonney Upwelling, but regional ocean circulation and climate patterns also influence the seasonal upwelling. The Flinders Current at the continental shelf-break along the Bonney Coast is part of a northern boundary current system off southern Australia (Middleton & Cirano 2002). The westward-flowing Flinders Current enhances open ocean-shelf water mass exchange that potentially preconditions wind-driven cool water upwelling by raising the thermocline on the continental shelf (Middleton & Cirano 2002, Middleton & Platov 2003). A seasonal coastal current opposes the Flinders Current with a strong south eastward flow in the winter months that reverses to a weak north westward flow in the summer (Middleton & Platov 2003). El Niño–Southern Oscillation (ENSO) conditions may also enhance upwelling in south eastern Australia during El Niño years due to the shoaling of the thermocline in the summer (Middleton et al. 2007).

Previous studies of numerous upwelling regions have identified a parabolic relationship between wind speed and productivity in Ekman-type upwelling systems (Cury & Roy 1989, Botsford et al. 2006). In these regions an 'optimal environmental window' has been defined where wind speed is strong enough to promote vertical mixing of nutrients to enhance productivity, but not so strong that it leads to turbulent mixing or advection of nutrients from the system that can reduce productivity (Cury and Roy 1989; Botsford et al. 2006). Botsford et al. (2003) suggest an optimal wind speed of 10–12 m s⁻¹ for primary productivity at a latitude and shelf width similar to the Bonney Coast (38.5°N, 35 km shelf width), and Cury and Roy (1989) suggest 5–6 m s⁻¹ for fish recruitment.

Here I investigate the relationship between upwelling and primary productivity of the regional Bonney Upwelling system determined from decadal time series of wind, sea surface temperature and surface chlorophyll. From the time series I develop three upwelling metrics (wind stress, plume area, and phytoplankton productivity approximated from satellite-derived chlorophyll *a* concentration) to determine predictive relationships amongst upwelling drivers and the biological response. The quantitative models developed in this study can be used to investigate potential effects on coastal wind-driven upwelling ecosystems due to climate change and variability at regional and global scales.

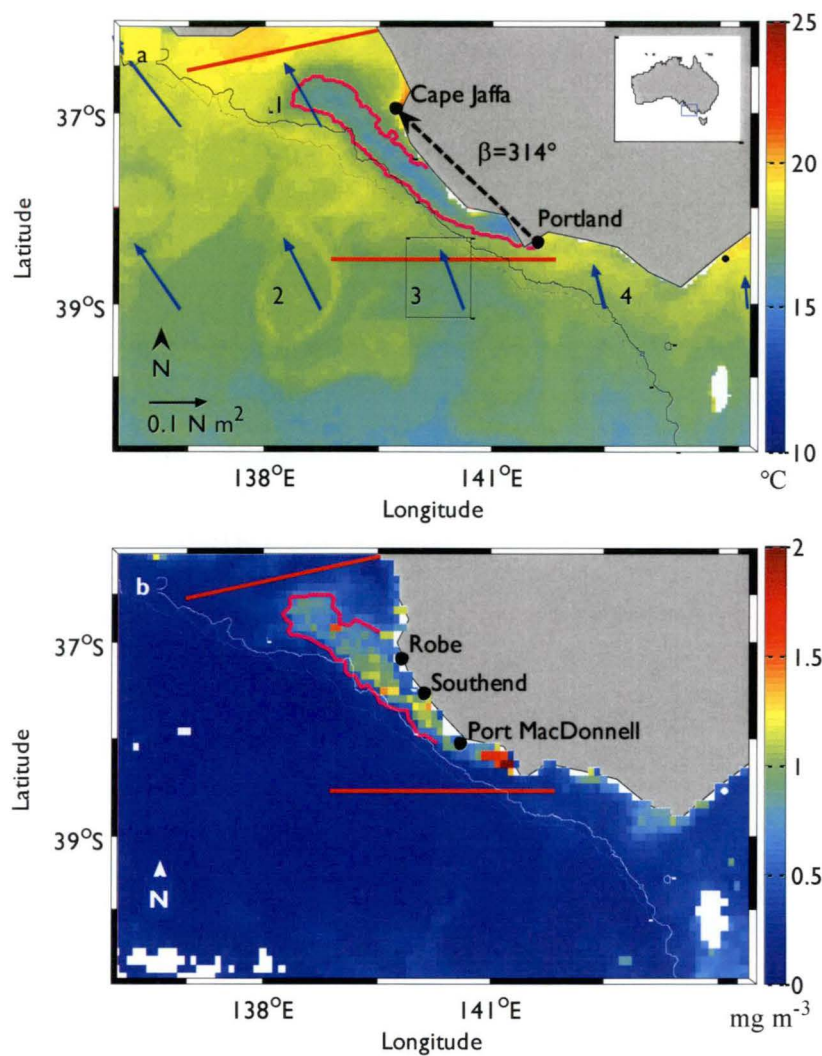


Fig. 3.1: (a) The Bonney Coast is encompassed by Cape Jaffa and Portland. NCEP-NCAR gridded wind locations (blue arrows) over the south eastern Australian ocean region. Numbered grid locations (1 to 4) identify wind values adjacent to the Bonney Coast. The boxed grid point (3) was used to represent wind values along the Bonney Coast, and developed into the upwelling wind index. The dashed black arrow along the coast indicates the dominant angle of the Bonney Coast near grid point 3 ($\beta \approx 314^\circ$). The 200 m contour represents the continental shelf (solid (a) black and (b) white lines). A polygon is defined by the northern and southern limits (red lines) and the 1000 m bathymetric contour defines the seaward edge of the upwelling region (dashed (a) black and (b) white lines) of the Bonney Coast upwelling region. The pink lines show the area of (a) anomalously low SST and (b) anomalously high SSC that represent the upwelling plume for each variable.

DATA

Wind

Upwelling-favourable wind stress was determined using wind data from the National Centre for Environmental Prediction–National Centre for Atmospheric Research (NCEP–NCAR) Reanalysis Project (Kalnay et al. 1996, Kistler et al. 2001). I used 6-hourly 10 m

NCEP–NCAR wind data from July 1993 to June 2007 that correspond with the temporal coverage of the satellite-derived sea surface temperature data. Wind data have a spatial resolution of 1.9° latitude by 1.88° longitude or $3.6 \times 10^4 \text{ km}^2$ in south eastern Australia (Fig. 3.1).

NCEP–NCAR grid locations closest to the Bonney Coast were identified (Fig. 3.1a). I used wind values at 39°S , 140.5°E (Fig. 3.1a, box 3) to represent the coastal wind that directly influences upwelling along the Bonney Coast. Daily mean wind speed was calculated from the 6-hourly wind fields, and a 5-day running mean was also generated.

Sea surface temperature and sea surface colour

The size of the upwelling sea surface temperature (SST) plume was determined using satellite-derived SST from National Oceanic and Atmospheric Administration's Advanced Very High Resolution Radiometer Local Area Coverage data. I used daily Commonwealth Scientific and Industrial Research Organisation 6-day composite SST data (Griffin et al. 2004) produced from data collected between October 1993 and June 2007. The spatial resolution of the data is 0.036° latitude by 0.042° longitude (14.6 km^2). Productivity in the upwelling-driven plume was estimated using satellite-derived sea surface colour (SSC) (chlorophyll *a*), based on Sea-viewing Wide Field-of-view Sensor (SeaWiFS) data from September 1997 to June 2007. SSC is often used to estimate phytoplankton biomass (Sathyendranath et al. 1991, Alvain et al. 2005), and although it has limitations in coastal regions, it is an appropriate proxy for upwelling systems where the primary productivity is high and variable. SSC data from the SeaWiFS satellite products are an 8-day composite with a spatial resolution of 0.0833° latitude by 0.0833° longitude (68.7 km^2).

SST and SSC data were analysed along the Bonney Coast between 36°S to 38.5°S , and to the 1000 m isobath (Fig. 3.1). This region includes coastal waters that are directly influenced by upwelling winds and shelf-scale oceanographic processes such as water mass and nutrient transport onto the continental shelf, and alongshore currents. Nearshore values within 3 km of the coast were removed due to possible land contamination in satellite observations.

METHODS

Model indices

Wind index

Upwelling wind indices have previously been defined as the wind stress component parallel to the coast (units: N m^{-2} ; Griffin et al. 1997, Mitchell-Innes 1999). Bakun (1973) defined a widely-used index based on offshore Ekman transport (units: $\text{m}^3 \text{ s}^{-1}$ per 100 meters of coastline). Other indices include the use of temperature gradients between upwelling and non-upwelling waters (Nykjaer & van Camp 1994, Shang et al. 2004), and the inclusion of

both wind and SST (Kuo et al. 2000) to represent upwelling intensity. In this study I follow Griffin et al. (1997) and define the wind index based on the wind stress parallel to the coast (τ'_v ; units: N m^{-2}) as:

$$\tau'_v = \rho_a C_d W^2 \sin(\alpha - \beta) \quad (3.1)$$

where W is wind speed, C_d is the drag coefficient ($C_d = 1.2 \times 10^{-3}$), ρ_a is air density ($\rho_a = 1.22 \text{ kg m}^{-3}$), α is wind direction, and β is the dominant angle (azimuth) of the selected coastline ($\beta = 314^\circ$) (Pond & Pickard 1983). With this index, positive (negative) values of τ'_v indicate upwelling (downwelling or relaxation).

SST index

Following Shang et al. (2004), the physical effect of upwelling-favourable winds was defined as a 1°C cooling from mean monthly SST off the Bonney Coast. Anomalously cool SST values ($\Delta \text{SST} \leq -1^\circ\text{C}$) were found for daily 6-day composite SST images and the largest continuous area was defined as the upwelling plume (ASST_a ; units: km^2) (Fig. 3.1a), and became the SST upwelling index. Smaller, isolated SST anomalies associated with the upwelling plume were occasionally present but contributed little to the overall area of the plume.

SSC index

SSC anomalies (SSC_a) were defined as chlorophyll a (Chl a) values $> 0.6 \text{ mg m}^{-3}$. Although this is less than thresholds in other more eutrophic regions (Fitch & Moore 2007: 0.8 mg m^{-3} ; Kahru & Mitchell 2000: 1 mg m^{-3}), southern Australia is generally oligotrophic with mean coastal SSC concentrations of $0.36 \pm 0.14 \text{ mg m}^{-3}$. Therefore a $\Delta \text{SSC} > 2$ standard deviations (0.6 mg m^{-3}) was regarded as an anomalous signal. I define the anomalously high SSC area (ASSC_a ; units: km^2) following the methods used to determined ASST_a (Fig. 3.1b). Additional steps to develop the SSC index ($[\text{Chl } a]$) were to sum the chlorophyll a within the anomalous region ($\sum \text{SSC}_a$), and divide by the area of the anomalous region (ASSC_a), such that $[\text{Chl } a] = \sum \text{SSC}_a / \text{ASSC}_a$ (units: $\text{mg m}^{-3} \text{ km}^{-2}$).

Time series analysis

Continuous wavelet transform analysis of the two upwelling activity indices, and one upwelling productivity index was performed to determine objectively the significant periodicities and their variability for each time series. A cross wavelet transform was used to assess the significant common periods and power, and provide an indication of the phase relationships among indices (Grinsted et al. 2004). For this analysis, each time series must have the same temporal range and time step. Therefore cross wavelet transforms were

performed between daily wind and $ASST_a$ (1994–2006), eight-day mean wind and $[Chl\ a]$ (1998–2006), and eight-day mean $ASST_a$ and $[Chl\ a]$ (1998–2006). I performed wavelet analysis using freely available software (see:

<http://www.pol.ac.uk/home/research/waveletcoherencece>)

Identification of significant factors and model development

I used analysis of variance (ANOVA) techniques and the Ryan-Einot-Gabriel-Welsch (REGWQ) multiple range test to identify significant differences among levels of the explanatory variables.

Generalised Additive Models (GAMs) were used initially to assess the shape of the relationship between the monthly response ($\ln[Chl\ a]$) and monthly predictors (wind; $ASST_a$) variables. Relationships between response and both predictors were linear, justifying the use of a multiple regression approach to build and assess quantitative relationships between the predictors and response. Additional predictor time series also considered were: the temperature of the upwelling plume, and Niño 3.4 and Southern Oscillation Index (SOI) to represent ENSO. Preliminary analysis indicated that these indices were not significant and did not improve the predictive skill of the models greatly above that obtained using wind and SST indices alone. However, a relationship was suggested between $[Chl\ a]$ and ENSO for the strongest El Niño events, but this relationship was not statistically significant, possibly due to the short time series.

Due to the temporal range of the SeaWiFS dataset, indices were evaluated for the period 1998–2006. They were initially lagged by periods of 0–3 months to assess if any phase lags existed between the variables. Zero lag was found to give the best relationships, as presented below. Models were validated using wind, SST, and SSC data for 2007 that were withheld from model development. Statistically significant results are defined as $p \leq 0.05$.

RESULTS

Significant time scales

The three indices (wind, $ASST_a$, $[Chl\ a]$) show significant annual periodicities over all years (Fig. 3.2), except the wind index for 1997–1998. The absent wind signal during 1997–1998 at the annual period coincides with the very strong 1997–1998 El Niño event. A semi-annual period is apparent for some years in both the $ASST_a$ and $[Chl\ a]$ indices. All indices show high interannual variability at shorter time scales (8 days to 2 months for wind and $ASST_a$, and 16 days to 2 months for $[Chl\ a]$) (Fig. 3.2). High frequency variability of the wind index is found throughout the entire time series. However, the high frequency variability in the $ASST_a$ and $[Chl\ a]$ indices occur only during the austral summer (November–April).

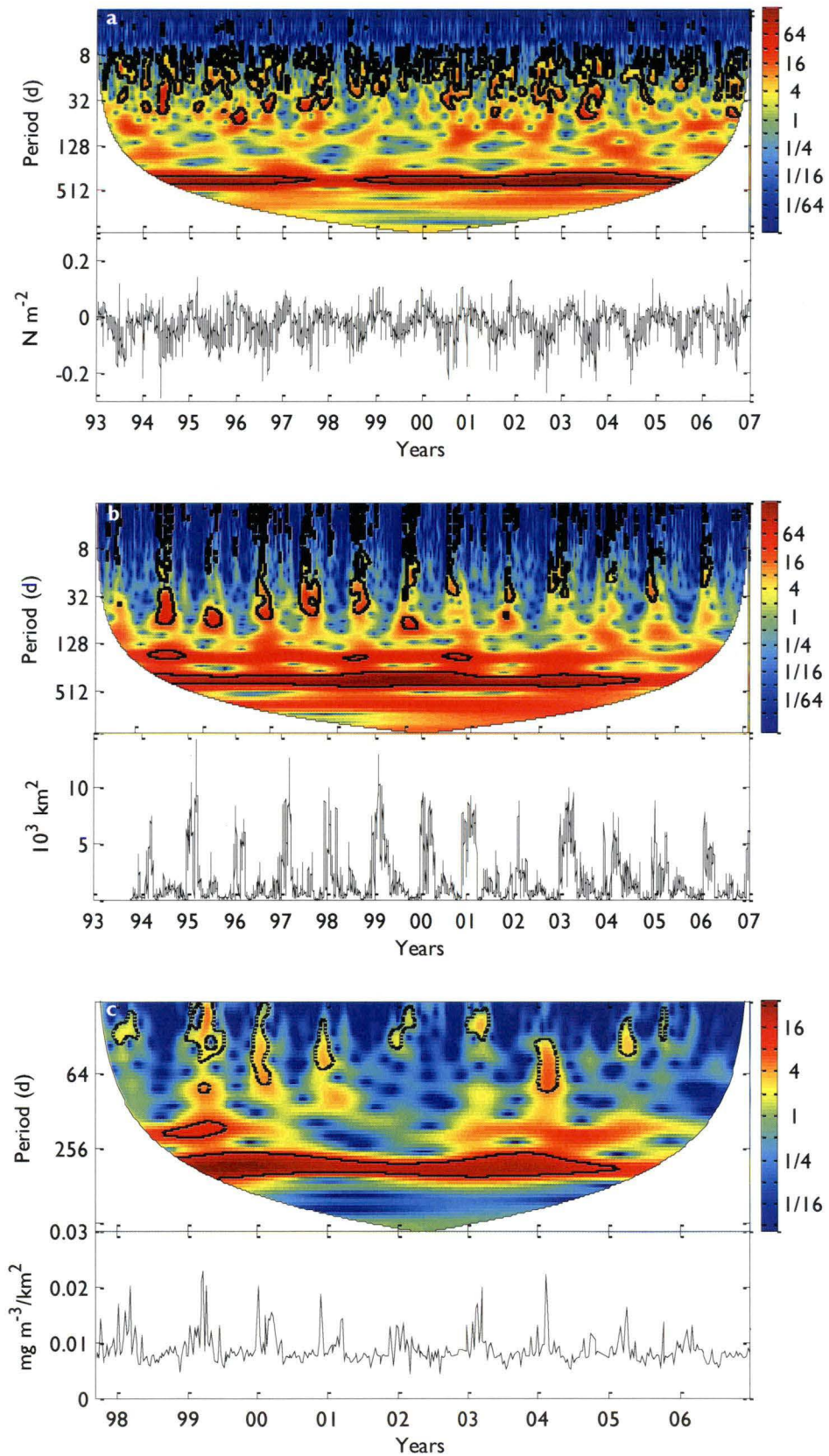


Fig. 3.2: Wavelet transform (colour bar indicates power, black contours = 5% significance) and time series of (a) daily alongshore wind stress (1994–2006) (positive wind stress is easterly and upwelling-favourable), (b) daily ASST_a (1994–2006), and (c) 8-day [Chl *a*] (1998–2006) for the Bonney Coast.

Cross-wavelet transforms amongst the three indices (not shown) indicate that there are significant relationships between the time series at the annual period indicating strong seasonal activity. The indices are in phase with one another, suggesting cause-and-effect relationships. Higher power is shared between $ASST_a$ and $[Chl\ a]$ than between wind and $[Chl\ a]$. Significant signals are evident at: 8 days to 2 months for wind and $ASST_a$; 16 days to 2–3 months for $ASST_a$ and $[Chl\ a]$; and 16 days to just over 1 month for wind and $[Chl\ a]$. However, coherent power between any two of the indices consistently occurs at a monthly period during the austral summer. Therefore I used mean monthly data to develop the multiple regression models. This analysis suggests the need for further examination of the variability of the three indices at the seasonal timescale, in which the year is divided into an 'upwelling season' and a 'non-upwelling season', and inter- and intra-upwelling season variability.

Seasonal variability

The annual signal apparent in the wind stress index relates to the cyclical pattern of upwelling-favourable wind along the Bonney Coast (Fig. 3.2a). There was a significant difference in percentage of days of upwelling-favourable winds between the upwelling season (November–April) and the non-upwelling season (May–October) of 48% and 17%, respectively ($F_{25}=106.15$, $p<0.0001$, $n=26$). In this study I define an upwelling event as one or more days of positive alongshore wind stress. Upwelling events occur 6.3 ± 2.4 times throughout May to October and 10.2 ± 1.9 times during November to April (Fig. 3.3a).

A significant difference was found between the two seasons based on wind stress intensity ($F_{4747}=1082.4$, $p<0.0001$, $n=4748$). Note that annual mean wind stress is westerly for both upwelling and non-upwelling seasons, but the numerous easterly wind events that occur between November and April result in a significant decrease in the strength of the mean westerly wind during the upwelling season (Fig. 3.3b). Therefore, during the upwelling season there was a weakening of the usual downwelling-favourable westerly wind stress that is stronger during the non-upwelling season (Fig. 3.3b). Maximum easterly wind stress occurs during the upwelling season (Fig. 3.2a). However, the Bonney Upwelling region was found to be a low-wind forced system with an overall wind speed of only 4.1 m s^{-1} . Duration of upwelling events in the upwelling season were significantly longer (8.9 ± 1.7 days) than in the non-upwelling season (4.5 ± 1.4 days) ($F_{212}=20.63$, $p<0.0001$, $n=213$) (Fig. 3.3a). Quiescent (low or downwelling wind stress) periods during the upwelling season were significantly shorter (10.1 ± 4.1 days) than during the non-upwelling period (26.5 ± 9.5 days) ($F_{224}=56.35$, $p<0.0001$, $n=225$) (Fig. 3.3a), implying that upwelling events occur more regularly in the upwelling season.

Similar to wind, both $ASST_a$ ($F_{4406}=1123.04$, $p<0.0001$, $n=4407$), and $[Chl\ a]$ ($F_{484}=166.02$, $p<0.0001$, $n=485$) show significant seasonal differences between the upwelling

and non-upwelling season. In the upwelling season of November to April, the largest upwelling plume area and maximal chlorophyll *a* response occurred (Fig. 3.3).

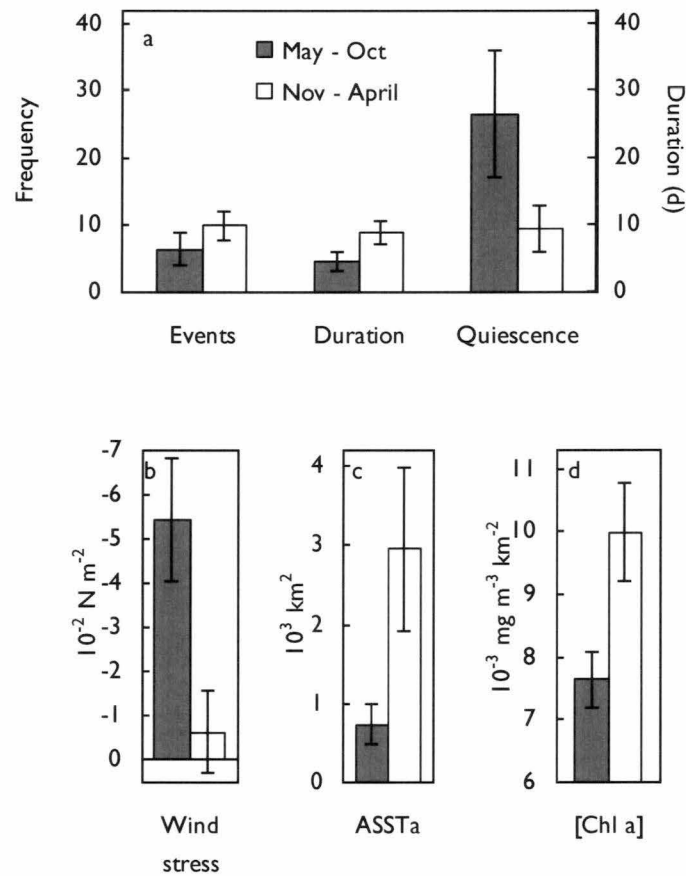


Fig. 3.3: Seasonal variability between the non-upwelling season (May–October) and the upwelling season (November–April) for (a) the mean frequency of upwelling events per season, duration of events (days), length of periods of quiescence between events (days), (b) the mean overall wind stress (N m^{-2}) (positive wind stress is easterly and upwelling-favourable), (c) ASST_a (km^2), and (d) [Chl *a*] ($\text{mg m}^{-3} \text{ km}^{-2}$). Error bars represent standard error around the mean.

Interannual variability

Significant interannual variability amongst upwelling seasons was found for wind stress intensity ($F_{2325}=8.13$, $p<0.0001$, $n=2326$), with overall mean wind stress of $-6.4 \pm 9.2 \times 10^{-3} \text{ N m}^{-2}$. The strongest upwelling-favourable wind stress occurred in 1998–1999 and 1999–2000, and was weakest in 1993–1994, 1997–1998, and 2005–2006. Weak upwelling-favourable wind stress in the upwelling season coincides with the 1993–1994, 1997–1998, and 2006–2007 El Niño years, however no wind stress signal is found for the 2002 to 2005 El Niño. Upwelling winds based on frequency and duration of events, and length of quiescent periods were variable among seasons, but not significantly different (Fig. 3.4a,b; Table 3.1). A significant difference was found amongst upwelling seasons for ASST_a

($F_{2230}=24.11$, $p<0.0001$, $n=2231$). The largest surface upwelling plume area was in 1998–1999, 2000–2001, and 2002–2003. The smallest anomalous SST area are found in 1993–1994, 2001–2002, 2004–2005, and 2005–2006 (Fig. 3.4c), coinciding with several weak El Niño events. The REGWQ test found two groupings for wind stress variability and three

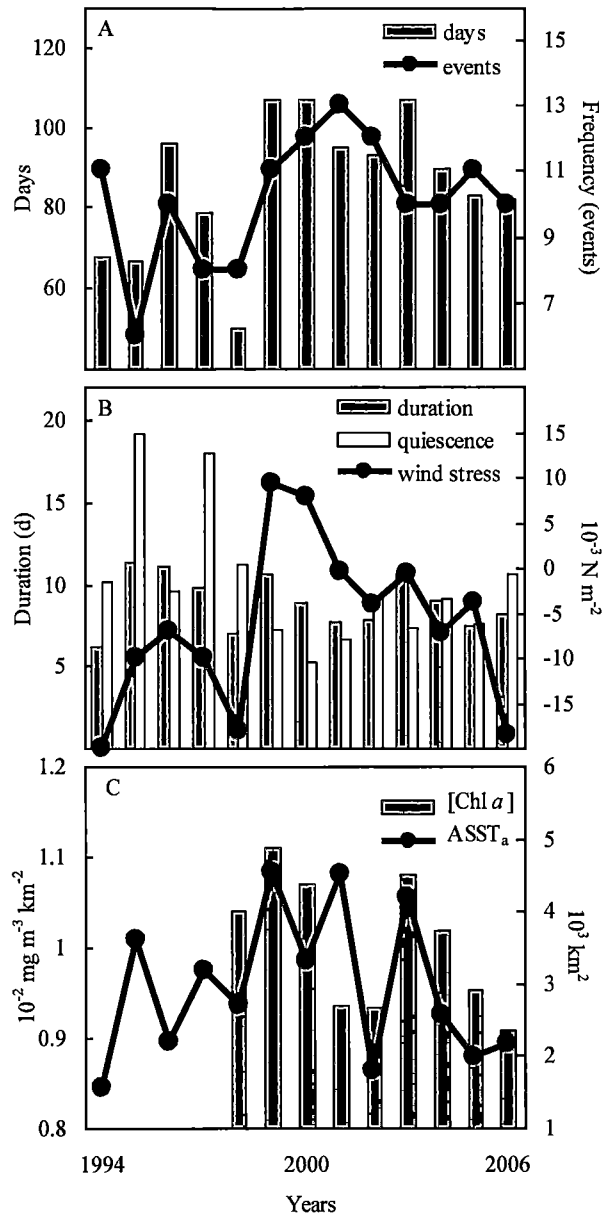


Fig. 3.4: Interannual variation of (a) number of upwelling days and frequency of upwelling events per year (b) mean annual duration of upwelling events and quiescent periods, and mean annual wind stress intensity (N m^{-2}), and (c) mean annual [Chl *a*] ($\text{mg m}^{-3} \text{ km}^{-2}$) and ASST_a (km^2) of the upwelling season (November–April).

Table 3.1: Interannual variability of the mean number of days of upwelling-favourable wind stress per year, the mean number of upwelling events per year, annual mean duration of upwelling events (d), wind stress (N m^{-2}), length of periods of quiescence between upwelling events (d), ASST_a (km^2), and $[\text{Chl } a]$ ($\text{mg m}^{-3} \text{ km}^{-2}$). *, **, *** Indicate significant interannual REGWQ groupings between years in ascending value order (e.g., * lowest grouping, *** highest grouping).

Seasons	Days	Events	Duration (d)	Wind stress (10^{-3} N m^{-2})	Quiescence (d)	ASST_a (10^3 km^2)	$[\text{Chl } a]$ ($10^{-2} \text{ mg m}^{-3} \text{ km}^{-2}$)
1994	68	11	6.2	-19.9 *	10.2	1.57 *	-
1995	67	6	11.3	-10 *	19.2	3.6 ***	-
1996	96	10	11.1	-7.07 *	9.6	2.19 *	-
1997	79	8	9.9	-10.1 *	18.0	3.17 **	-
1998	50	8	7.0	-18.0 *	11.3	2.7 *	1.04
1999	107	11	10.6	9.45 **	7.2	4.54 ***	1.11
2000	107	12	8.9	7.78 **	5.2	3.31 **	1.07
2001	95	13	7.8	-0.333 **	6.7	4.51 ***	0.936
2002	93	12	7.8	-4.04 **	9.3	1.81 *	0.935
2003	107	10	10.7	-0.698 **	7.4	4.2 ***	1.08
2004	90	10	9.0	-7.33 *	9.1	2.58 *	1.02
2005	83	11	7.5	-3.85 **	7.6	1.99 *	0.953
2006	82	10	8.2	-18.5 *	10.7	2.17 *	0.909
Mean	86.5 ± 17.4	10.2 ± 1.9	8.9 ± 1.7	-6.4 ± 9.2	10.1 ± 4.1	2.95 ± 1.03	1.01 ± 0.074

different groupings for ASST_a activity (Table 3.1), but El Niño years are found within most groupings. $[\text{Chl } a]$ showed no significant interannual difference among upwelling seasons ($F_{484}=2.44$, $p=0.01$, $n=485$). However, upwelling seasons of higher $[\text{Chl } a]$ are associated with favourable wind forcing and large upwelling plume area (Table 3.1), although this is not statistically significant.

The comparison between upwelling season variability and ENSO does not provide a consistent relationship. The strong 1997–1998 El Niño corresponds to an upwelling season that is characterised by infrequent upwelling events with short durations, long periods of quiescence between events, and low wind stress intensity. However, ASST_a and $[\text{Chl } a]$, had average anomalous area and concentration, respectively (Fig. 3.2). Years of weak El Niño events are inconsistent in wind pattern, having both frequent and infrequent upwelling events, short and long duration events, short and long periods of quiescence between events, and both high and low wind stress (Table 3.1). The SST surface plume and chlorophyll a response for weak El Niño years are variable as well (Table 3.1). Given that the development of any El Niño is unique, a longer time series is needed to characterise the effect on the Bonney Upwelling.

Intra-seasonal variability

Within the upwelling season, there was no significant monthly (November–April) difference in frequency of upwelling events. The difference in the number of upwelling days is marginally non-significant ($F_{55}=2.12$, $p=0.078$, $n=56$) amongst months of the upwelling season, and a significant ($F_{2355}=27.97$, $p<0.0001$, $n=2356$) difference was detected for the magnitude of the wind stress (Table 3.2). The REGWQ multiple range tests showed that February and January have the strongest upwelling wind stress that are significantly different from March, November and December, and April. Duration of upwelling wind events also shows a significant difference amongst months of the upwelling season ($F_{126}=3.81$, $p=0.0031$, $n=127$), indicating that upwelling-favourable winds are more persistent in January and February. Quiescent periods were not significantly different amongst months. The middle of the upwelling season (January–February) has stronger and more persistent upwelling wind events than found at the beginning and end of the season (Fig. 3.5a).

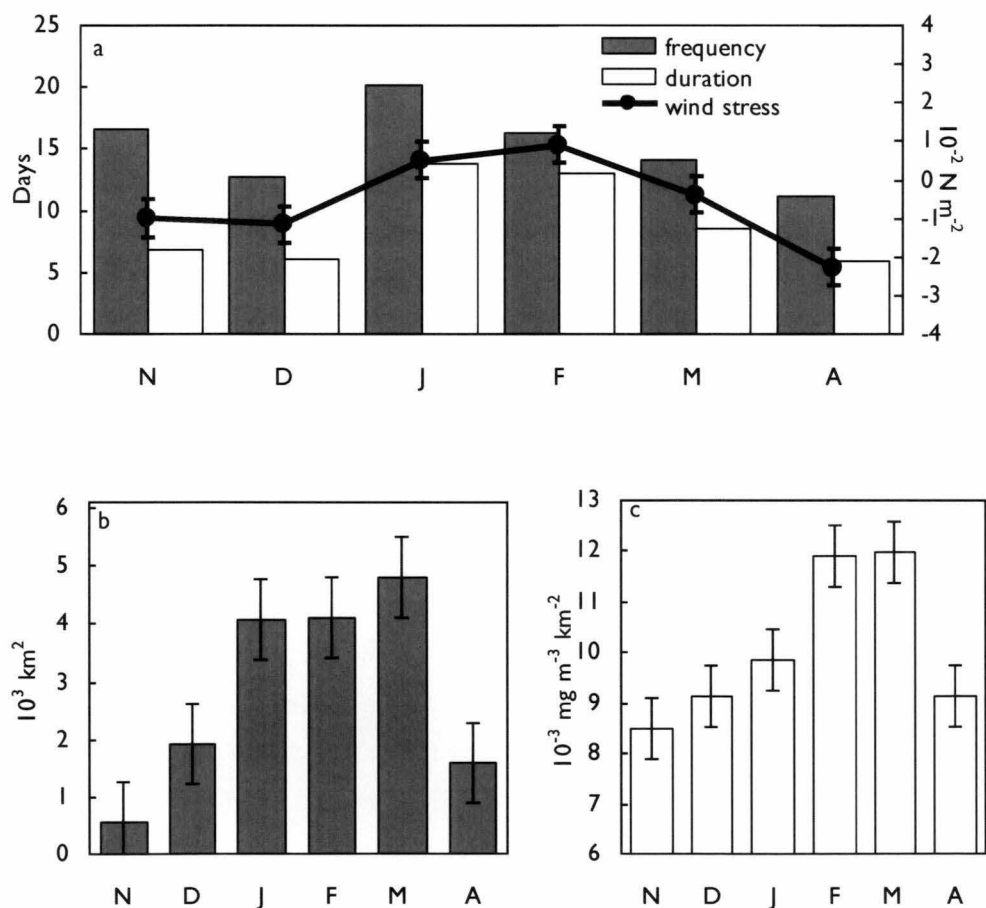


Fig. 3.5: Seasonal variation of (a) number of upwelling days per month, duration of upwelling events (d), and wind stress intensity (N m^{-2}), and (b) ASST_a (km^2) over 1994–2006, and (c) $[\text{Chl } a]$ ($\text{mg m}^{-3} \text{ km}^{-2}$) over 1998–2006 for the months within the upwelling season (November–April). Error bars represent standard errors of means.

REGIONAL-SCALE RELATIONSHIPS

ASST_a and [Chl *a*] both show significant differences within the upwelling season (ASST_a: $F_{2230}=178.22$, $p<0.0001$, $n=2231$; [Chl *a*]: $F_{182}=6.97$, $p<0.0001$, $n=183$). The largest anomalous SST area and chlorophyll concentration is in March (Table 3.2, Fig. 3.5b,c), which lags the wind stress slightly (Fig. 3.5).

All three indices have a similar pattern during the upwelling season with relatively low values at the beginning of the upwelling season (November), a maximum in the middle of the season (January–March) that then decreases to values typical of the non-upwelling season by the end of autumn (April–May).

Table 3.2: REGWQ multiple range test groupings and orders for frequency of upwelling days per month, wind stress intensity (N m^{-2}), and duration of upwelling events (d). Separate groupings delineated by commas, and are listed in descending order.

	REGWQ Grouping and order	<i>p</i>
Frequency (d)	Jan Nov Feb Mar Dec Apr	0.0778
Wind stress (N m^{-2})	Feb Jan, Mar Nov Dec, Apr	<0.0001
Duration (d)	Jan Feb, Mar, Nov Dec Apr	0.0031
ASST _a (km^2)	Mar, Feb Jan, Dec Apr, Nov	<0.0001
[Chl <i>a</i>] ($\text{mg m}^{-3} \text{ km}^{-2}$)	Mar Feb, Jan Apr Dec Nov	<0.0001

Upwelling index relationships

The first multiple regression relationship I present uses the 1998 to 2006 monthly alongshore wind (τ'_v) and ASST_a as predictor variables, and natural log-transformed [Chl *a*] as the response variable with no lag between indices. A significant positive relationship was found for both predictors ($F_{103}=49.00$, $p<0.0001$, $r^2=0.49$):

$$\ln[\text{Chl } a] = 0.9406 \tau'_v + 4.679 \times 10^{-5} \text{ASST}_a - 4.83 \quad (3.2)$$

Wind and ASST_a explain 50% of the variability of the natural log-transformed chlorophyll concentration in the Bonney Upwelling region.

The second relationship I examine is between 1998 to 2006 monthly wind and chlorophyll. A significant positive relationship was found for the predictor variable ($F_{104}=63.13$, $p<0.0001$, $R^2=0.38$):

$$\ln[\text{Chl } a] = 1.588 \tau'_v - 4.732 \quad (3.3)$$

Wind explains approximately 40% of the variability of the natural log transformed chlorophyll concentration in the Bonney Upwelling region. Niño 3.4 and SOI indices to represent ENSO were not significant predictors of [Chl *a*] and did not improve the skill of

either of the above models ($F_{104}=2.61$, $p=0.01$, $R^2=0.085$ and $F_{104}=1.89$, $p=0.102$, $r^2=0.055$, respectively).

I validated the wind and ASST_a and wind models (Eq. 3.2, 3.3) using 2007 wind, ASST_a, and [Chl *a*] data (Fig. 3.6). An examination of the total data set (1998–2007) for the wind and ASST_a model shows that the model simulates well the seasonal [Chl *a*] cycle; however it does not capture the magnitude of the variability (Fig. 3.6). The wind model also simulates the [Chl *a*] seasonal cycle, but the magnitude of the [Chl *a*] signal is reduced (Fig. 3.6). The coefficient of determination of the [Chl *a*] predicted from the wind and ASST_a and wind models for 2007 is $r^2=0.82$, ($F_{10}=20.5$, $p<0.0001$, $n=12$); and $r^2=0.19$ ($F_{11}=2.35$, $p<0.0001$, $n=12$), respectively. These results show that when used in simple linear models, the wind and ASST_a provide some prognostic skill for [Chl *a*] in this wind-driven upwelling ecosystem.

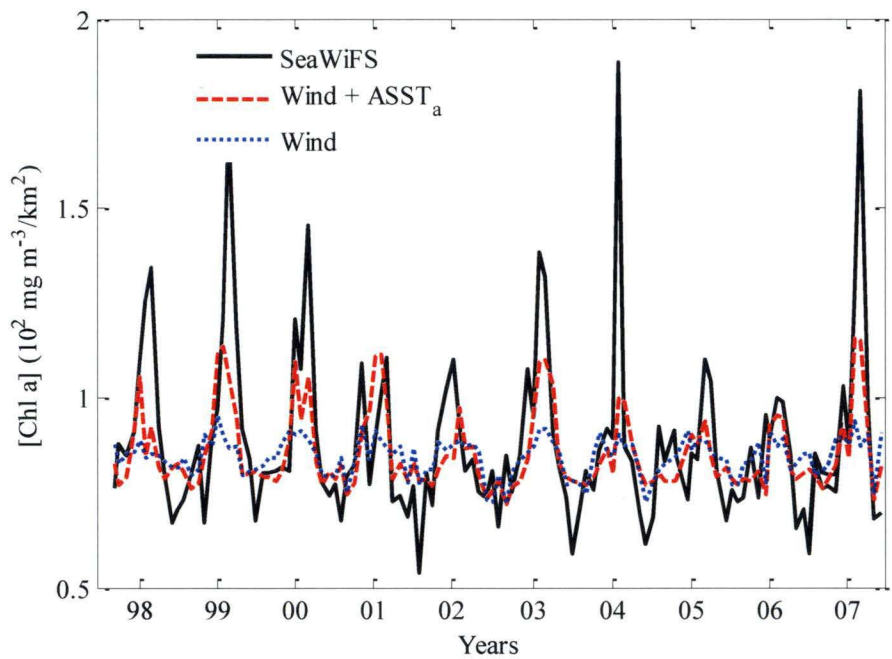


Fig. 3.6: A comparison of the observed [Chl *a*] as derived from the SeaWiFS satellite (solid line) against the modelled [Chl *a*] from wind + ASST_a (dashed line), and wind (dotted line).

DISCUSSION

I show that the Bonney Upwelling has distinct seasonal, inter-seasonal, and intra-seasonal variability, similar to many upwelling systems worldwide (Nykjaer & van Camp 1994, Mann 2000). I find the Bonney Coast to be a low-wind upwelling system with mean wind speeds of approximately 4 m s^{-1} , substantially less than the optimal wind speeds found in other upwelling systems (Cury & Roy 1989, Botsford et al. 2003). I find that a linear relationship between wind and marine primary productivity is applicable in low-wind systems. This

indicates that for these systems, higher wind speeds lead to greater nutrient input and enhanced phytoplankton productivity. Therefore, the models produced here are useful for low-wind regimes that do not exceed or attain the maximum wind-productivity threshold (so called optimal environmental window). The temporal variability for the Bonney Upwelling has a predictable pattern in both the driving forces and the biological response that enables us to develop simple predictive linear models to provide further understanding of low wind-forced coastal upwelling systems. These simple linear models are able to simulate the interannual variability of the chlorophyll *a* response to upwelling, however, do not capture intra-seasonal variability. However, as more ocean colour data becomes available and is incorporated into the models, their ability to capture intra-seasonal variability and their prognostic skill is likely to improve.

Along the Bonney Coast upwelling-favourable winds predominantly occur in the austral summer due to the southward migration of the subtropical ridge, which alters position from over the continent during the austral winter (May–October) to over the Great Australian Bight in the austral summer (November–April) (Sturman & Tapper 1996). Although the wind is the primary driver of the coastal upwelling, seasonal changes of the ocean circulation in the Great Australian Bight act to enhance the primary productivity associated with the upwelling winds. In the austral summer, the Flinders Current, a shelf break current, enhances the transport of open ocean water onto the narrow continental shelf (Herzfeld & Tomczak 1999, Middleton & Cirano 2002, Middleton & Platov 2003). The increased flux of open ocean water onto the continental shelf results in a shoaling of the thermocline (Fig. 3.7a) and increased nutrient concentrations below the mixed layer (Fig. 3.7b,c). The shallow thermocline and nutricline off the Bonney Coast in austral summer ensure the offshore Ekman flow is replaced by cooler and nutrient-rich water from depth (Kämpf et al. 2004).

In this study, high levels of $ASST_a$ and $[Chl\ a]$ are associated with consistent and persistent upwelling winds followed by a quiescent period of approximately 10 days, similar to other upwelling systems (Gonzalez-Rodriguez et al. 1992, Snyder et al. 2003). The 10-day quiescent period agrees with Bakun (1996), who suggested that calm periods five days or longer are sufficient to promote biological activity. Nutrients supplied to the euphotic zone during spring and summer are readily utilized due to the long duration of photosynthesis each day and relatively warm ambient surface water temperature. Phytoplankton respond to these favourable conditions (Brown & Field 1986), and result in a surface chlorophyll plume.

I found no clear relationship between inter-seasonal upwelling variability and ENSO. Many of the El Niño events that coincide with our time series are relatively weak (e.g., only slightly negative SOI values during 2002–2005). The ENSO cycle is generally 3 to 5 years, and our 13- and 10-year SST and SSC time series, respectively, are too short for

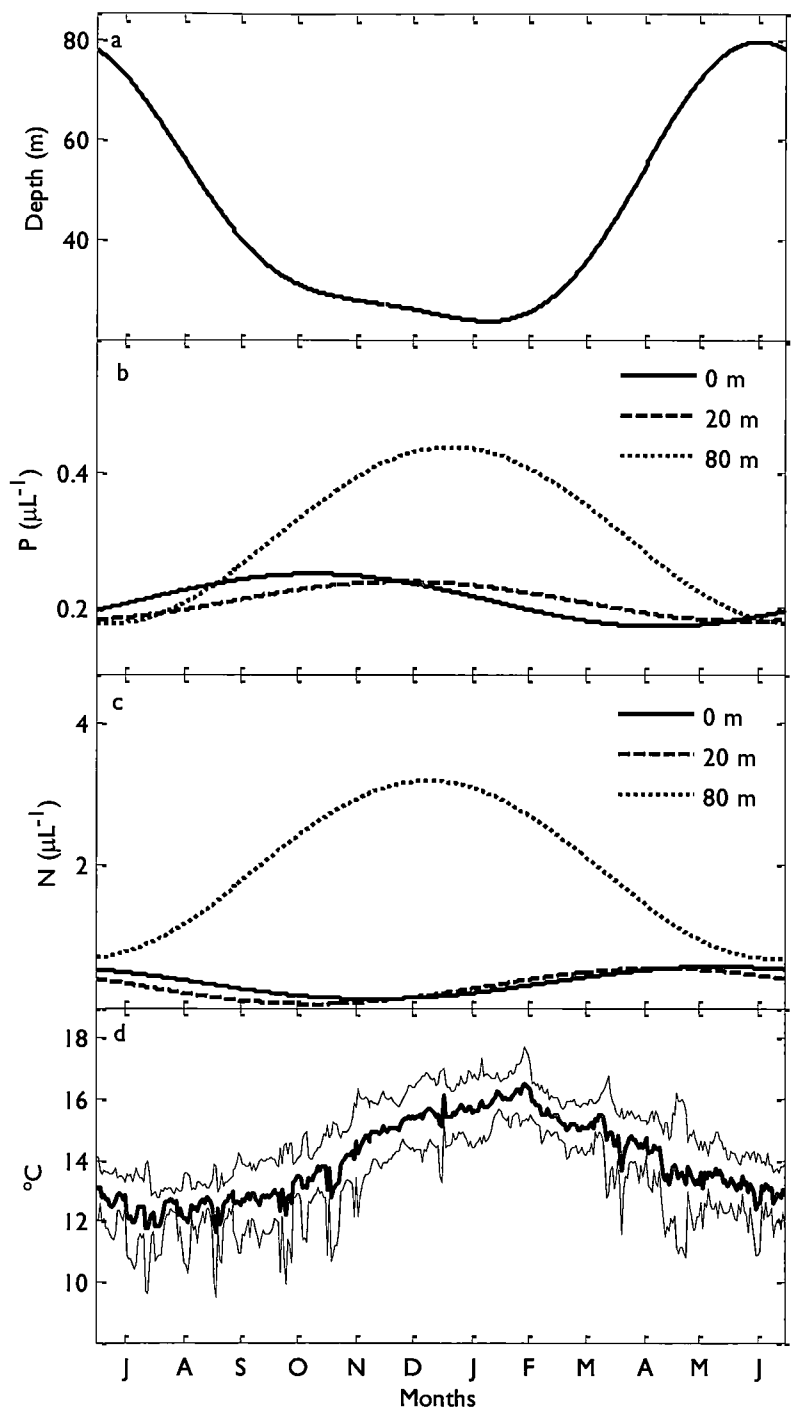


Fig. 3.7: CSIRO Atlas of Regional Seas (CARS; Dunn & Ridgway 2002, Ridgway et al. 2002) (a) mixed layer depth, and (b) phosphate and (c) nitrate concentration ($\mu\text{mol L}^{-1}$) at the surface (0 m), base of the summer mixed layer (20 m), and base of the winter mixed layer (80 m) on the continental shelf at a point off the Bonney Coast ($\sim 38.5^{\circ}$ latitude, 141° longitude) and (d) mean SST climatology (heavy line) ± 1 standard deviation (light lines) within the upwelling plume.

determining the relationship between the Bonney Upwelling and ENSO. However, I showed that the 1997–1998 El Niño that was characterised by rapid development and strong negative SOI did correspond to variability in upwelling wind forcing over the Bonney region. Middleton et al. (2007) suggested that El Niño events could shoal the thermocline during summer in south eastern Australia due to changes in regional ocean circulation. The 1997–1998 El Niño corresponds with weak upwelling wind stress and short wind event duration. However, no effect on $ASST_a$ and $[Chl\ a]$ was observed. The $ASST_a$ and $[Chl\ a]$ during the 1997–1998 El Niño may have been maintained by an anomalously shallow thermocline and nutricline. The sustained $ASST_a$ and $[Chl\ a]$ signal during the El Niño year of weak upwelling wind supports the suggestion that off the Bonney Coast during an El Niño year in the austral summer, the thermocline is anomalously shallow as a result of ocean circulation variability (Middleton et al. 2007). This also indicates that including a circulation index such as the strength of the Flinders Current may be beneficial to future studies on the relationship between Bonney Coast productivity and ENSO.

Our results indicate a distinct intra-seasonal pattern of upwelling wind and surface response similar to other seasonal upwelling systems that was characterised into four distinct phases that concur with phases found for the western Agulhas ('onset', 'sustained', 'quiescent', and 'downwelling') (Mitchell-Innes et al. 1999). I distinguish the first phase (onset), beginning in November and December at the start of the austral summer, by a variable wind pattern that is due to the faltering and shifting position of the subtropical high-pressure cell. The early upwelling season wind events along the Bonney Coast contribute to the priming of upwelling by weakening the pycnocline (Griffin et al. 1997, Richardson et al. 2003), while the Flinders Current shoals the pycnocline (Middleton & Platov 2003). Also, background environmental conditions are not yet favourable for phytoplankton growth due to low light levels and cool SST within the upwelling plume and on the shelf (Brown & Field 1986) ($\sim 14^\circ\text{C}$) (Fig. 3.7d).

The second distinct phase of upwelling (sustained) is the separation point between 'biologically irrelevant' and 'biologically relevant' upwelling, in which the upwelling winds are sufficient to overcome background ocean processes and translate into productivity-favourable conditions. In January and February, I found the strongest winds with frequent events of long duration along the Bonney Coast. This enables upwelling winds to penetrate the mixed layer, and bring nutrient-rich water into the surface layer. With increasing day length, radiant heating warms the SST plume ($\sim 16^\circ\text{C}$) (Fig. 3.7d). Due to sustained upwelling-favourable winds, and warmer, more stable conditions, $[Chl\ a]$ increases from January to February.

I observed the third phase (quiescent) to occur in March when winds begin to relax after having reached their peak in February along the Bonney Coast. Conditions are highly favourable for biological activity in the mature upwelling plume with relatively warm SST

(~15–16°C) (Fig. 3.7d), high light levels and low wind activity (Brown & Field 1986). This is consistent with Lasker's theory (1975, 1978) that it is the stable periods after a nutrient influx that are important for growth and production (Levasseur et al. 1984, Brown & Field 1986). I show the final phase (downwelling) to begin in April when downwelling-favourable winds that force surface water onshore dominate the system and similar conditions persist for the remainder of the year (May–October), ceasing enhanced primary production.

The analysis of the three upwelling indices enables us to clearly approximate a regular intra-seasonal cycle of primary production: the upwelling season begins slowly in November and December, peaks from January to March, and then declines from April. Although the Bonney Upwelling is driven by different atmospheric and oceanic circulation and is characterised by low-wind velocities, this intra-seasonal pattern is consistent with major seasonal upwelling systems (Gonzalez-Rodriguez et al. 1992, Snyder et al. 2003), and particularly concurs with the intra-seasonal phases characteristic of the western Agulhas upwelling system (Mitchell-Innes et al. 1999).

Given the in-phase, cause-and-effect relationship of the three upwelling indices I develop two linear models to predict chlorophyll concentration along the Bonney Coast. The first linear relationship I develop (wind and ASST_a) accounts for nearly 50% of the variability and indicates that consistent upwelling-favourable wind stress and a large SST plume lead to high levels of surface chlorophyll concentration. The second model shows that upwelling wind stress alone accounts for nearly 40% of the approximated primary productivity. Although the wind is the initial and primary driving force of the upwelling, its relationship with [Chl *a*] is weaker. This is due to the effect of other environmental factors, including light availability, ambient SST, depth of the thermocline and nutricline, and regional ocean circulation.

Although other environmental conditions influence primary productivity, the simple linear models developed here are able to simulate the seasonal upwelling-driven chlorophyll concentrations off the Bonney Coast. Due to the linearity of the relationships between wind and chlorophyll, these upwelling models are useful for assessing the effect of climate change and variability on chlorophyll concentration in low wind-forced coastal upwelling systems when considered with other environmental factors that affect biological activity. I note that if wind forcing increases with climate change as predicted (Bakun 1990) and exceeds the optimal threshold limit for primary productivity, additional terms may need to be added to the model to reflect the non-linear response to increased wind speed.

As the Bonney Upwelling supports feeding and fishing grounds for abundant marine life and is considered an important conservation area (Butler et al. 2002), it is imperative to understand the connection between the ecosystem-driving process of the upwelling and its associated biology. In this study I have shown that the Bonney Upwelling is a predictable regional system whose temporal variability conforms to larger and more intensely studied

wind-driven upwelling systems. Here they are combined in simple linear relationships with wind stress; however, I note that other systems may have more complex relationships to environmental influences. The models I develop in this study show skill in predicting interannual [Chl *a*] variability, and provide a simple way to monitor the variability of regional upwelling that may help assess the effect of changing climate. The simple models I develop in this study provide a method of assessing the effect of decadal or longer variability of approximated primary production in low wind-forced upwelling systems at regional and global scales.

**REGIONAL-SCALE RELATIONSHIPS:
PHYSICS TO FISHERIES PRODUCTIVITY**

4

4 REGIONAL-SCALE RELATIONSHIPS BETWEEN OCEAN PHYSICS AND FISHERIES PRODUCTIVITY

Environmental Mechanisms Driving Variability in Catch Rates of Two Contrasting Marine Species: Arrow Squid (*Nototodarus gouldi*) and Gummy Shark (*Mustelus antarcticus*) in an Australian Upwelling Region

Anne-Elise Nieblas^{a,b,*}, Malcolm Haddon^c, Bernadette M. Sloyan^{c,d}, Alan J. Butler^c and
Anthony J. Richardson^{e,f}

^a University of Tasmania, School of Zoology, Sandy Bay, Tasmania, Australia.

^b Commonwealth Scientific and Industrial Research Organisation (CSIRO) Climate Adaptation
Flagship National Research Flagship, CSIRO Marine and Atmospheric Research, Hobart, Tasmania,
Australia.

^c CSIRO Wealth from Oceans National Research Flagship, CSIRO Marine and Atmospheric
Research, Hobart, Tasmania, Australia.

^d Centre for Australian Weather and Climate Research, CSIRO Marine and Atmospheric Research,
Hobart, Tasmania, Australia

^e CSIRO Climate Adaptation National Research Flagship, CSIRO Marine and Atmospheric Research,
Cleveland, Queensland, Australia.

^f School of Mathematics and Physics, University of Queensland, St Lucia, Queensland, Australia.

*Corresponding author: Anne.Nieblas@csiro.au

ACKNOWLEDGEMENTS

A.E.N. is supported by a joint Commonwealth Scientific and Industrial Research Organisation (CSIRO)–University of Tasmania Ph.D. scholarship in Quantitative Marine Science (QMS). I thank the Australian Fisheries Management Authority (AFMA) for fish catch data and Mike Fuller for his help with AFMA data manipulation. I thank the following agencies for environmental data: 1) sea surface temperature – National Oceanic and Atmospheric Administration (NOAA) and National Aeronautics and Space Administration (NASA), 2) Sea-viewing Wide Field-of-view Sensor ocean colour – NASA, 3) wind – National Centre for Environmental Prediction–National Centre for Atmospheric Research, and 4) altimetry – Ssalto/Duacs. Satellite data were accessed using the Spatial Dynamics Ocean Data Explorer (SDODE) – customised software provided by Alistair Hobday, Klaas Hartmann, Jason Hartog, and Sophie Bestley. I thank Harry Hendon and James Risbey for the discussion and their advice regarding the effects of the Indian Ocean Dipole in south eastern Australia.

INTRODUCTION

Links between ocean physics and fish are individual, varied and complex and can have impacts on several stages within the life cycle of many species. Environmental fluctuations can affect the timing and extent of prey availability (Cushing 1975), influence growth rates and trophic interactions (Bailey & Houde 1989, Houde 1989), regulate larval feeding success, and control dispersal to, or retention within, nursery areas (Bakun 1996, Chapter 2.2). Whilst it is generally accepted that fish populations are influenced by the physical environment, these impacts are moderated through complex inter- and intra-species relationships (Gargett 1997a), and statistical corroboration of “physics to fish” relationships can be difficult to achieve. Quantitative models can be used to characterize and predict fish variability in relation to their environment, and can aid in understanding changes in their population and catch rates. As seafood constitutes nearly 10% of human diets world-wide (Burke et al. 2000), and fisheries are economically important in many countries, it is important to understand fish population dynamics, and assess the potential impacts of climate change on fisheries.

The majority of marine species’ early life stages involve planktonic eggs and larvae (e.g. teleost fish or squid) that are enormously affected by the environment in that their transport and survival are at the whim of the physical ocean. It is believed that the survival and growth of these stages are driven by key oceanographic features necessary for successful recruitment that a) enrich the water column by supplying nutrients and thus enhancing primary production; b) concentrate and aggregate primary producers and larvae through convergence zones or water column stability; and c) retain or transport eggs and larvae within or towards suitable nursery habitat (Bakun 1996, Agostini & Bakun 2002, Chapter 2.2).

In contrast, a minority of species have reproductive strategies involving low fecundity, long gestation periods, and live birth of relatively well-developed juveniles (e.g. chondrichthyans). These species are expected to show relatively successful early survival and recruitment to fisheries that are comparatively little influenced by environmental variability (Walker 1998, Watters et al. 2003). However, environmental influences, such as ambient temperature or ocean productivity, may impact such species through changes in growth rates, which in turn affect stock productivity and hence catches taken by a fishery. In addition, the environment may influence catch rates by affecting the availability of individuals to the fishery. Highly mobile species may aggregate in an area due to a higher likelihood of feeding success, beneficial reproductive conditions, or good nursery regions (Nakamura 1969, Humston et al. 2000). Low mobility species may be concentrated by frontal formation due to regional circulation variability (Bradbury et al. 2003).

Here I investigate statistical relationships between the physical environment and the catch rates of two marine species with very different life histories to elucidate whether predictive models can be developed to improve our understanding of fishery dynamics and assess any potential impacts to biomass due to climate change. I examined commercial catch rates of arrow squid (*Nototodarus gouldi*) and gummy shark (*Mustelus antarcticus*) in an Australian upwelling region, the Bonney Upwelling. Both species are commercially important, but have markedly different reproductive and life history patterns and are thus likely to be driven differently by the environment. I focus on the Bonney Upwelling region because it has clearly-defined seasonality in atmospheric, oceanographic, and primary productivity responses (Nieblas et al. 2009) that should provide distinct relationships between the environment and living resources. I describe the interannual and seasonal variability of catch rates in both the arrow squid and gummy shark fisheries. I use catch and effort data as a proxy for fish abundance, reproductive success, or availability to the fishery and relate it to environmental indices that describe regional oceanography as well as indices that specifically describe upwelling dynamics. Based on these relationships, I develop statistical models that can be used in a predictive manner to assess fisheries dynamics and the impacts of climate change on arrow squid and gummy shark off the Bonney Coast.

MARINE SPECIES AND UPWELLING REGION DETAILS

Arrow Squid (*Notodarus gouldi*)

Arrow squid are widespread in southern Australia and northern New Zealand (Stark et al. 2005). They are targeted by Australia's largest jig fishery, which is seasonally-productive and valued at nearly \$1.2M in 2002–2003 (Australian Fisheries Management Authority 2004). They are also a valuable by-product year-round in the South East Scalefish and Shark Fishery trawl sector. Arrow squid live for less than 1 year, are multiple batch spawners, hatch throughout the year with up to 4 main intra-annual cohorts (Jackson et al. 2003), and are genetically well-mixed throughout their range (Triantafillos et al. 2004).

Many squid have r-selected characteristics (Boletzky 1981), including rapid growth rates, high fecundity, and relatively low and variable recruitment (MacArthur & Wilson 1967). Although they are aggressive predators, squid also fill similar ecological roles to small pelagic fish as they are a neritic, pelagic, schooling species, capable of rapid population response, with pelagic egg “balloons” (O'Shea et al. 2004) and planktonic paralarvae that feed in upper ocean planktonic communities (Bakun & Csirke 1998). However, their life history stages are even more rapid than small pelagic fish, with faster growth rates and shorter life spans (Jackson et al. 2005) that require a high caloric intake and relatively low energy expenditure (Bakun & Csirke 1998). Squid have inherent life history flexibility that enables rapid individual responses to fluctuating conditions, especially temperature and food

availability, that influence the timing and success of spawning, hatching, growth, recruitment, and reproductive maturity (Forsythe 1993, Jackson & Moltschaniwskyj 2001, Stark 2008).

Gummy Shark (*Mustelus antarcticus*)

The gummy shark, endemic to southern Australia, is targeted as part of Australia's South East Scalefish and Shark Fishery, and was valued at nearly \$16M in 2006–2007 (Australian Fisheries Management Authority 2008). Stock assessments have shown that since the inception of gillnets as the main method of fishing, gummy shark abundance has clearly been reduced. Recent assessments, however, suggest that the fishery is maintained close to the maximum sustainable yield (Walker 1994, 1998, Pribac et al. 2005).

Gummy sharks have K-selected characteristics (MacArthur & Wilson 1967) and are relatively long-lived (11–16 years), with low fecundity at 1–57 pups every 1–2 years, and gestation periods of up to 12 months (Walker 2007). Ovulation takes place in October to December and parturition is complete by the following December. Newborn and juvenile gummy sharks aggregate in many areas across southern Australia, but there is no known nursery ground (Kailola et al. 1993). They recruit to the fishery after 2 yrs (Walker 1992).

Generally, it is believed that environmental conditions do not strongly affect shark early life history as the pups are born relatively well-developed, and consequently recruitment is highly dependent on stock size rather than environmental influences (Bonfil 1994). However, density-dependent effects due to reduction in population (e.g. from fishing pressure, changes in predation, cannibalism, competition, or disease, Holden 1973), can result in compensatory increases in fecundity and or growth when more food is available (Holden 1973, Sosebee 2005). This can induce earlier maturity and greater fecundity for each age class (Holden 1973). Climate change will lead to changes in background environmental conditions, which in turn may change primary productivity thus altering food availability (Chapter 2.1). Any subsequent trophic cascades may impact the growth, availability or the migration patterns of gummy shark.

Bonney Upwelling Region

Coastal upwelling regions often have oceanographic conditions beneficial for successful recruitment (enrichment, concentration, and retention) (Chapter 2.2). However, there may be a trade-off between the benefits of enhanced productivity and the detriment of offshore transport of eggs and larvae, depending on regional circulation and coastal topography. Australia is unique in that large-scale upwelling is absent off the West Australian coast due to the poleward-flowing Leeuwin Current that suppresses otherwise upwelling-favourable wind forcing (Hanson et al. 2005b). Consequently, upwelling around Australia occurs only in smaller, regional systems. The Bonney Upwelling in south eastern Australia (Fig. 4.1) is Australia's largest and most predictable coastal upwelling (Butler et al. 2002) and has

physical forcing similar to larger wind-driven global upwelling systems, although wind-forcing along this coast is much weaker (Nieblas et al. 2009). Weak wind conditions, limit phytoplankton biomass due to less nutrient enrichment from weaker vertical mixing, but do not lead to turbulent mixing or excessive advection of particles (i.e. eggs and larvae) out of the system (Cury & Roy 1989).

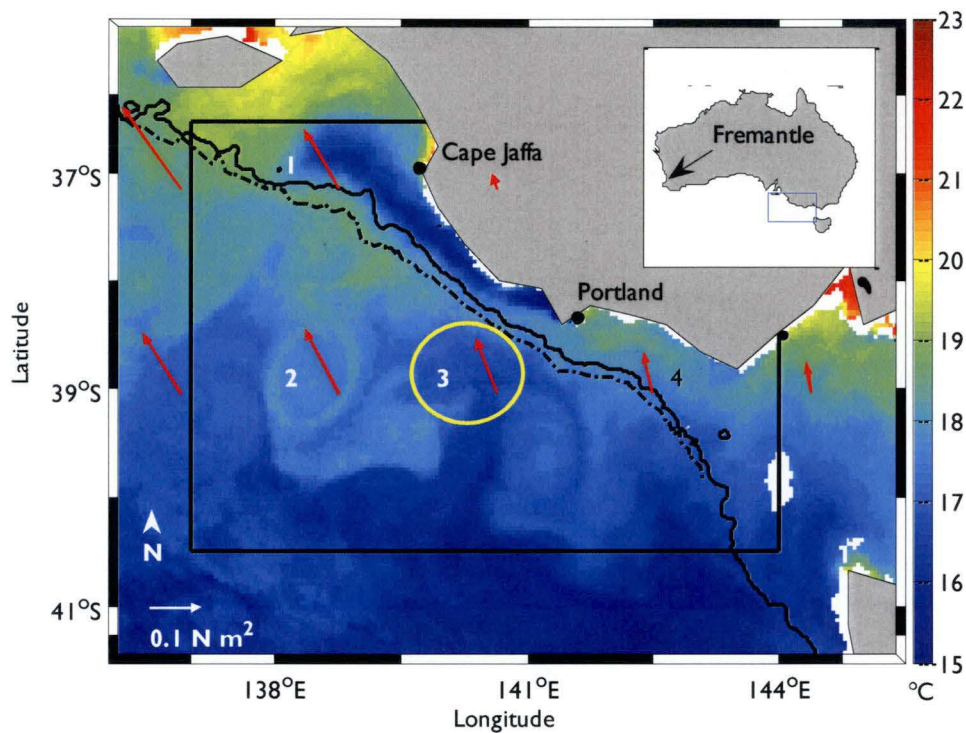


Fig. 4.1: The Bonney Coast with the $\sim 15^{\circ}\text{C}$ upwelling plume. The South East Scalefish and Shark Fishery zone 50 is shown by the black box. Red arrows indicate reanalysed wind positions and the yellow-circled vector 3 value at 39°S , 140.5°E is used to represent wind stress that directly influences the Bonney Coast. Black full and dashed lines represent the 200- and 1000-m contours, respectively, and the colour bar represents sea surface temperature ($^{\circ}\text{C}$).

The Bonney Upwelling is driven by the seasonal latitudinal migration of the subtropical ridge that drives westerly, downwelling favourable winds in the austral winter (Rochford 1975) and south easterly, upwelling-favourable winds in the austral spring and summer (Lewis 1981, Schahinger 1987, Griffin et al. 1997). Regional ocean circulation and climate patterns also influence upwelling variability. The westward-flowing Flinders Current at the continental shelf break (Middleton & Cirano 2002) enhances open ocean-shelf water exchange that preconditions wind-driven coastal upwelling by lifting the thermocline on the continental shelf (Middleton & Cirano 2002, Middleton & Platov 2003). A seasonal coastal current opposes the Flinders Current with strong south eastward flow in the winter months that reverses to a weak north westward flow in the summer (Middleton & Platov 2003). Upwelling appears to be marginally related to El Niño–Southern Oscillation (ENSO)

variability (Nieblas et al. 2009) due to teleconnections affecting the Leeuwin Current. During El Niño (La Niña) events, the Leeuwin Current is weakened (strengthened), which in turn shoals (deepens) the thermocline off the Bonney Coast (Middleton et al. 2007). The majority of upwelling activity occurs during the austral summer from November to April, and the development, peak, and decline of upwelling activity follows four distinct phases: “onset,” “sustained,” “quiescent,” and “downwelling” (Mitchell-Innes et al. 1999, Nieblas et al. 2009).

The Bonney Upwelling marine ecosystem has the key ocean triad features during its summer upwelling season. Enrichment processes occur throughout the summer, and peak by February to March during the sustained and quiescent periods (Chapter 2.2, Nieblas et al. 2009). Upwelling creates effective frontal convergences (Lutjeharms & Stockton 1987, Moita et al. 2003) that potentially concentrate and aggregate primary production and prey for both juvenile and adult marine organisms (Gonovi & Grimes 1992). Depending on the time of spawning, retention in the system can be maintained by onshore transport due to downwelling winds prior to the upwelling season, but can also occur at the frontal edges of the upwelling plume (Chapter 2.2). Additionally, circulation at the time of upwelling is generally north westward (Middleton & Platov 2003), towards regions of coastal nursery habitat (Chapter 2.2).

DATA

Fisheries data

Catch records for arrow squid and gummy shark were obtained from the Australian Fisheries Management Authority logbook dataset for the South East Scalefish and Shark Fishery zone 50, directly off the Bonney Coast (Fig. 4.1). Records were included if they specifically named arrow squid *Nototodarus gouldi* and gummy shark *Mustelus antarcticus*. Only records where continuous “normal fishing activity” occurred were used, which included 12,103 catch records from 2003 to 2008 for arrow squid in the trawl fishery, and 28,888 catch records from 1998 to 2008 for gummy shark in the gillnet fishery. Trawl fishery data are used as arrow squid is a non-target species, and therefore the effects of effort are less influential on catch rates for the than for the jig fishery. Catches were reported in tonnes (t) of total fish caught, excluding discards. Catch per unit effort (CPUE) was calculated as catch divided by hours fished for arrow squid (unit: t hour⁻¹). No consistent measure of effort was recorded for the gummy shark fishery, and catches were used to represent daily hauls by individual fishers in the gillnet fishery (unit: t day⁻¹). The small number of zero values (<1%) was excluded from time series of both species, as they had little or no influence on the catch rate mean or variability and would unnecessarily increase the complexity required for model development. Distributions of catches were selected to include depths representative of the bulk of the records. Records of arrow

squid reported as being caught below 600 m ($n=104$) and of gummy shark caught below 200 m ($n=39$) were excluded from analyses. Because normality tests are unhelpful with very large numbers of records, as in the present study, a visual inspection of residual values was used and indicated that a natural log transformation was necessary for both species and the resulting distributions were effectively normal (Fig. 4.2). Mean monthly values of catch rates were then used for further analysis.

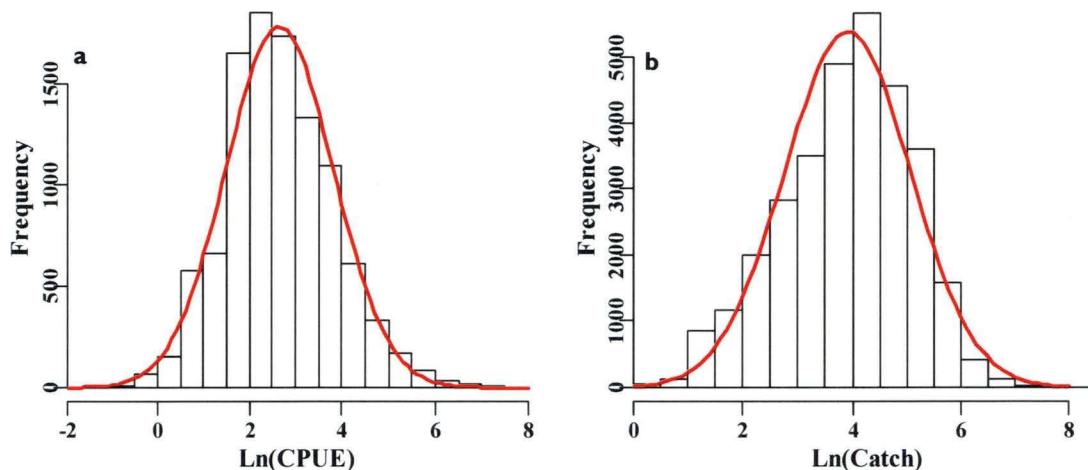


Fig. 4.2: Histogram of the natural log of (a) arrow squid CPUE and (b) gummy shark catch. Red lines indicate a normal distribution curve.

There are several caveats associated with the use of fish catch data as an index of abundance. First, fish catch is generally standardised by effort using statistical techniques to create a relative abundance index that attempts to account for biases such as effort creep and variations in catchability (Maunder & Punt 2004, Bishop et al. 2008). Standardisation techniques are challenging, as many factors that affect catch rate cannot be fully taken into account (e.g. vessel, depth, skipper experience) (Harley et al. 2001, Maunder et al. 2006, Bishop et al. 2008). However, here I attempt to explain the majority of the variance in catch rates using environmental variables. I assume that CPUE is linearly related to abundance and that catchability is constant, though there are several examples where this does not hold (e.g. Hilborn & Walters 1987, Harley et al. 2001). I believe that it is reasonable to assume constant catchability because I am using arrow squid data in a multi-species fishery that does not manage by quota or specifically target the species (Tilzey 1994, Stark 2008). I have selected a relatively small subset of the data (2003–2008 compared to 1986–2008 of consistent reporting) with relatively stable catch in comparison to the highly variable full time series (Sahlqvist 2007). In addition, Walker (1994, 1998) and Pribac et al. (2005) confirm that comparatively stable catch rates of gummy sharks occurred after the initial stages of exploitation in the 1960s and 1970s, and despite large changes in the fishing effort during this period including a quota managed system since 2001, recruitment rates appear

to be relatively stable (McLoughlin & Wood 2008). Second, logbook data have their own weaknesses in terms of handling of discards, and the general difficulty of data collection and data quality control (Chassot et al. 2007). The Australian Fisheries Management Authority fisheries logbook program has been in existence for >40 years, with high coverage and sufficient consistency in the reporting by Commonwealth fisheries operating in Australian waters in the recent period (Rohan 1999).

Environmental data

Our focus was to assess whether relationships exist between arrow squid or gummy shark abundance and key oceanographic variables at a variety of spatial scales that described conditions specific to the seasonal upwelling off the Bonney Coast. These key variables were calculated using a variety of data sources. Six-hourly 10 m wind data were taken from the National Center for Environmental Prediction–National Center for Atmospheric Research Reanalysis Project (Kalnay et al. 1996). Sea surface temperature (SST) data was taken from local area coverage National Oceanic and Atmospheric Administration's Advanced Very High Resolution Radiometer that was processed into daily 6-day composites (Griffin et al. 2004). Eight-day Sea-viewing Wide Field-of-view Sensor ocean colour images were used to represent chlorophyll *a* concentration in surface waters. Despite limitations in coastal regions, ocean colour is an extensively used (e.g. Sathyendranath et al. 1991, Alvain et al. 2005) and appropriate proxy for phytoplankton biomass in upwelling systems where primary productivity is high and variable. Weekly TOPEX/POSEIDON, Jason-1, Jason-2, ERS-1, ERS-2, GFO, and Envisat composite satellite altimetry data was used to provide Sea Surface Height anomaly (SSHa) data. Altimeter products were produced by Ssalto/Duacs and distributed by AVISO, with support from CNES ([http:// www.aviso.oceanobs.com/duacs/](http://www.aviso.oceanobs.com/duacs/)). Tide gauge data were provided by the Permanent Service for Mean Sea Level (Woodworth & Player 2003), and were linearly detrended to remove long-term trends in mean sea level not relevant to this study.

Environmental indices

Regional environmental indices were developed for the South East Scalefish and Shark Fishery zone 50 (Fig. 4.1) from monthly mean estimates of satellite-derived SST (SST_R ; units: °C), altimetry (SSH_{AR} ; units: m), and chlorophyll *a* concentration (SSC_R ; units: $mg\ m^{-3}$). Local (Portland) and distant (Fremantle) tide gauge data (Fig. 4.1) measure sea level height variability and respectively represent the strength of the seasonally-reversing coastal current off the Bonney Coast (PORT; units: m; Middleton et al. 2007) and the Leeuwin Current that flows poleward along the Western Australian coast and eastward along the southern Australian shelf towards the Bonney Coast (FRE; units: m, Feng et al. 2003). In addition, large-scale climate indices that represent ENSO and Indian Ocean Dipole (IOD)

impacts on Bonney Upwelling are included as these may influence atmospheric or oceanographic conditions along the Bonney Coast (e.g. Ashok et al. 2003, England et al. 2006, Middleton et al. 2007). The Southern Oscillation Index (SOI) and the Nino 3.4 index were used to represent ENSO, and the Dipole Mode Index (DMI) was used to represent the IOD.

Indices directly related to upwelling were developed according to methods described in Nieblas et al. (2009). The upwelling wind index is defined here as the wind stress component parallel to the coast (UI ; units: $N\ m^{-2}$). With UI , positive (negative) values indicate upwelling (downwelling or relaxation). I used values at $39^{\circ}S$, $140.5^{\circ}E$ to represent coastal wind that directly influences upwelling along the Bonney Coast (Fig. 4.1). The area of the upwelling plume indicates the physical effect of upwelling-favourable winds on the surface of the ocean. I define this as the largest continuous area with a $1^{\circ}C$ cooling from mean monthly SST off the Bonney Coast ($Area_{UI}$; units: km^2). I also identified mean temperature within the upwelling plume ($Temp_{UI}$; units: $^{\circ}C$). To estimate the response of primary productivity to upwelling, I summed the chlorophyll concentration within the largest continuous region of anomalous values ($>0.6\ mg\ m^{-3}$) and divided by the area of the plume to give an approximation of phytoplankton biomass of the upwelling plume. A visual inspection of residuals indicated that a log normal transformation of chlorophyll data was necessary ($LnSSC_{UI}$; units: $mg\ m^{-3}\ km^{-2}$).

ANALYSIS METHODS

Time series analysis

Time series analyses were performed between all environmental indices and arrow squid and gummy shark log transformed catch rate data to find the most appropriate lag times for the environmental variables. This was achieved using lag plots and autocorrelation and partial autocorrelation functions to determine the significance of the lags. Time lags are common in nature and this method has been used for many environment-fish relationships (e.g. Thorrold et al. 1994, Kim et al. 1997, Downton & Miller 1998). Lag periods with the highest absolute correlation coefficients (r) and lowest significant p-values ($\alpha = 0.05$) were chosen for each environmental index.

Model development

I built a log-linear model and used step-wise regression to determine the relationship between environmental predictors and natural log-transformed arrow squid and gummy shark catch rates. Since the Bonney Upwelling is a low-wind system compared to eastern-boundary upwelling regions (Nieblas et al. 2009), primary productivity is not generally affected by the deleterious effects of turbulence and advection (Cury & Roy 1989). Therefore, a linear relationship between upwelling wind stress and primary productivity is

expected for the Bonney Upwelling (Nieblas et al. 2009) and nonlinearities are not considered. Environmental indices that had been lagged according to the time series analysis described previously were manually added in a forward manner and model fits were compared using the Akaike Information Criterion (AIC), adjusted coefficients of determination (r^2), and p-values from an Analysis of Variance (ANOVA) test. If a predictor variable decreased the AIC or increased the adjusted r^2 by 1% or more, and was significant at the 0.05 level in the ANOVA, it was included in the model. Many predictors were not orthogonal (i.e. they are correlated); however they were each assessed as to whether they significantly explained additional variance of fisheries CPUE. Models were created using the base time period of 2003–2007 for arrow squid and 1998–2007 for gummy shark. Data from 2008 was withheld from model development and was used to validate models. Additional retrospective analyses were performed by removing years of data to compare the consistency of results and the capacity for prediction of the modified models based on reduced datasets.

RESULTS

Interannual variability of fisheries

There was significant interannual variability in squid catch from 2003–2008 ($F_{71}=2.88$, $p=0.021$, $n=72$). A total of 71 t to 169 t of squid were caught each year in the trawl fishery off the Bonney Coast (Fig. 4.3a), with an overall annual mean catch of 107.7 t during this 6-year period. Highest catches were in 2003 (169.22 t), which was significantly higher than the catches in 2007–2008. Lowest catches were in 2004–2006, with mean annual catch for this period of 73.2 t.

Catch of gummy sharks has significant interannual variability from 1998–2008 in the gillnet fishery off the Bonney Coast ($F_{143}=10.75$, $p<0.0001$, $n=144$). Catches ranged from 68.1 t in the year of lowest catch (2001) to 131.1 t in the year of highest catch (2000) (Fig. 4.3b), with mean annual catch reaching 91.4 t. The first four years of gummy shark catch (1998–2001) fluctuating widely between the highest and the lowest catch. After 2001, catches steadily increase (Fig. 4.3b).

Seasonal variability of fisheries

Catches of arrow squid are strongly seasonal, with the majority of squid caught in the trawl fishery in the late austral summer to early austral winter. Catches peak in April to May, and lowest catches were taken in early spring (October–December) (Fig. 4.3c). Gummy shark have an almost opposite seasonal trend, with peak catches in early austral spring to summer and lowest catches in autumn and winter (Fig. 4.3d). These seasonal signals indicate that, although peak catches may occur in particular periods of the year, both arrow squid and gummy shark are available at least at some level off the Bonney Coast throughout the year.

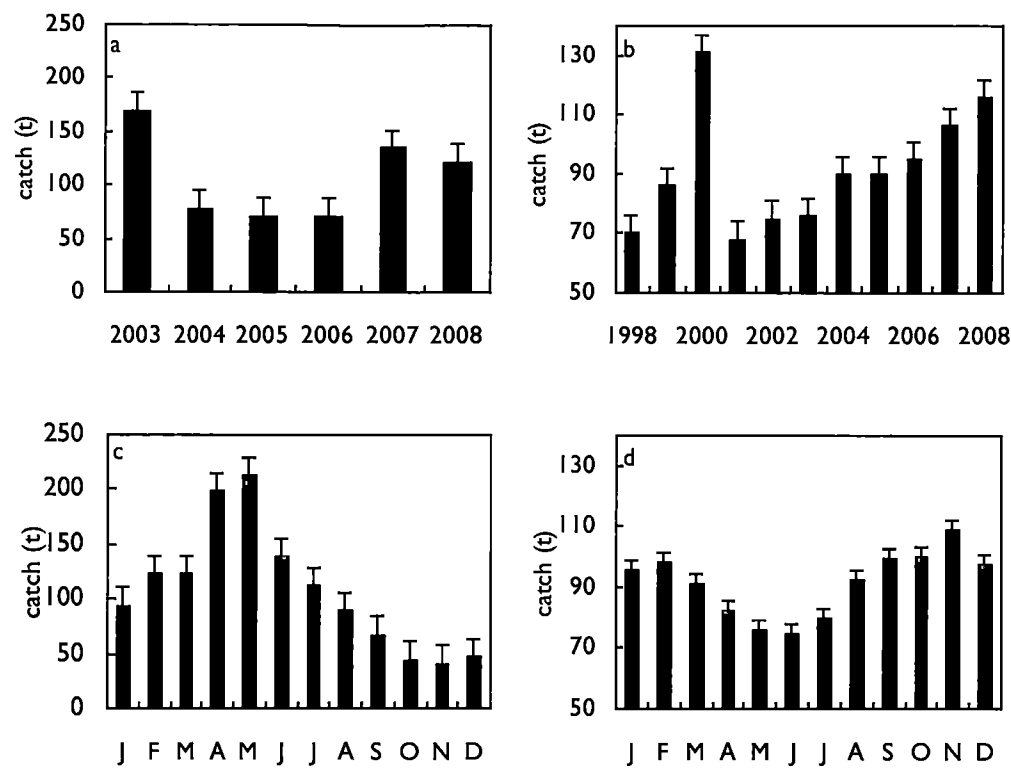


Fig. 4.3: Interannual and seasonal variability of (a,c) arrow squid and (b,d) gummy shark catch (t) in South East Scalefish and Shark Fishery zone 50. Error bars represent standard errors of means.

Table 4.1: Optimal lag periods of environmental indices for arrow squid and gummy shark catch rates. Lag periods expressed in months. Only significant ($\alpha = 0.05$) correlation coefficients, r , listed. Ln represents a natural logarithmic transformation.

Environmental index	Abbreviation	Arrow squid		Gummy shark	
		Optimal lag (months)	r	Optimal lag (months)	r
Upwelling wind stress	UI	-3	0.57	-10	0.26
Upwelling plume area	Area _{UI}	-2	0.71	-9	0.34
Upwelling plume temperature	Temp _{UI}	-2	0.59	-9	0.28
Ln(Upwelling plume productivity)	LnSSC _{UI}	-3	0.63	-9	0.30
Regional temperature	SST _R	-2	0.69	-9	0.29
Regional altimetry	SSHa _R	-5	-0.61	-5	0.4
Regional productivity	SSC _R	-	-	-1	0.31
Fremantle sea level	FRE	-5	-0.59	-24	0.42
Portland sea level	PORT	-5	-0.55	-10	-0.27
Southern Oscillation Index	SOI	-	-	-32	-0.53
Nino 3.4	Nino	-13	-0.28	-31	0.58
Dipole Mode Index	DMI	-	-	-1	0.30

Time series analysis

Optimal lag periods of environmental indices related to arrow squid abundance were generally short, between 2–5 months, with the exception of Nino 3.4, which had a lag of 13 months (Nino₋₁₃, Table 4.1). Environmental indices directly related to upwelling had significant positive correlations with arrow squid CPUE at lags of about a season (2–3 months). All measures of sea level were negatively related to arrow squid CPUE with 5 months lag (SSH_{aR,-5}, PORT₋₅, and FRE₋₅). Area_{UI} had the highest correlation with arrow squid at a lag of 2 months (Area_{UI,-2}, $r=0.71$, Table 4.1), and most variables had a correlation coefficient greater than 0.5. However, SSC_R, SOI, and DMI were not significantly correlated with squid abundance at any time lag.

A wider and more variable range of optimal lag periods of between 1–32 months was found for environmental indices correlated with the abundance of the relatively long-lived gummy shark (Table 4.1). Correlation coefficients between catch and environmental variables were weaker for gummy sharks (0.26–0.58) than for arrow squid, however all environmental indices were significantly correlated to gummy shark catch at some lag period. Nino 3.4 had the highest correlation to gummy shark at a 31 month lag (Nino₋₃₁, $r=0.58$, Table 4.1), and upwelling wind stress had the lowest at a 10 month lag (UI₋₁₀, $r=0.26$, Table 4.1). Upwelling-related and regional indices were related to gummy shark abundance at shorter lags, between 1–10 months, whereas larger-scale or remote indices were related to gummy shark abundance at longer lags, between 24 (FRE₋₂₄) and 32 months (SOI₋₃₂). DMI was an exception as a large-scale predictor, with an optimal lag of only 1 month (DMI₋₁).

Linear models

The time series analyses indicated that all environmental indices chosen for this study have some relationship with either arrow squid or gummy shark at optimal lag periods; they were therefore input in a stepwise fashion to multiple linear regression models. The best model fit for natural log of arrow squid CPUE from 2003–2007 (MI_{squid}) included a Year factor to account for annual variability of abundance, with SSH_{aR,-5}, Area_{UI,-2}, and Nino₋₁₃ as predictor variables (adjusted $r^2=77.3\%$, AIC=29.68) (Table 4.2; Fig. 4.4a). A mean of all Year factor estimates was taken so that the model could be used for future prediction. Year explained 10.4% of variance of arrow squid catch rates, and SSH_{aR,-5} contributed an additional 59.9% to model fit. Area_{UI,-2} and Nino₋₁₃ contributed a further 6.1% and 0.9%, respectively to the overall fit. Although Nino₋₁₃ was only marginally non-significant ($p<0.08$) in the ANOVA, it added nearly 1% to the overall fit and reduced the AIC (Table 4.2). This indicated that it contributed important extra explanatory power to the model and was therefore included. All other predictors were significant, with Year, SSH_{aR,-5}, and Nino₋₁₃

being negatively related, and $Area_{UL,-2}$ being positively related to arrow squid (Table 4.3; Fig. 4.5).

Retrospective validation for arrow squid CPUE was performed using MI_{squid} with data that had been abridged from the full time series to include just 2003–2006 and 2003–2005. Both MI_{squid} retrospective models performed well and described 74.7% and 76.3% of the variability, respectively (Table 4.4). The full and abridged MI_{squid} predicted 76.8–80.4% of the withheld 2008 $\ln(CPUE)$ data (Table 4.4). MI_{squid} was plotted with separate Year factors (2004–2007) ($M_{squid,Year}$; Fig. 4.4a) to examine how well the mean Year factor predicted the squid index. A visual inspection showed that the time series of arrow squid

Table 4.2: Best fit step-wise linear modelling of environmental predictors against arrow squid CPUE (2003–2007) and gummy shark catch (1998–2007) with adjusted coefficients of determination ($adj\ r^2$) and the Akaike Information Criterion (AIC) indicating goodness-of-fit. Significance codes for each predictor variable in the ANOVA are represented as ***' <0.001, '**' <0.01, '*'<0.05, '~'<0.1.

Arrow squid		Predictors			Adj r^2	AIC	
	$\ln(CPUE_{\text{squid}})$	Year*			0.104	109.57	
	$\ln(CPUE_{\text{squid}})$	Year***	$SSH_{R,-5}$ ***		0.703	44.13	
	$\ln(CPUE_{\text{squid}})$	Year**	$SSH_{R,-5}$ ***	$Area_{UL,-2}$ ***	0.764	31.21	
MI_{squid}	$\ln(CPUE_{\text{squid}})$	Year***	$SSH_{R,-5}$ ***	$Area_{UL,-2}$ ***	$Nino_{-13} \sim$	0.773	29.68
Gummy shark							
	$\ln(Catch_{\text{shark}})$	Year***			0.427	-26.49	
	$\ln(Catch_{\text{shark}})$	Year***	$SST_{R,-10}$ ***		0.602	-69.44	
	$\ln(Catch_{\text{shark}})$	$Nino_{-31}$ ***			0.291	-8.55	
	$\ln(Catch_{\text{shark}})$	$Nino_{-31}$ ***	FRE_{-24} ***		0.434	-34.75	
	$\ln(Catch_{\text{shark}})$	$Nino_{-31}$ ***	FRE_{-24} ***	DML_{-1} **	0.473	-42.33	
MI_{shark}	$\ln(Catch_{\text{shark}})$	$Nino_{-31}$ ***	FRE_{-24} ***	DML_{-1} **	UL_{-10} **	0.509	-49.76

$\ln(CPUE)$ and $M_{squid,Year}$ is reasonably well predicted by MI_{squid} (Fig. 4.4a), indicating good predictive ability for the models.

The step-wise linear modelling for gummy shark was a two-part analysis. Initially, a Year factor was included, explaining 42.7% of the variance, and only $SST_{R,-9}$ contributed subsequent significant variability (17.5%). Both predictors had significant positive relationships to the natural log of gummy shark catch, and the model had a relatively high adjusted r^2 of 0.602 (Table 4.2; Fig. 4.4b):

$$\ln(Catch_{shark}) = 2.56 + 0.49 + 7.5 \times 10^{-2} SST_{R,-9} \tag{4.1}$$

However, the multi-year trend was lost with the mean Year factor, limiting the predictive ability of Eq. 4.1 (Fig. 4.4b). Therefore, instead of the Year factor, Nino₋₃₁ was input into the model and explained 29.1% of the variance. A visual examination of the

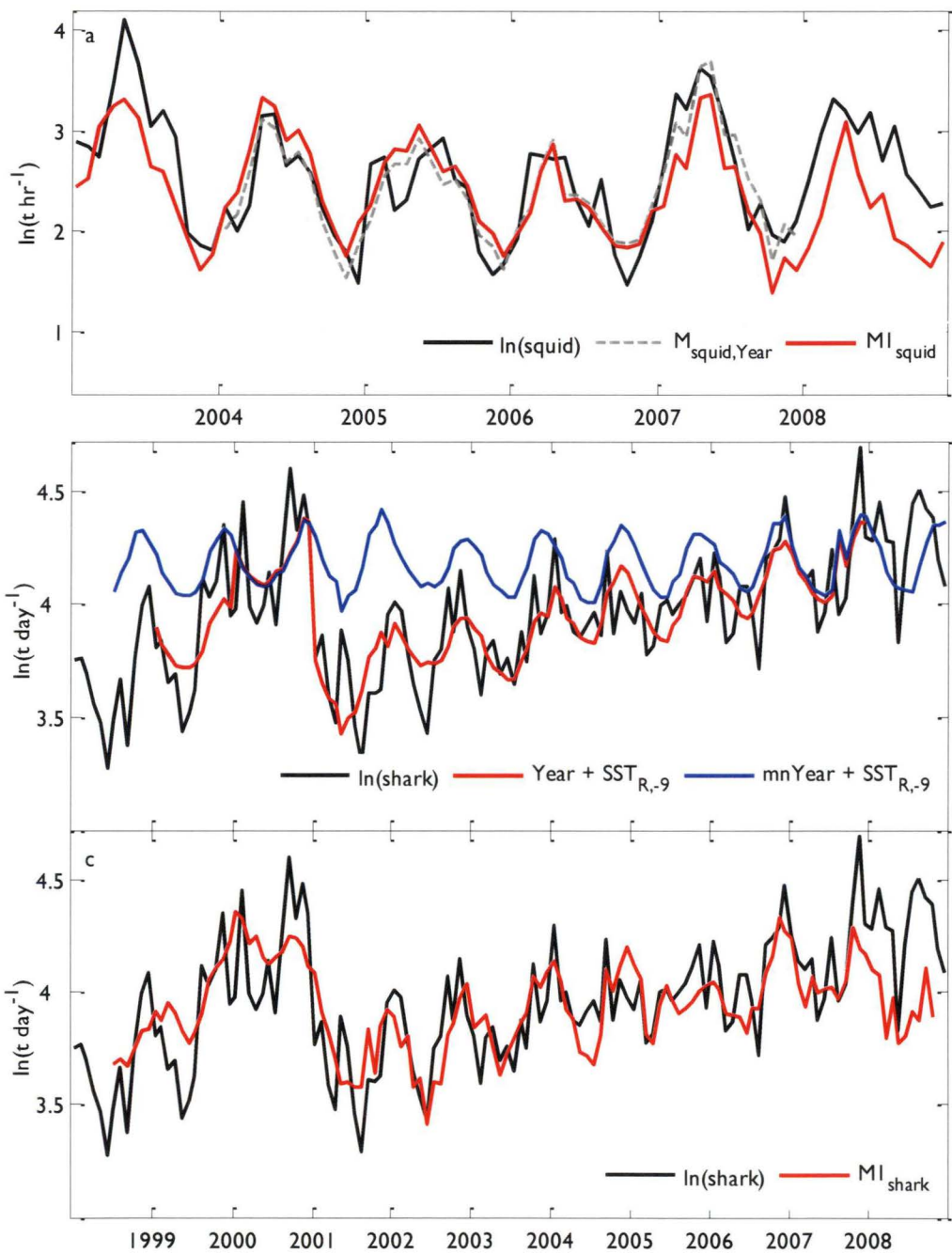


Fig. 4.4: (a) 2003–2008 arrow squid $\ln(\text{CPUE})$ time series (black) with full MI_{squid} linear model with each year parameter value (grey, dashed), full MI_{squid} with mean year parameter value (red), predicted until 2008. (b) 1998–2008 gummy shark $\ln(\text{catch})$ time series (black) with the optimal linear model using the Year factor ($\text{Year} + SST_{R,-9}$; red), and mean Year factor ($\text{mnYear} + SST_{R,-9}$; blue), predicted until 2008. (c) 1998–2008 full MI_{shark} linear model (red), predicted until 2008.

Table 4.3: Models for arrow squid and gummy shark with optimal predictive performance (MI). Mn refers to the mean year parameter.

Response	Adj r^2	AIC	Predictors				
Arrow squid ln(CPUE)			Intercept	Mn(Year)	SSH _{a_R-5}	Area _{UI-2}	Nino ₋₁₃
MI _{squid}	0.77	29.68	2.83	-0.326	-9.25	9.31×10 ⁻⁵	-0.13
Gummy shark ln(catch)			Intercept	Nino ₋₃₁	FRE ₋₂₄	DML ₁	UI ₋₁₀
MI _{shark}	0.51	-49.76	3.96	9.02×10 ⁻²	-6.37×10 ⁻⁴	0.15	1.78

Table 4.4: Best models parameter estimates and retrospective analysis of environmental predictors against arrow squid CPUE and gummy shark catch. Mean of all year factor estimates listed. Adjusted coefficients of determination (Adj r^2) show goodness-of-fit. Significance codes of each predictor in the ANOVA are represented as '***' <0.001, '**' <0.01, '*' <0.05, '~' <0.1. 2008 column represents Adj r^2 of each model's 2008 predictions against 2008 arrow squid CPUE or gummy shark catch data.

MI _{squid}								Predicted 2008
Data range	Adj r^2	AIC	Intercept	Year	SSH _{a_R-5}	Area _{UI-2}	Nino ₋₁₃	Adj r^2
2003–2007	0.773	29.68	2.83	-0.326 ***	-9.25 ***	9.31×10 ⁻⁵ ***	-0.127 ~	0.768
2003–2006	0.747	27.36	2.81	-0.422 ***	-10.03 ***	8.33×10 ⁻⁵ *	-6.17×10 ⁻²	0.804
2003–2005	0.763	22.28	2.87	-0.519 ***	-9.64 ***	8.3×10 ⁻⁵ *	-0.133	0.770
MI _{shark}								Predicted 2008
Data range	Adj r^2	AIC	Intercept	Nino ₋₃₁	FRE ₋₂₄	DML ₁	UI ₋₁₀	Adj r^2
1998–2007	0.509	-49.76	3.96	9.02×10 ⁻² ***	-6.37×10 ⁻⁴ ***	0.15 **	1.78 **	0.24
1998–2006	0.485	-45.97	3.95	8.80×10 ⁻² ***	-5.86×10 ⁻⁴ ***	0.12 *	1.68 **	0.20
1998–2005	0.488	-43.48	3.93	8.82×10 ⁻² ***	-5.52×10 ⁻⁴ ***	0.06	1.75 **	0.30

model fit based on this one variable showed that $Nino_{-31}$ appeared to capture much of the between-year variability in the shark CPUE time series. Other environmental variables also significantly contributed to the model fit and reduced the AIC, including FRE_{-24} , DMI_{-1} , and UI_{-10} , which described an additional 14.4%, 3.9%, and 3.6% of the variance, respectively (Table 4.2). The final model for 1998–2007 (MI_{shark}) described 50.9% of the variance of gummy shark catch rates, and a visual inspection revealed that this model accounts for most of the large multi-year trend (Fig. 4.4c). All predictors have significant positive relationships with the natural log of catch, except FRE_{-24} which has a significant negative relationship (Table 4.3; Fig. 4.6).

Retrospective analyses were performed to validate the final model of gummy shark catch using MI_{shark} with 1998–2006 and 1998–2005 data. The percent of variance described by the retrospective models for MI_{shark} (1998–2006: 49%, 1998–2005: 49%) was similar to that described by the full model (51%). However, the significance of DMI_{-1} changed between the different models and became less significant with sequential removal of data (Table 4.4). The full MI_{shark} and the 1998–2006 and 1998–2005 retrospective MI_{shark} did not predict the withheld 2008 $\ln(\text{catch})$ well (24%, 20%, and 30%, respectively; Table 4.4). This significant decline in predictive ability for 2008 indicated that the final data period had a large impact on model development for gummy sharks.

Visual inspection of MI_{shark} shows relatively good fit to the gummy shark CPUE time series until the final 19 months (April 2007–October 2008), when the model considerably under fits the data (Fig. 4.4c). This failure was driven by the $Nino_{-31}$ signal, which declined and flattened at the end of the time series (Fig. 4.4c). Though the model fit was worse in the final stages of the time series, a visual examination indicated that DMI_{-1} (Fig. 4.6) increased in the final two years. It is possible that this variable drove the model fit for the final years. The possibility that some variables have greater effect on the model at distinct periods in the time series suggested that there were nonlinearities or thresholds in their relationship to gummy shark catch, which are not accounted for using linear models. Whether these variables are spurious or a result of nonlinearities that are not constant throughout necessitates a longer time series for a more complete examination. Additionally, the diminished fit in the final 19 months indicated that something besides ENSO, the IOD, and upwelling activity was affecting gummy shark catch rates during this period. The failure of all models in 2007–2008 indicates that the environmental variables included do not sufficiently predict gummy shark for all years of this time series, or the gummy shark time series is not long enough for accurate predictions to be made.

DISCUSSION

I find that two species with contrasting life history characteristics (r- and K-selected) have distinct interannual and seasonal variability in their catch rates. This variability can be

robustly predicted using regional and large-scale environmental variables for squid. Variation in the squid species I examine is mostly related to regional and upwelling-specific environmental conditions at a lag of approximately one season, with only a marginal influence by ENSO. Conversely, the shark species examined here is more directly related to large-scale environmental conditions at longer lag periods, and less strongly impacted by upwelling-specific and regional conditions. However, the models I developed for gummy shark indicate that the relationship is not entirely consistent throughout time. Ocean physics may affect early life stages, growth, or availability of individuals to the fishery. Availability may be related to whether this region attracts individuals as a feeding ground or a reproductive centre for spawning or mating. For both species, it is difficult to distinguish from the available catch data what are the exact causal links between catch rates and environmental indices. Here, I discuss potential sources for the correlations I developed; however a manipulative approach with discrete sampling (e.g. fine-scale spatial modelling of squid recruitment data, or tagging or tracking studies for shark) might provide the means to identify the underlying causal mechanisms between physics and fish.

Arrow squid

The arrow squid MI_{squid} has a very tight fit ($r^2=0.77$) and follows the observed CPUE closely, indicating close coupling between arrow squid catch rates and their environment. This has been observed for other species of squid worldwide, such as *Illex argentinus* in the South Atlantic (Waluda et al. 1999), *Loligo forbesi* in the North Sea (Pierce & Boyle 2003), *L. vulgaris reynaudii* in South Africa (Roberts & Sauer 1994), and *L. pealei* and *I. illecebrosus* in the north west Atlantic (Brodziak & Hendrickson 1999, Dal et al. 2007). Environmental variables examined in this study are not orthogonal, and the strong linkages between them contribute to the difficulty in explaining the mechanisms behind their relationship to squid CPUE. The predictive heuristic model of arrow squid CPUE consists of three variables with regional- to large-spatial scales, over a range of lag periods (2–13 months). These predictors ($SSH_{AR,-5}$, $Area_{UI,-2}$, and $Nino_{-13}$) are strongly related to the regional summer upwelling that occurs off the Bonney Coast, indicating that upwelling may be the dominant environmental driver of arrow squid catches within the South East Scalefish and Shark Fishery zone 50.

As the catch of arrow squid in any year is a mix of several within-year cohorts (Jackson et al. 2003), relationships developed in this study may be explained by the influence that environmental conditions have on squid recruitment, growth, or availability to the fishery. Previous studies have shown that environmental conditions during hatching are important indicators of abundance in squid (Waluda et al. 1999, Agnew et al. 2000, Yatsu et al. 2000, Waluda et al. 2004) and similar to small pelagic fish, squid early life stages are likely to be governed by the “ocean triad” of enrichment, concentration and retention (Bakun

1996, Bakun & Csirke 1998, Chapter 2.2). Additionally, like most other species of squid, arrow squid have rapid growth to reach sexual maturity within their life span (1 yr; Jackson et al. 2005), which requires a high caloric intake with relatively low energy expenditure (Bakun & Csirke 1998). Thus, regions where there are large amounts of concentrated food would lead to faster growth rates. Finally, arrow squid are thought to make relatively small-scale ontogenetic migrations (Stark 2008), therefore individuals may migrate to regions to spawn where ocean triad conditions are suitable seasonally, thus enhancing egg and larval survival and overall recruitment success.

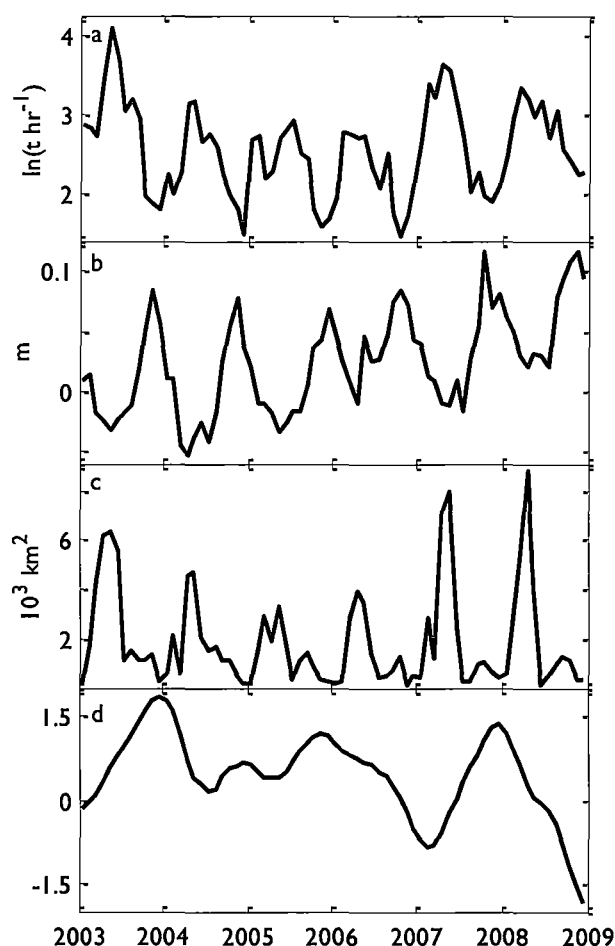


Fig. 4.5: Time series of (a) arrow squid $\ln(\text{CPUE})$ and environmental variables with incorporated optimal lag periods, including (b) negatively-related $\text{SSHa}_{R,-5}$, (c) positively-related $\text{Area}_{UI,-2}$, and (d) negatively-related $\text{Nino}_{-1.3}$.

The majority of the variance accounted for by MI_{squid} is explained by the negatively-related SSHa_R lagged over 5 months. November to December is 5 months prior to peak arrow squid catches (April–May), during the onset phase of summer upwelling along the Bonney Coast (Nieblas et al. 2009). $\text{SSHa}_{R,-5}$ may encompass the variability of several upwelling indices, especially the indices that represent the seasonal variability of the regional

circulation. Low sea surface height in November (Fig. 4.5b), is due to a divergence at the coast and offshore movement of water caused by south easterly (upwelling-favourable) winds along the Bonney Coast. During this period, the pycnocline weakens (Griffin et al. 1997) and shoals because of the influence of the Flinders Current (Middleton & Platov 2003), which may also impact sea level. Productivity begins to increase due to the upwelling of nutrient-rich water in the euphotic zone, and the temperature within the upwelling plume warms from $\sim 13^{\circ}\text{C}$, but remains relatively cool around $14\text{--}15^{\circ}\text{C}$ (Nieblas et al. 2009). Though arrow squid have a protracted spawning period, with hatching occurring throughout the year, peak hatching is from August to November (Uozumi 1998, Jackson et al. 2005) with up to four main cohorts (Jackson et al. 2003). This is just prior to the onset of upwelling conditions, when winds are still downwelling-favourable (Nieblas et al. 2009) and push surface water onshore; this is likely to retain eggs and paralarvae nearshore in preferred nursery habitat (Stark 2008). It is possible that by the onset of upwelling conditions, this main cohort has grown out of its planktonic stage and can actively avoid offshore transport, as well as take advantage of concentrated food due to the enhanced productivity of upwelling.

Area_{UI} is positively related to CPUE when lagged over 2 months. A lag of two months from peak arrow squid catch coincides with the peaks of Area_{UI} (February–March) (Fig. 4.5c), during the sustained enrichment phase of the Bonney Upwelling when strong south easterly winds penetrate the mixed layer most effectively (Nieblas et al. 2009). Peak productivity occurs within this phase, due to favourable background environmental conditions for phytoplankton growth, including more persistent upwelling-favourable winds, warmer temperatures, and longer days (Nieblas et al. 2009). The majority of studies that have focused on environmental influences on squid growth rates have found a link between growth and either ocean productivity or ocean temperature (e.g. Forsythe 1993, Villanueva 2000, Pierce et al. 2005, Jackson et al. 2003). As the Bonney Upwelling is a low-wind system (Nieblas et al. 2009), it is unlikely that the majority of upwelling events are sufficiently strong to advect particles out of the system. Therefore, large regions of frontal convergence along the edge of the upwelling plume can aggregate phytoplankton and zooplankton. These conditions may be beneficial for squid eggs and paralarvae that are transported and trapped within the upwelling front and hatch into regions of highly concentrated food resources (Bakun & Csirke 1998), or are transported onshore when upwelling wind events relax (Bjorkstedt & Roughgarden 1997). Additionally, with a larger upwelling plume, indicating greater upwelling productivity (Nieblas et al. 2009), more phytoplankton is available as a food source, increasing and concentrating the available prey for arrow squid. The two month delay between peak upwelling activity and squid abundance may be due to the time it takes for secondary productivity (e.g. zooplankton) to increase in biomass. The timing of mobile predator foraging often coincides with the

zooplankton peak (Croll et al. 2005). Squid have a strong physiological response to water temperature (Forsythe 1993), therefore the additional benefit of warmer frontal conditions and increases in both regional and upwelling plume temperature may enhance growth rates for paralarvae, juveniles, and adults (Brandt 1993) and may increase catch levels.

Nino₋₁₃ is weakly negatively-associated with squid CPUE at a lag of greater than a year, which suggests that arrow squid catch rates might be influenced by La Niña events. Effects of La Niña on south eastern Australian circulation are even less well understood than El Niño, but a possible impact on regional circulation may be related to the enhanced flow of the Leeuwin Current during La Niña (Feng et al. 2003), which may deepen the thermocline off the Bonney Coast and reduce summer upwelling. Previous studies have also found that squid abundance is related to large-scale climate indices (Roberts & Sauer 1994, Dal et al. 2000, Stark 2008), due to atmospheric teleconnections that cause large- and regional-scale changes to ocean circulation. ENSO has a 3–5 year cycle and the current time series of 6 years is currently too short to be definitive.

The summer upwelling conditions generally appear favourable for paralarvae and juveniles, provided they are not transported out of the system before they can reap the benefits of enhanced productivity. I have also shown that the upwelling conditions may impact adult squid by affecting the growth rate during particular months, and thereby improving catch through increasing available biomass due to larger body mass. Alternatively, migrating adults may be attracted to the region due to enhanced feeding opportunities. Although it is the primary driver of the upwelling, UI was not a significant predictor for squid abundance, which may be due to its high correlation with other variables. Alternatively, the monthly resolution of upwelling winds may conceal important wind events on the scale of days to over a week along the Bonney Coast (Nieblas et al. 2009). Though squid may respond to wind events on a shorter time scale than shown in this study, the resolution of consistent reporting of fish catch data used in this study (monthly) is not sufficient to resolve the relationship. These results indicate that upwelling conditions represented by the models as SSH_{R,-5}, Area_{UI,-2} and Nino₋₁₃ act as a complex interplay of environmental influences, which may affect both the survival and growth of arrow squid pre- and post-recruit stages, and may also impact the spatial distribution of post-recruit arrow squid within the Bonney Coast region. An exact knowledge of causal processes, although desirable, is usually not possible and is not essential for predictive modelling purposes (Agnew et al. 2000). As shown, the simple linear models developed here are able to simulate seasonal changes in abundance of squid catch rate off the Bonney Coast in a robust manner with good predictive ability.

Gummy shark

The final gummy shark model (MI_{shark}) fits the observed catch data well ($r^2=0.51$), until April 2007. This indicates that catch variability is related to environmental data for gummy shark, but not sufficiently consistently to be used for predictive purposes at this time. Sharks in general are slow-growing, late-to-mature, long-lived, and have small brood sizes (Smith et al. 1998). Gummy sharks are born well-formed at 30–35 cm (Last & Stevens 1994), and environmental variability is likely to have little effect on survival of juveniles and recruitment to the fishery (Walker 1998). It is therefore remarkable that our model describes their catch variability so well across approximately nine years of data. However, female gummy sharks are known to undertake long migrations (Last & Stevens 1994). Consequently, the variability in catch described by our model may be due to effects on catchability by changing availability of sharks to the fishery, drawn to the region during beneficial periods for growth, feeding, or reproduction. However, gummy sharks grow relatively quickly, have relatively high productivity (for sharks), and recruit to the fishery after 2 years (Walker 1998). Prior to recruitment, density-dependent effects and food availability affect gummy shark survival and growth (Walker 1998); therefore environmental conditions that affect food availability may filter through to changes in gummy shark abundance.

MI_{shark} is substantially different to MI_{squid} , as a larger proportion of the shark catch variability is attributable to large-scale climate indices. $Nino_{-31}$ accounts for the majority of the predictive capacity in the absence of the other environmental variables. FRE_{-24} significantly contributes to the model and is an indicator of the strength of the Leeuwin Current. The Leeuwin Current is strongest during the austral winter and weakest during the austral summer. The multi-year variability of the current is strongly affected by ENSO, becoming weaker (stronger) with El Niño (La Niña) events. $Nino_{3.4}$ is negatively correlated to FRE and is lagged a year (at ~ 3 years) behind FRE (at 2 years) in its association with gummy shark. $Nino_{3.4}$ measures ENSO signals in the middle of the Pacific Ocean, and FRE indicates ENSO signals off the south western coast of Australia. Therefore the difference in lag periods is due to the spatial separation of the respective indices locations. It is likely that the association with gummy shark for both of these climate indices is explained by regional variations in south eastern Australia due to ENSO; however, the additional capacity added to the model by FRE may also incorporate the seasonal trend of the Leeuwin Current.

A causal mechanism for the correlation between gummy shark and ENSO is difficult to identify. ENSO effects in south eastern Australia are thought to shoal the thermocline and enable upwelling winds to be more effective at driving productivity (Nieblas et al. 2009). Gummy shark catch is high

throughout the upwelling season (November–March) (Fig. 4.3d). El Niño conditions off the Bonney Coast may make this region attractive to the gummy shark due to enhanced and aggregated prey, and thus improved feeding success. The 2–3 year lag period suggests that the enhanced productivity of the region during El Niño years affects either the growth and survival of pre-recruits, or the reproductive success of female gummy sharks. Migrations undertaken by female gummy sharks (Last & Stevens 1994) may be linked to finding regions where their reproductive success may be enhanced through higher caloric intake in higher productivity regions.

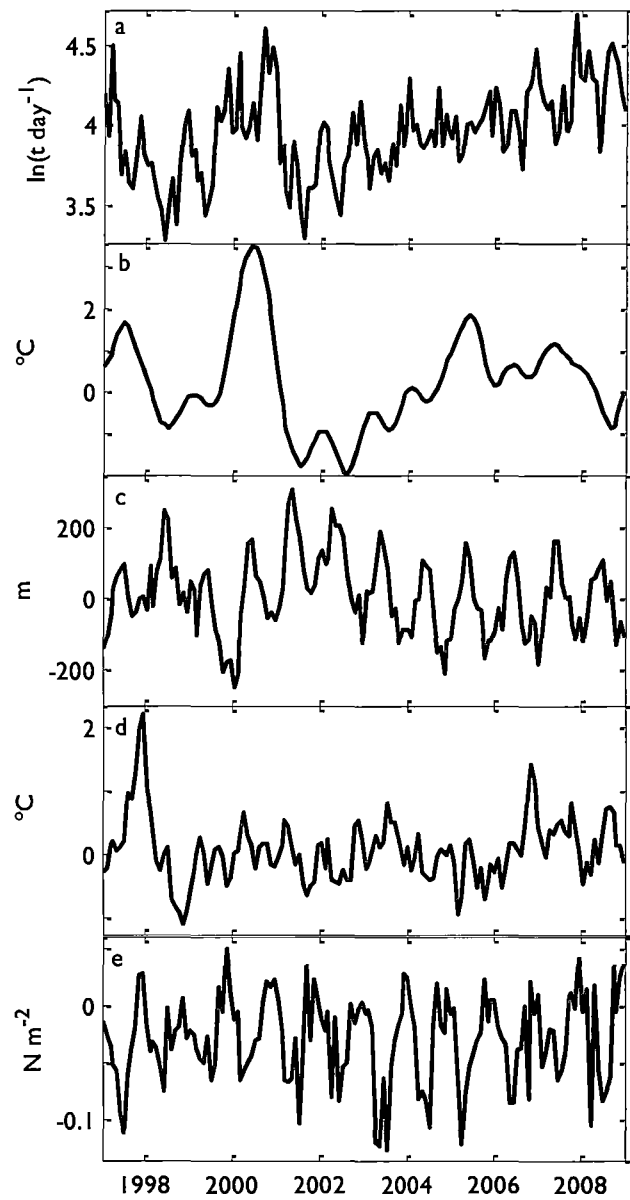


Fig. 4.6: Time series of (a) gummy shark $\ln(\text{catch})$ and environmental variables with incorporated optimal lag periods, including (b) positively-related Nino_{-31} , (c) negatively-related FRE_{-24} , (d) positively-related DMI_{-1} , and (e) positively-related UL_{10} .

Gummy shark catches are also positively related to the Indian Ocean Dipole at a lag time of only 1 month. Little is known about the effects of the IOD on ocean circulation in south eastern Australia. IOD is thought to have two effects on the strength of the Leeuwin Current. The Leeuwin Current is indirectly affected by the IOD connection to ENSO, with enhanced current strength occurring during positive IOD and El Niño conditions (Harry Hendon, pers. comm.), or changes in the subtropical winds south and west of Australia (England et al. 2006). If this relationship between IOD and circulation exists, it is as surprising as it is unexpected that a large climate index could have such an immediate effect on gummy shark, especially when ENSO has such a delayed effect. It is, however, theoretically possible for effects of the IOD to travel to south eastern Australia within the 1 month time frame, potentially through a (fast) propagating coastal Kelvin wave (Potemra 2001) or changes in subtropical winds. Currently, I am unable to describe a causal mechanism for the link between IOD and gummy shark; however, as indicated by the short lag time, it is most likely influencing the availability of the shark to the fishery or perhaps the behaviour of the fishers, rather than impacting growth or recruitment. However, the MI_{shark} retrospective analysis indicates that DML_{-1} only contributes significantly for 2008 and may be spurious. A longer time series of gummy shark data is necessary to determine whether DML_{-1} continues to significantly contribute to variability in gummy shark catches.

The remaining significant environmental indices are all directly related to upwelling, including the strength of alongshore wind stress and the productivity within the upwelling plume. The peak in gummy shark catch rates is in November (Fig. 4.3d), which is positively related to wind stress 10 months previously in the preceding January. January is within the sustained phase of the Bonney Upwelling (Nieblas et al. 2009). During this phase, phytoplankton growth accelerates and regional productivity increases due to more favourable conditions, potentially impacting on the growth of gummy shark, especially smaller fish about to recruit to the fishery.

The influence of the environment on gummy shark abundance is difficult to interpret because it occurs over longer time-periods than for squid, and involves large-scale climate indices whose regional influences are currently not fully understood. Additionally, monthly means of catch per day are used as a measure of abundance, which does not account for changes in fishing effort that may be a large driver of gummy shark patterns. Further, it is difficult to interpret the causal mechanism behind the model because gummy sharks are not known to respond to their environment in the way that I have shown in our model (e.g. Walker 1998; Watters et al. 2003). I argue that gummy shark juveniles or young could potentially be affected by environmental conditions relating to ENSO, the effect of which occurs on catches 2–3 years later. However, gummy shark also show similar interactions with their environment to squid in that they are influenced by some shorter-time scale and regionally-based environmental cues. Similar to squid, the environmental

conditions appear to affect the availability of individuals to the fishery due to the relative attractiveness of enhanced productivity. The models developed for gummy sharks have a remarkable fit until April 2007 when the model fails. This suggests that the environment is very influential, but there are other factors affecting gummy shark that override environmental influences during some periods. These additional factors are currently unknown and may be biological in origin (e.g. density dependence, diet), fisheries-related (e.g. changes in quotas, closures), or physical factors that I have not accounted for here.

CONCLUSION

I have examined species with contrasting life histories to assess whether it is possible to predict an index of their abundance based on environmental variables, and to consider the causal mechanism underlying such relationships. I have shown that for both a short- and a long-lived species with disparate migratory behaviours and reproductive strategies (batch spawner with pelagic paralarvae versus viviparous live bearers), environmental variables play an important role in the recruitment or growth of individuals, or availability of individuals to the fishery. However, the underlying mechanisms between the two species and environmental indices are very different. Catches of arrow squid are closely linked to regional and seasonal upwelling variability and only slightly influenced by ENSO. In contrast, gummy shark are mostly impacted by longer-term and large-scale indices such as ENSO, and only moderately affected by interannual and seasonal upwelling activity. Gummy shark also have considerable additional variation that is not explained by any variable in this study. The different associations for the two species are likely to be a consequence of differences in each species' life history characteristics and ecology; however an empirical approach should be used to investigate the exact causal mechanisms driving these relationships.

I have developed simple linear models that predict the abundance of two disparate species in a seasonal Australian upwelling region. The models for squid are robust to validation and have good predictive skill, despite the fact that they do not consider nonlinearities. The model for gummy sharks is not sufficiently robust to be used in a predictive manner without further investigation with a longer time series. With climate change, nonlinearities and interactions between environmental variables, productivity, and catches may become more important and it would be desirable to investigate specific mechanisms that underlie the observed correlations (Gargett 1997b). Finally, the relationships described here have been developed to be used to predict arrow squid and gummy shark abundance at interannual and decadal time-scales into the future. I show that environmental data can be useful for standardising fisheries-dependent catch data using fisheries-independent variables, and also used as predictive models to assess the impacts of climate change on fisheries biomass. These predictions should help inform sustainable management of resources both at present and into the future.

CLIMATE CHANGE IMPACTS

5

5 PROJECTIONS OF THE IMPACTS OF CLIMATE CHANGE ON REGIONAL-SCALE UPWELLING PHYSICS, PRIMARY PRODUCTIVITY, AND FISHERIES PRODUCTIVITY

Impacts of Climate Change on Environment, Primary Productivity, and Tertiary Productivity of Arrow Squid (*Nototodarus gouldi*) in an Australian Upwelling Region

Anne-Elise Nieblas^{1,2*}, Bernadette M. Sloyan^{3,4}, Malcolm Haddon⁴, Alan J. Butler⁴, Anthony J. Richardson^{5,6}

¹ School of Zoology, University of Tasmania, Hobart, Tasmania, Australia.

² Commonwealth Scientific and Industrial Research Organisation (CSIRO) Climate Adaptation National Research Flagship, CSIRO Marine and Atmospheric Research, Hobart, Tasmania, Australia.

³ Centre for Australian Weather and Climate Research, CSIRO Marine and Atmospheric Research, Hobart, Tasmania, Australia

⁴ CSIRO Wealth from Oceans National Research Flagship, CSIRO Marine and Atmospheric Research, Hobart, Tasmania, Australia

⁵ CSIRO Climate Adaptation National Research Flagship, CSIRO Marine and Atmospheric Research, Cleveland, Queensland, Australia.

⁶ School of Mathematics and Physics, University of Queensland, St Lucia, Queensland, Australia.

*Corresponding author: Anne.Nieblas@csiro.au

ACKNOWLEDGEMENTS

A.E.N. is supported by a joint Commonwealth Scientific and Industrial Research Organisation–University of Tasmania Ph.D. scholarship in Quantitative Marine Science. I thank the Australian Fisheries Management Authority for fish catch data and Mike Fuller for his help with data manipulation. I thank the following agencies for environmental data: 1) sea surface temperature – National Oceanic and Atmospheric Administration and National Aeronautics and Space Administration (NASA), 2) Sea-viewing Wide Field-of-view Sensor ocean colour – NASA, and 3) wind – National Centre for Environmental Prediction–National Centre for Atmospheric Research. Satellite data were accessed using the Spatial Dynamics Ocean Data Explorer – customised software provided by Alistair Hobday, Klaas Hartmann, Jason Hartog, and Sophie Bestley. I thank the modelling groups for providing climate model data for analysis, the Program for Climate Model Diagnosis and Intercomparison for collecting and archiving the model output, and the JSC/CLIVAR Working Group on Coupled Modeling for organising the model data analysis activity. The multi-model data archive is supported by the Office of Science, U.S. Department of Energy.

INTRODUCTION

Climate change is having substantial and discernable impacts on the physical environment and will likely have unprecedented effects on organisms (Walther et al. 2002), including changes in abundance and phenology, and changes to ecosystem structure and functioning (Stenseth et al. 2002, Parmesan 2006). The majority of studies on the impacts of climate change have focused on terrestrial systems, with very few studies investigating marine systems (Richardson & Poloczanska 2008). However, the majority of earth system heating by greenhouse gases is absorbed by the ocean, especially in the upper 700 m (Murphy et al. 2009). Most marine organisms inhabit this upper layer, indicating that marine ecosystems are likely to be affected by climate change. As marine fisheries provide up to 16% of global animal protein (FAO 2007) and oceans account for ~63% of global ecosystem services (Costanza et al. 1997), it is imperative to determine the potential impacts that climate change will have on the marine environment

Changes in the distribution, abundance, phenology, community composition and physiology of marine species will occur as a result of climate change (Poloczanska et al. 2007), due to the effects of changing environmental forcing. Changes in abundance of species may occur at both larval and adult stages due to changes in reproductive success, and growth. Spawning and recruitment success of many marine species with pelagic eggs and larvae are governed by the ocean features of concentration, retention, and enrichment (Bakun 1996), which are themselves controlled by environmental parameters (Walther et al. 2002, Chapter 2.2). The spawning and migration behaviours of many marine organisms coincide with productivity peaks, therefore changes in seasonality of productivity drivers (i.e. alongshore upwelling wind stress) could lead to trophic mismatches at larval and adult stages (Edwards & Richardson 2004, Henson & Thomas 2007). Further, changes to productivity and temperature patterns can have direct physiological influences on growth and mortality of species (Walther et al. 2002).

Coastal upwelling zones are the most productive marine environments. They constitute <1% of the ocean by area, but account for >20% of global ocean productivity (Pauly & Christensen 1995). They are characterised as regions with alongshore wind stress that drives surface water offshore, drawing cool, nutrient-rich water into the surface euphotic zone. This enhances primary productivity that in turn supports a rich abundance of marine fauna. Under climate change, upwelling wind stress has been predicted to intensify (Bakun 1990), which has been supported by observations (Schwing & Mendelssohn 1997, Mendelssohn & Schwing 2002). Changing wind forcing could have profound effects on the productivity of marine ecosystems (Snyder et al. 2003).

Most major upwelling systems are located along eastern boundaries of ocean basins (Pond & Pickard 1983, Mann & Lazier 1996), such as off the coasts of the USA, Peru,

Namibia, and South Africa. Australia is unique in that large-scale upwelling is absent off the West Australian coast due to the poleward-flowing Leeuwin Current that suppresses otherwise upwelling-favourable wind forcing (Hanson et al. 2005a). Consequently, upwelling around Australia occurs only in smaller, regional systems. The Bonney Upwelling in south eastern Australia (Fig. 5.1) is Australia's largest and most predictable coastal upwelling (Butler et al. 2002) and has physical forcing similar to the larger wind-driven upwelling systems on eastern boundaries of ocean basins (Nieblas et al. 2009).

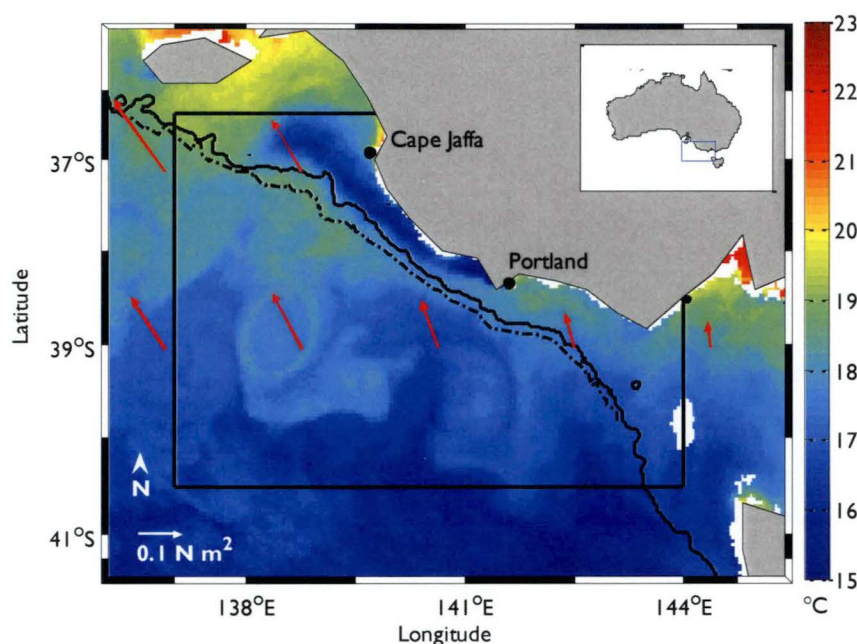


Fig. 5.1: The Bonney Coast off south eastern Australia with schematic coastline. The colour bar represents sea surface temperature ($^{\circ}\text{C}$), and the upwelling plume is signified by cool ($\sim 15^{\circ}\text{C}$) water off the coast. Red arrows represent observed wind stress, the continental shelf is represented by the 200 m (black line) and 1000 m (dashed black line) contours. The black box represents the South East Scalefish and Shark Fishery zone 50.

The Bonney Upwelling is driven by the seasonal latitudinal migration of the subtropical ridge (Linacre & Hobbs 1977, Sturman & Tapper 1996) that drives westerly, downwelling favourable winds in the austral winter (Rochford 1975) and south easterly, upwelling-favourable winds in the austral spring and summer (Lewis 1981, Schahinger 1987, Griffin et al. 1997). Regional ocean circulation and large-scale climate indices (El Niño–Southern Oscillation (ENSO)) also influence upwelling variability. The westward-flowing Flinders Current at the continental shelf break enhances open ocean-shelf water exchange that preconditions wind-driven coastal upwelling by lifting the thermocline on the continental shelf (Middleton & Cirano 2002). A seasonal coastal current opposes the Flinders Current, with strong south eastward flow during winter that reverses to a weak north westward flow in summer (Middleton & Cirano 2002, Middleton & Platov 2003). The

Bonney Coast upwelling is weakly related to ENSO variability (Middleton et al. 2007, Nieblas et al. 2009) due to teleconnections via the Leeuwin Current. During El Niño (La Niña) events, the Leeuwin Current is weakened (strengthened), which in turn shoals (deepens) the thermocline off the Bonney Coast (Nieblas et al. 2009). The majority of the upwelling activity is during the austral summer from November to April, and the development, peak, and decline of upwelling activity follows four distinct phases: “onset,” “sustained,” “quiescent,” and “downwelling” (Mitchell-Innes et al. 1999, Nieblas et al. 2009).

In addition to alongshore wind stress, environmental conditions such as wind speed, thermocline structure, and temperature influence upwelling-driven productivity, and are likely to be affected by climate change (Meehl et al. 2007, Coma et al. 2009). An “optimal environmental window” has been defined where wind speed is strong enough to promote vertical mixing, but not so strong as to lead to vigorous turbulent mixing or advection from the system ($5\text{--}6\text{ m s}^{-1}$ for fish productivity; Cury & Roy 1989). The Bonney Upwelling is currently considered a low-wind system, with mean wind speed of 4.1 m s^{-1} (Nieblas et al. 2009). The depth of the thermocline is an important determinant of marine productivity, as upwelling wind stress must effectively mix nutrient-rich water from below the surface mixed layer into the euphotic zone to stimulate phytoplankton growth. Temperature may have multiple impacts on upwelling-driven productivity, including influences on stratification of the surface layer and on water column stability that can be favourable for phytoplankton growth and spawning success of fish (Lasker 1975, 1978). However, temperature effects that induce stratification may also suppress upwelling activity and limit the amount of new nutrients reaching the surface layer (Bopp et al. 2001).

The Bonney Upwelling supports a productive fishing ground, including one of Australia’s oldest and most valuable fisheries, the Commonwealth South East Scalefish and Shark Fishery (Tilzey 1994). Only Commonwealth data were available in this study, and though small pelagic fish are common throughout the region, these fisheries operate under Australian state (South Australian and Victoria) control. However, arrow squid (*Nototodarus gouldi*) are widespread in southern Australia (Stark et al. 2005) and are targeted by the Commonwealth’s largest jig fishery. This jig fishery was valued at ~\$1.2M in 2002–2003 (Australian Fisheries Management Authority 2004) and arrow squid are also a valuable by-product year-round in the South East Scalefish and Shark Fishery trawl sector. Of the Commonwealth species caught in the region, squid have the third highest catch in tonnes (t) and are the only r-selected species (Boletzky 1981) in the top 20 species by catch in the region.

As r-selected species, squid have rapid growth rates, high fecundity, and relatively low and variable recruitment (MacArthur & Wilson 1967). Although they are aggressive predators, squid also fill similar ecological roles to small pelagic fish as they are a neritic, pelagic, schooling species, capable of rapid population response (O’Shea et al. 2004). They

also have pelagic egg “balloons” and planktonic paralarvae that feed in upper ocean planktonic communities (Bakun & Csirke 1998). However, their life histories are even more rapid than small pelagic fish, with faster growth rates and shorter life spans (Jackson et al. 2005), which require a high caloric intake and relatively low energy expenditure (Bakun & Csirke 1998). Squid have inherent life history flexibility that enables rapid individual responses to fluctuating conditions, especially temperature and food availability that influence the timing and success of spawning, hatching, growth, recruitment, and reproductive maturity (Forsythe 1993, Jackson & Moltschanowskyj 2001, Stark 2008). Thus arrow squid constitute a convenient candidate species for examining the impacts of a changing climate on fisheries productivity, particularly that of small pelagic predators.

Here, I investigate potential impacts of climate change on a regional upwelling ecosystem using two likely emissions scenarios from an ensemble of seven different climate models. I develop environmental indices that represent temperature and upwelling wind stress and speed off the Bonney Coast. I validate 20th century climate model simulations of regional-scale environmental indices against observations. Log-linear models are used to examine change in phytoplankton and arrow squid in the Bonney Upwelling ecosystem. These models define a set of environmental and biological relationships, which are then used with climate model variables to simulate future abundance. These statistical biophysical models assess the projected seasonal and monthly change in phytoplankton productivity and fisheries productivity of a commercially-important species of squid (arrow squid) off the Bonney Coast. I discuss the benefits and limitations of the model results, and the wider implications for the Bonney Upwelling ecosystem. Models that examine the impacts of climate change are relatively new to marine ecosystems. This study investigates the impacts of climate change by developing simple biophysical models that link ocean and atmospheric projections to primary and fisheries productivity.

METHODS

Data

The data sources and methods used in this study are summarised in Fig. 5.2. Environmental data were gathered from a variety of sources to validate the climate models, compare with statistical models of chlorophyll production (Nieblas et al. 2009), and develop a viable squid catch rate biophysical model. I used six-hourly 10 m wind data that were taken from the National Center for Environmental Prediction–National Center for Atmospheric Research Reanalysis Project (NCEP–NCAR) (Kalnay et al. 1996). Sea surface temperature (SST) data were taken from local area coverage National Oceanic and Atmospheric Administration’s Advanced Very High Resolution Radiometer (AVHRR) that was processed into daily 6-day composites (Griffin et al. 2004). Eight-day Sea-viewing Wide Field-of-view Sensor (SeaWiFS)

ocean colour images were used to represent chlorophyll *a* concentration in surface waters. Despite limitations in coastal regions, ocean colour is an extensively used (e.g.

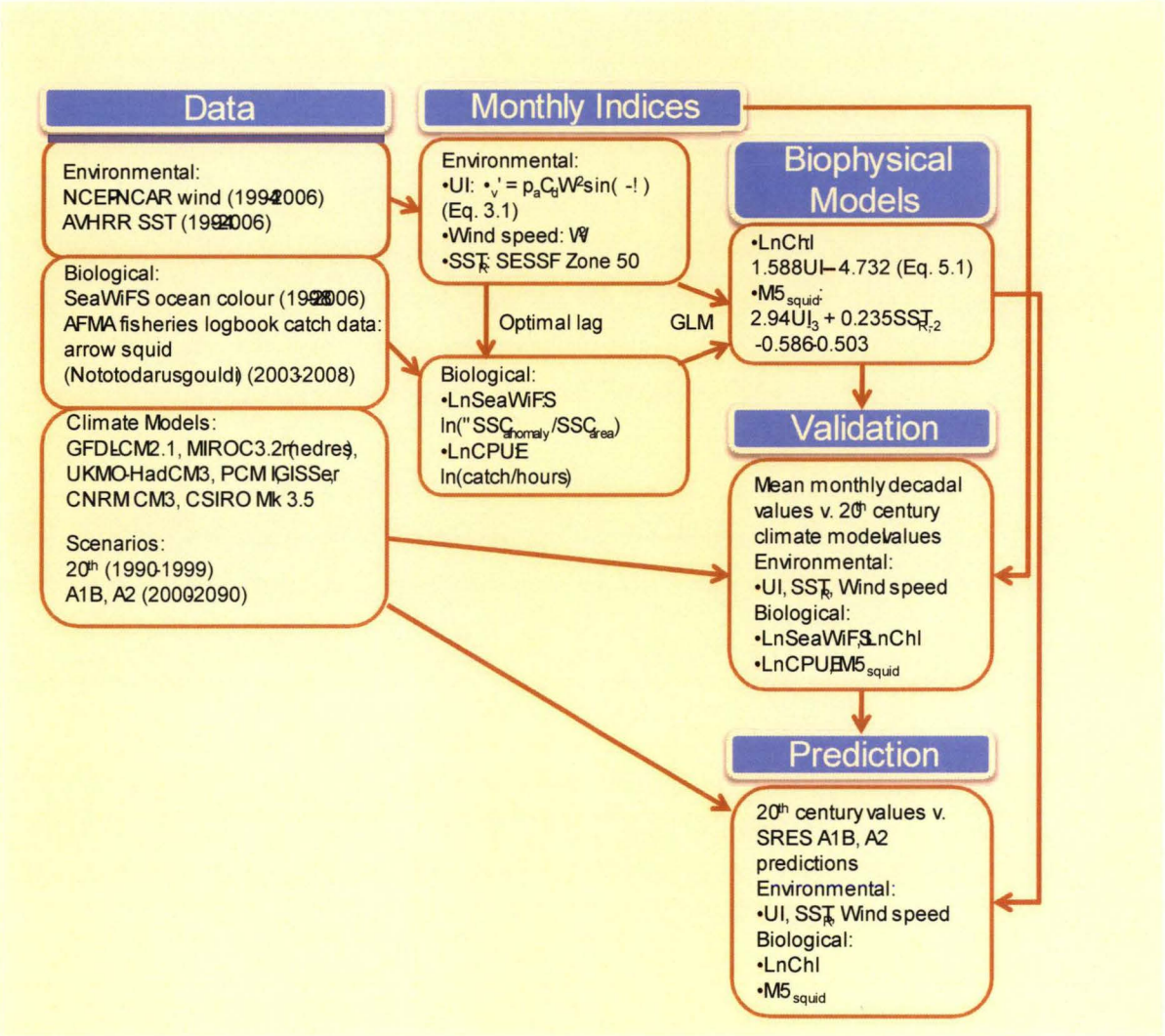


Fig. 5.2: Schematic diagram of the data sources and methods used in this study.

Sathyendranath et al. 1991, Alvain et al. 2005) and an appropriate proxy for phytoplankton biomass in upwelling systems where primary productivity is high and variable. I refer throughout the text to NCEP–NCAR wind, AVHRR SST, and SeaWiFS chlorophyll as “observations”, though they are derived from a reanalysis model and satellite data.

Australian Fisheries Management Authority (AFMA) logbook catch dataset was used to develop the biophysical statistical model of arrow squid catch rates. Catches were obtained from the South East Scalefish and Shark Fishery zone 50, directly off the Bonney Coast (Fig. 5.1). Detailed methods for handling these data are explained in Chapter 4. There are several caveats associated with the use of catch data as an index of abundance for harvested marine resources, which are discussed in Chapter 4. Nevertheless, I believe I make reasonable assumptions regarding the quality and handling of the data.

I examined two emissions scenarios for 7 climate models as described by the Special Report of Emissions Scenarios deemed to be the most realistic for current CO₂ emissions: A1B and A2 (Nakicenovic et al. 2001). The A1B scenario (approximately linear CO₂ emissions) describes an affluent world of decreasing fertility and mortality and increasing equity in international productivity and economic development. This scenario portrays relatively high demands of energy and materials, which is somewhat mitigated by increased technological and structural efficiency. The A2 scenario describes a more “business-as-usual” approach with similar population growth patterns to the current period, slow convergence of international development, and slow uptake and use of efficient technology, including delayed development of renewable energy. Other scenarios (e.g. B1, B2) describe more strongly developed mitigation measures. However as climate is currently tracking closest to the highest emissions scenario (A1FI, Rahmsdorf et al. 2007), these scenarios were deemed too optimistic to warrant further investigation.

From the climate models I obtained simulated (20th century) and predicted (21st century) A1B and A2 monthly environmental variables to be used in the chlorophyll *a* concentration (Chl) production and squid catch rate biophysical models. These included 2-dimensional wind stress (τ), wind speed, and SST. I developed ensemble means from seven climate models (Table 5.1; details of IPCC climate models can be found online at [www-pcmdi.llnl.gov/ipcc/about_ipcc.php](http://www.pcmdi.llnl.gov/ipcc/about_ipcc.php)). Climate models have coarse spatial resolution (0.3°–5° longitude (x) by 0.3°–4° latitude (y)). I did not correct for systematic model drift of environmental variables in this study as it is much smaller than changes due to the selected forcing scenarios (Sloyan & Kamenkovich 2007).

Environmental indices

Environmental indices in this study are defined similar to Nieblas et al. (2009) and Chapter 4. The upwelling wind index is defined as the wind stress component parallel to the coast (UI; units: N m⁻²). Positive (negative) UI indicates upwelling (downwelling or relaxation). Wind speed (units: m s⁻¹) was calculated to assess whether the Bonney Upwelling system shifted within the optimal environmental window for biological production. For both UI and wind speed, I used observational values at 39°S, 140.5°E (Fig. 5.1) and climate model values closest to this location to represent coastal wind that directly influenced upwelling along the Bonney Coast. Monthly mean observational and climate model SST values were determined for the South East Scalefish and Shark Fishery zone 50 (Fig. 5.1) (SST_R; units: °C). Following Nieblas et al. (2009), the present-day response of primary productivity to upwelling was determined from SeaWiFS Chl. The largest continuous region of anomalous chlorophyll (>0.6 mg m⁻³) was divided by the area of the plume to give an approximation of phytoplankton biomass of the upwelling plume. A visual inspection of residuals indicated that a log normal transformation of Chl data was necessary (LnChl; units: mg m⁻³ km⁻²).

Table 5.1: Details of climate models used in this study. Geophysical Fluid Dynamics Laboratory (GFDL); the National Oceanic and Atmospheric Administration (NOAA); Model for Interdisciplinary Research on Climate 3.2 medium-resolution (MIROC3.2 (medres)); the Center for Climate System Research (CCSR); the National Institute for Environmental Studies (NIES); the Frontier Research Center for Global Change (FRCGC); the Japan Agency for Marine-Earth Science and Technology (JAMSTEC); the U.K. Met Office Hadley Centre Coupled Model, version 3 (UKMO-HadCM3); Parallel Climate Model, version 1.1 (PCM 1); the National Center for Atmospheric Research; the Goddard Institute of Space Studies Model E/Russel (GISSer); the National Aeronautics and Space Administration (NASA); the Centre National de Recherches Meteorologiques (CNRM); and the Commonwealth Scientific and Industrial Research Organisation (CSIRO).

Climate model	Institution	Horizontal resolution	Temporal range (monthly)
GFDL-CM2.1	NOAA/GFDL	lon: 1° lat: 1°-0.33°	20th: 1861-2000 A1B: 2001-2300 A2: 2001-2100
MIROC3.2 (medres)	CCSR/NIES/FRCGC (JAMSTEC)	lon: 0.28° lat: 0.19°	20th: 1850-2000 A1B: 2001-2300 A2: 2001-2100
UKMO-HadCM3	Hadley Centre for Climate Prediction	lon: 1.25° lat: 1.25°	20th: 1860-1999 A1B: 2000-2199 A2: 2000-2099
PCM 1	NCAR	lon: 2.81° lat: ~2.79°	20th: 1890-1999 A1B: 2000-2199 A2: 2000-2099
GISSer	NASA/GISS	lon: 5° lat: 4°	20th: 1880-2003 A1B: 2004-2300 A2: 2004-2100
CNRM CM3	CNRM	lon: 2° lat: 1.5°-0.5°	20th: 1860-1999 A1B: 2000-2300 A2: 2000-2100
CSIRO Mk 3.5	CSIRO, Marine and Atmospheric Research	lon: 1.87° lat: 0.84°	20th: 1871-2000 A1B: 2001-2300 A2: 2001-2100

Biophysical models

To develop predictions of how climate change may affect upwelling productivity I employed a linear model developed in Nieblas et al. (2009) that predicts nearly 40% of the variability of LnChl based on upwelling wind stress:

$$\text{LnChl} = 1.588\text{UI} - 4.732 \quad (5.1)$$

This model tends to under-predict the magnitude of phytoplankton peaks evident in SeaWiFS data, which is exacerbated by the log transformation. However, it captures the seasonal variability of the upwelling-driven chlorophyll signal (Fig. 5.3a).

I also develop a log-linear model to describe how log-transformed arrow squid catch rates relate to environmental variables. Models developed in Chapter 4 consider several environmental variables that were not compatible, or could not be easily derived from climate models (e.g. SeaWiFS Chl and sea level). In order to estimate Chl, Eq. 5.1 is forced with climate model output, which makes this estimate more uncertain. Sea level is a diagnostic variable in the climate models that can be defined by several methods (see http://www-pcmdi.llnl.gov/ipcc/standard_output.html). It is not clear how each climate model calculates this variable, or if the climate model variable is equivalent to altimetric sea level. Therefore, I build a biophysical squid model using only UI, wind speed, and SST. From Chapter 4, I expect that the simpler model developed for use with climate models should provide a reasonably accurate prediction.

Cross correlations and lag plots were used to find the most appropriate lag times between observational log-transformed arrow squid catch rate data and the useable environmental indices. I then built a log-linear model and used step-wise regression to determine the optimum relationship between natural log-transformed arrow squid catch rates and environmental indices. I used the Akaike Information Criterion (AIC), adjusted coefficients of determination (r^2), and p-values from an Analysis of Variance test to assess the model fit against observations. Models were created using the base time period of 2003–2007 and data from 2008 was withheld from model development to validate model predictions. In addition, retrospective analyses were performed by removing years of data to compare the consistency of results and the capacity for prediction of the models based on reduced datasets. These validations were performed with present-day observations before applying climate model-derived variables to the final biophysical model.

Impacts of climate change emissions scenarios analysis

Ensemble means of physical variables for 20th century climate models (SST, u , v , and τ) were compared to observational data to examine how well climate model variables simulate the seasonality and magnitude of observational environmental indices. I defined the 20th century climate model mean as a 10-yr period (1990–1999) and compared to mean observational wind and SST data from 1994–2006 (Nieblas et al. 2009). To assess the impact of climate change on upwelling drivers, I compare decadal means of 20th century (1990–1999) with two emissions scenarios (A1B, A2) for the late 21st century (2090–2099). I then developed ensemble means of the 20th century run, and the A1B and A2 climate scenarios using all climate models (Table 5.1) to assess change over 100 years. Recent

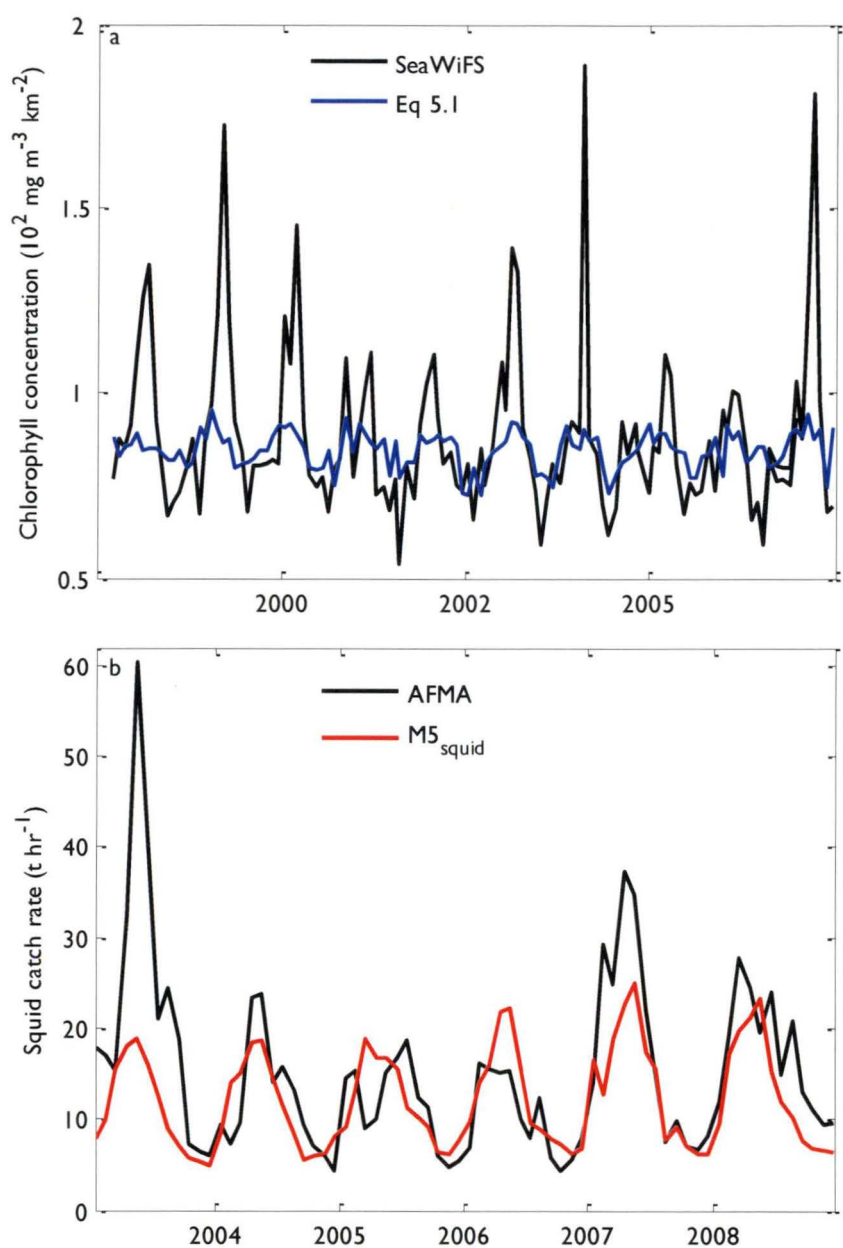


Fig. 5.3: (a) Chl of the Bonney Upwelling plume ($\text{mg m}^{-3} \text{ km}^{-2}$) as measured from SeaWiFS satellite data (black) and predicted by Eq. 5.1 (blue). (b) Squid catch rate (t hr^{-1}) for the South East Scalefish and Shark Fishery zone 50 as reported by AFMA logbook data (black) and predicted by $M5_{\text{squid}}$ (red).

studies have shown that projections made by different models can be extremely variable (e.g. Pearson et al. 2006), which may undermine the usefulness of the prediction (Araújo & New 2007). An ensemble approach to studying the impacts of climate change has been advocated to incorporate the variability in projections from multiple models (Araújo & New 2007).

I forced the biophysical LnChl and squid models with environmental indices derived from climate model 10-yr ensemble means to predict the relative phytoplankton biomass and squid abundance and assess potential future change. I compared mean monthly 20th century (1990–1999) climate model-based predictions against mean monthly observational LnChl (1998–2006; as in Nieblas et al. 2009) and squid logbook data (2003–2007; Chapter 4), and modelled LnChl and squid forced with present-day observational environmental indices. I assessed the long-term change in phytoplankton biomass and squid abundance using similar methods to assess change in upwelling drivers.

RESULTS

Arrow squid predictive model

UI was significantly and positively related to arrow squid abundance at a seasonal lag of 3 months (Table 5.2) (UI_{-3} ; $r=0.57$) and SST_R at 2 months ($SST_{R,-2}$; $r=0.69$). Wind speed was not significantly related to arrow squid abundance. The optimally-lagged environmental indices were input in a sequential fashion to log-linear models. The best model fit for natural log of arrow squid CPUE from 2003–2007 ($M5_{squid}$) included a Year factor to account for annual variability of abundance, with UI_{-3} , and $SST_{R,-2}$ as predictor variables (adjusted $r^2= 66.2\%$, $AIC=52.81$) (Table 5.2; Fig. 5.3b). A mean of all Year factor estimates was taken so that the model could be used for future prediction. Year explained 10.4% of variance for catch rates of arrow squid, UI_{-3} contributed an additional 35.9% to model fit and $SST_{R,-2}$ contributed a further 19.9% to the overall fit (Table 5.2). A visual inspection showed that $M5_{squid}$ follows the time series of AFMA catch data well, with the exception of 2003, when the location of a peak in catch is predicted by the model but not its magnitude (Fig. 5.3b).

Table 5.2: Best fit step-wise linear modelling of observed environmental predictors against arrow squid CPUE (2003–2007) with adjusted coefficients of determination (Adj r^2) and the Akaike Information Criterion (AIC) indicating goodness-of-fit. ‘ln’ represents the natural log. Significance codes for each predictor variable in the ANOVA are represented as *** $p < 0.001$, ** $p < 0.01$, * $p < 0.05$.

Arrow squid		Predictors			Adj r^2	AIC
	ln(CPUE _{squid})	Year*			0.104	109.57
	ln(CPUE _{squid})	Year**	UI ₋₃ ***		0.463	79.76
M5 _{squid}	ln(CPUE _{squid})	Year***	UI ₋₃ ***	SST _{R,-2} ***	0.662	52.82

Retrospective validation for arrow squid CPUE was performed using $M5_{squid}$ with data that had been reduced from the full time series to include just 2003–2006 and 2003–2005. The $M5_{squid}$ retrospective models performed well and described 61.2% and 58.0% of the variability, respectively (Table 5.3). The full and reduced $M5_{squid}$ models described 88.1–88.3% of the withheld 2008 ln(CPUE) data (Table 5.3). Parameter values remained

consistently significant throughout the analyses and indicated that the models are robust, giving more confidence in their use for predictions.

Table 5.3: Model parameter estimates and retrospective analysis of observed environmental predictors against arrow squid CPUE. Mean of all year factor estimates listed. Adjusted coefficients of determination (adj r^2) show goodness-of-fit. Significance codes of each predictor in the ANOVA are represented as *** p < 0.001, ** p < 0.01, * p < 0.05. 2008 column represents adjusted r^2 of each model's 2008 predictions against 2008 arrow squid CPUE.

Mode	Data range	Adj r^2	AIC	Intercep				2008 predictions
				t	Year	UI ₋₃	SST _{R,-2}	Adj r^2
M5 _{squid}	2003–		52.8		–	2.94**		
	2007	0.662	1	–0.503	0.586***	*	0.235***	0.880
	2003–		47.1		–	1.91**		
	2006	0.612	8	–0.608	0.647***	*	0.240***	0.884
	2003–		42.0			2.70**		
	2005	0.580	8	–0.497	–0.596**	*	0.234**	0.881

Validation of 20th century climate model simulations for physical and biological indices

The 20th century climate models simulations (1990–1999) were compared to present-day observed data (1994–2006) for each physical variable. SST_R was well-resolved by climate models and related strongly to the seasonal cycle of observations ($r^2=0.70$ – 0.87) (Fig. 5.4a). This is not unexpected as temperature varies latitudinally and is linearly related to atmospheric warming, although it also depends on ocean circulation. Climate models tended to predict warmer SST_R in the austral summer–autumn than observed, but most did reasonably well at predicting the austral winter–spring values (Fig. 5.4a). The majority of climate models did not predict the u (east–west) component of wind speed as well ($r^2=0.02$ – 0.25) as the v (north–south) component ($r^2=0.60$ – 0.76) (Fig. 5.4b, c). This indicates that the migration of the subtropical ridge is well-modelled; however the position of these ridges is not correct due to the coarse model grid. Climate model UI related reasonably well to observed UI ($r^2=0.31$ – 0.49). This reasonable simulation is explained by the predominantly north-south orientation of the Bonney Coast ($\beta=315^\circ$) and that the v -component of the wind is simulated well by climate models. Most climate models captured summer UI well; however they over-predicted the westerly, downwelling-favourable (negative) wind stress (Fig. 5.4d). Ensemble means of the 20th century simulation showed some differences to the observed UI in the transition period between the mostly negative (downwelling, March–April) and mostly positive (upwelling, November–December) phases, although the seasonal signal was similar (Fig. 5.4d).

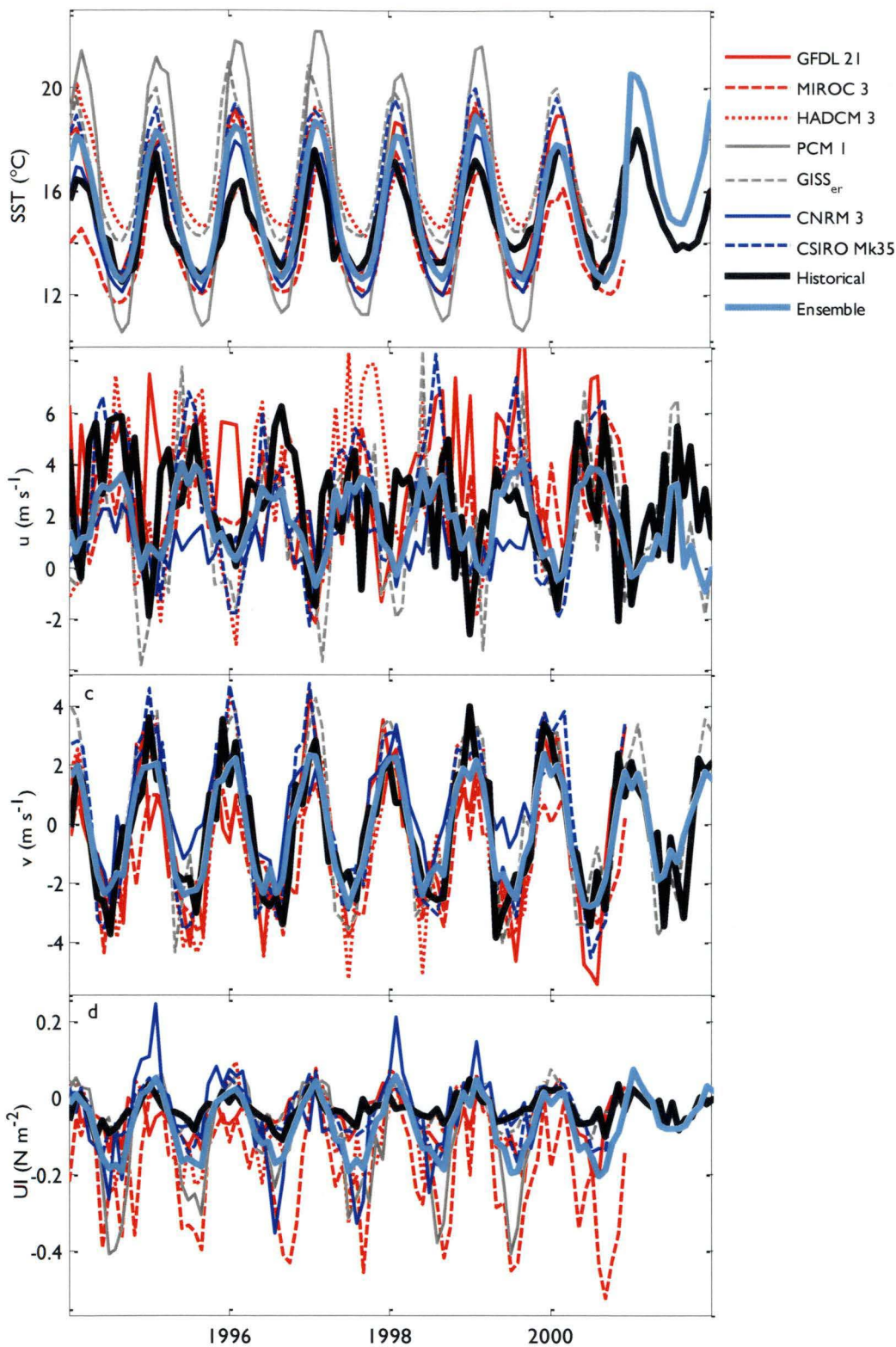


Fig. 5.4: Climate model 20th century (a) SST ($^{\circ}\text{C}$), (b) u -component of wind speed (m s^{-1}), (c) v -component of wind speed (m s^{-1}), and (d) UI (N m^{-2}) plotted against present day observations. Cyan lines represent the ensemble means of the seven different climate models. Model name abbreviations as listed in Table 5.1.

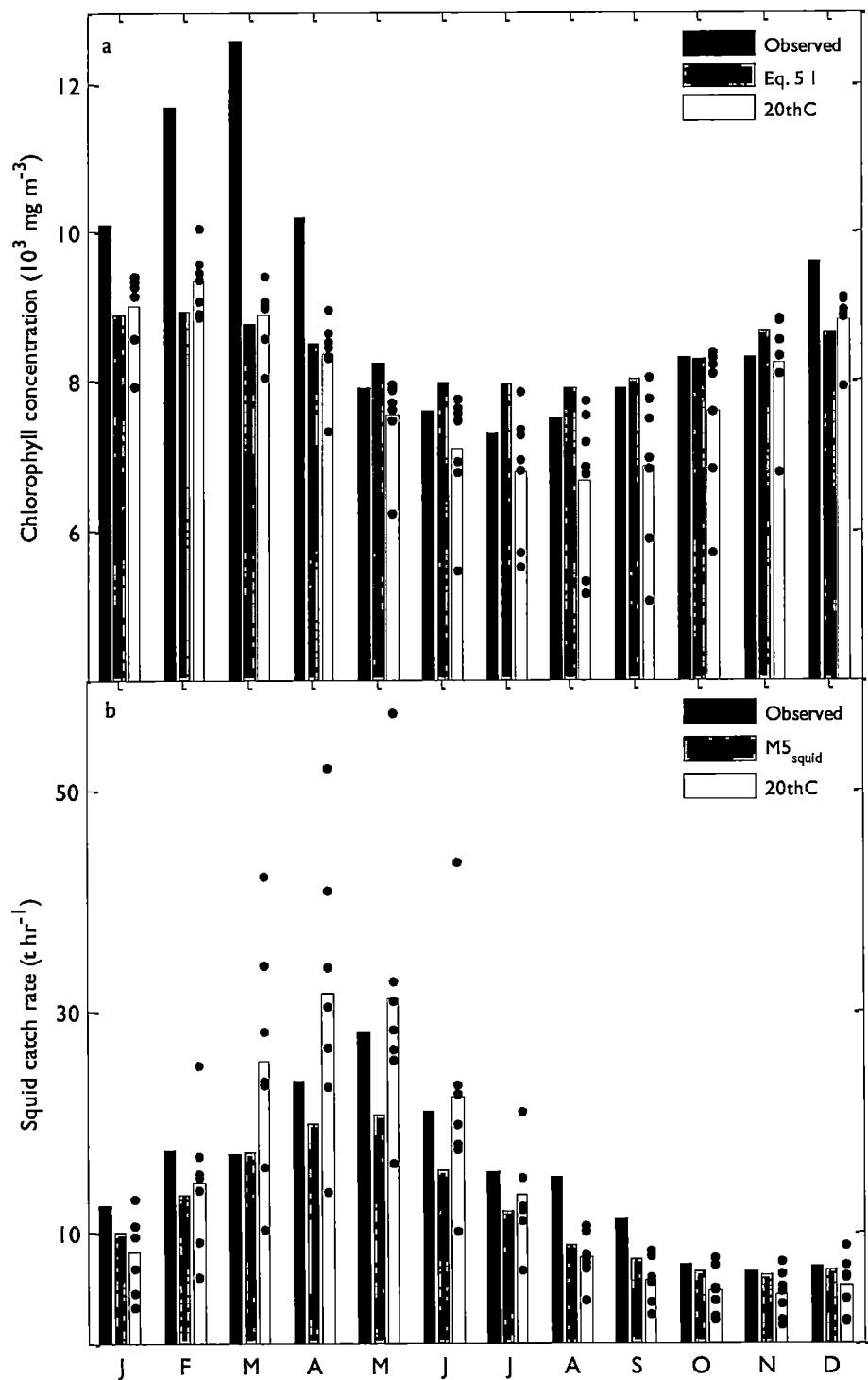


Fig. 5.5: Mean monthly (a) Chl for Eq 5.1 and 20th century climate models and (b) squid catch rates for M5_{squid} and 20th century climate models plotted against present-day observations. Black dots represent individual climate model predictions for the 20th century.

The simulations of the biophysical models forced by 20th century climate model data matched well the seasonal signal of the biophysical model simulations forced by observations (Fig. 5.5). Climate models simulate Chl well and especially in the upwelling season (November–April) in comparison to observationally-modelled Chl (Fig. 5.5a). Simulations by the biophysical model derived both from observations and climate models underestimate the magnitude of observed Chl peaks in January to March when Chl is highest, but did reasonably well the rest of the year (Fig. 5.5a). Similarly, biophysical models forced by environmental observations under-predict AFMA catch rates for all months except those of lowest catch (October–December) when the model matches well with observations. Biophysical squid models forced by climate models compare well to observations throughout the year with slight over-predictions in times of high catch due to increased variance with an increased mean (February–June) (Fig. 5.5b).

21st century climate projections

Sea surface temperature

Climate model projections of sea surface temperature were consistent amongst models and for each emission scenario (A1B and A2). Both scenarios of 21st century climate predict that SST will warm by 1–2°C throughout the year (Fig. 5.6a), although A2 consistently predicts warmer temperatures than A1B. Though slightly warmer than present-day observations, 20th century runs indicated that in the beginning of the upwelling season (November), SST in zone 50 was 14.3°C. This was projected to increase to 15.7°C under A1B and 16.2°C under A2. SST was projected to peak at the same time as 20th century runs (February) at 20.4°C by A1B and 20.8°C by A2, which is 1.6–2°C warmer than the 20th century ensemble mean. SST will decline again in April to May, and reach its lowest point in September (Fig. 5.6a).

Wind speed

Compared to the 20th century climate model run, the 21st century scenarios indicate that wind speed is not expected to change dramatically throughout the year. A1B generally predicted higher wind speeds throughout the year than A2 (not shown). Percent change of mean wind speed across climate scenarios were marginal and indicated a change of between 5–6% from both scenarios for the November to April upwelling season. A 3% increase for A1B and a 1.7% decrease for A2 were projected for the downwelling season. If these percent changes were applied to the present-day observed mean of 4.1 m s⁻¹, they would not substantially change the mean wind speed of the upwelling season in relation to the optimal environmental window of 5–6 m s⁻¹, and the Bonney Upwelling would remain a low-wind system.

Upwelling index

Compared to the ensemble means of their 20th century runs (1990–1999), the decadal monthly ensemble means of both A1B and A2 (2091–2099) climate scenarios predicted that UI will become more easterly (positive and upwelling-favourable) throughout the year in the late 21st century (Fig. 5.6b). A2 projected a larger positive shift in UI than A1B, and they both showed the largest change in November to April.

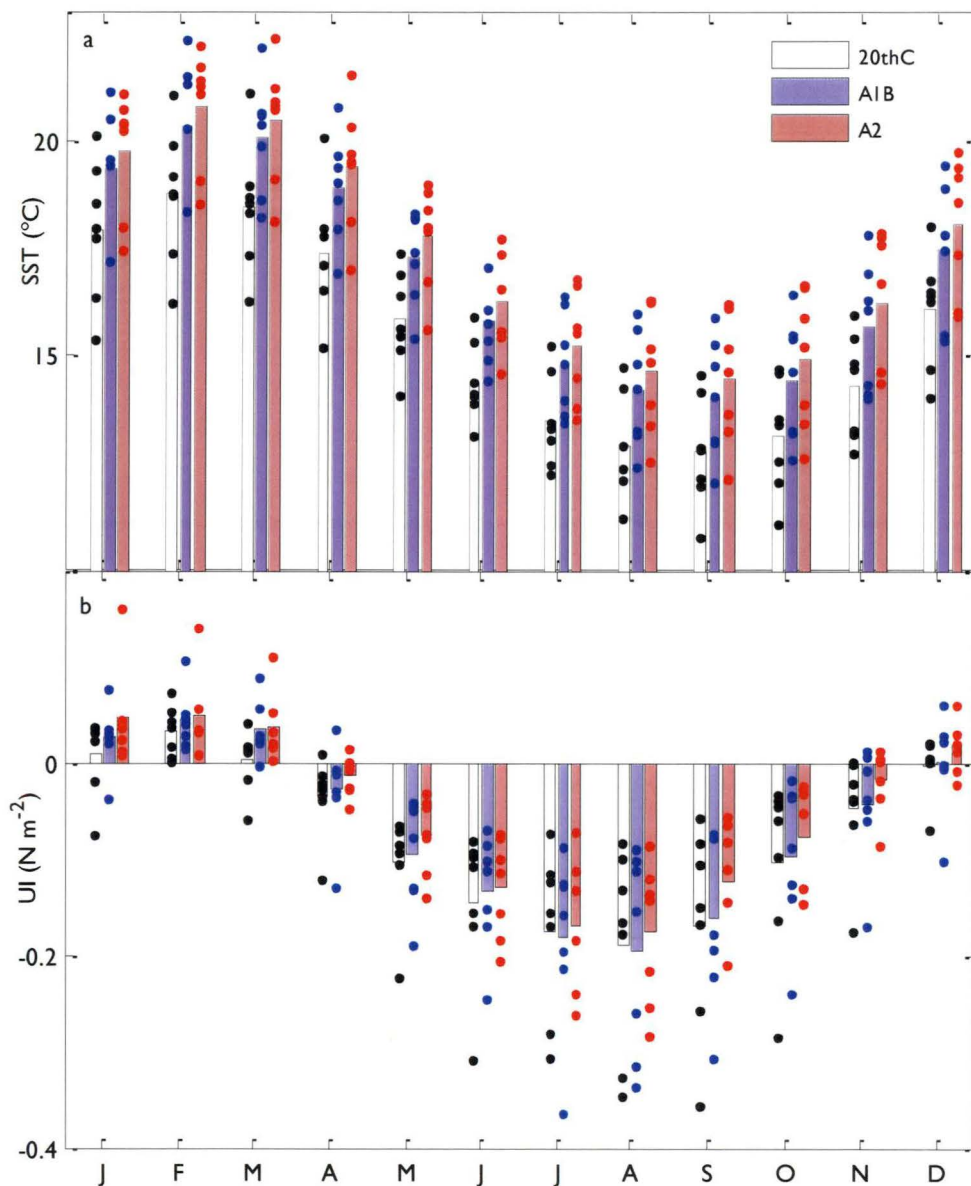


Fig. 5.6: Climate model ensemble means for the 20th century (1990–1999; white bar), and 21st century A1B (2090–2099; blue bar), and A2 (2090–2099; red bar) scenarios for (a) SST (°C), and (b) the wind stress-based upwelling index (N m⁻²). Individual model and scenario predictions for the 20th century (black dot) and projections of the 21st century A1B (blue dot) and A2 (red dot) scenarios are given to show the full range of model predictions.

Both climate scenario means indicated that westerly (negative) downwelling winds were strong and dominant in May to October. In November, the climate scenarios predicted a weakening of the westerlies, indicating more easterly (positive) upwelling-favourable wind events. A1B predicted a slight weakening and A2 showed a dramatic weakening of westerly winds from the 20th century ensemble mean (Fig. 5.6b). In December, the 20th century climate models showed UI as slightly negative, indicating westerly winds were diminishing but still dominant and easterly winds were becoming stronger or more frequent. A1B was slightly positive in December, indicating easterly winds will begin to dominate this period for this scenario of the 21st century. A2 predicted that UI will become strongly positive in December, indicating more frequent easterly upwelling wind events and perhaps stronger events than in the 20th century. A1B and A2 projections for January and February both showed UI to become more positive relative to the 20th century mean (Fig. 5.6b). In March, the 20th century mean indicated that upwelling-favourable easterly winds slacken, as wind stress was near zero but still positive. In contrast, both A1B and A2 predicted that upwelling-favourable winds dominated during this period. In April, A1B indicated that downwelling, westerly, strongly-negative winds dominate once more, while A2 projected only weak westerly winds that did not become strongly negative until May (Fig. 5.6b).

Ensemble means from the climate models predicted that the seasonal timing of upwelling wind stress will remain relatively unchanged, although the transition period to upwelling conditions (November–December) may be shorter, and the transition period to downwelling conditions (March–May) may either be more rapid with fewer and shorter periods of quiescence, or may be delayed by one month in comparison to 20th century wind stress. In addition, both A1B and A2 predicted more frequent or perhaps stronger easterly wind stress.

Projections of change in the biological system

Chlorophyll concentration

In comparison to 20th century runs, both A1B and A2 scenarios predicted Chl to increase throughout the year with small changes in winter, and larger changes from November to March (Fig. 5.7a). In September, A2 predicted a large increase in Chl in comparison to 20th century values, but A1B showed little change. Chl continued to increase steadily for both scenarios until January, when both A1B and A2 showed large increases in Chl in comparison to the model 20th century. A1B predicted Chl to peak in February, and A2 predicted the peak for January to February (Fig. 5.7a). Both predicted that Chl would begin to decline by March. By April, almost no change is predicted from 20th century predictions for A1B, though A2 still shows higher Chl. Both scenarios indicated that Chl declines during

the austral winter (May–August), but higher values were maintained by both scenarios throughout the year when compared to the model 20th century (Fig. 5.7a).

Arrow squid catch rates

Both climate scenarios projected an increase in arrow squid catch rate throughout the year in comparison to 20th century values (Fig. 5.7b). A2 predicted higher values than A1B, but both scenarios predicted most change during the period of peak catch (March–June), which is lagged slightly behind peak productivity driven by upwelling activity. Catch was lowest in September to December. Between January and June, 21st century predictions surpassed 20th century catch rates. Both 21st century catch rates peaked in April. Predicted catch rates remained high in May and June, but were projected to decline significantly by July as SST begins to cool at the end of the upwelling season (Fig. 5.7b).

DISCUSSION

In this study, I show that a regional upwelling ecosystem is sensitive to effects of climate change at both lower and higher trophic levels. I find that climate models predict wind stress along the Bonney Coast to become more upwelling-favourable throughout the year; with some change in seasonal cycle. However, no substantial change in mean wind speed is expected, indicating that the Bonney Upwelling will remain a low-wind upwelling ecosystem. The SST of the region is projected to rise by 1–2°C throughout the year.

These changes in physical forcing and background conditions of the Bonney Upwelling are projected to positively impact primary and fisheries productivity (as measured by chlorophyll and squid catch rate, respectively), assuming all other inter- and intra-species, community, and biophysical relationships remain unchanged. Our models project an increase of between 10–20% of chlorophyll concentration and a 40–70% increase in squid catch rates in the late 21st century relative to the late 20th century. I assume that the food web is stable, therefore, a much larger increase of Chl than our model predicts is necessary to maintain the predicted increase in squid catch rates due to more successful recruitment, faster growth rates and more biomass in the late 21st century. I note that Eq. 5.1 severely under-predicts chlorophyll concentration, indicating that there may be a much larger increase in Chl into the late 21st century. In addition, arrow squid have the ability to exploit ecological loopholes that may mitigate the effects of lower than necessary primary productivity in the ecosystem. However, due to uncertainties and assumptions of these predictions I believe their value lies with the general sign of change, rather than the approximate value of change.

Concerns have been raised regarding the ability of large spatial resolution climate models, such as those used in this study, to predict changes in upwelling (Bakun et al. 2009). Results of our validation indicate that, especially for temperature and wind stress, climate

models perform reasonably well at predicting regional-scale environmental indices for the Bonney Upwelling region. Ensemble means from seven climate models used in our study consistently predict upwelling-favourable winds to intensify into the 21st century for both climate scenarios examined. The high pressure subtropical ridge that dominates climate patterns in south eastern Australia (Sturman & Tapper 1996) is predicted to shift southwards, and this is supported by empirical evidence (Thresher et al. 2004). With this shift, zonal westerly (downwelling) winds that currently dominate during winter would have a weaker effect on the Bonney Coast and south easterly (upwelling-favourable) winds would be more frequent and potentially stronger throughout the year, in accordance with our results. This indicates that more confidence can be given to predictions made in

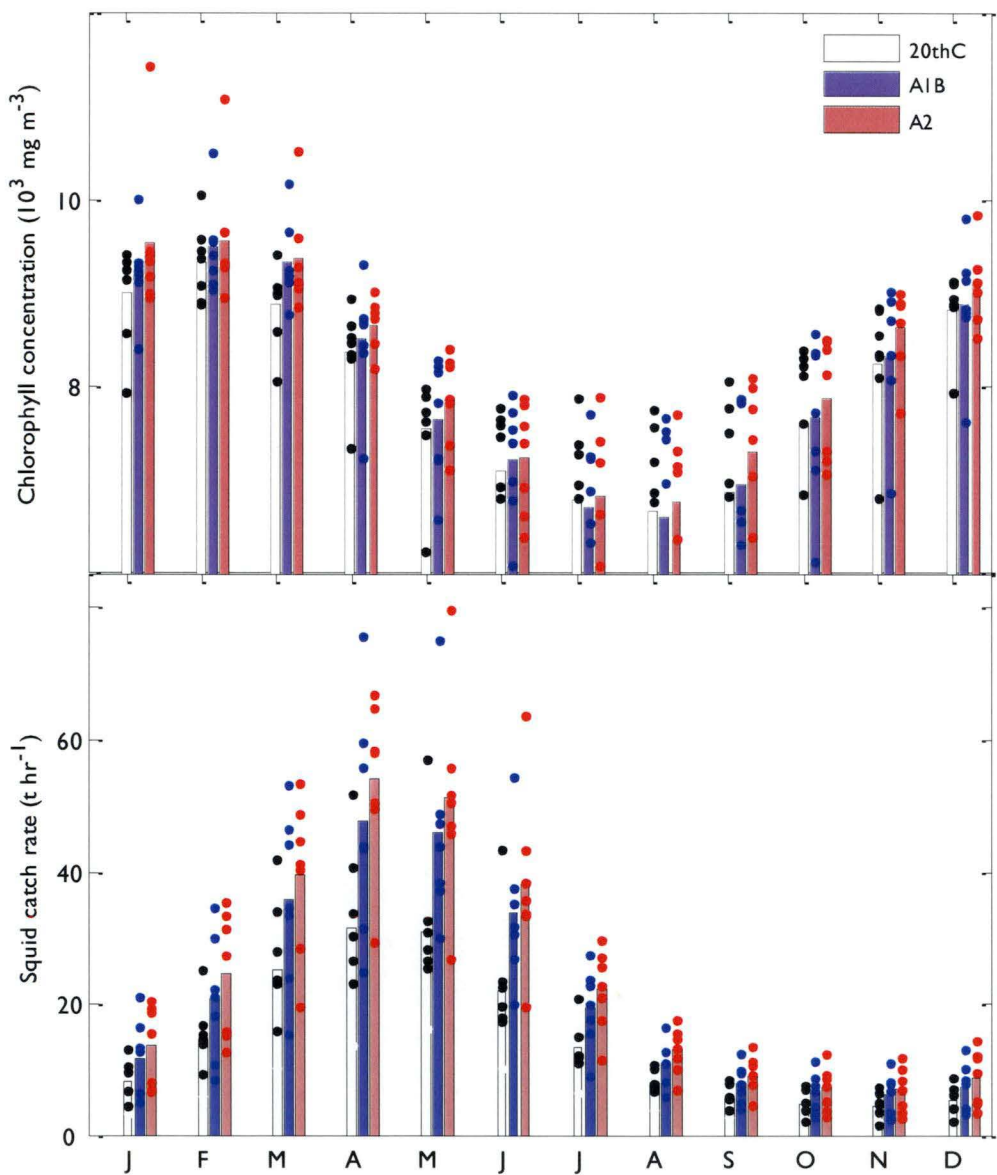


Fig. 5.7: As for Fig. 5.6, but for (a) Chl of the upwelling plume ($\text{mg m}^{-3} \text{ km}^{-2}$) and (b) squid catch rate (t hr^{-1}).

upwelling systems controlled by large-scale climate patterns that are well captured by climate models, as off the Bonney Coast.

The present-day environmental and biological indices were assumed to be accurate approximations of the environmental and ecosystem conditions. The biophysical statistical models I used and developed for Chl and squid catch rates describe ~40% and ~66% of present-day variability. These models lack biological interactions, evolutionary change and adaptations, and species dispersal and assume equilibrium between species and current environmental conditions. I did not consider effects of changes to other biotic, abiotic, or anthropogenic interactions (e.g. effects of ocean acidification, species adaptations, or changes in fishing practices). The models used in this study are different from bioclimate envelope models, which currently constitute the prevailing method in modelling the impacts of climate changes on plants and animals (Peterson et al. 2002, Thuiller et al. 2005, Araújo et al. 2006). Our models use methods that are routinely used with fisheries data to examine changes in abundance rather than distribution as with bioclimate envelope models. Regardless, the models used here are valuable tools for predicting potential impacts on marine species and ecosystems due to climate change. These predictions can provide hypotheses to refine future studies and inform policy decisions.

Impacts of climate change on the physical upwelling forcing

It is the prevailing theory that upwelling wind stress is likely to intensify with climate change (Bakun 1990). However, I expect the Bonney Upwelling will remain a low-wind forced system. I show temperature may increase throughout the year, potentially enhancing surface mixed layer stratification (Bopp et al. 2001); however, intensified wind stress leading to vertical mixing throughout the upwelling season may potentially mitigate this effect. In addition, El Niño conditions may become more frequent as climate change progresses (Trenberth & Hoar 1997), potentially shoaling the thermocline off the Bonney Coast (Middleton et al. 2007, Nieblas et al. 2009).

The onset phase of the Bonney Upwelling, which historically begins in November to December at the start of the austral summer, is characterised by variable, weakly westerly wind stress due to the faltering and shifting position of the subtropical ridge (Nieblas et al. 2009). Sustained upwelling is defined as the phase where upwelling winds become sufficiently strong and frequent to overcome background ocean processes and penetrate the mixed layer (Mitchell-Innes et al. 1999, Nieblas et al. 2009). By the end of the 21st century, both climate scenarios predict a rapid shift from onset conditions in November to sustained upwelling conditions by December. The ensemble means I develop find 1–2°C change in SST above the 20th century run throughout the year. The long-term trend may mask cooling driven by enhanced upwelling of deep waters (Schwing & Mendelssohn 1997), and SSTs should not be considered as indicative of upwelling strength

at these temporal and spatial scales (Di Lorenzo et al. 2005). I find temperatures that were typical for the sustained phase of the upwelling season in the 20th century (17°C in February, based on 20th century simulations) are predicted during November to December in the 21st century. Therefore, it appears that conditions previously confined to the sustained upwelling phase may occur earlier in the upwelling season (November–December) in the 21st century.

Historically, the sustained phase of upwelling is from January to February, March is typically the quiescent phase when upwelling winds relax, and April indicates the end of upwelling conditions off the Bonney Coast (Nieblas et al. 2009). Both climate scenarios differ from this pattern. A1B and A2 predict wind stress to remain strongly upwelling-favourable in March. Also, A1B predicts a rapid swing to downwelling conditions in April, with limited or no quiescent phase. In contrast, A2 becomes only weakly westerly in April (a delayed quiescent phase), and strong downwelling conditions do not occur until May, indicates that the A2 scenario predicts the upwelling season to extend by a month. SST_R remains warm throughout this period (18°C–20.5°C).

Impacts of climate change on upwelling-driven phytoplankton biomass

Our study indicates that in the future, under climate conditions A1B and A2, Chl will be higher throughout the year than currently in response to enhanced upwelling wind stress, particularly during the November to April upwelling season. However, a variety of other factors may influence phytoplankton growth and biomass including changes in regional and remote circulation (e.g. ENSO) that affect vertical thermocline structure, and nutrient supply (Bakun et al. 2009). Primary productivity is related to mean wind speed by the optimal environmental window. As mean wind speed is not projected to change substantially, deleterious effects of turbulence on phytoplankton are unlikely. Ocean temperatures are predicted to be warmer earlier (November–December) and may lead to earlier and elevated blooms, depending on the type of phytoplankton dominant in the region (Edwards & Richardson 2004), and the optimal temperature range of the community. Invasions of warmer-water species may change current communities and affect the bloom levels (Nehring 1996). The model I use predicts phytoplankton biomass to increase relative to current levels in the winter downwelling season as wind stress becomes less negative (May–October) and SST_R remains relatively warm (~16°C) until June. In addition, fewer downwelling wind events indicate a shallower thermocline during this period. These environmental conditions are beneficial for phytoplankton growth of the present community (Nieblas et al. 2009).

Changes in the intra-annual pattern of upwelling may affect productivity peaks, whose magnitudes are not well-modelled in our study (Fig. 5.3a). Quiescent periods are necessary for optimal productivity (Lasker 1975, 1978). Nieblas et al. (2009) find maximum

Chl peaks during periods of quiescence, when upwelling wind stress weakens but nutrient concentrations remain high. Climate model scenarios indicate contrasting influences on intra-annual Chl peaks. A1B predictions indicate Chl may have lower peaks than currently found due to less frequent quiescent periods. Alternatively, A2 predictions indicate a shift in peak biomass due to a delayed quiescent phase. In contrast, phytoplankton may have a longer growing season if predictions of earlier and longer sustained upwelling conditions are correct.

Impacts of climate change on higher trophic levels

I find that arrow squid are significantly and positively related to environmental conditions (UI_{-3} and SST_{R-2}), similar to previous studies (Waluda et al. 1999, Agnew et al. 2000, Yatsu et al. 2000, Waluda et al. 2004, Chapter 4). Based on these relationships, predicted increases in easterly wind stress and warmer regional SST of the Bonney upwelling region are found to have positive effects on arrow squid catch rates, with a longer period of peak catch (March–June) than presently observed (April–June). A lag of two to three months from peak fisheries logbook arrow squid catch rates (January–March) coincides with peak productivity of the historically sustained and quiescent enrichment phases of the Bonney Upwelling (Nieblas et al. 2009). Peaks in phytoplankton productivity may not be maintained at current levels if quiescent periods are limited, as suggested by the A1B scenario. However, increased mean productivity will enhance food availability and feeding success rate throughout the food web. The delay currently seen between peak upwelling activity and squid abundance may be due to the time it takes for secondary productivity (i.e. zooplankton) to increase in biomass, as the timing of the foraging of mobile predators often coincides with the zooplankton peak (Croll et al. 2005). If productivity peaks are delayed, as suggested by A2, the flexibility and plasticity of arrow squid life history, and multiple cohorts throughout the year (Jackson et al. 2003) may enable the population to adapt relatively easily to trophic mismatches.

Future warming may have conflicting effects on squid. Squid have a strong physiological response to water temperature (Keyl et al. 2008), and warming conditions have been shown to accelerate their life histories, enhance growth rate (Forsythe 1993) and shorten life spans (Pech & Jackson 2008). However, the perceived benefit of warming is complicated, as hatchlings emerge at smaller sizes, which will likely impact the size-at-age of adults, and require more energy (i.e. productivity) for growth (Pech & Jackson 2008). This may influence population structure and abundance as smaller individuals invest higher relative energy into lower reproductive yields (Pech & Jackson 2008).

Though potentially smaller with enhanced warming, arrow squid early life history stages may be able to withstand more turbulent, advective, or frequent mixing that will occur with increased upwelling wind stress. Smaller arrow squid may be able to avoid

passive transport more easily as their paralarvae are hatched at a relatively well-developed state (Keyl et al. 2008) and develop active swimming abilities sooner than paralarvae from larger arrow squid. Further, as the Bonney Upwelling is predicted to remain a low-wind system, it is unlikely that the majority of upwelling events will be sufficiently strong to negatively impact squid paralarvae. Arrow squid may also be affected by changes in the size of the upwelling plume that will increase with intensified upwelling-favourable wind stress. Large regions of frontal convergence along the edge of the upwelling plume can aggregate phytoplankton and zooplankton. These conditions may be beneficial for squid eggs and paralarvae that are transported and trapped within the upwelling front and hatch into regions of highly concentrated food resources (Bakun & Csirke 1998).

Squid have many flexible life history traits that enable them to respond to changing environmental conditions with plasticity (Jackson & O'Dor 2001). With changing environmental and trophic conditions due to the effects of climate change, "loopholes" (Bakun & Broad 2003) or ecological niches that were formerly occupied by other species may be left open by species that were previously competitors or predators. Similar to other species of ommastrephid squid (e.g. *Dosidicus gigas*), arrow squid may be able to fill these gaps (Tam et al. 2008), especially if competitor or predator species are either less able to adapt than squid, or have been overfished (Sibert et al. 2006, Zeidberg & Robison 2007). Cannibalism can be viewed as a beneficial trait that ensures efficient use of food resources and the maximum production of healthy, reproductively successful squid. At a population level, cannibalism may be helpful in conditions of high population densities, conditions of reduced prey availability, or in conditions of severe interspecific competition (Polis 1981).

CONCLUSIONS

The aim of this study is to give an indication of the types of change that may occur in a regional upwelling ecosystem due to climate change. I used an ensemble climate model approach of 7 different climate models to provide robust and more reliable predictions. Our study indicates that for both climate scenarios (an A2 "business-as-usual" approach to greenhouse gas emissions, and an A1B approach with some mitigation measures), climate change will substantially impact physical forcing of upwelling drivers, upwelling-driven primary productivity, and regional fisheries productivity of at least one species. Here, the impacts of changes to physical forcing are projected to enhance phytoplankton biomass and squid catch rates. However, I have discussed many factors that may alter these predictions to some degree, including abiotic, biotic, and anthropogenic effects not specifically analysed here. I note that it is important to explore further historical relationships to improve the understanding of ecosystem interactions for more comprehensive predictions of future change. Though primary productivity is expected to increase with enhanced upwelling, it

would be misleading to assert that this change is beneficial for all higher trophic levels, as substantial community and ecosystem regime shifts may occur. Finally, this study contributes methods to develop a systematic approach to assessing the potential impacts of climate change in marine ecosystems.

DISCUSSION 6

6 GENERAL DISCUSSION

There are several themes throughout this thesis that provide insight into the relationships between the environment and primary and fisheries productivity; they include trophic control, the ocean triad (Bakun 1996), and the optimal environmental window (Cury & Roy 1989). This study investigated the value of these large-scale ecological concepts in the Australian context, quantitatively testing the theory of trophic control, using the ocean triad as a conceptual guide for a comparative study, and applying the empirical rule encapsulated in the optimal environmental window to place Australian ecosystems in a global context. These three general principles provide a useful guide of marine ecosystem function at large and regional scales.

A regional-scale analysis of the main environmental drivers of primary and fisheries productivity was performed for the Bonney Upwelling ecosystem. The Bonney Upwelling is characterised as a low-wind system relative to the optimal environmental window (Nieblas et al. 2009). This characterisation sets the context for what kinds of quantitative relationships amongst environmental variables, primary productivity, and fisheries productivity can be built for this system. The relationships developed here describe present-day variability and can potentially be used to project biological response to environmental change. The theory of bottom-up dynamics and the ocean triad were utilised to enhance understanding of key underlying environmental mechanisms driving the relationships between physics and the marine organisms considered here. The identification of these relationships is important to help develop an ecosystem approach to fisheries.

LARGE-SCALE SYNTHESIS

Bottom-up relationships exist throughout diverse marine habitats around Australia, similar to temperate and warm temperate habitats in the northern hemisphere (Ware and Thomson 2005, Chassot et al. 2007). Primary productivity acts as the limiting factor, determining the carrying capacity for fisheries productivity (Richardson & Schoeman 2004). This relationship provides a general principle for examining environmental interactions with fisheries productivity, i.e. if physical forces alter primary productivity, fisheries productivity can be expected to be affected. This principle is generally asserted for Australian ecosystems (e.g. Harris et al. 1992, Ward et al. 2001), but has not been tested over a large scale before in Australia. Here, I successfully test this theory for diverse marine ecosystems. In contrast to Frank et al. (2006) I did not find any consistent latitudinal pattern for trophic control varying from top-down in higher latitudes and bottom-up in lower latitudes. In addition, the bottom-up relationship is not strong across all functional groups, nor at small

spatial and short temporal scales where other environmental factors can influence fisheries productivity to a greater degree.

The ocean triad conceptual framework (Bakun 1996) describes the underlying environmental mechanisms that drive fisheries productivity. Through a series of comparative case studies, I find that enrichment, concentration, and retention features are a consistent characteristic in the productive ecosystems. The influence of these three key ocean features differs among species with diverse life histories. However, these case studies clearly show that particular environmental and oceanographic characteristics are critical for providing adequate conditions for successful recruitment and fisheries productivity. The triad framework is difficult to test in a strictly quantitative manner (Cole & McGlade 1998), but qualitative comparative analyses across different habitats and species is informative. Although this study indicates that large-scale conceptual guides and environmental variables are useful to understanding ecosystem function, there is a need to examine species and ecosystems individually to determine underlying mechanisms driving variability.

REGIONAL-SCALE SYNTHESIS

The Bonney Upwelling region is a highly productive and commercially-important fishing area in Australia (Butler et al. 2002). The seasonal, interannual, and intraseasonal patterns of upwelling are similar to large-scale eastern boundary upwelling systems (Nieblas et al. 2009). The Bonney Upwelling is a low-wind system (Nieblas et al. 2009) relative to the optimal environmental window for biological productivity developed for eastern boundary upwelling systems (Cury & Roy 1989). This indicates that for the present-day, upwelling wind forcing is relatively weak, and biological productivity is linearly related to upwelling wind stress.

Primary productivity in the Bonney Upwelling can be predicted effectively using simple measures of upwelling drivers. In particular, the alongshore wind stress, which represents the strength of the upwelling forcing, and the size of the upwelling plume, which indicates the effectiveness of the wind at drawing nutrient-rich water to the surface (Nieblas et al. 2009). Phytoplankton biomass responds in a predictable manner to these environmental drivers and the relationships can be used for future predictions.

Further investigations of higher trophic levels reveal that environmental forcing is important for different types of marine organisms. Species with r-selected traits have rapid population expansion and turn over, and respond rapidly to their environment (MacArthur & Wilson 1967). In contrast, K-selected species have much slower growth and longer-lived individuals, so their populations are less influenced by short-term or small-scale environmental variability (MacArthur & Wilson 1967). Using arrow squid as a representative r-selected species in the Bonney Upwelling, I find that this species is highly responsive to the environment, as has been shown for other squid species (Roberts &

Sauer 1994, Brodziak & Hendrickson 1999, Waluda et al. 1999, Pierce & Boyle 2003, Dal et al. 2007). This relationship has a time lag of approximately one season, and indicates that the abundance of squid off the Bonney Coast is closely related to upwelling, the local dominant environmental feature. Interestingly, the K-selected species investigated, gummy shark, is also found to be significantly related to the environment. However, this relationship occurs at much longer time scales (10 months–3 years) and is related to a large-scale ocean process (ENSO) that influences both the local environment (Middleton et al. 2007) and the large-scale ocean circulation and ocean-atmosphere interactions (Cole 2001).

The statistical models developed in this study are valuable indicators of abundance that explain a useful proportion of the present-day variability of both species examined. These simple models have important implications as present-day management tools, because they can predict abundances 2 months (squid) and 10 months (shark) in advance. Generalised linear models are often used to standardise fish catch rates (with respect to, for example, vessel size, depth, day/night, etc.) to remove biases within the data (Maunder & Punt 2004). Environmental data are not generally used in this process (Maunder & Punt 2004), but the models built here clearly indicate that environmental variables can provide useful information to help standardise fish catch data. Finally, these models can also be used for predictive purposes, although at present the squid model is the only one viable for predictions. The predictive use of the gummy shark biophysical model is limited due to instabilities in the model.

IMPLICATIONS OF CLIMATE CHANGE FOR AUSTRALIAN FISHERIES

This study finds that the physical environment strongly influences both primary and fisheries productivity. This indicates that climate change, which is causing rapid changes to the physical marine environment, will affect marine ecosystems (Brierley & Kingsford 2009). This study introduces simple methods for predicting the consequences of climate change on particular components of marine ecosystems. Though the models are applied only to phytoplankton and arrow squid in the Bonney Upwelling, this technique can be applied to other species and habitats.

Two 21st century CO₂ emission scenarios (A1B and A2) predict the Bonney Upwelling system to remain a low-wind system in terms of the optimal environmental window for biological production. However, the alongshore wind stress driving the Bonney Upwelling is expected to intensify with climate change, similar to theoretical predictions (e.g. Bakun 1990), and observations for eastern boundary upwelling systems (Snyder et al. 2003, Bakun et al. 2009). The predicted intensification of upwelling wind stress is due to changes in the migration of the subtropical high pressure system that drives upwelling off the Bonney Coast. This large-scale climate pattern is well-predicted by climate models,

though the exact location of the high-pressure ridge differs between climate models. The methods I use indicate that the climate models are simulating present-day conditions well; therefore I have more certainty using model projections. More confidence can be given to predictions made in these types of upwelling systems, alleviating some concerns regarding the validity of using climate model data to predict changes in upwelling systems (Bakun et al. 2009). However, I note that this may not be the case for all systems.

The intensification of upwelling causes mean phytoplankton biomass to be greater than it is currently throughout the year relative to the 20th century, resulting in potentially beneficial conditions for fisheries productivity (Brown et al. 2009). However, depending on the climate scenario used to make predictions, upwelling seasonality is also predicted to alter, potentially shifting phytoplankton blooms earlier (A1B) or later (A2). Though not modelled in our study, this change in timing could have serious implications for higher trophic level species that time their behaviour with present-day peaks in productivity, potentially leading to trophic mismatches (Edwards & Richardson 2004).

In the future, changed environmental conditions may have beneficial consequences for arrow squid off the Bonney Coast, as their biomass is expected to increase markedly. However, the perceived benefit of more upwelling and warmer SST should be cautiously interpreted. Though the Bonney Upwelling will likely remain a low-wind system, more frequent and intense upwelling events may create advective conditions, and lack of quiescence may reduce phytoplankton blooms and lower food availability. These changes could have negative impacts on squid paralarvae, potentially influencing recruitment success. Temperature effects may have both positive and negative consequences for squid populations (Pech & Jackson 2008). However, extreme consequences of the predictions of environmental change suggest that squid may be able to fill ecological “loopholes” (Bakun & Broad 2003) made empty by local extinctions due to changing environmental conditions or overfishing (Sibert et al. 2006, Zeidberg & Robison 2007).

FUTURE WORK

This study investigates impacts of climate change on primary and fisheries productivity for a regional upwelling system. The analysis and interpretation of results provide useful productivity projections in this region. The Bonney Upwelling is the largest and most predictable regional upwelling in Australia (Butler et al. 2002), so it provides a good benchmark for comparative analysis. The methods developed in this study could be applied to other regional upwelling systems around Australia and in other parts of the world. A comparative study among regional upwelling ecosystems may enable general principles to be developed. In addition, it would be useful to compare the physical and biological characteristics of the Bonney Upwelling to large-scale eastern boundary upwelling systems. It is clear that the Bonney Upwelling has similar physical and biological characteristics to

these systems but on a much smaller scale (Nieblas et al. 2009). A comparative quantitative analysis could provide further understanding to the mechanisms that drive the upwelling and how the Bonney Upwelling fits in the global context.

A particular value of the models used in this study is their simplicity. The models developed in this thesis are simple statistical models that predict change through time and are driven by environmental variables. These contrast with many ecological models that predict change through space, and are driven by biological interactions (e.g. trophic linkages). The linear approach used for the models here was shown to be valid for the marine organisms examined. However, a variety of other methods could be employed to make this modelling approach more widely applicable and include more complex physical and ecosystem interactions. In addition, the approach taken here focuses mainly on a 2-dimensional perspective. Using 3-dimensional model fields could add further information to the models developed in this thesis. Further, the spatial resolution of general circulation models is not yet ideal for coastal systems, and the biophysical relationships could be refined as model resolution improves. It would be valuable to include threshold and density-dependent effects to give a better representation of the interactions of marine species with their environment and between individuals (Hulme 2005). Additionally, a clearer interpretation of the results from the models would arise if fisheries-independent data were used to better resolve environment impacts on particular aspects of a species' life history (e.g. recruitment, growth). In addition, these methods could be applied to multi-species analyses by incorporating interspecies interactions (e.g. Batchelder & Kashiwai 2007). With this additional information, these models could feed information into a "whole-of-system" modelling approach. This approach combines the influences and interactions of many aspects of the marine ecosystem including physical, biological, and human components to provide comprehensive information for integrated adaptive management (Fulton et al. 2004).

CONCLUSION

This study followed a path from testing large-scale theory to regional-scale biophysical modelling. I have shown that bottom-up trophic control operates in Australia, with primary productivity acting as the limiting factor for fisheries productivity at the large scale. However, primary productivity is not the only driver of fisheries productivity, especially at small spatial and short temporal scales. A variety of key oceanographic conditions are necessary for successful recruitment and fisheries productivity, as shown for many different habitats and species. The relative importance of different ocean features is dependent on individual life histories of the different species. Therefore, the large-scale analysis indicated the value of examining individual species and habitats. I then focussed the study on the Bonney Upwelling because it is a particularly productive habitat that has clear

environmental forcing. The physical drivers were shown to reliably predict upwelling-driven phytoplankton biomass and the abundance of higher trophic level marine organisms. These models are informative for understanding present-day variability, but also can be used in a predictive sense to assess the impacts of climate change. I present results that indicate that climate change will have significant impacts on the physical drivers of the Bonney Upwelling ecosystem. The biological response to this change will be complex; however, mean phytoplankton and squid abundance are expected to increase. This study demonstrates an examination of physical-biological interactions on a range of scales. It provides a simple, useful approach for assessing complex interactions and the biological response to physical change for important marine ecosystems.

REFERENCES

- ABARE (2008) Australian fisheries statistics 2007., Australian Bureau of Agricultural and Resource Economics, Canberra, Australia
- Agnew DJ, Hill SL, Beddington JR (2000) Predicting the recruitment strength of an annual squid stock: *Loligo gahi* around the Falkland Islands. Canadian Journal of Fisheries and Aquatic Science 57:2479-2487
- Agostini V, Bakun A (2002) 'Ocean triads' in the Mediterranean Sea: physical mechanisms potentially structuring reproductive habitat suitability (with example application to European anchovy, *Engraulis encrasicolus*). Fisheries Oceanography 11:129-142
- Alpine JE, Hobday AJ (2007) Area requirements and pelagic protected areas: is size an impediment to implementation? Mar Freshw Res 58:558-569
- Alvain S, Moulin C, Dandonneau Y, Bréon F (2005) Remote sensing of phytoplankton groups in case I waters from global SeaWiFS imagery. Deep-Sea Research I: Oceanographic Research Papers 52:1989-2004
- Alvain S, Moulin C, Dandonneau Y, Loisel H (2008) Seasonal distribution and succession of dominant phytoplankton groups in the global ocean: A satellite view. Global Biogeochem Cy 22:GB3001, doi:3010.1029/2007GB003154
- Arájo MB, Thuiller W, Pearson RG (2006) Climate warming and the decline of amphibians and reptiles in Europe. Journal of Biogeography 33:1712-1728
- Araújo MB, New M (2007) Ensemble forecasting of species distributions. Trends in Ecology and Evolution 22:42-47
- Ashok K, Guan Z, Yamagata T (2003) Influence of the Indian Ocean Dipole on the Australian winter rainfall. Geophysical Research Letters 30:1821, doi:1810.1029/2003GL017926
- Australian Fisheries Management Authority (2004) Draft assessment report: Southern squid jig fishery, Australian Government
- Australian Fisheries Management Authority (2008) Gillnet sector fact sheet - gummy shark. Australian Government
- Australian Fisheries Management Authority (2009a) Northern Prawn Fishery. Australian Government
- Australian Fisheries Management Authority (2009b) Southern and Eastern Scalefish and Shark Fishery. Australian Government
- Badeck FW, Bondeau A, Böttcher K, Doktor D, Lucht W, Schaber J, Sitch S (2004) Responses of spring phenology to climate change. New Phytol 162:295-309
- Bailey KM, Houde ED (1989) Predation on eggs and larvae of marine fishes and the recruitment problem. Advances in Marine Biology 25:1-67
- Baines PG, Edwards RJ, Fandry CB (1983) Observations of a new baroclinic current along the western continental slope of the Bass Strait. Aust J Mar Freshw Res 34:155-157

- Bakun A (1973) Coastal upwelling indices, west coast of North America, 1946-71. Report No. NMFS SSRF-671, U.S. Dep. Commer.
- Bakun A (1990) Global climate change and intensification of coastal ocean upwelling. *Science* 247:198-201
- Bakun A (1993) The California Current, Benguela Current, and Southwestern Atlantic Shelf Ecosystems: A comparative approach to identifying factors regulating biomass yields. In: Sherman K, Alexander LM, Gold B (eds) *Large Marine Ecosystems - Stress, Mitigation, and Sustainability*. American Association for the Advancement of Science, Washington, D.C.
- Bakun A (1996) Patterns in the ocean: Ocean processes and marine population dynamics, Vol. University of California Sea Grant, in cooperation with Centro de Investigaciones Biologicas de Noroeste, San Diego, California, USA, and La Paz, Baja California Sur, Mexico
- Bakun A (1998) Ocean triads and radical interdecadal stock variability: bane and boon for fishery management science. In: Pitcher TJ, Hart PJB, Pauly D (eds) *Reinventing Fisheries Management*. Chapman & Hall, London, p 331-358
- Bakun A (2006) Wasp-waist populations and marine ecosystem dynamics: Navigating the "predator pit" topographies. *Progress in Oceanography* 68:271-288
- Bakun A, Broad K (2003) Environmental 'loopholes' and fish population dynamics: comparative pattern recognition with focus on El Niño effects in the Pacific. *Fisheries Oceanography* 12:458-473
- Bakun A, Csirke J (1998) Environmental processes and recruitment variability. In: Rodhouse PG, Dal EG, O'Dor R (eds) *Squid recruitment dynamics*. FAO, Rome, p 105-124
- Bakun A, Field DB, Redondo-Rodriguez A, Weeks SJ (2009) Greenhouse gas, upwelling-favourable winds, and the future of coastal ocean upwelling ecosystems. *Glob Change Biol*:doi: 10.1111/j.1365-2486.2009.02094.x
- Bakun A, Parrish R (1990) Comparative studies of coastal pelagic fish reproductive habitats: the Brazilian sardine (*Sardinella aurita*). *J Cons int Explor Mer* 46:269-283
- Bakun A, Parrish R (1991) Comparative studies of coastal pelagic fish reproductive habitats: the anchovy (*Engraulis anchoita*) of the southwestern Atlantic. *ICES J Mar Sci* 48:343-361
- Bakun A, Weeks S (2004) Greenhouse gas buildup, sardines, submarine eruptions and the possibility of abrupt degradation of intense marine upwelling ecosystems. *Ecol Lett* 7:1015-1023
- Barth J, Menge B, Lubchenco J, Chan F, Bane J, Kirincich A, McManus M, Nielsen K, Pierce S, Washburn L (2007) Delayed upwelling alters nearshore coastal ocean ecosystems in the northern California current. *PNAS* 104:3719-3724
- Batchelder H, Kashiwai M (2007) Ecosystem modeling with NEMURO within the PICES Climate Change and Carrying Capacity program. *Ecol Model* 202:7-11
- Bishop J, Venables WN, Dichmonth CM, Sterling DJ (2008) Standardizing catch rates: is logbook information by itself enough? *ICES Journal of Marine Science* 65:255-266
- Bjorkstedt EP, Roughgarden J (1997) Larval transport and coastal upwelling: An application of HF radar in ecological research. *Oceanography* 10:64-67
- Bobko SJ, Berkeley SA (2004) Maturity, ovarian cycle, fecundity, and age-specific parturition of black rockfish (*Sebastes melanops*). *Fish Bull, US* 102:418-429
- Boletzky SV (1981) Reflexions sur les strategies de reproduction chez les cephalopodes. *Bulletin de la Societe Zoologie Francaise* 106:293-304
- Bonfil R (1994) Overview of world elasmobranch fisheries. *FAO Fisheries Technical Paper* 341:1-119
- Bopp L, Monfray P, Aumont O, Dufresne J-L, Le Treut H, Madec G, Terray L, Orr JC (2001) Potential impact of climate change on marine export production. *Global Biogeochemical Cycles* 15:81-99
- Botsford LW, Lawrence CA, Dever EP, Hastings A, Largier J (2003) Wind strength and biological productivity in upwelling systems: an idealized study. *Fish Oceanogr* 12:245-259
- Botsford LW, Lawrence CA, Dever EP, Hastings A, Largier J (2006) Effects of variable winds on biological productivity on continental shelves in coastal upwelling systems. *Deep-Sea Research II* 53:3116-3140
- Boyd PW, Doney SC (2002) Modelling regional responses by marine pelagic ecosystems to global climate change. *Geophys Res Lett* 29:1806, 1810.1029/2001GL014130
- Bradbury IR, Snelgrove PVR, Pepin P (2003) Passive and active behavioural contributions to patchiness and spatial pattern during the early life history of marine fishes. *Marine Ecology Progress Series* 257:233-245
- Brandt SB (1993) The effect of thermal fronts on fish growth: A bioenergetics evaluation of food and temperature. *Estuaries* 16:142-159
- Brierley AS, Kingsford MJ (2009) Impacts of climate change on marine organisms and ecosystems. *Curr Biol* 19:R602-R614

- Brink K, Abrantes F, Bernal P, Dugdale R, Estrada M, Hutchings L, Jahnke R, Müller P, Smith R (1995) Group Report: How Do Coastal Upwelling Systems Operate as Integrated Physical, Chemical, and Biological Systems and Influence the Geological Record? The Role of Physical Processes in Defining the Spatial Structures of Biological and Chemical Variables. In: Summerhayes C, Emeis K-C, Angel M, Smith R, Zeitzschel B (eds) *Upwelling in the Ocean: Modern Processes and Ancient Records*. John Wiley & Sons, Berlin, p 103-124
- Brodziak J, Hendrickson L (1999) An analysis of environmental effects on survey catches of squids *Loligo pealei* and *Illex illecebrosus* in the northwest Atlantic. *Fisheries Bulletin*, US 97:9-24
- Brown CJ, Fulton EA, Hobday AJ, Matear RJ, Possingham HP, Bulman C, Christensen V, Forrest RE, Gehrke PC, Gribble NA, Griffiths SP, Lozano-Montes H, Martin JM, Metcalf SJ, Okey TA, Watson R, Richardson AJ (2009) Effects of climate-driven primary production change on marine food webs: implications for fisheries and conservation. *Global Change Biology*:10.1111/j.1365-2486.2009.02046.x
- Brown PC, Field JG (1986) Factors limiting phytoplankton production in a nearshore upwelling area. *J Plankton Res* 8:55-68
- Bruce BD, Bradford RW, Neira FJ, Miskiewicz AG, Jordan AR (2001a) Larval fish database. Report No. FRDC Project No. 98/103, CSIRO Marine and Atmospheric Research
- Bruce BD, Condie SA, Sutton CA (2001b) Larval distribution of blue grenadier (*Macruronus novaezelandiae* Hector) in south-eastern Australia: further evidence for a second spawning area. *Mar Freshw Res* 52:603-610
- Bruce BD, Evans K, Sutton CA, Young JW, Furlani DM (2001c) Influence of mesoscale oceanographic processes on larval distribution and stock structure in jackass morwong (*Nemadactylus macropterus*: Cheilodactylidae). *ICES J Mar Sci* 58:1072-1080
- Bruce BD, Neira FJ, Bradford RW (2001d) Larval distribution and abundance of blue and spotted warehou (*Seriola lalandi* and *S. punctata*: Centrolophidae) in south-eastern Australia. *Mar Freshw Res* 52:631-636
- Burford MA, Rothlisberg PC (1999) Factors limiting phytoplankton production in a tropical continental shelf ecosystem. *Estuar Coast Shelf S* 48:541-549
- Burford MA, Rothlisberg PC, Revill AT (2009) Sources of nutrients driving production in the Gulf of Carpentaria, Australia - a shallow tropical shelf system. *Mar Freshw Res* 60:1044-1053
- Burford MA, Rothlisberg PC, Wang Y (1995) Spatial and temporal distribution of tropical phytoplankton species and biomass in the Gulf of Carpentaria, Australia. *Mar Ecol Prog Ser* 118:255-266
- Burke L, Kura Y, Kassem K, Revenga C, Spalding M, McAllister D (2000) *Pilot analysis of global ecosystems: Coastal ecosystems*, Washington, DC
- Butler A, Althaus F, Furlani D, Ridgway K (2002) Assessment of the conservation values of the Bonney upwelling area: a component of the Commonwealth Marine Conservation Assessment Program 2002-2004: report to the Environment Australia, CSIRO Marine Research
- Cai W (2006) Antarctic ozone depletion causes an intensification of the Southern Ocean super-gyre circulation. *Geophys Res Lett* 33:L03712, doi:10.1029/2005GL024911
- Catchpole A, Aulicims A (1999) Southern oscillation and the northern Australian prawn catch. *Int J Biometeorol* 43:110-112
- Cayula J-F, Cornillon P (1992) Edge detection algorithm for SST images. *J Atmos Ocean Tech* 9:67-80
- Chassot E, Mélin F, Le Pape O, Gascuel D (2007) Bottom-up control regulates fisheries production at the scale of eco-regions in European seas. *Marine Ecology Progress Series* 343:45-55
- Christensen V, Guénette S, Heymans JJ, Walters CJ, Watson R, Zeller D, Pauly D (2003) Hundred-year decline of North Atlantic predatory fishes. *Fish and Fisheries* 4:1-24
- Clarke TA (1982) Distribution, growth, and reproduction of the lightfish *Maurollicus muelleri* (Sternoptychidae) off South-East Australia. Report No. 145, CSIRO Marine Laboratories, Cronulla
- Clementson LA, Parslow JP, Turbull AR, McKenzie DC, Rathbone CA (2001) Optical properties of waters in the Australasian sector of the Southern Ocean. *J Geophys Res* 106:31611-31625
- Cole J (2001) Enhanced: A Slow Dance for El Nino. *Science* 291:1496-1497
- Cole J, McGlade J (1998) Clupeoid population variability, the environment and satellite imagery in coastal upwelling systems. *Rev Fish Biol Fish* 8:445-471
- Collie JS, Richards KJ, Steele JH (2004) Regime shifts: can ecological theory illuminate the mechanisms? *Progress in Oceanography* 60:281-302
- Coma R, Ribes M, Serrano E, Jiménez E, Salat J, Pascual J (2009) Global warming-enhanced stratification and mass mortality events in the Mediterranean. *Proceeding of the National Academy of Sciences of the United States of America* 106:6176-6181

- Commonwealth of Australia (2006) A guide to the Integrated Marine and Coastal Regionalisation of Australia Version 4.0, Department of the Environment and Heritage, Canberra, Australia
- Condie SA, Dunn JR (2006) Seasonal characteristics of the surface mixed layer in the Australasian region: implications for primary production regimes and biogeography. *Mar Freshw Res* 57:569-590
- Condie SA, Loneragan NR, Die DJ (1999) Modelling the recruitment of tiger prawns *Penaeus esculentus* and *P. semisulcatus* to nursery grounds in the Gulf of Carpentaria, northern Australia: implications for assessing stock-recruitment relationships. *Mar Ecol Prog Ser* 178:55-68
- Costanza R, d'Arge R, de Groot R, Farber S, Grasso M, Hannon B, Limburg K, Naeem S, O'Neill RV, Paruelo J, Raskin RG, Sutton P, van den Belt M (1997) The value of the world's ecosystem services and natural capital. *Nature* 387:253-260
- Cresswell GR, Golding TJ (1980) Observations of a south-flowing current in the southeastern Indian Ocean. *Deep-Sea Res* 1 27:449-466
- Crococ PJ, van der Velde TD (1995) Seasonal, spatial and interannual variability in the reproductive dynamics of the grooved tiger prawn *Penaeus semisulcatus* in Albatross Bay, Gulf of Carpentaria, Australia: the concept of effective spawning. *Mar Biol* 122:557-570
- Croll D, Marinovic B, Benson S, Chavez F, Black N, Ternullo R, Tershy B (2005) From wind to whales: trophic links in a coastal upwelling system. *Marine Ecology Progress Series* 289:117-130
- Cury P, Bakun A, Crawford RJM, Jarre-Teichmann A, Quiñones RA, Shannon LJ, Verheye HM (2000) Small pelagics in upwelling systems: patterns of interaction and structural changes in "waspy-waist" ecosystems. *ICES J Mar Sci* 210:603-618
- Cury P, Roy C (1989) Optimal environmental window and pelagic fish recruitment success in upwelling areas. *Canadian Journal of Fisheries and Aquatic Science* 46:670-680
- Cury P, Shannon L, Shin Y-J (2003) The functioning of marine ecosystems: a fisheries perspective. In: Sinclair M, Valdimarsson G (eds) *Responsible fisheries in the marine ecosystem*. FAO, Rome, p 103-123
- Cushing DH (1971) Upwelling and the production of fish. *Adv Mar Biol* 9:255-334
- Cushing DH (1975) *Marine ecology and fisheries*, Vol. Cambridge University Press, Cambridge
- Cushing DH (1992) A short history of the Downs stock of herring. *ICES J Mar Sci* 49:437-443
- Dall W, Hill B, Rothlisberg PC, Staples D (1990) Biology of Penaeidae. In: *Adv Mar Biol*, Vol 27. Academic Press, London, p 283-314
- Daskalov G, Grishin A, Rodionov S, Mihneva V (2007) Trophic cascades triggered by overfishing reveal possible mechanisms of ecosystem regime shifts. *PNAS* 104:10518-10523
- Dal E, Hendrickson L, Colbourne E, Drinkwater K, Showell M (2007) Ocean climate effects on the relative abundance of short-finned (*Illex illecebrosus*) and long-finned (*Loligo pealeii*) squid in the northwest Atlantic Ocean. *Fisheries Oceanography* 16:303-316
- Dal EG, Colbourne EB, Drinkwater KF (2000) Environmental effects on recruitment of short-finned squid (*Illex illecebrosus*). *ICES Journal of Marine Science* 57:1002-1013
- Di Lorenzo E, Miller A, Schneider N, McWilliams J (2005) The Warming of the California Current System: Dynamics and Ecosystem Implications. *Journal of Physical Oceanography* 35:336-362
- Dimlich W, Breed W, Ward T (2004) Relative importance of gulf and shelf waters for spawning and recruitment of Australian anchovy, *Engraulis australis*, in South Australia. *Fish Oceanogr* 13:310-323
- Downton MW, Miller KA (1998) Relationships between Alaskan salmon catch and North Pacific climate on interannual and interdecadal time scales. *Canadian Journal of Fisheries and Aquatic Science* 55:2255-2265
- Dunn JR, Ridgway KR (2002) Mapping ocean properties in regions of complex topography. *Deep-Sea Res* 1 49:591-604
- Durand M-H, Curry P, Mendelssohn R, Roy C, Bakun A, Pauly D, (eds) (1998) *Global Versus Local Changes in Upwelling Systems*, Vol. ORSTOM editions, Paris
- Dyer LA, Letourneau D (2003) Top-down and bottom-up diversity cascades in detrital vs. living food webs. *Ecol Lett* 6:60-68
- Edwards M, Richardson A (2004) Impact of climate change on marine pelagic phenology and trophic mismatch. *Nature* 430:8881-8884
- Elsberry RL, Garwood RW (1978) Sea-surface temperature anomaly generation in relation to atmospheric storms. *Bull Am Meteorol Soc* 59:786-789
- England M, Ummenhofer C, Santoso A (2006) Interannual Rainfall Extremes over Southwest Western Australia Linked to Indian Ocean Climate Variability. *Journal of Climate* 19:1948-1969
- FAO (2007) *The state of world fisheries and aquaculture 2006*

- Feng M, Meyers G, Pearce A, Wijffels S (2003) Annual and interannual variations of the Leeuwin Current at 32°S. *Journal of Geophysical Research* 108:3355, doi:10.1029/2002JC001763
- Feng M, Weller E, Hill K (2009) The Leeuwin Current, NCCARF Publication 05/09
- Fitch DT, Moore JK (2007) Wind speed influence on phytoplankton bloom dynamics in the Southern Ocean Marginal Ice Zone. *J Geophys Res* 112:C08006, doi:10.1029/2006JC004061
- Forbes AMG (1984) The contribution of local processes to seasonal hydrology of the Gulf of Carpentaria. *Océanographie Tropicale* 19:193-201
- Forbes AMG, Church JA (1983) Circulation in the Gulf of Carpentaria. II. Residual currents and mean sea level. *Aust J Mar Freshw Res* 34:11-22
- Forsythe JW (1993) A working hypothesis of how seasonal temperature change may impact the field growth of young cephalopods. In: Okutani T, O'Dor RK, Kubodera T (eds) *Recent Advances in Fisheries Biology*. Tokai University Press, Tokyo, p 133-143
- Frank KT, Petrie B, Choi JS, Leggett WC (2005) Trophic cascades in a formerly cod-dominated ecosystem. *Science* 308:1621-1623
- Frank KT, Petrie B, Shackell NL, Choi JS (2006) Reconciling differences in trophic control in mid-latitude marine ecosystems. *Ecol Lett* 9:1096-1105
- Frederiksen M, Edwards M, Richardson AJ, Halliday NC, Wanless S (2006) From plankton to top predators: bottom-up control of a marine food web across four trophic levels. *J Anim Ecol* 75:1259-1268
- Fulton EA, Smith ADM, Punt AE (2004) Ecological indicators of the ecosystem effects of fishing: final report, Report No. R99/1546, Australian Fisheries Management Authority, Canberra
- Gargett A (1997a) The optimal stability 'window': a mechanism underlying decadal fluctuations in North Pacific salmon stocks? *Fisheries Oceanography* 6:109-117
- Gargett AE (1997b) Physics to fish: Interactions between physics and biology on a variety of scales. *Oceanography* 10:128-131
- Gill AE (1982) *Atmosphere-Ocean Dynamics*, Vol. Academic Press, New York
- Gill P (2004) Ecological linkages within the Bonney Upwelling blue whale feeding area. Ph.D. thesis, Deakin University
- Gill PC (2002) A blue whale (*Balaenoptera musculus*) feeding ground in a southern Australian coastal upwelling zone. *Journal of Cetacean Research Management* 4:179-184
- Gonovi JJ, Grimes CB (1992) The surface accumulation of larval fishes by hydrodynamic convergence within the Mississippi River plume front. *Continental Shelf Research* 12:1265-1276
- Gonzalez-Rodriguez E, Valentin JL, André DL, Jacob SA (1992) Upwelling and downwelling at Cabo Frio (Brazil): comparison of biomass and primary productivity responses. *J Plankton Res* 14:289-306
- Gray CA (1996) Intrusions of surface sewage plumes into continental shelf waters: interactions with larval and presettlement juvenile fishes. *Mar Ecol Prog Ser* 139:31-45
- Griffin D, Middleton J (1992) Upwelling and internal tides over the inner New South Wales continental shelf. *Journal of Geophysical Research* 97:14,389-14,405
- Griffin DA, Rathbone CE, Smith GP, Suber KD, Turner PJ (2004) A decade of SST satellite data. Report No. NOOC2003/020, CSIRO Marine Research, Hobart
- Griffin DA, Thompson PA, Bax NJ, Bradford RW, Hallegraeff GM (1997) The 1995 mass mortality of pilchard: no role found for physical or biological oceanographic factors in Australia. *Marine and Freshwater Research* 48:27-42
- Grinsted A, Moore J, Jevrejeva S (2004) Application of the cross wavelet transform and wavelet coherence to geophysical time series. *Nonlinear Proc Geophys* 11:561-566
- Gunn JS, Bruce BD, Furlani DM, Thresher RE, Blaber SJM (1989) Timing and location of spawning of blue grenadier, *Macrurus novaezelandiae* (Teleostei: Merlucciidae), in Australian coastal waters. *Aust J Mar Freshw Res* 40:97-112
- Gunn JS, Young JW (1996) Environmental determinants of the movement and migration of juvenile southern bluefin tuna, Australian Society for Fish Biology, Sydney
- Häder D-P, Kumar HD, Smith RC, Worrest RC (2003) Aquatic ecosystems: effects of solar ultraviolet radiation and interactions with other climatic change factors. *Photochem Photobiol Sci* 2:39-50
- Hallegraeff GM, Beardall J, Brett S, Doblin M, Hosja W, de Salas M, Thompson P (2009) Phytoplankton and climate change, NCCARF Publication 05/09
- Hanson C, Pattiaratchi C, Waite A (2005a) Seasonal production regimes off south-western Australia: influence of the Capes and Leeuwin Currents on phytoplankton dynamics. *Marine and Freshwater Research* 56:1011-1026
- Hanson CE, Pattiaratchi CB, Waite AM (2005b) Sporadic upwelling on a downwelling coast: Phytoplankton responses to spatially variable nutrient dynamics off the Gascoyne region of Western Australia. *Continental Shelf Research* 25:1561-1582

- Hanson CE, Waite AM, Thompson PA, Pattiaratchi CB (2007) Phytoplankton community structure and nitrogen nutrition in Leeuwin Current and coastal waters off the Gascoyne region of Western Australia. *Deep-Sea Res II* 54:902-924
- Hardman-Mountford NJ, Richardson AJ, Boyer DC, Kreiner A, Boyer HJ (2003) Relating sardine recruitment in the Northern Benguela to satellite-derived sea surface height using a neural network pattern recognition approach. *Prog Oceanogr* 59:241-255
- Hare JA, Cowan RK (1993) Ecological and evolutionary implications of the larval transport and reproductive strategy of bluefish *Pomatomus saltatrix* *Mar Ecol Prog Ser* 98:1-16
- Harley C, Hughes A, Hultgren K, Miner B, Sorte C, Thornber C, Rodriguez L, Tomanek L, Williams S (2006) The impacts of climate change in coastal marine systems. *Ecol Lett* 9:228-241
- Harley SJ, Ransom AM, Dunn A (2001) Is catch-per-unit-effort proportional to abundance? . *Canadian Journal of Fisheries and Aquatic Science* 58:1760-1772
- Harris G, Nilsson C, Clementson L, Thomas D (1987) The water masses of the east coast of Tasmania: Seasonal and interannual variability and the influence on phytoplankton biomass and productivity. *Aust J Mar Freshw Res* 38:569-590
- Harris GP, Griffiths FB, Clementson LA (1992) Climate and the fisheries off Tasmania - interactions of physics, food chains and fish. *S Afr J Mar Sci* 12:585-597
- Hays G, Richardson A, Robinson C (2005) Climate change and marine plankton. *Trends Ecol Evol* 20:337-344
- Hearn WS (1986) Mathematical models for evaluating marine fisheries. Ph.D. thesis, University of New South Wales
- Hendiarti N, Siegel H, Ohde T (2004) Investigation of different coastal processes in Indonesian waters using SeaWiFS data. *Deep-Sea Res II* 51:85-97
- Henson S, Thomas A (2007) Interannual variability in timing of bloom initiation in the California Current System. *Journal of Geophysical Research* 112:C08007, doi: 08010.01029/02006JC003960
- Herzfeld M, Tomczak M (1999) Bottom-driven upwelling generated by eastern intensification in closed and semi-closed basins with a sloping bottom. *Mar Freshw Res* 50:613-627
- Hilborn R, Walters CJ (1987) A general model for simulation of stock and fleet dynamics in spatially heterogeneous environments. *Canadian Journal of Fisheries and Aquatic Science* 44:1366-1369
- Hobday A, Matear R (2005) Review of Climate Impacts on Australian Fisheries and Aquaculture: implications for the effects of Climate Change., Canberra, Australia
- Hobday AJ, Okey TA, Poloczanska ES, Kunz TJ, Richardson AJ, (eds) (2006) Impacts of climate change on Australian marine life, Canberra, Australia
- Hobday AJ, Poloczanska ES, Matear R (2008) Introduction: Climate and Australian fisheries and aquaculture, Report to the Department of Climate Change, Canberra, Australia
- Hoegh-Guldberg O (1999) Climate change, coral bleaching and the future of the world's coral reefs. *Mar Freshw Res* 50:839-866
- Hoegh-Guldberg O (2005) Marine ecosystems and climate change. In: Lovejoy T, Hannah L (eds) *Climate Change and Biodiversity*. Yale University Press, New Haven, CT, USA, p 256-271
- Holden MJ (1973) Are long-term sustainable fisheries for elasmobranchs possible? *Fish Stocks and Recruitment. Rapports et Proces-Verbaux des Reunions Conseil International Pour l'Exploration de la Mer*, p 360-367
- Houde ED (1989) Subtleties and episodes in the early life of fishes. *Journal of Fish Biology (Suppl A)* 35:28-38
- Hughes L (2000) Biological consequences of global warming: Is the signal already apparent? *Trends Ecol Evol* 15:56-61
- Hughes L (2003) Climate change and Australia: Trends, projections and impacts. *Austral Ecology* 28:423-443
- Hughes T, Szmant A, Steneck R, Carpenter R, Miller S (1999) Algal blooms on coral reefs: What are the causes? *Limnol Oceanogr* 44:1583-1586
- Hulme PE (2005) Adapting to climate change: is there scope for ecological management in the face of a global threat? *J Appl Ecol* 42:784-794
- Humston R, Ault JS, Lutcavage M, Olson DB (2000) Schooling and migration of large pelagic fishes relative to environmental cues. *Fisheries Oceanography* 9:136-146
- Hunter MD, Price PW (1992) Playing chutes and ladders: Heterogeneity and the relative roles of bottom-up and top-down forces in natural communities. *Ecology* 73:724-732
- Husby D, Nelson C (1982) Turbulence and vertical stability in the California Current. *California Cooperative Oceanic Fisheries Investigations Reports XXIII*:113-129
- Hynd JS, Robins JP (1967) Tasmanian Tuna Survey report of first operational period. Report No. 22, CSIRO Australia

- IPCC (2007a) Climate Change 2007: Impacts, Adaptation and Vulnerability, Cambridge
- IPCC (2007b) Climate Change 2007: The Physical Science Basis, Intergovernmental Panel on Climate Change, Cambridge
- Jackson G, O'Dor R (2001) Time, space and the ecophysiology of squid growth, life in the fast lane. *Vie et milieu* 51:205-215
- Jackson GD, McGrath Steer BL, Wotherspoon S, Hobday AJ (2003) Variation in age, growth and maturity in the Australian arrow squid *Nototodarus gouldi* over time and space - what is the pattern? *Marine Ecology Progress Series* 264:57-71
- Jackson GD, Moltschaniwskyj NA (2001) Temporal variation in growth rates and reproductive parameters in the small near-shore tropical squid *Lololus noctiluca*; is cooler better? *Marine Ecology Progress Series* 218:167-177
- Jackson GD, Wotherspoon S, McGrath Steer BL (2005) Temporal population dynamics in arrow squid *Nototodarus gouldi* in southern Australian waters. *Marine Biology* 146:975-983
- Jenkins GP, Black KP, Hamer PA (2000) Determination of spawning areas and larval advection pathways for King George whiting in southeastern Australia using otolith microstructure and hydrodynamic modelling. I. Victoria. *Mar Ecol Prog Ser* 199:231-242
- Jordan A, Pullen G, Marshall J-A, Williams H (1995) Temporal and spatial patterns of spawning in jack mackerel, *Trachurus declivis* (Pisces: Carangidae), during 1988-91 in eastern Tasmanian waters. *Mar Freshw Res* 46:831-842
- Kahru M, Håkansson B, Rud O (1995) Distributions of the sea-surface temperature fronts in the Baltic Sea as derived from satellite imagery. *Cont Shelf Res* 15:663-679
- Kahru M, Mitchell T (2000) Influence of the 1997-98 El Niño on the surface chlorophyll in the California Current. *Geophys Res Lett* 27:2937-2940
- Kailola PJ, Williams MM, Stewart PC, Reichelt RE, McNee A, Grieve C (1993) Australian fisheries resources, Vol. Bureau of Resource Sciences, Canberra, Australia
- Kalnay E, Kanamitsu M, Kistler R, Collins W, Deven D, Gandin L, Iredell M, Saha S, White G, Woollen J, Zhu Y, Leetmaa A, Reynolds B, Chelliah M, Ebisuzaki W, Higgins W, Janowiak J, Mo KC, Ropelewski C, Wang J, Jenne R, Joseph D (1996) The NCEP/NCAR 40-year reanalysis project. *Bulletin of the American Meteorological Society* 77:437-471
- Kämpf J, Doubell M, Griffin DA, Matthews RL, Ward TM (2004) Evidence of a large seasonal coastal upwelling system along the southern shelf of Australia. *Geophys Res Lett* 31:L09310, doi:09310.01029/02003GL019221
- Keyl F, Argüelles J, Mariátegui L, Tafur R, Wolff M, Yamashiro C (2008) A hypothesis on range expansion and spatio-temporal shifts in size-at-maturity of jumbo squid (*Dosidicus gigas*) in the eastern Pacific Ocean. *California Cooperative Oceanic Fisheries Investigations Reports* 49:119-128
- Kim S, Jung S, Zhang CI (1997) The effect of seasonal anomalies of seawater temperature and salinity on the fluctuation of yields of small yellow croaker *Pseudosciaena polyactis*, in the Yellow Sea. *Fisheries Oceanography* 6:1-9
- Kingsford MJ, Suthers IM (1994) Dynamic estuarine plumes and fronts: importance to small fish and plankton in coastal waters of NSW, Australia. *Cont Shelf Res* 14:655-672
- Kistler R, Kalnay E, Collins W, Saha S, White G, Woollen J, Chelliah M, Ebisuzaki W, Kanamitsu M, Kousky V, van den Dool H, Jenne R, Fiorino M (2001) The NCEP-NCAR 50-year reanalysis: Monthly means CD-ROM and documentation. *Bull Am Meteorol Soc* 82:247-268
- Kloser R, Ryan T, Sakov P, Young J, Stanley C, Davis T (1998) Assessment of acoustics as a research tool to determine the distribution, biomass and behaviour of southern bluefin tuna schools and their prey in the Great Australian Bight. Report No. 2, CSIRO, Hobart, Tasmania
- Knuckey IA, Sivakumaran KP (2001) Reproductive characteristics and per-recruit analyses of blue warehou (*Seriola lalandi*): implications for the South East Fishery of Australia. *Mar Freshw Res* 52:575-587
- Kudela R, Dugdale R (2000) Nutrient regulation of phytoplankton productivity in Monterey Bay, California. *Deep-Sea Res* 47:1023-1053
- Kuo N-J, Zheng Q, Ho C-R (2000) Satellite observation of upwelling along the western coast of the South China Sea. *Remote Sens Environ* 74:463-470
- Larcombe J, McLoughlin K, (eds) (2007) Fishery status reports 2006: status of fish stocks managed by the Australian government, Bureau of Rural Sciences, Canberra
- Lasker R (1975) Field criteria for survival of anchovy larvae: the relation between inshore chlorophyll maximum layers and successful first feeding. *Fisheries Bulletin*, US 73:453-462
- Lasker R (1978) The relations between oceanographic conditions and larval anchovy food in the California Current: Identification of factors contributing to recruitment failure. *Rapports et Proces-Verbaux des Reunions* 173:212-230.
- Last PR, Stevens JD (eds) (1994) Sharks and rays of Australia, Vol 1. CSIRO, Australia

- Lawrence GC (1978) Comparative growth, respiration and delayed feeding abilities of larval cod (*Gadus morhua*) and haddock (*Melanogrammus aeglefinus*) as influenced by temperature during laboratory studies. *Mar Biol* 50:1-7
- Levasseur M, Therriault J-C, Legendre L (1984) Hierarchical control of phytoplankton succession by physical factors. *Mar Ecol Prog Ser* 19:211-222
- Lewis RK (1981) Seasonal upwelling along the south-eastern coastline of South Australia. *Australian Journal of Marine and Freshwater Research* 32:843-854
- Linacre E, Hobbs H (1977) The Australian climatic environment, Vol. John Wiley, Brisbane
- Lough JM (2008) Shifting climate zones for Australia's tropical marine ecosystems. *Geophys Res Lett* 35:L14708, doi:10.1029/2008GL034634
- Lutjeharms JRE, Stockton PL (1987) Kinematics of the upwelling front off southern Africa. *South African Journal of Marine Science* 5:35-49
- Lyle JM, Ford WB (1993) Review of trawl research 1979-1987, with summaries of biological information for the major species, Department of Primary Industry and Fisheries, Taroona, Tasmania
- MacArthur RH, Wilson EO (1967) The theory of island biogeography, Vol. Princeton University Press, Princeton NJ
- Mann KH (2000) Ecology of coastal waters, with implications for management, Vol. Blackwell Science, Boston
- Mann KH, Lazier JRN (1996) Dynamics of Marine Ecosystems, Vol. Blackwell Scientific, Oxford, UK
- Maunder MN, Punt AE (2004) Standardizing catch and effort data: a review of recent approaches. *Fisheries Research* 70:141-159
- Maunder MN, Sibert JR, Fonteneau A, Hampton J, Kleiber P, Harley SJ (2006) Interpreting catch per unit effort data to assess the status of individual stocks and communities. *ICES Journal of Marine Science* 63:1373-1385
- Maxwell JGH, Cresswell GR (1981) Dispersal of Tropical Marine Fauna to the Great Australian Bight by the Leeuwin Current. *Aust J Mar Freshw Res* 32:493-500
- McClain CR, Feldman GC, Hooker SB (2004) An overview of the SeaWiFS project and strategies for producing a climate research quality global ocean bio-optical time series. *Deep-Sea Res II* 51:5-42
- McClatchie S, Middleton J, Ward T (2006) Water mass analysis and alongshore variation in upwelling intensity in the eastern Great Australian Bight. *J Geophys Res* 111:C08007, doi:10.1029/2004JC002699
- McEdward LRE (1995) The Ecology of Marine Invertebrate Larvae, Vol. CRC Press, Boca Raton
- McLoughlin K, Wood R (2008) Fisheries status reports, Bureau of Rural Sciences, Canberra
- Meehl GA, Stocker TF, Collins WD, Friedlingstein P, Gaye AT, Gregory JM, Kitoh A, Knutti R, Murphy JM, Noda A, Raper SCB, Watterson IG, Weaver AJ, Zhao Z-C (2007) Global Climate Projections., Cambridge University Press, Cambridge, UK
- Mendelsohn R, Schwing F (2002) Common and uncommon trends in SST and wind stress in the California and Peru-Chile current systems. *Progress in Oceanography* 53:141-162
- Menge BA, Daley BA, Wheeler PA, Dahlhoff E, Sanford E, Strub PT (1997) Benthic-pelagic links and rocky intertidal communities: Bottom-up effects on top-down control? *PNAS* 94:14530-14535
- Metcalf SJ (2009) Qualitative modelling to aid ecosystem analyses for fisheries management in a data-limited situation. Ph.D. thesis, University of Tasmania
- Micheli F (1999) Eutrophication, fisheries, and consumer-resource dynamics in marine pelagic ecosystems. *Science* 285:1396-1398
- Middleton J, Cirano M (2002) A northern boundary current along Australia's southern shelves: The Flinders Current. *Journal of Geophysical Research* 107:3129, doi:10.1029/2000JC000701
- Middleton JF, Arthur C, Van Ruth P, Ward TM, McClean JL, Maltrud ME, Gill P, Levings A, Middleton S (2007) El Niño effects and upwelling off South Australia. *Journal of Physical Oceanography* 37:2458-2477
- Middleton JF, Platov G (2003) The mean summertime circulation along Australia's southern shelves: A numerical study. *Journal of Physical Oceanography* 33:2270-2287
- Mitchell-Innes BA, Richardson AJ, Painting SJ (1999) Seasonal change in phytoplankton biomass on the Western Agulhas Bank, South Africa. *South African Journal of Marine Science* 21:127-233
- Moita MT, Oliveira PB, Mendes JC, Palma AS (2003) Distribution of chlorophyll *a* and *Gymnodinium catenatum* associated with coastal upwelling plumes off central Portugal. *Acta Oecologia* 24:S125-S132
- Moore TS, Il, Marra J, Alkatiri A (2003) Response of the Banda Sea to the southeast monsoon. *Mar Ecol Prog Ser* 261:41-49

- Moriarty DJW, O'Donohue MJ (1993) Nitrogen fixation in seagrass communities during summer in the Gulf of Carpentaria, Australia. *Aust J Mar Freshw Res* 44:117-125
- Munday PL, Kingsford MJ, O'Callaghan M, Donelson JM (2008) Elevated temperature restricts growth potential of the coral reef fish *Acanthochromis polyacanthus*. *Coral Reefs* 27:927-931
- Murphy DM, Solomon S, Portmann RW, Rosenlof KH, Forster PM, Wong T (2009) An observationally based energy balance for the Earth since 1950. *Journal of Geophysical Research* 114:D17107, doi:10.1029/2009JD012105
- Myers RA, Barrowman NJ, Hutchings JA, Rosenberg AA (1995) Population dynamics of exploited fish stocks at low population levels. *Science* 269:1106-1109
- Nakamura H (1969) Tuna Distribution and Migration, Vol. Fishing News (Books) Ltd, London
- Nakicenovic N, Alcamo J, Davis G, de Vries B, Fenhann J, Gaffin S, Gregory K, Grübler A, Jung TY, Kram T, La Rovere EL, Michaelis L, Mori S, Morita T, Pepper W, Pitcher H, Prines L, Riahi K, Roehrl A, Rogner H-H, Sankovski A, Schlesinger M, Shukla P, Smith SE, Swart R, van Rooijen S, Victor N, Dadi Z (2001) Special Report on Emissions Scenarios, Intergovernmental Panel on Climate Change
- Nehring S (1996) Establishment of thermophilic phytoplankton species in the North Sea: biological indicators of climatic changes? *ICES Journal of Marine Science* 55:818-823
- Neira FJ, Lyle JM, Keane JP (2009) Shelf spawning habitat of *Emmelichthys nitidus* in south-eastern Australia - Implications and suitability for egg-based biomass estimation. *Estuar Coast Shelf S* 81:521-532
- Nelson WR, Ingham MC, Schaaf I (1977) Larval transport and year class strength of Atlantic menhaden, *Brevoortia tyrannus*. *Fish Bull*, US 75:23-41
- Nieblas AE, Sloyan BM, Hobday AJ, Coleman R, Richardson AJ (2009) Variability of biological production in low wind-forced regional upwelling systems: a case study off southeastern Australia *Limnology and Oceanography* 54:1548-1558
- Nilsson CS, Cresswell GR (1981) The formation and evolution of East Australian Current warm-core eddies. *Prog Oceanogr* 9:133-183
- Nykjaer L, van Camp L (1994) Seasonal and interannual variability of coastal upwelling along northwest Africa and Portugal from 1981 to 1991. *J Geophys Res* 99:14197-14208
- O'Hara TD, Poore GCB (2000) Patterns of distribution for southern Australian marine echinoderms and decapods. *J Biogeogr* 27:1321-1335
- O'Shea S, Bolstad KS, Ritchie PA (2004) First records of egg masses of *Nototodarus gouldi* McCoy, 1888 (Mollusca: Cephalopoda: Ommastrephidae), with comments on egg-mass susceptibility to damage by fisheries trawl. *New Zealand Journal of Marine and Freshwater Research* 31:161-166
- Oke PR, England MH (2004) Oceanic response to changes in the latitude of the Southern Hemisphere subpolar westerly winds. *J Clim* 17:1040-1054
- Oke PR, Schiller A, Griffin DA, Brassington GB (2005) Ensemble data assimilation for an eddy-resolving ocean model. *Q J Roy Meteor Soc* 131:3301-3311
- Pace ML, Cole JJ, Carpenter SR, Kitchell JF (1999) Trophic cascades revealed in diverse ecosystems. *Trends Ecol Evol* 14:483-488
- Pandolfi JM, Bradbury RH, Sala E, Hughes TP, Bjørndal KA, Cooke RG, McArdle D, McClenachan L, Newman MJH, Paredes G, Warner RR, Jackson JBC (2003) Global Trajectories of the Long-Term Decline of Coral Reef Ecosystems. *Science* 301:955-958
- Parnesan C (2006) Ecological and Evolutionary Responses to Recent Climate Change. *Annual Review of Ecology, Evolution, and Systematics* 37:637-669
- Parnesan C, Yohe G (2003) A globally coherent fingerprint of climate change impacts across natural systems. *Nature* 421:37-42
- Parrish RHA, Bakun A, Husby DM, Nelson CS (1983) Comparative climatology of selected environmental processes in relation to eastern boundary current pelagic fish reproduction. In: Sharp GD, Csirke J (eds) *Proceedings of the expert consultation to examine changes in abundance and species composition of neritic fish resources*. FAO Fish. Rep., p 1224pp.
- Pauly D, Christensen V (1995) Primary production required to sustain global fisheries. *Nature* 374:255-257
- Payá I, Ehrhardt NM (2005) Comparative sustainability mechanisms of two hake (*Merluccius gayi gayi* and *Merluccius australis*) populations subjected to exploitation in Chile. *Bull Mar Sci* 76:261-286
- Pearson RG, Thuiller W, Araújo MB, Martinez-Meyer E, Brotons L, McClean C, Miles L, Segurado P, Dawson TP, Lees DC (2006) Model-based uncertainty in species range prediction. *Journal of Biogeography* 33:1704-1711
- Pech GT, Jackson GD (2008) The potential impacts of climate change on inshore squid: biology, ecology and fisheries. *Reviews in Fish Biology and Fisheries* 18:373-385

- Pennington J, Mahoney K, Kuwahara V, Kolber D, Calienes R, Chavez F (2006) Primary production in the eastern tropical Pacific: A review. *Prog Oceanogr* 69:285-317
- Peñuelas J, Filella I (2001) Responses to a warming world. *Science* 294:793-794
- Peterson AT, Ortega-Huerta MA, Bartley J, Sánchez-Cordero V, Soberón J, Buddemeier RH, Stockwell DRB (2002) Future projections for Mexican faunas under global climate change scenarios. *Nature* 416:626-629
- Peterson L, Abbott M, Anderson D, Caulet J-P, Conté M, Emeis K-C, Kemp A, Summerhayes C (1995) Group Report: How Do Upwelling Systems Vary through Time? In: Summerhayes C, Emeis K-C, Angel M, Smith R, Zeitzschel B (eds) *Upwelling in the Ocean: Modern Processes and Ancient Records*. John Wiley & Sons, Berlin, p 285-311
- Philippart CJM, van Aken HM, Beukema JJ, Bos OG, Cadée GC, Dekker R (2003) Climate-related changes in recruitment of the bivalve *Macoma balthica*. *Limnol Oceanogr* 48:2171-2185
- Phillips JA (2001) Marine macroalgal biodiversity hotspots: why is there high species richness and endemism in southern Australian marine benthic flora? *Biodivers Conserv* 10:1555-1577
- Pickett MH, Schwing FB (2006) Evaluating upwelling estimates off the west coasts of North and South America. *Fish Oceanogr* 15:256-269
- Pierce D (2004) Future Changes in Biological Activity in the North Pacific due to Anthropogenic Forcing. *Climatic Change* 62:389-418
- Pierce GJ, Boyle PR (2003) Empirical modelling of interannual trends in abundance of squid (*Loligo forbesi*) in Scottish waters. *Fisheries Research* 59:305-326
- Pierce GJ, Zuur AF, Smith JM, Begona Santos M, Bailey N, Chen C-S, Boyle PR (2005) Interannual variation in life-cycle characteristics of the veined squid (*Loligo forbesi*) in Scottish waters. *Aquatic Living Resources* 18:327-340
- Pinaud D, Weimerskirch H (2007) At-sea distribution and scale-dependent foraging behaviour of petrels and albatrosses: a comparative study. *Journal of Animal Ecology* 76:9-19
- Poiner IR, Staples DJ, Kenyon R (1987) Seagrass communities of the Gulf of Carpentaria, Australia. *Aust J Mar Freshw Res* 38:121-131
- Polis GA (1981) The evolution and dynamics of intraspecific predation. *Ann Rev Ecol Syst* 12:225-251
- Poloczanska ES, Babcock RC, Butler A, Hobday AJ, Hoegh-Guldberg O, Kunz TJ, Matear R, Milton DA, Okey TA, Richardson AJ (2007) Climate change and Australian marine life. *Oceanography and Marine Biology: An Annual Review* 45:407-478
- Pond S, Pickard GL (1983) *Introductory dynamical oceanography*, Vol. Pergamon Press, Oxford
- Potemra JT (2001) Contribution of equatorial Pacific winds to southern tropical Indian Ocean Rossby waves. *Journal of Geophysical Research* 106:2407-2422
- Pribac F, Punt AE, Walker TI, Taylor BL (2005) Using length, age and tagging data in a stock assessment of a length selective fishery for gummy shark (*Mustelus antarcticus*). *Journal of Northwest Atlantic Fishery Science* 35:267-290
- Prince J (2001) Ecosystem of the South East fishery (Australia), and fisher lore. *Mar Freshw Res* 52:431-449
- Rahmstorf S, Cazenave A, Church JA, Hansen JE, Keeling RF, Parker DE, Somerville RCJ (2007) Recent climate observations compared to projections. *Science* 316:709
- Redfield AC (1958) The biological control of chemical factors in the environment. *Am Sci* 64:205-221
- Richardson AJ, Bakun A, Hays GC, Gibbons MJ (2009a) The jellyfish joyride: causes, consequences and management actions. *Trends Ecol Evol* 24:312-322
- Richardson AJ, McKinnon D, Swadling KM (2009b) *Zooplankton and climate change*, NCCARF Publication 05/09
- Richardson AJ, Mitchell-Innes BA, Verheye HM, Fowler JL, Field JG (2003) Seasonal and event-scale variation in growth of *Calanus agulhensis* (Copepoda) in the Benguela upwelling system and implications for spawning of sardine *Sardinops sagax*. *Mar Ecol Prog Ser* 254:239-251
- Richardson AJ, Poloczanska ES (2008) Under-resourced, under threat. *Science* 320:1294-1295
- Richardson AJ, Schoeman DS (2004) Climate impact on plankton ecosystems in the northeast Atlantic. *Science* 305:1609-1612
- Richardson KM, Pinkerton MH, Boyd PW, Gall MP, Zeldis J, Oliver MD, Murphy RJ (2004) Validation of SeaWiFS data from around New Zealand. *Adv Space Res* 33:1160-1167
- Ridgway K, Dunn JR, Wilkin JL (2002) Ocean interpolation by four-dimensional weighted least squares - Application to the waters around Australasia. *J Atmos Ocean Tech* 19:1357-1375
- Ridgway KR (2007) Seasonal circulation around Tasmania: An interface between eastern and western boundary dynamics. *J Geophys Res* 112:C10016, doi:10.1029/2006JC003898
- Ridgway KR, Godfrey JS (1997) Seasonal cycle of the East Australian Current. *J Geophys Res* 102:22,921-22,936

- Roberts MJ, Sauer WHH (1994) Environment: the key to understanding the South African chokka squid (*Loligo vulgaris reynaudii*) life cycle and fishery? *Antarctic Science* 6:249-258
- Rochford DJ (1975) Oceanography and its role in the management of aquatic ecosystems. *Proceedings of the Ecological Society of Australia* 8:67-83
- Rochford DJ (1977) A review of a possible upwelling situation off Port MacDonnell, SA. CSIRO Division of Fisheries and Oceanography 81:1-17
- Roemmich D, Gilson J, Davis R, Sutton P, Wijffels S, Riser S (2007) Decadal spinup of the South Pacific subtropical gyre. *J Phys Oceanogr* 37:162-173
- Roemmich D, McGowan J (1995) Climatic Warming and the Decline of Zooplankton in the California Current. *Science* 267:1324-1326
- Roessig JM, Woodley CM, Cech JJ, Jr., Hansen LJ (2004) Effects of global climate change on marine and estuarine fishes and fisheries. *Rev Fish Biol Fish* 14:251-275
- Rohan G (1999) Ensuring monitoring contributes to the pursuit of management objectives: An Australian Fisheries Management Authority perspective, FAO, Sydney, Australia
- Rothlisberg PC, Church JA (1994) Processes controlling the larval dispersal and postlarval recruitment of penaeid prawns. In: Sammarco PW, Heron M (eds) *Coastal and Estuarine Studies 45 - The Bio-Physics of Marine Larval Dispersal*. American Geophysical Union, Washington D.C., p 352
- Rothlisberg PC, Craig PD, Andrewartha JR (1996) Modelling penaeid prawn larval advection in Albatross Bay, Australia: Defining the effective spawning population. *Mar Freshw Res* 47:157-168
- Rothlisberg PC, Jackson CJ, Pendrey RC (1987) Larval ecology of penaeids of the Gulf of Carpentaria, Australia. I. Assessing the reproductive activity of five species of *Penaeus* from the distribution and abundance of the zoeal stages. *Aust J Mar Freshw Res* 38:1-17
- Rothlisberg PC, Pollard PC, Nichols PD, Moriarty DJW, Forbes AMG, Jackson CJ, Vaudrey D (1994) Phytoplankton community structure and productivity in relation to the hydrological regime of the Gulf of Carpentaria, Australia, in Summer. *Aust J Mar Freshw Res* 45:265-282
- Rothlisberg PC, Staples DJ, Crocos PJ (1985) The life history of the banana prawn *Penaeus merguensis* in the Gulf of Carpentaria. In: Rothlisberg PC, Hill BJ, Staples DJ (eds) *Second Australian National Prawn Seminar, NPS2: Cleveland, Australia*, p 125-136
- Rothlisberg PC, White NJ, Forbes AMG (1989) Hydrographic atlas of the Gulf of Carpentaria. Report No. 209, CSIRO Marine Laboratories
- Roughan M, Middleton JH (2002) A comparison of observed upwelling mechanisms off the east coast of Australia. *Cont Shelf Res* 22:2551-2572
- Roy C, Porteiro C, Cabanas JM (1995) The optimal environmental window hypothesis in the ICES area: the example of the Iberian sardine. *ICES Coop Res Rep* 206:57-65
- Rutlant J, Montecino V (2002) Multiscale upwelling forcing cycles and biological response off north-central Chile. *Revista Chilena de Historia Natural* 75:217-231
- Rykaczewski RR, Checkley DM, Jr (2008) Influence of ocean winds on the pelagic ecosystem in upwelling regions. *Proceeding of the National Academy of Sciences of the United States of America* 105:1965-1970
- Ryther JH (1969) Photosynthesis and fish production in the sea. *Science* 166:72-76
- Sahlqvist P (2007) Southern Squid Jig Fishery, Bureau of Rural Sciences, Canberra
- Saltaug A, Godø OR (2000) Standardisation of commercial CPUE. *Fish Res* 49:271-281
- Sathyendranath S, Platt T, Horne E, Harrison W, Ulloa O, Outerbridge R, Hoepffner N (1991) Estimation of new production in the ocean by compound remote sensing. *Nature* 353:129-133
- Schahinger RB (1987) Structure of coastal upwelling events observed off the south-east coast of South Australia during February 1983-April 1984. *Australian Journal of Marine and Freshwater Research* 38:439-459
- Scheffer M, Carpenter SR (2003) Catastrophic regime shifts in ecosystems: linking theory to observations. *Trends Ecol Evol* 18:648-656
- Schwing F, Mendelssohn R (1997) Increased coastal upwelling in the California Current System. *Journal of Geophysical Research* 102:3421-3438
- Serra R, Cury P, Roy C (eds) (1998) The recruitment of the Chilean sardine (*Sardinops sagax*) and the 'Optimal Environmental Window', Vol. ORSTOM, Paris
- Shang SL, Zhang CY, Hong HS, Shang SP, Chai F (2004) Short-term variability of chlorophyll associated with upwelling events in the Taiwan Strait during the southwest monsoon of 1998. *Deep-Sea Res II* 51:1113-1127
- Shaw MR, Zavaleta ES, Chiariello NR, Cleland EE, Mooney HA, Field CB (2002) Grassland Responses to Global Environmental Changes Suppressed by Elevated CO₂. *Science* 298:1987-1990

- Shepherd SA, Bryars S, Kirkegaard I, Harbison P, Jennings JT (2008) Natural history of Gulf St. Vincent, Vol 496. Royal Society of South Australia Inc., Adelaide
- Sibert J, Hampton J, Kleiber P, Maunder M (2006) Biomass, Size, and Trophic Status of Top Predators in the Pacific Ocean. *Science* 314:1773-1776
- Sloyan BM, Kamenkovich IV (2007) Simulation of Subantarctic Mode and Antarctic Intermediate Waters in climate models. *Journal of Climate* 20:5061-5080
- Smith KA (2000) Active and passive dispersal of *Centroberyx affinis* (Berycidae) and *Gonorhynchus greyi* (Gonorynchidae) larvae on the Sydney shelf. *Mar Freshw Res* 51:229-234
- Smith KA (2003) Larval distributions of some commercially valuable fish species over the Sydney continental shelf. *Proceedings of the Linnean Society of New South Wales* 124:1-11
- Smith KA, Gibbs MT, Middleton JH, Suthers IM (1999) Short term variability in larval fish assemblages of the Sydney shelf: tracers of hydrographic variability. *Mar Ecol Prog Ser* 178:1-15
- Smith KA, Suthers IM (1999) Displacement of diverse ichthyoplankton assemblages by a coastal upwelling event on the Sydney shelf. *Mar Ecol Prog Ser* 176:49-62
- Smith R (1968) Upwelling. *Oceanography and Marine Biology Annual Review* 6:11-46
- Smith SE, Au DW, Show C (1998) Intrinsic rebound potentials of 26 species of Pacific sharks. *Marine and Freshwater Research* 49:663-678
- Snyder MA, Sloan LC, Diffenbaugh NS, Bell JL (2003) Future climate change and upwelling in the California Current. *Geophysical Research Letters* 30:1823, doi:10.1029/2003GL017647
- Sommer U, Stibor H, Katechakis A, Sommer F, Hansen T (2002) Pelagic food web configurations at different levels of nutrient richness and their implications for the ratio fish production:primary production. *Hydrobiologia* 484:11-20
- Sosebee KA (2005) Are density-dependent effects on elasmobranch maturity possible? *Journal of Northwest Atlantic Fishery Science* 35:115-124
- Staples DJ, Vance DJ (1985) Short-term and long-term influences on the immigration of postlarval banana prawns *Penaeus merguensis*, into a mangrove estuary of the Gulf of Carpentaria, Australia. *Marine Ecology Progress Series* 23:15-29
- Stark KE (2008) Ecology of the arrow squid (*Nototodarus gouldi*) in southeastern Australian waters: A multi-scale investigation of spatial and temporal variability. Ph.D. thesis, University of Tasmania
- Stark KE, Jackson GD, Lyle JM (2005) Tracking arrow squid movements with an automated acoustic telemetry system. *Marine Ecology Progress Series* 299:167-177
- Stenseth NC, Mysterud A, Ottersen G, Hurrell JW, Chan K-S, Lima M (2002) Ecological effects of climate fluctuations. *Science* 297:1292-1296
- Sturman A, Tapper N (1996) The weather and climate of Australia and New Zealand, Vol. Oxford University Press, Auckland
- Summerhayes CP, Emeis K-C, Angel MV, Smith RL, Zeitzschel B (1995) Upwelling in the Ocean: Modern Processes and Ancient Records. In: Summerhayes C, Emeis K-C, Angel M, Smith R, Zeitzschel B (eds) *Upwelling in the Ocean: Modern Processes and Ancient Records*. John Wiley & Sons, Berlin, p 1-37
- Suthers IM, Waite AM (2007) Coastal Oceanography and Ecology. In: Connell SD, Gillanders BM (eds) *Marine Ecology*. Oxford, New York, p 630
- Tam J, Taylor MH, Blaskovic V, Espinoza P, Ballon RM, Diaz E, Wosnitza-Mendo C, Argüelles J, Purca S, Ayon P, Quipuzcoa L, Gutierrez D, Goya E, Ochoa N, Wolff M (2008) Trophic modeling of the Northern Humboldt Current Ecosystem, Part I: Comparing trophic linkages under La Niña and El Niño conditions. *Progress in Oceanography* 79:352-365
- Thorrold SR, Shenker JM, Maddox ED, Mojica R, Wishinski E (1994) Larval supply of shorefishes to nursery habitats around Lee Stocking Island, Bahamas. II. Lunar and oceanographic influences. *Marine Biology* 118:567-578
- Thresher RE, Bruce BD, Furlani DM, Gunn JS (1988) Distribution, advection, and growth of larvae of the southern temperate gadoid, *Macruronus novaezelandiae* (Teleostei: Merlucciidae), in Australian coastal waters. *Fish Bull, US* 87:29-48
- Thresher RE, Rintoul SR, Koslow JA, Weidman C, Adkins J, Proctor C (2004) Oceanic evidence of climate change in southern Australia over the last three centuries. *Geophysical Research Letters* 31:L07212, doi:10.1029/2003GL018869
- Thuiller W, Lavorel S, Araújo MB, Sykes MT, Prentice IC (2005) Climate change treats to plant diversity in Europe. *Proceeding of the National Academy of Sciences of the United States of America* 102:8245-8250
- Tilzey RDJ, Zann-Schuster M, Klaer NL, Williams MJ (1990) The south east fishery: biological synopsis and catch distributions for seven major commercial fish species
- Tilzey RDJe (1994) The South East Fishery, Vol. Bureau of Resource Sciences, Parkes, ACT

- Tranter D, Carpenter D, Leech G (1986) The coastal enrichment effect of the East Australian Current eddy field. *Deep-Sea Research* 33:1705-1728
- Trenberth KE, Hoar TJ (1997) El Niño and climate change. *Geophysical Research Letters* 24:3057-3060
- Triantafillos L, Jackson GD, Adams M, McGrath Steer BL (2004) An allozyme investigation of the stock structure of arrow squid *Nototodarus gouldi* (Cephalopoda: Ommastrephidae) from Australia. *ICES Journal of Marine Science* 61:829-835
- Tuck GNe (2006) Stock assessment for the South East Scalefish and Shark Fishery 2004-2005, Australian Fisheries Management Authority and CSIRO Marine and Atmospheric Research, Hobart
- Ullman DS, Cornillon PC (2000) Evaluation of front detection methods for satellite-derived SST data using in situ observations. *J Atmos Ocean Tech* 17:1667-1675
- Uozumi Y (1998) Fishery biology of arrow squids, *Nototodarus gouldi* and *N. sloanii* in New Zealand waters. *Bulletin of National Research Institute of Far Seas Fisheries* 35:1-11
- Vieira S, Wood R, Causer R (2008) Australian fisheries surveys report 2008: results for selected fisheries 2005-06 and 2006-07, Fisheries Resources Research Fund, Canberra
- Villanueva R (2000) Effect of temperature on statolith growth of the European squid *Loligo vulgaris* during early life. *Marine Biology* 136:449-460
- Vooren CM (1972) Post-larvae and juveniles of tarakihi (Teleostei: Cheilodactylidae) in New Zealand. *New Zeal J Mar Freshw Res* 6:601-618
- Walker TI (1992) Fishery simulation model for sharks applied to the gummy shark, *Mustelus antarcticus* Günther, from southern Australian waters. *Australian Journal of Marine and Freshwater Research* 43:195-212
- Walker TI (1994) Fishery model of gummy shark, *Mustelus antarcticus*, for Bas Strait. In: Bishop I (ed) *Resource Technology '94 New Opportunities Best Practice*. The University of Melbourne, Melbourne, p 422-438
- Walker TI (1998) Can shark resources be harvested sustainably? A question revisited with a review of shark fisheries. *Marine and Freshwater Research* 1998:553-572
- Walker TI (2007) Spatial and temporal variation in the reproductive biology of gummy shark *Mustelus antarcticus* (Chondrichthyes : Triakidae) harvested off southern Australia. *Marine and Freshwater Research* 58:67-97
- Walther GR, Hughes L, Vitousek P, Stenseth NC (2005) Consensus on climate change. *Trends Ecol Evol* 20:648-649
- Walther GR, Post E, Convery P, Menzel A, Parmesan C, Beebee TJC, Fromentin J-M, Hoegh-Guldberg O, Bairlein F (2002) Ecological responses to recent climate change. *Nature* 416:389-395
- Waluda CM, Trathan PN, Rodhouse PG (1999) Influence of oceanographic variability on recruitment in the *Illex argentinus* (Cephalopoda: Ommastrephidae) fishery in the South Atlantic. *Marine Ecology Progress Series* 183:159-167
- Waluda CM, Trathan PN, Rodhouse PG (2004) Synchronicity in southern hemisphere squid stocks and the influence of the Southern Oscillation and Trans Polar Index. *Fisheries Oceanography* 13:255-266
- Ward T, Hoedt F, McLeay L, Dimmlich W, Jackson G, Rogers P, Jones K (2001) Have recent mass mortalities of the sardine *Sardinops sagax* facilitated an expansion in the distribution and abundance of the anchovy *Engraulis australis* in South Australia? *Mar Ecol Prog Ser* 220:241-251
- Ward TM, Goldsworthy SD, Rogers PJ, Page B, McLeay LJ, Dimmlich WF, Baylis AMM, Einoder L, Wiebkin A, Roberts M, Daly K, Caines R, Huveneers C (2008) Ecological importance of small pelagic fishes in the Flinders Current System, South Australian Research and Development Institute (Aquatic Sciences), Adelaide
- Ward TM, McLeay LJ, Dimmlich WF, Rogers PJ, McClatchie S, Matthews R, Kämpf J, Van Ruth PD (2006) Pelagic ecology of a northern boundary current system: effects of upwelling on the production and distribution of sardine (*Sardinops sagax*), anchovy (*Engraulis australis*) and southern bluefin tuna (*Thunnus maccoyii*) in the Great Australian Bight. *Fish Oceanogr* 15:191-207
- Ware DM, Thomson RE (2005) Bottom-Up Ecosystem Trophic Dynamics Determine Fish Production in the Northeast Pacific. *Science* 308:1280-1284
- Watters GM, Olson RJ, Francis RC, Fiedler PC, Polovina JJ, Reilly SB, Aydin KY, Boggs CH, Essington TE, Walters CJ, Kitchell JF (2003) Physical forcing and the dynamics of the pelagic ecosystem in the eastern tropical Pacific: simulations with ENSO-scale and global-warming climate drivers. *Canadian Journal of Fisheries and Aquatic Science* 60:1161-1175

- Wolanski E, Ridd P (1990) Mixing and trapping in Australian coastal waters. In: Cheng RT (ed) Coastal and Estuarine Studies, Vol 38. Springer-Verlag, New York, p 165-183
- Woodworth PL, Player R (2003) The Permanent Service for Mean Sea Level: An update to the 21st century. *Journal of Coastal Research* 19:287-295
- Worm B, Myers RA (2003) Meta-analysis of cod-shrimp interactions reveals top-down control in oceanic food webs. *Ecology* 84:162-173
- Worm B, Sandow M, Oschlies A, Lotze H, Myers R (2005) Global Patterns of Predator Diversity in the Open Oceans. *Science* 309:1365-1369
- Wyrski K (1960) The surface circulation in the Coral and Tasman seas. Tech Pap Div Fish Oceanogr CSIRO, Australia 8:1-44
- Yatsu A, Watanabe T, Mori J, Nagasawa K, Ishida Y, Meguro T, Kamei Y, Sakurai Y (2000) Interannual variability in stock abundance of the neon flying squid, *Ommastrephes bartramii*, in the North Pacific Ocean during 1979-1998: impact of driftnet fishing and oceanographic conditions. *Fisheries Oceanography* 9:163-170
- Young JW, Bradford RW, Lamb TD, Lyne VD (1996) Biomass of zooplankton and micronekton in the southern bluefin tuna fishing grounds of eastern Tasmania. *Mar Ecol Prog Ser* 138:1-14
- Young JW, Lamb TD, Russell W, Bradford RW (1997) Feeding ecology and annual variation in diet of the southern bluefin tuna (*Thunnus maccoyii*) in relation to the coastal and oceanic waters off eastern Tasmania. *Environ Biol Fish* 50:275-291
- Young JW, Nishida T, Stanley C (1999) A preliminary survey of the summer hydrography and plankton biomass of the eastern Great Australian Bight, Australia. Southern Bluefin Tuna Recruitment Monitoring and Tagging Program, CSIRO, Hobart
- Zeidberg LD, Robison BH (2007) Invasive range expansion by the Humboldt squid, *Dosidicus gigas*, in the eastern North Pacific. *Proceeding of the National Academy of Sciences of the United States of America* 104:12948-12950